

Photochemical Harpoons:

Covalent labels for multi-protein complexes

A thesis submitted in partial fulfilment of the requirements for the
degree of Doctor of Philosophy.

By

Fathi A. Smida

2013

School of Science and Technology
Nottingham Trent University
Clifton Lane
Nottingham
NG11 8NS
United Kingdom

Declaration.

I hereby certify that the work embodied in this thesis is the result of my own investigations except where reference has been made to published literature.

Abstract.

The identification of the biomolecular interaction partners of small bioactive molecules is a fundamental problem in drug discovery and cell biology. This thesis describes the development of fluorescent chemical probes to identify the biomolecular targets of the known organophosphate toxin, phenyl saligenin phosphate (PSP), and the cardioprotective agent diazoxide.

PSP is an organophosphate toxin that irreversibly inhibits hydrolase enzymes such as trypsin and chymotrypsin along with the common organophosphate target acetylcholine esterase. PSP is also suspected of affecting many other cell functions and may interact with a large number of cellular proteins. In this work phenyl saligenin phosphate has been synthesised and its inhibitory effect on the action of transglutaminase 2 (TGase2) demonstrated. Analogues of PSP containing an attached dansyl amide fluorescent group have been prepared and incubated with purified enzymes trypsin, chymotrypsin and TGase2. SDS-PAGE analysis demonstrates effective fluorescent labelling and a covalent interaction between the toxin analogue and the enzymes.

The K_{ATP} channel opener, diazoxide displays marked cardioprotective effects and is reported to bind to mitochondrial K_{ATP} channels. However, the molecular structure of these channels is still largely unknown. This thesis describes the design and the synthesis of a chemical tool to covalently attach fluorescently labels to the proteins which will bind diazoxide.

Chemical tools for fluorescent labelling of diazoxide targeted proteins have been prepared. Each consists of a photochemically activated reactive 'barb' and coupled fluorescent component linked to modified diazoxide bait. In developing these molecules, a range of functionalised diazoxide bait components were prepared and

tested for retained biological activity compared to the parent compound. Two active analogues were linked to either benzophenone or diazirine (photoreactive) and dansyl amide (fluorescent) components. The non-specific photochemical reactivity of these labelling compounds with bovine serum albumin was established. The incubation and photolysis with mitochondrial extracts showed selective photo labelling of only three biomolecular components. The identification of these biomolecules is the subject of ongoing investigation.

Acknowledgements.

First of all, I praise God, the almighty, merciful and passionate, for providing me this opportunity and granting me the capability to complete my thesis.

I would like to express my deep thanks to my supervisor Dr Chris Garner for all his support, and guidance throughout my studies, also for his encouragement, enthusiasm and advice have inspired me during the research and writing of this thesis.

A big thank you also to my supervision team: Dr John Dickenson and Dr Alan Hargreaves, for their expertise and advice in the biology side of the research and for giving me a part of their priceless time. I cannot forget Dr Manuel Galiñanes for the collaboration for doing an essential biological work. Also big thanks for Dr Quentin Hanley who gave me the opportunity to do the UV irradiation experiments with his well-established machine, for Prof John Wallis for his help and advices and for my friends Salem and Wesam for their help in running the gel electrophoresis.

A big thank you to all the people in the lab, who have made the labs enjoyable places in which to conduct research. I would like to thank Dr Pat Huddleston for his help with his expertise and knowledge in the practical chemistry.

I am most grateful to the Libyan Ministry of Higher Education for offering me the scholarship to pursue my PhD study.

Many thanks go to my very close friend Ismail and all other friends for being great friends, and helping me to leave work at work when I needed to relax.

I sincerely wish to give my deepest appreciation to my wife and son for their patience and support. My completion of this thesis would not have been possible without their presence with me in the U.K during my study.

Finally, my biggest thanks go to mother, father, my brothers and sisters who have in one way or another helped me achieve this thesis. Without all of your support, this couldn't have been done.

Dedication.

To my parents

To my wife and son

To all my brothers, sisters and dearest friends

Without whom this thesis could never have been complete

List of acronyms, abbreviations and symbols.

5-HD	5-hydroxydecanoate
ABP	Activity based probe
Ac	Acetyl
ACh	Acetylcholine
AChE	Acetylcholinesterase enzyme
ADP	Adenosine diphosphate
AFBP	Affinity-based probes
aq.	Aqueous
Ar	Aryl / heteroaryl
ATP	Adenosine triphosphate
Boc	Di tert-butyloxycarbonyl
br	Broad
BSA	Bovine serum albumin
CAD	Coronary artery disease
d	Doublet
d.	Day
DCM	Dichloromethane
dd	Doublet of doublets
DMAP	4-dimethylaminopyridine
DMF	N, N-dimethylformamide
DMSO	Dimethylsulfoxide
eq.	Equivalents
Et	Ethyl
Fig.	Figure
FP	Fluorescent Protein
GFP	Green fluorescent protein
h.	Hour
HMQC	Heteronuclear Multiple Quantum Coherence
HRMS	High Resolution Mass Spectrum

I/R	Ischaemia/reperfusion
ICAT	Isotope-coded affinity tagging
IPC	Ischaemia preconditioning
ISC	Intersystem crossing
IUPAC	International Union of Pure and Applied Chemist
K _a	Acidity constant
K _{ir}	Inwardly rectifying potassium channel subunit
LG	Leaving Group
m	Meta
m	Multiplet
m. /min.	Minutes
MAP-2	Microtubules associated protein-2
Me	Methyl
mol	Mole
μM	Micromolar
Mp	Melting Point
MS	Mass spectrometry
NEt ₃	Triethylamine
NFH	Neurofilament heavy chain
NIQ	Naphthylisoquinoline
NMR	Nuclear Magnetic Resonance
NTE	Neuropathy target esterase enzyme
NTE	Neuropathy Target Esterase
Nu	Nucleophile
<i>o</i>	Ortho
OP	Organophosphate
OPIDN	Organophosphate-induced delayed neuropathy
OPIDP	Organophosphate-induced delayed polyneuropathy
<i>p</i>	Para
PAGE	Polyacrylamide gel electrophoresis

PAL	Photoaffinity labelling
PEG	Polyethylene glycol
Ph	Phenyl
PPC	Pharmacological preconditioning
ppm	Parts per million
PSP	Phenyl saligenin phosphate
py	Pyridine
q	Quintet
R _f	Retention Factor
ROS	Reactive oxygen species
s	Singlet
S	Chemical shift (ppm)
SCOTP	Saligenin cyclic ortho-tolylphosphate
SDS	Sodium dodecyl sulphate
SUR	Sulfonylurea receptor
t	Triplet
tBu	<i>Tert</i> -butyl
TGase	Transglutaminase enzyme
THF	Tetrahydrofuran
TLC	Thin Layer Chromatography
TOCP	Tri-ortho-cresyl phosphate
TPCP	Tri-para-cresyl phosphate
UV	Ultraviolet
UV	Ultra-violet
<i>vic</i>	Vicinal

List of figures.

FIGURE 1 <i>MONASTROL PREPARATION</i>	4
FIGURE 2 <i>STRUCTURE OF A CHEMICAL PROBES</i>	8
FIGURE 3 <i>REACTIVE GROUPS</i>	9
FIGURE 4 <i>MECHANISM OF THE FOUR PRIMARY CLASSES OF CHEMICAL PROBE</i>	10
FIGURE 5 <i>LINKER STRUCTURE</i>	12
FIGURE 6 <i>TAGS USED FOR LABELLING</i>	13
FIGURE 7 <i>PHOTOAFFINITY LABELLING; (I) INCUBATION OF CELL LYSATE WITH TAGGING MOLECULE; (II) IRRADIATION; (III) FLUORESCENCE DIRECTED PURIFICATION</i>	15
FIGURE 8 <i>PHOTOREACTIVE GROUPS USED IN TAGGING BIOMOLECULES</i>	16
FIGURE 9 <i>POSSIBLE REACTION MODES OF THE REACTIVE INTERMEDIATES FORMED UPON IRRADIATION OF ARYL AZIDES</i>	18
FIGURE 10 <i>SOME METHODS OF AZIDES PREPARATION</i>	19
FIGURE 11 <i>INTERMEDIATES AND REACTIONS IN DIAZIRINE PHOTOLYSIS</i>	21
FIGURE 12 <i>BENZOPHENONE IRRADIATION MECHANISMS</i>	22
FIGURE 13 <i>STREPTAVIDIN PROTEIN AND BIOTIN TAG COMPLEX MOLECULE</i>	23
FIGURE 14 <i>BIOTIN-AVIDIN INTERACTIONS FOR PROTEIN TARGET IDENTIFICATION</i>	24
FIGURE 15 <i>PHOTOCLEAVABLE LINKER FOR (ICAT) PROBES</i>	25
FIGURE 16 <i>JABLONSKI ELECTRONIC-STATE DIAGRAM FOR SIMPLE FLUORESCENCE</i>	26
FIGURE 17 <i>DANSYLATED AND FULLY FUNCTIONALIZED DIONCOPHYLLINE ALKALOID</i>	32
FIGURE 18 <i>PHOTOAFFINITY CAPTURE COMPOUND FOR HUMAN CARBONIC ANHYDRASE II INHIBITERS</i>	33
FIGURE 19 <i>GENERAL STRATEGY OF THE PROJECT</i>	35
FIGURE 20 <i>METRIFONATE, USED FOR SCHISTOSOMIASIS TREATMENT</i>	37
FIGURE 21 <i>INHIBITION OF ACETYLCHOLINESTERASE BY ORGANOPHOSPHATE; A. ACh HYDROLYSIS AChE, B. DE-ACTIVATION OF AChE</i>	38
FIGURE 22 <i>TOXINS BIND TO TARGETS OTHER THAN ACETYLCHOLINESTERASE</i>	39
FIGURE 23 <i>ORGANOPHOSPHATES KNOWN TO INDUCE OPIDN</i>	41
FIGURE 24 <i>STRATEGY OF ORGANOPHOSPHATE PROTEIN TARGETING</i>	46

FIGURE 25 POSSIBLE MECHANISMS OF THE INHIBITION AND BINDING OF SALIGENIN PHOSPHATE WITH BIOMOLECULES	47
FIGURE 26 SALIGENIN-PHOSPHONATE AND PHOSPHATE ANALOGUES	48
FIGURE 27 ORGANOPHOSPHATE NEUROTOXIN LINKED WITH FLUORESCENT TAG	48
FIGURE 28 SALIGENIN PHOSPHATE WITH BODIPY VIA ALKYL LINKER	52
FIGURE 29 NMR SPECTRA FOR COMPOUND 13	59
FIGURE 30 CLEAVAGE SITE AND REACTION PRODUCT RELEASED BY TRYPSIN	60
FIGURE 31 EFFECT OF PSP ON TRYPSIN ACTIVITY	61
FIGURE 32 CLEAVAGE SITE AND SUBSTRATE RELEASED BY CHYMOTRYPSIN	62
FIGURE 33 EFFECT OF PSP ON CHYMOTRYPSIN ACTIVITY	62
FIGURE 34 BIOTIN CADAVERINE ASSAY FOR TGASE 2 ACTIVITY.....	63
FIGURE 35 IN VITRO EFFECTS OF DIFFERENT CONCENTRATIONS OF PSP ON TGASE 2 ACTIVITY	64
FIGURE 36 INCUBATION OF DANSYLATED SALIGENIN PHOSPHATE WITH TRYPSIN AND CHYMOTRYPSIN	65
FIGURE 37 INCUBATION OF DANSYLATED SALIGENIN PHOSPHATE WITH TRANSGLUTAMINASE 2.....	66
FIGURE 38 HYPOTENSIVE VASODILATORS; DIAZOXIDE, CROMAKALIM AND PINACIDIL	73
FIGURE 39 K_{ATP} BLOCKERS; GLIBENCLAMIDE AND SODIUM 5-HYDROXYDECANOATE.....	73
FIGURE 40 PROPOSAL STRUCTURE OF THE MITO K_{ATP} CHANNE	75
FIGURE 41 IDENTIFICATION STRATEGY FOR THE PROTEIN TARGET OF DRUG MOLECULE	75
FIGURE 42 MODULAR LINKED PHOTOREACTIVE BARB AND FLUORESCENT TAG WITH A SMALL BINDING BAIT MOLECULE	79
FIGURE 43 RETROSYNTHESIS OF DIAZIRINE	80
FIGURE 45 ^{13}C NMR FOR <i>E</i> AND <i>Z</i> DIASTEREOMER	82
FIGURE 46: SYMMETRIC POSSIBLE ISOMERS OF COMPOUND 6.....	83
FIGURE 46 MOLECULAR STRUCTURE OF 36.....	94
FIGURE 47 MECHANISM OF LDH ASSAY.....	102
FIGURE 48 REDUCTION OF MTT TO FORMAZAN.....	102
FIGURE 49 DIAZOXIDE ANALOGUES TESTED IN CELL VIABILITY ASSAYS	105
FIGURE 50 LDH AND MTT ASSAYS RESULTS.....	105
FIGURE 51 ELABORATION PLAN FOR THE ANALOGUES 43 AND 47	106
FIGURE 52 NMR SPECTRA FOR COMPOUND 54	110

FIGURE 53 <i>NMR SPECTRA FOR COMPOUND 55</i>	111
FIGURE 54 <i>NMR SPECTRA FOR COMPOUND 56</i>	112
FIGURE 55 <i>EXCITATION AND EMISSION FOR 54</i>	115
FIGURE 56 <i>EXPOSURE OF BSA PROTEIN MIXED WITH THE THREE COMPOUNDS IN 10 MINUTES</i>	117
FIGURE 57 <i>EXPOSURE OF BSA PROTEIN MIXED WITH THE TWO COMPOUNDS FOR 30 MINUTES 54A, 56A AND FOR 60 MINUTES 54B, 56B</i>	117
FIGURE 58 <i>INCUBATION OF MOLECULES 54, 55 AND 56 WITH MITOCHONDRIAL EXTRACT</i>	119
FIGURE 59 <i>SPECIFICITY TARGETING TEST</i>	120

Table of Contents.

<i>Declaration.</i>	<i>I</i>
<i>Abstract.</i>	<i>II</i>
<i>Acknowledgements.</i>	<i>IV</i>
<i>Dedication.</i>	<i>VI</i>
<i>List of acronyms, abbreviations and symbols.</i>	<i>VII</i>
<i>List of figures.</i>	<i>X</i>
<i>Table of Contents.</i>	<i>XIII</i>
<i>1.</i>	<i>Chapter 1: Introduction</i>
.....	<i>1</i>
1.1 Background	1
1.2 Genetic methods	6
1.3 Affinity methods	7
1.3.1 Tagging biomolecules using reactive sites	7
1.3.2 Tagging proteins with no reactive sites	14
1.3.2.1 Photoaffinity labelling (PAL)	14
1.3 The project plan	34
<i>2.</i>	<i>Chapter 2: Organophosphates</i>
.....	<i>36</i>
2.1 Introduction	36
2.1.1 Acute toxicity mechanism of organophosphorus compounds	37
2.1.2 Other organophosphate targets	38
2.1.3 Organophosphate-induced delayed neuropathy (OPIDN)	40
2.1.4 The effect of phenyl saligenin phosphate (PSP) on the phosphorylation of neurofilament heavy chain (NFH) and MAP kinase activation (ERK1/2)	42
2.1.5 The effect of phenyl saligenin phosphate PSP on serine/threonine phosphorylation	43
2.1.6 The effect of phenyl saligenin phosphate PSP on the neurite outgrowth and the activity of NTE	43

2.1.7 The effect of phenyl saligenin phosphate on transglutaminase activity	44
2.1.8 Aim of investigation	45
2.2 Results and Discussion.....	46
2.2.1 Synthesis of phenyl saligenin phosphate	48
2.2.2 Preparation of 2-chloro-4H-benzo[d] [1, 3, 2]dioxaphosphinine 2-oxide	49
2.2.3 Reaction of saligenin phosphate with 1, 6 hexane diol.....	50
2.2.4 Preparation of saligenin phosphate with a linker for attachment to a fluorescent tag	50
2.2.5 Preparation of BODIPY- FL fluorescent component with linker	52
2.2.6 Dansylamide with PEG linker	55
2.2.7 Dansylamide with six carbon alkyl linker	56
2.2.8 Coupling the organophosphate compound with the florescent tag	57
2.2.9 Coupling the organophosphate compound 2 with dansyl amide 12	58
2.2.10 Biological testing	60
2.3 Conclusion	67
3.....Chapter 3: The mK_{ATP} activator “diazoxide”	68
1. Introduction.....	68
3.1.2 Introduction to cardioprotection	69
3.1.3 Potassium channel activation and diazoxide	72
3.1.4 Structure of the mK_{ATP} channel	74
3.1.5 Aim of investigation	75
3.2 Results and discussion	77
3.2.1 Preparing the Photoaffinity compound (α -trifluoro diazine)	80
3.2.2 Preparation of fluorescent tag (dansylamide) with linker	84
3.2.3 Coupling barb with molecule of fluorescent tag and linker	85
3.2.4 Preparation of substituted diazoxides as “baits”	90
3.2.5 Substitutions on diazoxide.....	92
3.2.6 Biologically active testing for the modified diazoxide results	100
3.2.7 Fully functionalised diazoxide tagging molecules.....	106

3.2.8 Photolysis investigation of the fully functional molecules 54, 55 and 56	115
3.2.9 Investigation of mitochondrial component targets of diazoxide analogues.	118
3.2.10 Incubation of diazirine compound 55 with the mitochondrial extract	120
3.3 Conclusion	122
4. Chapter 4: Experimental.....	123
4.1 General.....	123
4.2 Reagents and Solvents	123
4.3 Purification Processes	123
4.4 Instrumentation.....	124
4.5 Experimental of Chapter 2.....	125
4.5.1 Synthesis of phenyl saligenin phosphate-1	125
4.5.2 The preparation of 2-chloro-4H-1,3,2-benzodioxaphosphorin-2-oxide-2	125
4.5.3 Preparation of N-Boc-6-aminohexan-1-ol-3.....	126
4.5.4 Synthesis of a BODIPY	126
4.5.4.2 Ethyl 3-(1H-pyrrol-2-yl) propionate-5	127
4.5.5 5-(Dimethyl amino)naphthalene-1-sulfonamide-9	130
4.5.6 5-(Dimethylamino)-N-(2-(2-(2 hydroxyethoxy)ethoxy) ethyl) naphthalene-1-sulfonamide-10	131
4.5.7 5-(Dimethylamino)-N,N-bis(2-(2-(2-hydroxyethoxy)ethoxy)ethyl)naphthalene-1-sulfonamide- 10a	132
4.5.8 N-(6-hydroxy-hexyl)-5-dimethylamino-naphthalene-1-sulfonamide 12	132
4.5.9 Coupling the organophosphate compound with fluorescent tag-13.....	133
4.6 Experimental of Chapter 3.....	134
4.6.1 4-Bromobenzyl alcohol-O-(<i>tert</i> -butyldimethylsilyl) ether -14	135
4.6.2 4-[(<i>tert</i> -butyldimethylsiloxy)methyl]-2,2,2-trifluoroacetophenone -15.....	136
4.6.3 4-[(<i>tert</i> -Butyldimethylsiloxy)methyl]-2,2,2-trifluoroacetophenone-oxime-16.....	137
4.6.4 4-[(<i>tert</i> -Butyldimethylsiloxy)methyl]-2,2,2-trifluoroacetophenone-O-(4 toluenesulphonyl)oxime-17	137
4.6.5 3-[α -(<i>tert</i> -Butyldimethylsiloxy)-4-tolyl]-3-trifluoromethyl diaziridine-18	138
4.6.6 (4-(3-(trifluoromethyl)diaziridin-3-yl)phenyl)methanol-19	139

4.6.7 3-[α - (<i>tert</i> -Butyldimethylsiloxy)-4-tolyl]-3-trifluoromethyl diazirine-20	139
4.6.8 4-[3-Trifluoromethyl-3H-diazirin-3-yl) benzyl alcohol-21	140
4.6.9 3-(4-(Bromomethyl)phenyl)-3-(trifluoromethyl)-3H-diazirine-22	141
4.6.10 <i>N</i> -Allyl-5-(dimethylamino)naphthalene-1-sulfonamide-23.....	141
4.6.11 A model reaction using benzyl alcohol-24	142
4.6.12 Coupling of diaziridine with fluorescent component-25	143
4.6.13 5-(Dimethylamino)- <i>N</i> -(6-hydroxyhexyl)- <i>N</i> -(4-(3-(trifluoromethyl)-3H-diazirin-3-yl)benzyl)naphthalene-1-sulfonamide-26.....	144
4.6.14 Coupling the benzophenone with the dansyl amide-27a	145
4.6.15 <i>N</i>-(4-Benzoylbenzyl)-5-(dimethylamino)-<i>N</i>-(6-hydroxyhexyl)naphthalene-1-sulfonamide-27	146
4.6.16 <i>N</i> -(4-Benzoylbenzyl)-5-(dimethylamino)- <i>N</i> -(2-(2-(2 hydroxyethoxy)ethoxy)ethyl)naphthalene-1-sulfonamide-28	147
4.6.17 3-Methyl-4H-benzo[1,2,4]thiadiazine 1,1-dioxide-33.....	148
4.6.18 3-Methyl-7-nitro-4H-1,2,4-benzothiadiazine-1,1-dioxide-34.....	148
4.6.19 7-Bromo-3-methyl-4H-benzo[e][1,2,4]thiadiazine 1,1-dioxide-35	149
4.6.20 5,7-Dibromo-3-methyl-4H-benzo[e][1,2,4]thiadiazine 1,1-dioxide-36.....	149
4.6.21 5-Bromo-2-amino-benzenesulfonamide-37	150
4.6.22 3,5-Dibromo-2-aminobenzenesulfonamide-38	150
4.6.23 2-Amino-5-vinyl-benzenesulfonamide-40.....	151
4.6.24 2-Amino-4-vinylbenzenesulfonamide 40a	152
4.6.25 3-Methyl-7-vinyl-4H-benzo[e][1,2,4]thiadiazine 1,1-dioxide-41.....	153
4.6.26 2-Amino-5-(2-hydroxy-ethyl)-benzenesulfonamide-42	154
4.6.27 7-(2-Hydroxyethyl)-3-methyl-4H-benzo[e][1,2,4]thiadiazine 1,1-dioxide-43	154
4.6.28 2-Amino-4-bromobenzenesulfonamide-44.....	155
4.6.29 6-Bromo-3-methyl-4H-benzo[e][1,2,4]thiadiazine 1,1-dioxide-45	156
4.6.30 2-Amino-6-chlorobenzenesulfonamide-46	157
4.6.31 8-Chloro-3-methyl-4H-benzo[e][1,2,4]thiadiazine 1,1-dioxide-47	159
4.6.32 4-(1,1-Dioxido-4H-benzo[e][1,2,4]thiadiazin-3-yl)butanoic acid-48.....	159

4.6.33	4-(7-Bromo-1,1-dioxido-4H-benzo[e][1,2,4]thiadiazin-3-yl)butanoic acid-49	160
4.6.34	4-(5,7-Dibromo-1,1-dioxido-4H-benzo[e][1,2,4]thiadiazin-3-yl)butanoic acid-50	160
4.6.35	Hybrid with the non-substituted diazoxide-52	161
4.6.36	4-(8-Chloro-1,1-dioxido-4H-benzo[e][1,2,4]thiadiazin-3-yl)butanoic acid-53	162
4.6.37	Benzophenone-hybrid with 8-chloro- diazoxide-54	162
4.6.38	Diazirine alkyl linker hybrid with 8-chloro diazoxide-55	163
4.6.39	Benzophenone and PEG linker hybrid with 8-chlorodiazoxide-56	164
4.6.40	4-(1,1-Dioxido-7-vinyl-4H-benzo[e][1,2,4]thiadiazin-3-yl)butanoic acid-57	165
4.6.41	Benzophenone-hybrid with 7-vinyl diazoxide-58	165
4.7	Biological experimental	167
4.7.1	UV irradiation test	167
4.7.2	SDS Polyacrylamide Gel Electrophoresis	167
4.7.3	Incubation of the mitochondrial extract proteins with the diazoxide molecules.....	170
References	172

1. Chapter 1: Introduction

1.1 Background

Naturally occurring substances have been used for medicinal purposes for thousands of years and until relatively recent times, all drugs were obtained from Nature, often by serendipity, and the means by which these medicines worked was little understood. The advent of modern biochemistry has given rise to the concept of a drug, as a low molecular weight compound (< 1 kDa) which interacts selectively with specific biomolecules to give a potent pharmacological response.¹ As the processes that regulate living organisms have been progressively elucidated, and biochemical science has developed, the process of drug discovery has also changed. Modern drug discovery involves chemical synthesis of large number of both structurally diverse and systematically varied compounds, which are then tested for activity using sophisticated and rapid biological screening techniques.²

One of the main objectives in drug discovery is identification of new chemical entities that are more likely to bind the target protein to have a desired biological action. High-throughput screening of huge chemical libraries has been a main source of identification of new lead compounds. In conjunction with this, the study of the biochemical mechanism of action of natural small molecules and new drugs has become central to understanding the function and importance of many classes of proteins, including intracellular receptors membrane, signalling proteins and proteins carrying out and regulating the cell cycle, and to the process of drug discovery.^{3, 4}

In the biological system, many proteins are activated and/or deactivated by various ligands to transduce inputs into proper cellular responses. Understanding the types of

protein targets and the mechanism of molecular interactions between small bioactive ligands and those proteins is important for successful drug design and discovery.⁵

The study of genomic information has provided an increasing number of potential drug targets that can be screened,⁶ and many high-throughput screens traditionally employed to identify potential drugs use biochemical assays involving purified target protein.⁷ These methods directly seek to find small molecules which will affect a known target protein however, a high number of compounds of recent interest come from screens involving cell culture or complete organism.^{8, 9} While the chance for discovering new drugs or drug usages by these assays is good, these leads give no unambiguous indication of the probable targets. To compound matters, advances in chemical synthesis and high throughput biological screening have not been matched by advances in the identification of the biological targets of small molecules.¹⁰

As it stands, there are currently many drugs for which the biological target are completely unknown and in order to further understand how these drugs work, identification of these protein targets is essential. It has been estimated that the biomolecular targets of at least half of the drugs dating from the pre-molecular period, when drugs action were discovered using complete tissues, and biological activity was just indicated by tissue-based responses are unknown. Currently, 37% of drugs come from phenotypic screens,^{11, 12} and the biomolecule targets for a number of novel drugs remains unknown.

To further complicate matters, drugs selected for, or considered to specifically modify activity of a target protein, may also bind various other proteins. Multi-target drugs generally interact with a lower affinity than a drug with a single target, as high affinity binding to many different targets it is not expected, but this is not necessarily a

weakness. For instance, Memantine, currently used in the treatment of Alzheimer's disease, shows no high affinity for any of particular protein but targets multiple proteins with relatively low affinity and exhibits lower of side effects than alternative single target drugs with high binding affinities.¹¹

Conversely, the study of the effects of small biologically active molecules and drugs can give an opportunity examine protein function in general. In such studies protein activity can be quickly switched on or off by small molecules in a controlled manner, which cannot be found in any other methods allowing the role of these proteins to be probed. The main problem of widespread use of small molecules for studying biology is the difficulty of identifying compounds that can specifically modify the function of a given protein.¹³ This problem can be addressed by the elucidation of the biomolecular targets of known biologically active molecules.¹³

There are a number of methods that have been applied to the identification of protein targets of small molecules and drugs which are outlined below. One instructive example of the drug discovery using high-throughput phenotypic screening process coupled with identification of the novel target is the case of Monastrol.

Monastrol is a cell-permeable small molecule inhibitor discovered by Schreiber and Mayer. This compound was identified from a phenotypic screen of 35 000 compounds involving cell mitosis, and was subsequently shown to inhibit kinesin Eg5, a motor protein important for spindle bipolarity. Monastrol has since proved to be a powerful tool for the investigation of cellular processes as it can quickly perturb the function of a protein target and unlike taxol does not target tubulin.¹⁴ The mode of action of Monastrol was identified from the observation that it inhibits the formation of bipolar spindles in a dose-dependent manner, and the morphological effect was found to be

similar to that seen in antibody inhibition of Eg5 in *Xenopus* egg extracts.¹⁵ In this case, systematic large scale screening allowed the identification of the small bioactive compound however identification of the target required a much more specific approach.

Monastrol is an illustration example of the use of parallel synthesis to generate drug lead compounds. Its synthesis involves the multi component cyclocondensation of an aldehyde, β -lacto ester and urea, which leads itself to rapid combine synthesis. Indeed, Monastrol can be easily synthesized using a microwave protocol, employing ethyl acetoacetate, 3-hydroxybenzaldehyde, and thiourea (Figure 1).¹⁶

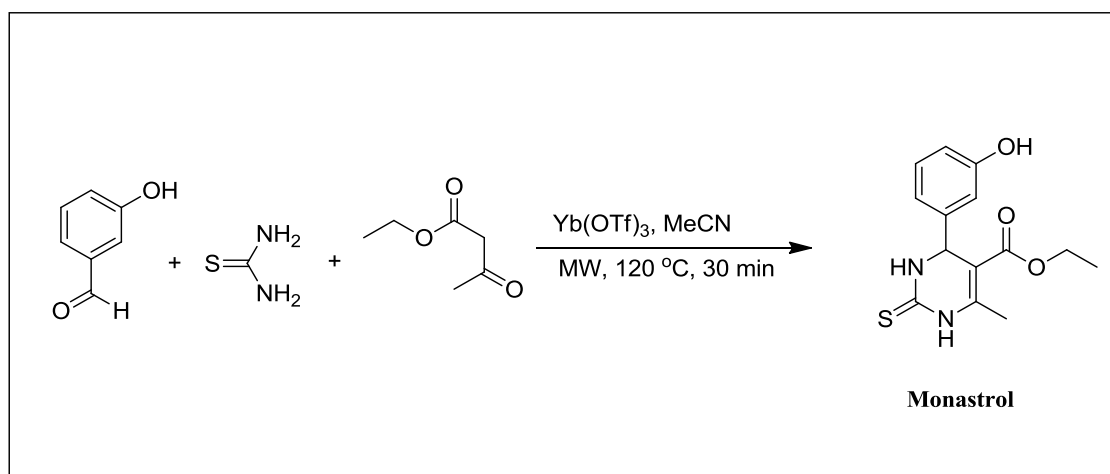


Figure 1 *Monastrol preparation*

Identification of protein function and the mechanisms of balancing functions in life using small molecules as probes is an area of great interest and activity. In the biological system, many proteins are activated and/or deactivated by various ligands to transduce inputs into proper cellular responses. Understanding the types of protein targets and the mechanism of molecular interactions between small bioactive ligands and those proteins is important for successful drug design and discovery.⁵

One of the main objectives in drug discovery is identification of new chemical entities that are more likely to bind the target protein to have a desired biological action.

Recently, the study of genomic information has provided an increasing number of potential drug targets that can be screened.⁶ High-throughput screening of huge chemical libraries has been a main source of identification of new lead compounds. In conjunction with this, many three-dimensional structures for several drug targets have been developed aiding the design of new leads.

The high-performance computing platforms have successfully screened large chemical databases to identify a wide range of targets. There are two essential methods for virtual screening. First, a ligand-based approach aims to detect molecules which have similar physical and chemical properties to known drugs that are expected to interact with the target.¹⁷ Second, a receptor-based approach aims to utilise the molecular recognition between a drug and a target protein to select out chemical entities that bind strongly to the active sites of biologically relevant targets for which the three-dimensional structures are known or inferred.¹⁸

In addition, small biologically active molecules and drugs can give an opportunity to examine protein function in general. Protein activity can be modified by these small molecules in a controlled manner, which cannot be achieved by any other methods, allowing the role of these proteins to be probed. However, the main problem limiting a widespread use of small molecules for studying biology is the difficulty of identifying compounds that can specifically modify the function of a given protein.¹³

Ad hoc methods have been used to identify the protein targets of many small molecules and drugs, which have led to a deeper knowledge of the physiological functions of many proteins and sometimes the pathophysiology of diseases, which the drugs are used to treat. Modern chemical biology, high-throughput phenotypic screening, together with an increase in the number of drugs have resulted in the emergence of small molecules as tools to perturb and elucidate biological processes.¹³

Even when small molecules are known to cause phenotype responses, the identification of biological targets is a problem. Therefore, the targets identification has been addressed via many methods: including genome-wide genetic approaches, affinity purification, molecular profiling strategies and *in silico* computational modelling and automated prediction of drug targets. Affinity purification and genetics are the most popular methods used for target identification and each application has its strengths and weaknesses.

1.2 Genetic methods

In essence, the genetic method for target identification is to carry out genetic perturbation of an organism and select for clones that have resistance to action of a certain small molecule by screening.¹⁹ The identification of the gene(s) that created the resistance can then help to determine the target of a small molecule. It is possible for the bacterial and yeast cells to select resistant clones which are made by mutations. After these resistant clones are isolated, genomic DNA can be extracted and sequenced, and compared with the wild type cells. From this it is possible to identify the mutation on the gene that provides increase to resistance to the drug under investigation. For example the target of the immunosuppressive of antiproliferative Rabamycin was identified by means of yeast genetics.²⁰ While effective, these genetic approaches require a considerable amount of work to produce clones, and such genetic modification is not always possible.

This approach is further limited, as many mammalian cellular pathways do not exist in yeast. Hence, yeast genetics are not valid for many small molecules which affect specific processes in mammalian cells. Furthermore, some small molecules cannot be used in yeast due to a poor permeability of yeast cells. Some of these problems have

been addressed by a similar approach using mammalian cells which can easily be mutagenized, to select for clones which have resistance to a specific small molecule.²¹

1.3 Affinity methods

Chemical methods are essential in chemical biology and provide an alternative route for direct identification of target proteins in biomolecules mixtures as well as their ligand binding site structures. Affinity purification is a powerful method which can be applied to identify targets of small molecules and drugs, which show biological activity only in mammalian cells or whole organisms. These analyses are based on the affinity between the ligand and the target protein, affinity-based chemical modification introduces a useful tag for analysing the target protein.²²

For example, single-molecular imaging with a fluorophore visualizes target biomolecules in complex systems for imaging of the localization of these biomolecules and processing the flow of bioactive compounds in cell units.²³ Affinity labelling is limited by the necessity to specifically attach the required tag on the target protein. Generally the method requires the presence of nucleophilic residues near to a ligand binding site in order to avoid non-specific introduction of the tag at a site different from the binding site or onto other parallel biomolecules.²⁴

1.3.1 Tagging biomolecules using reactive sites

Tagging biomolecules using reactive sites have found much application in the field of enzyme identification. A principal component of this field is the proposal of specific protein-modifying reagents that can be applied for functional studies of enzyme families within a complex proteome. These chemical probes are designed to covalently bind to a target enzyme in such a way that it can be then identified and/or purified by tagging the protein of interest.²⁵ The probes can be prepared to react with diverse families or

subfamilies of enzymes. With this area, much work has focused on activity based probes (ABPs) which modify the enzyme using covalent bond formation. Other probes can target non-catalytic residues on proteins and enzymes, and these affinity-based probes (AFBPs) should have a high selectivity and, tight binding to tag the proteins.

In general, chemical probes are being increasingly applied in the field of proteomics and have good capability to help in drug target identification, validation, and drug discovery. In the most basic form, chemical probes consist of three functional elements;²⁶ i) a reactive group for covalent reaction with the enzyme, ii) a linker, that can modulate reactivity and specificity of the reactive group, iii) and a tag for identification and purification.(Figure 2).

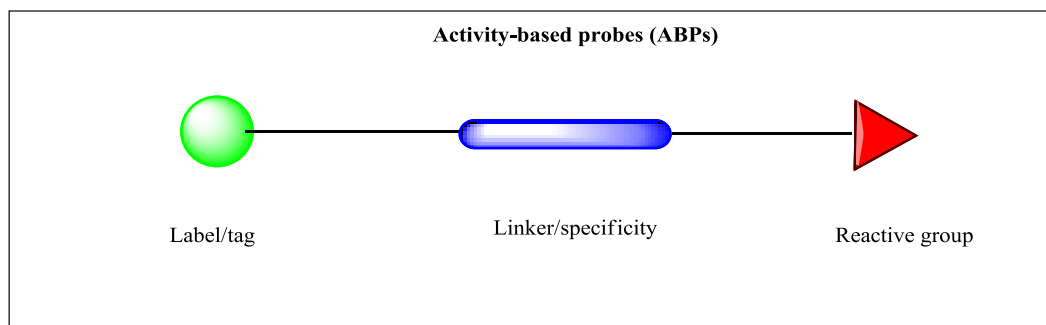


Figure 2 *Structure of a chemical probe*

1.3.1.1 Reactive groups

One of the major difficulties in designing a chemical probe is finding a reactive group that can undergo selective covalent modification of a target protein. The group must be reactive towards a specific residue on a protein but at the same time unreactive towards other species within the cell or cell extract (Figure 3).

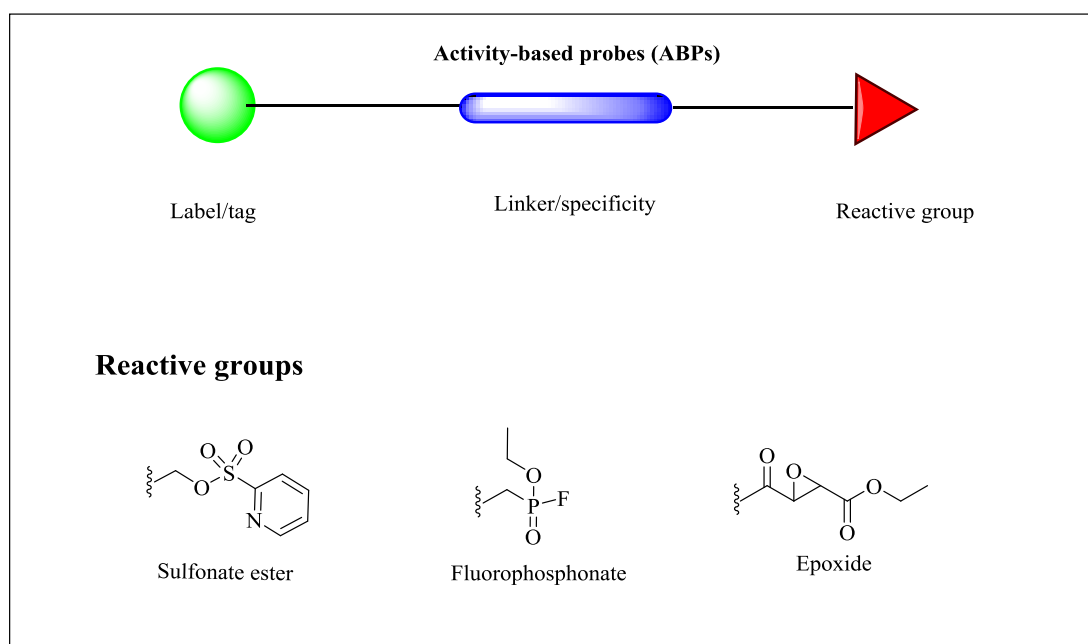


Figure 3 *Reactive groups*

In general, most of the successful chemical probes are based on the chemistries of the enzyme active site, and are, effectively, covalent, mechanism-based inhibitors of the enzyme. Generally, four general classes of reactive groups are used to design chemical probes (Figure 4).

Probe type	Mechanism
I: Mechanism-based ABP	
II: Suicide substrate ABP	
III: Affinity alkylating ABP	
IV: General alkylating	

Figure 4 Mechanism of the four primary classes of chemical probe

The first two types (I and II) require active target enzymes to react with the probe are based on enzyme reaction mechanism or suicide inhibitors. For the mechanism-based probes (type I), the reactive nucleophile is the catalytic residue of the enzyme normally involved in reaction with a substrate. The selectivity of this probe uses knowledge of catalytic mechanism and is often uses chemistry specific to the nucleophilic atom used by the enzyme class. The suicide inhibitor ABPs (type II) contain a 'masked electrophile' that is uncovered after the probe functions as substrate for the target enzyme. Once unmasked, the electrophile reacts with adjacent nucleophilic residues in

the active site. Affinity alkylating probes (AFBPs, type III) have affinity-based labelling groups that need only a strong nucleophile or electrophile nearby the active-site pocket and do not require a fully active enzyme. As such these probes rely upon guest/host recognition to bring the reaction partners together. The final class of reactive groups used (type IV) contains non-specific alkylating groups that react with targets based only on the reactivity of nucleophilic amino acid residues such as cysteine. This class of probe has recently found much application in bulk proteomic analysis by mass spectrometry.²⁷

1.3.1.2 Linkers

The linker section of a chemical probe connects the reactive group to the tag used for identification and/or purification. The linker section has multiple purposes. Its primary function is to separate the reactive group and the tag to avoid steric hinderance that could either block reaction of the reactive group or access to the tag during purification process. Linkers often used are a long-chain alkyl or polyethylene glycol (PEG) spacer, the choice of linker can control hydrophobicity and alkyl linker can confer membrane permeability, while the PEG linker can confer water solubility to hydrophobic probes. Polypeptide linkers have also been used. (Figure 5).²⁸

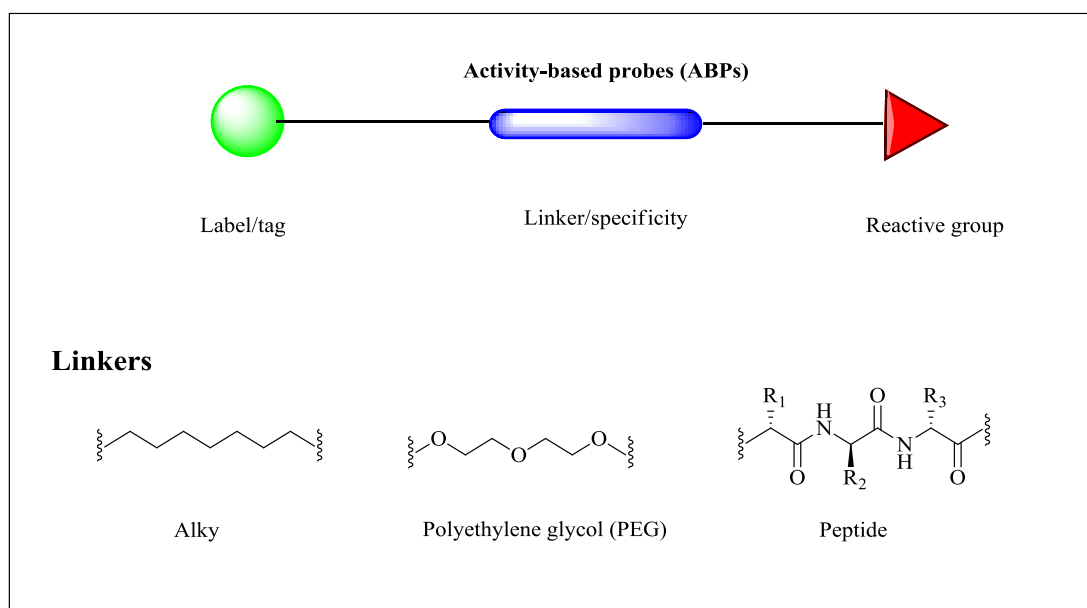


Figure 5 *Linker structure*

1.3.1.3 Tags

The function of the tag on a chemical probe is to enable identification, and often purification, of probe-modified proteins. The most commonly applied tags are biotin, fluorescent, and radioactive tags. The simplest method to separate proteins involves gel electrophoresis, and tags used in a probe must be suitable for use with SDS-PAGE methods. Fluorescent and radioactive tags have several advantages over biotin. Both fluorescence and radioactivity detection methods are more sensitive than streptavidin-biotin detection methods (Figure 6).²⁹

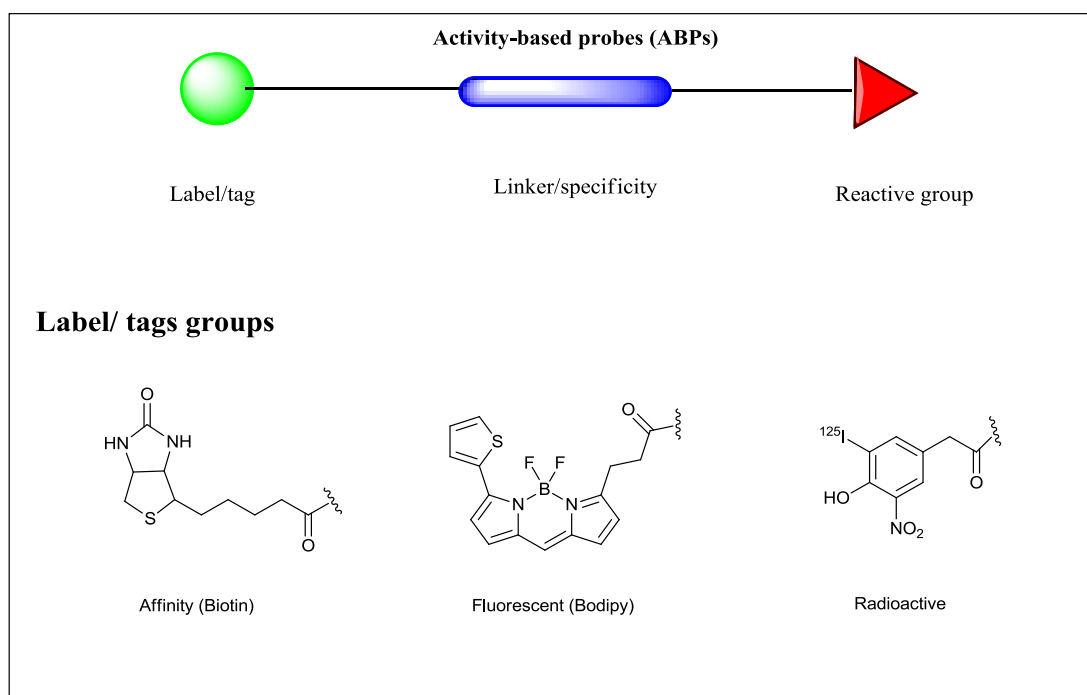


Figure 6 *Tags used for labelling*

In addition, fluorescent tagging methods have an added advantage, in that tags emitting different wavelengths can be used. For example using different coloured fluorescent tags in different experiments allows all results to still be obtained on a single gel.^{30, 31}

Despite the benefits of fluorescent and radioactive tags, biotin still remains the most commonly used tag since it allows both a gel-based detection and a method for purification of labelled enzymes on streptavidin – agarose beads. The use of very large peptides or proteins tags holds much promise by providing a high selectivity to a chemical probe and simplicity of isolation, but it also has disadvantages, specifically the peptide tags are large in size, hard to integrate into small molecule skeletons and greatly alter the cell permeability of probes.³²

1.3.2 Tagging proteins with no reactive sites

As discussed above, the content labelling of enzymes can be achieved by exploiting the reactive nature of enzyme active sites, however it is highly desirable to be able to tag proteins that are not enzymes in order to identify and elucidate their functions. Indeed, chemical probes can be applied to study all aspects of proteomics from protein expression and identification to cellular localization and regulation.²⁶ Chemical proteomics has the potential to uncover these targets in a rapid, systematic and comprehensive manner through design, synthesis, and application of relevant probes.

1.3.2.1 Photoaffinity labelling (PAL)

The concept of photoaffinity labelling (PAL) was introduced by Frank Westheimer in the early 1960s,³³ and has since become one of the most common methods used in biology for the specific detection of the protein targets of bioactive ligands. The identification of interacting partners allows immediate access to the discovery of medicinal leads. The method of photoaffinity labelling enables the direct identification of target protein through the formation of a covalent bond between a ligand and its specific receptor.³⁴ This technique is based on ligand-receptor complex formation between a photoreactive probe and receptor protein which, when exposed to ultra violet light, results in carbene or nitrene reactive intermediates which facilitate covalent attachment of the probe to receptor binding site of the ligand (Figure 7).^{35, 36}

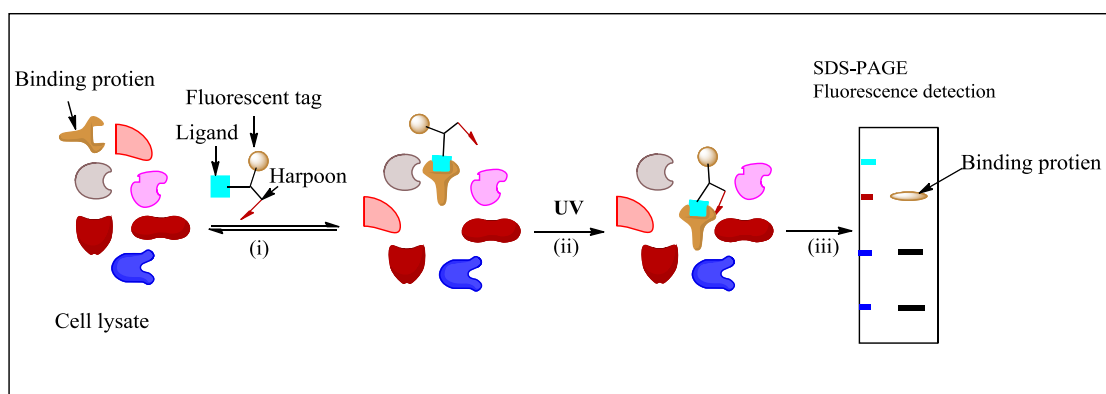


Figure 7 *Photoaffinity labelling; (i) incubation of cell lysate with tagging molecule; (ii) irradiation; (iii) fluorescence directed purification*

1.3.2.1.1 Photoactivating groups

The main role of photoreactive groups attached to a ligand is to provide covalent binding between the ligand and receptor. The success of a photoaffinity labelling experiment relies on the selection of appropriate photoactivating groups which is crucial in this process.³⁷ There are several considerations in selecting reactive groups for a photoaffinity labelling experiment. Generally, the photophore size should not be very large, in order to avoid a negative effect on the binding affinity of ligand-receptor due to a steric interference. The photophore should be also chemically activated under ultra violet light irradiation, and the photo-activated lifespan under ultra violet should also be considered. The covalent attachment of photophore to its active binding receptor site must occur before dissociation of the ligand receptor complex, which can only happen when the duration of the activation lifespan is short.

On the other hand, if the photophore remains very close to the binding site, more efficient covalent attachment will be achieved when a photophore with a long excited state is chosen. Furthermore, the wavelengths used for activation of photophore should not negatively cause damage to the target protein of interest.³⁴ Nitrene or carbene reactive intermediates are strong electrophiles with the ability to selectively react with

nucleophilic hetero atoms (N, O or S) or even double bonds, but also inert groups such as C-H and N-H sigma bonds.

The most widely used photoreactive groups are phenylazides, phenyldiazirines and benzophenones due to their ease of handling, simple synthesis and commercial availability (Figure 8).³⁸

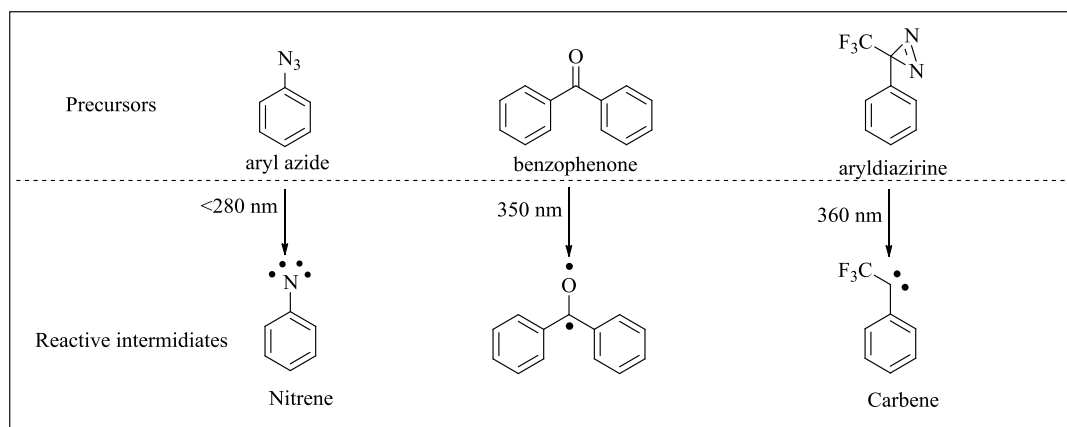


Figure 8 Photoreactive groups used in tagging biomolecules

The photolysis of azides produces a nitrene intermediate while carbene intermediates are generated by a diazirine precursor. Carbenes are generally considered better reactive intermediates than nitrenes, and for instance, carbenes are more reactive in crosslinking reactions with nitrogen-carbon bonds than nitrenes, especially in amino acid sequence identification.

These photoreactive groups require different wavelengths of light to activate the photolysis process. A wavelength of 300 nm is required for the azide photolysis, which upon prolonged irradiation, may affect bio-macromolecules. On the other hand, carbene precursors require a longer wavelength of $\sim 360\text{ nm}$ which is less damaging to proteins.³⁹

Benzophenone derivatives are also a powerful agent for efficient crosslinking,³⁴ and benzophenones offer advantages which make them attractive for reaction with target proteins over the use of diazirine and azide photo probes. The photo-dissociation is a potential side reaction in diazirine and azide chemistry while with benzophenone this

phenomenon does not occur. Similar to carbenes, the carbonyl group can be excited at approximately 360 nm to generate a triplet excitation state which shows high reactivity with C-H bonds even in the presence of water.³⁹

Comparative irradiation studies of these three photophores types in living cells suggest that the irradiation needed for the generation of active species from azide and benzophenone may cause cell death, because long irradiation times are needed to integrate the photophores into cell membrane surface biomolecules. On the other hand, the carbene precursor – 3-phenyl-3-(trifluoromethyl) diazirine (TPD) – did not promote cell death in the generation of active species, but the other photophores are effective in photoaffinity experiments *in vitro*.⁴⁰

1.3.2.1.2 Mechanisms of action of the photophores

All the three photophore molecules have different reactivity profiles in reaction with the biomolecule targets. The mechanisms of action depend on the reactive intermediates generated during the course of the reaction, which can possibly lead to a variation of products.

i) Phenyl azide potential mode of reaction

The photochemistry of aryl azides is quite rich and is illustrated by reactions of phenyl azide. The irradiation of the aryl azide **A1** with UV light with a wavelength of 280 nm, leads to the release of nitrogen (N₂) and a singlet nitrene **A2** is produced. This highly reactive intermediate has a short lifetime and quickly converts into other reactive intermediates.⁴¹ Intersystem crossing (ISC) can lead to a triplet nitrene **A3**.⁴² These two nitrenes have different modes of reaction; however the product is the same C-H insertion product **A4**. The singlet nitrene acts as an electrophile and undergoes a direct insertion reaction with C-H bonds, while the triplet nitrene behaves as a diradical which can abstract a hydrogen radical from the adjacent C-H then bind with the resultant

carbon radical **A9**. Singlet nitrenes can also rapidly rearrange into the appropriate benzazirine **A5** and dehydroazepine **A7**, which can react with the adjacent nucleophile producing **A6** and **A8** correspondingly. Finally the highly reactive nitrene is also susceptible to aerobic oxidation from the triplet state to form the nitro compound **A10** (Figure 9).⁴³

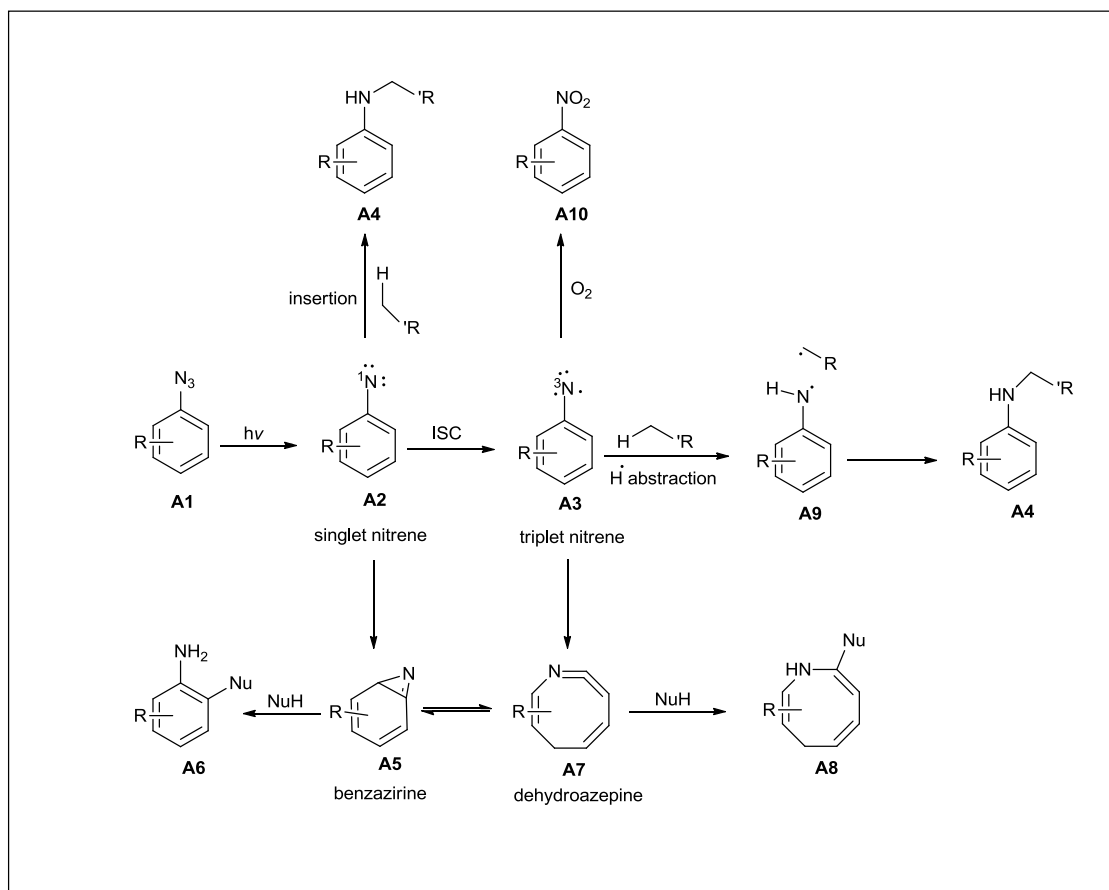


Figure 9 Possible reaction modes of the reactive intermediates formed upon irradiation of aryl azides

In addition, a non-specific labelling generated from rearrangements of short lived phenylnitrenes result in undesirable ketenimines.⁴⁴

The preparation of aryl azides is relatively simple and aryl azides can be obtained from the corresponding amines in one or two synthetic steps. The most common route is the

diazotization of the amine with subsequent addition of sodium azide.⁴⁵ A superior preparatory method utilises triflyl azide (TfN₃), to derivative the amine directly in one step reaction with high yield.⁴⁶ Recently, a more stable reagent imidazole-1-sulfonyl azide has been developed, which gave a good conversion under mild conditions (Figure 10).⁴⁷

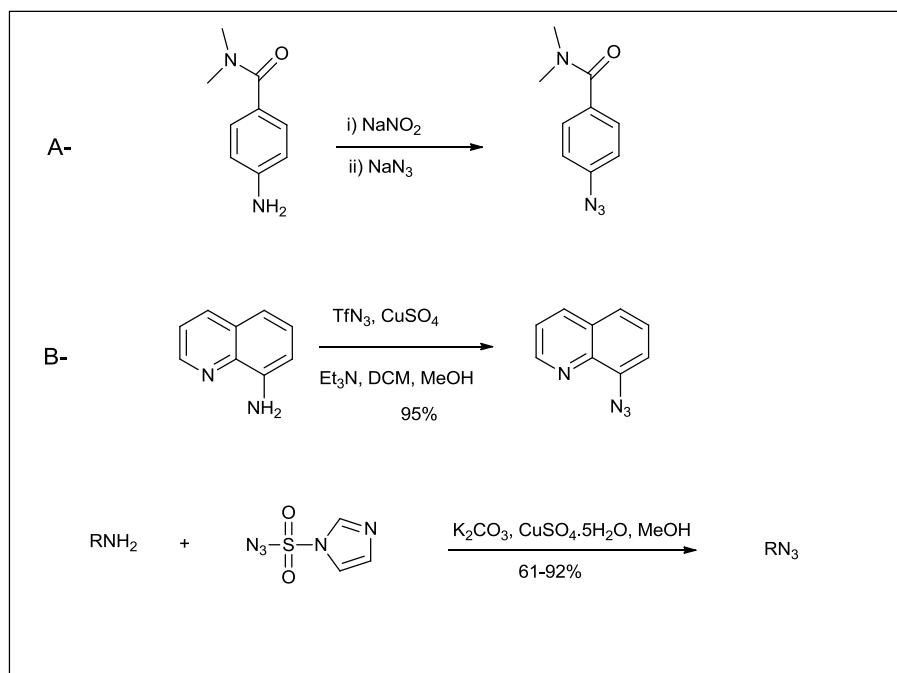


Figure 10 *Some methods of azides preparation*

ii) Diazirine possible modes of reaction

Diazirines are increasingly finding utility as carbene precursors for biological tagging.⁴⁸ When alkyl or aryl diazirines are exposed to UV light of 360 nm, molecular nitrogen is released with formation of a singlet carbene **D2**, along with about 30% rearrangement to form the diazo-isomer **D3**. This diazo compound may then be slowly converted into the singlet carbene at the wavelengths normally used for irradiation. The diazo compound is fairly long-lived and potentially has time to diffuse and undergo both labelling or hydrolysis reactions. The rearrangement process can be suppressed by the introduction of CF₃ group α to the diazirine and 3-aryl-3-(trifluoromethyl)-3H-diazirine **D1** was

developed by Brunner and co-workers as a photoaffinity labelling substrates.⁴⁹ Singlet carbene **D2** is considerably short-lived ($t_{1/2} \sim 1$ ns) and can convert to a triplet state **D10** by intersystem crossing (ISC). Singlet and triplet carbenes show similar reactions compared to the analogous nitrenes. A singlet carbene can behave as an electrophile, nucleophile or ambiphile, depending on the nature of its substituents, while triplet carbenes react as diradicals. The produced singlet carbenes can quickly give insertion reactions; with insertion into hydroxyl groups **D4** usually giving a higher yield than for C-H insertions **D5**.⁵⁰ Insertion into N-H amine bond can lead to produce intermediate **D6**, which can give undesired by-products. N-H insertion products can easily lose HF, forming enamine **D7**, which can be hydrolysed in presence of water to the corresponding ketone **D9**. As a result, the covalently bonded biomolecule target may be lost.⁵⁰ The triplet carbene behaves in a similar fashion to the triplet nitrene with the C-H bond, firstly abstracting the hydrogen to form the radical **D11**, which combines with the produced radical to give the same net product as in the singlet carbene insertion **D5**. Alternatively, a second H-abstraction may occur to give reduced the intermediate to **D12**. Undesired oxidation reaction may also occur from the triplet carbene intermediate in presence of oxygen, affording the corresponding ketone **D13** (Figure 11).⁵¹

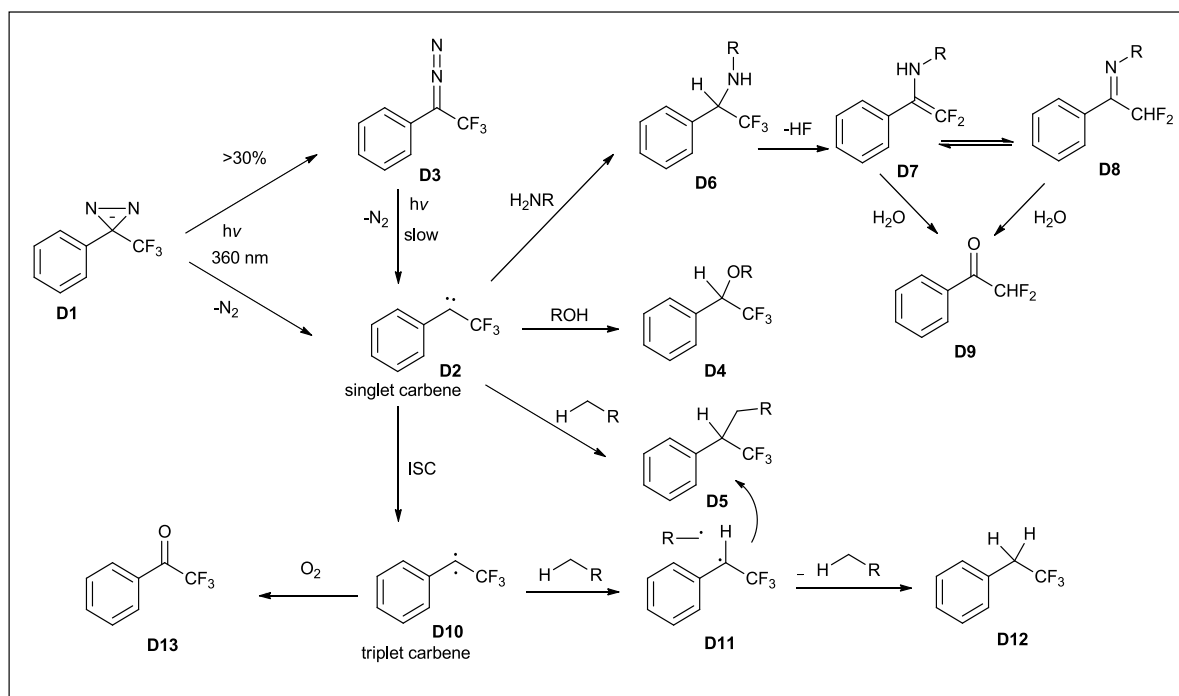


Figure 11 *Intermediates and reactions in diazirine photolysis.*

iii) Benzophenone possible mechanism of action

In contrast to the diazirine and nitrene, benzophenone does not react irreversibly to form a reactive intermediate. The benzophenone **B1** upon irradiation with the UV light at ≈ 350 nm forms a benzhydryl diradical **B2**. This is a reversible excitation and the compound reverts to a stable ground state in the absence of a suitable reaction partner. In the presence of a suitable hydrogen atom source, abstraction of hydrogen occurs to create the active species and the rate of this step is dependent on the nature of X-H bond.⁵² Generally, C-H bond cleavage is preferred to O-H bond cleavage, especially when hydrogen abstraction creates a stable carbon radical, for example, at the α -positions in α -amino acids, at benzylic or tertiary carbon centres and adjacent to heteroatoms. As a result of reaction of the benzhydryl diradical **B2** with an amino acid α -centre **B3**, a ketyl formula **B4** and alkyl radical **B5** are produced, which after a fast recombination create a benzhydryl **B6**. The major benefits of using the benzophenone

group are: it is more reactive toward C-H bonds than nitrenes and less prone to intermolecular rearrangements than the carbene. Moreover, when the diradical interacts with water it forms a hydrate **B7**, which can then dehydrate to reform the ketone. One unproductive side reaction is the homodimerization of ketyl **B4** to give benzopinacol **B8** however, because of the difference in reaction rates of hydrogen abstraction and recombination, only a small amount of this by-product is generally formed (Figure 12).

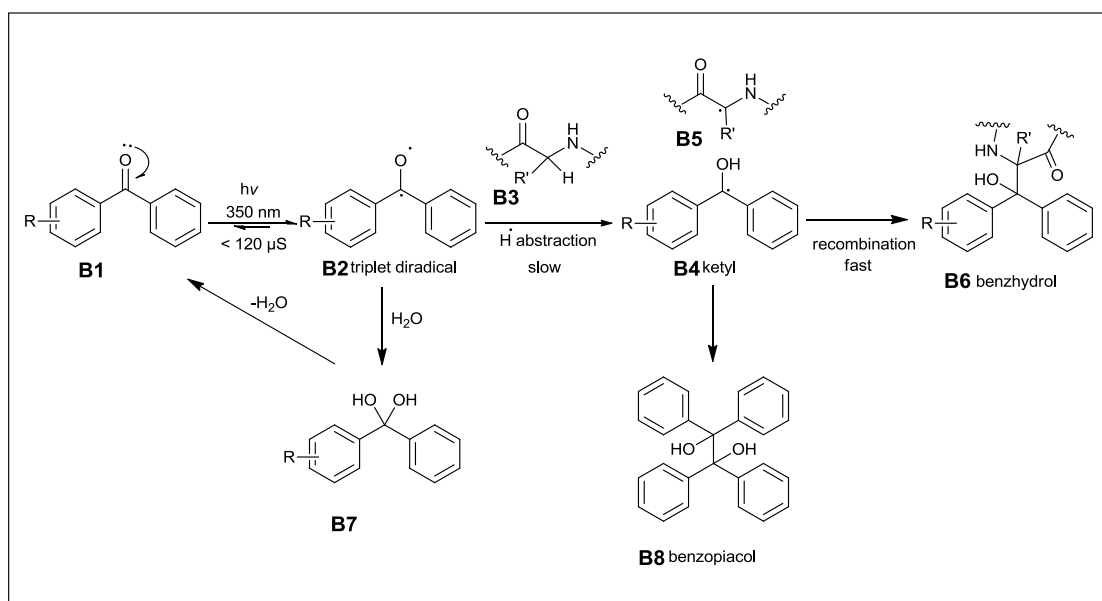


Figure 12 *Benzophenone irradiation mechanisms*

1.3.2.2 The use of tags in photoaffinity labelling experiments

To be effective, photochemical labelling requires the attachment of some other function to allow tracking or identification of the targeted proteins. Tags historically used are radioactive isotopes, or biotin. Recently, many biochemical studies have used fluorescent tags to detect ligand-receptor complexes and facilitate isolation. Whatever method is used, tagging strategy is fundamentally important for the observation of the new protein targets.⁵³ The interaction of receptors and ligands can be also identified when the photoaffinity labelling is combined with mass spectrometry (MS). In such an

experiment the tagged protein is identified by a characteristic change in mass of the protein, and detection by mass spectrometry.³⁴

i) Biotin Tags

Purification and identification of probe-bound proteins is the key step for the use of chemical probes to proteomics. The most popular widely utilized affinity tag in ABPs is biotin which has a particular strong non-covalent affinity for avidin and streptavidin proteins.⁴⁰ By using this intervention, proteins can be purified and/or immobilized by efficiently using affinity tags of streptavidin/avidin interaction and can be used in a wide variety of biotechnological and biochemical applications (Figure 13).

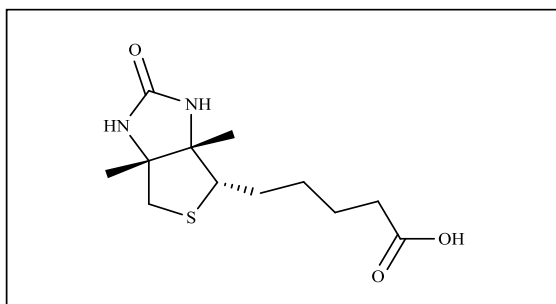


Figure 13 Streptavidin protein and biotin tag complex molecule

Biotin is a vitamin exists mostly in all cells, whereas avidin is a protein extracted from chicken egg white. Streptavidin is a bacterial protein similar to avidin, isolated from *Streptomyces avidinii*, and is more commonly used than avidin. Biotin is an effective handle which can be bound to immobilliable streptavidin or avidin allowing purification of the probe labelled enzyme and isolation of the targeted protein. Biotin- streptavidin binding is very fast and stable under various conditions of pH and temperature.^{54, 55} The biotin-streptavidin interaction bond is one of the strongest known non-covalent interactions ($K_d = 10^{-15}M$)⁵⁶ allowing for quantitative binding of low abundance biotinylated enzymes.⁵⁷ The mechanics of such an assay is that streptavidin is fitted to a

solid surface, like a magnetic bead, or biosensor chip, and biotin is linked to molecules of interest, for example a protein, nucleic acid or antibody (Figure 14).

Although derived tags are useful in protein isolations, its use is hampered *in vivo* applications since incorporation of this moiety confers poor cell permeability on the biomolecule probes. This disadvantage limits its uses as an affinity tag in ABP applications and therefore biotin was mainly utilised *in vitro* applications for target isolation.⁴⁰

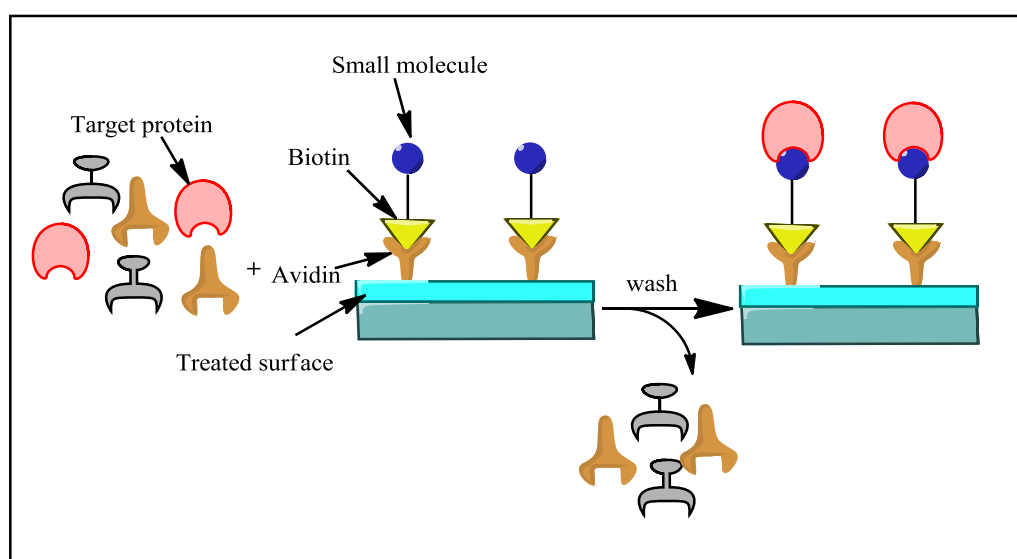


Figure 14 Biotin-avidin interactions for protein target identification

The strong binding interaction of biotin with streptavidin has further disadvantages as it cannot be easily removed from streptavidin resins without using harsh conditions, for example by treatment with formamide and using high temperatures, which may lead to denaturing target proteins and streptavidin molecules.⁵⁵ For this reason, probe design has recently focussed on the inclusion of cleavable linkers between the reactive group and the biotin tag that allow mild and selective elution of the probe-bound proteins from the solid support. A photocleavable linker has been reported for use with isotope-coded affinity tagging (ICAT) probes (Figure 15) and other types of cleavable linkers are under development.⁵⁸

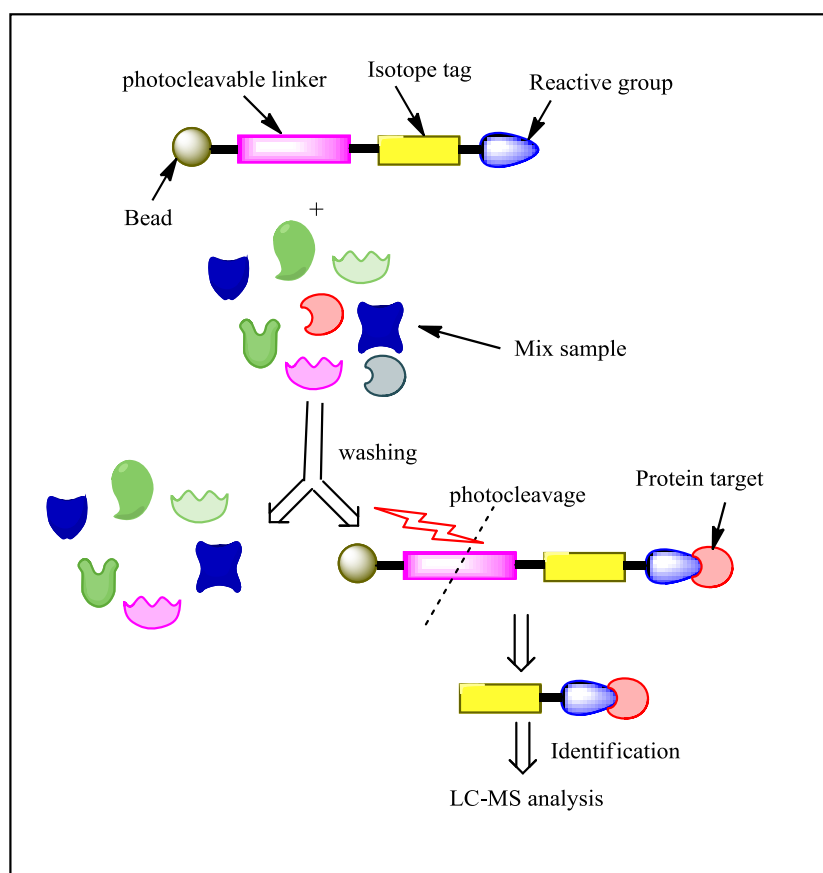


Figure 15 *Photocleavable linker for (ICAT) probes*

ii) Fluorescent Tags.

Fluorescence is a phenomenon where a fluorophore or fluorescent dye (generally polyaromatic hydrocarbons or heterocycles) absorbs a light at a specific wavelength which then leads to emission of visible light at a lower wavelength. The absorbance of the light by such molecule or atom leads to promotion of electrons in the valance orbitals, generally at a specific wavelength of UV light. The fluorescence then occurs via a three-stage route within such fluorescent molecules, outlined in the Jablonski electronic-state diagram shown in (Figure 16).

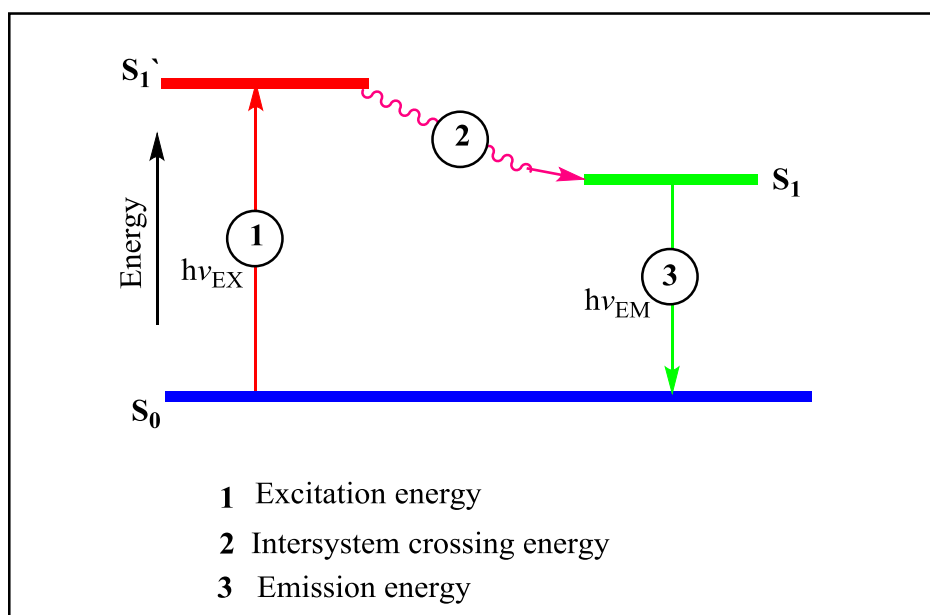


Figure 16 *Jablonski electronic-state diagram for simple fluorescence*

Excitation state

A photon of energy $h\nu_{\text{EX}}$ is supplied by a UV light source absorbed by the fluorescence dye, generating an excited singlet state (S_1'). This process differentiates fluorescence from chemiluminescence, wherein the excited state is occurred by a chemical reaction.

Excited-State Lifetime

The excited state continues for a limited time (normally 1–10 nanoseconds). In this time, conformational changes of fluorophore may occur and fluorophores are also subject to many interactions with the molecular environment. Once excitation occurs, the energy of S_1' is degraded via intersystem crossing, leading to a relaxed singlet excited state (S_1), which initiates fluorescence emission.

Fluorescence Emission

The emission occurs when the photon energy $h\nu_{\text{EM}}$ is emitted and the fluorescent molecule returns to the ground state S_0 . The emission is lower than the excitation

energy, because part of the energy is lost during the excited state lifetime; the emission wavelength is longer than in the excitation wavelength $h\nu_{EX}$. This difference in the energy is called the Stokes shift. The Stokes shift is essential to the fluorescence performance, since it allows emission photons to be sensed with a low background isolated from excitation photons.

In the fluorescence process, not all molecules excited by the absorption return back to the ground state (S_0) by fluorescence emission. The quantum yield of the fluorescence is the ratio of the number of photons emitted compared to the number of photons absorbed, and is a measure of the efficiency of the fluorescence process.⁵⁹ Both the Stokes shift and quantum yield are important factors in choosing effective fluorescent tags.

In the life sciences, fluorescence is generally used as a safe way of tracking and analysing biological molecules via fluorescent emission at a specific wavelength.⁶⁰ The fluorescence can be affected by the background emission from the excitation light, as relatively few cellular components are naturally fluorescent. The fluorescence has become one of the most useful methods in the field of the biological molecule purification and detection processes, this is because of many reasons. First is the variation of the wavelength can be used in the fluorescence detection of the biomolecules, allowing the application of such fluorophores in different environments, since some biomolecules fluoresce under a certain wavelengths of light. Second because of the efficient quantum yield, fluorescence can be applied with the very low abundances of biomolecules. Finally the availability and the ease of laboratory preparation give more advantages of using the fluorescent labelling than the other dyes. Fluorophores need not only be small molecules and the development of fluorescent proteins (FPs) has revolutionised biomolecular tagging. Initial efforts in protein fluorescent labelling *in vivo* was performed after the genetic sequences of green

fluorescent proteins (GFPs) from the jellyfish *Aequorea victoria*. GFP was firstly used for labelling proteins of interest in 1994.⁶¹ Later after Osamu Shimomura, Martin Chalfie and Roger Y. Tsien won The Noble Prize in chemistry in 2008 for discovering and developing GFP. This protein has become well recognized as an indicator of gene expression and to target protein in cells and organisms. However, the size and the narrow range of the fluorescent spectra of GFPs may limit their application. As a result there are necessities to find alternative smaller fluorophores with wide range of different properties and emitted wavelength spectra.

Synthetic chemistry has introduced fluorescent probes of small molecular size with improved photochemical properties, which can offer variety of colours. The small fluorescent molecules are widely used in many biological applications and each of these molecules has advantages and disadvantages (Table 1).

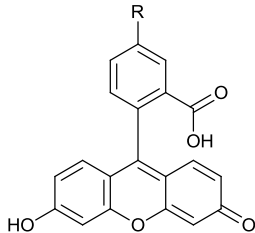
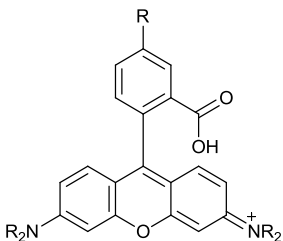
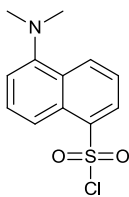
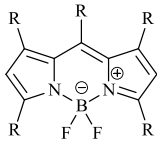
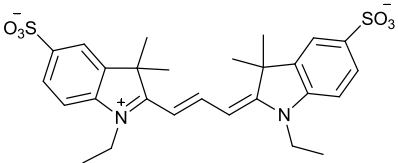
The fluorophore	Advantages	Disadvantages
Fluorescein 	Relative high absorptivity; excellent quantum yield; high water solubility; inexpensive; stable to solid-phase peptide synthesis method	Fast photobleaching; pH sensitive below 7; Relative broad emission; self- quenching; lack of cell permeability.
Rhodamine 	Readily excited, more photostable than fluorescein.	Low quantum yield (1/4 of fluorescein); complex absorption complex; lack of cell permeability.
Dansyl sulphonamide 	Fluorescent as dansyl amide and not chloride; large stokes shifts; inexpensive	Environmental- dependent quantum yields and emission maxima.
BODIPY 	High extinction coefficients; excellent photostability; high fluorescence quantum yields; narrow emission bandwidth; good photostability; pH insensitive; no ionic charge; non-polar; minimal effect on electrophoresis mobility; cell permeable.	More expensive than rhodamine and fluorescein, shows unstability under the majority of solid phase synthesis, lack of rapid photobleaching
Cyanine 	pH insensitive (3–10); DMSO tolerance; good aqueous solubility; superior photostability; stable to standard peptide synthesis	Expensive

Table 1 *The advantages and disadvantages of the most common fluorophores*

In many biological and biochemical investigations, tagging proteins with an effective small molecule fluorophores can lead to *in vivo* and *in vitro* investigations of their functions and structures.⁶²

There are several problems that could negatively affect the generation of a good fluorescence. For instance, fluorophores can absorb photons, but sometimes does not result in high rate of excitement, this can lead to high brightness level within the fluorescence. This very bright light affects the visibility of fluorescence and cannot be clearly detected and the good fluorescence observation can be detected in the dark.⁶³

Generally, establishing a powerful fluorescent label requires maximising the number of emitted photons. This can be performed via a high absorption/quantum yield. On the other hand, the efficiency of photo-induced-chemical alteration must be also considered, because this can negatively cause production of non-fluorescent molecules.⁶⁴

The fluorophore performance and photostability can be affected by undesirable phenomenon that decreases both the quantum yield and the number of emitted photons. These affecting factors are underlined as photoblinking and photobleaching.

Photoblinking is a phenomenon described as reversible reduction or fading of the emitted light proceeding in an average time of microseconds to seconds, which is significantly longer than the emission from the singlet state (normally 1-10 ns). Photoblinking is also can be as result of the triplet state excitation,⁶⁵ and it can also cause a bad measurement of single molecule by affecting the process timescale. It may be difficult to discriminate the case of prolonged time photoblinking from permanent photobleaching.

Photobleaching occurs when a fluorophore molecule becomes unable to fluoresce, because of photon-induced chemical damage and covalent binding modification. During the transition from the excited singlet state to the excited triplet state,

irreversible covalent interaction may occur between the fluorescent molecule and another molecule in the environment. This interaction occurs because the triplet state is relatively longer than the singlet state, which allows the excited molecule to have sufficient time to undergo chemical modification. The main factors affecting the photobleaching of a fluorophore are the molecular structure and the nature of environment. Limiting these variable changes is crucial to improve the photostability. Photobleaching can be minimised by decreasing the lifetime of the fluorophore triplet state by limiting the exposure time or by lowering the excitation energy. Lowering the oxygen levels may also reduce photobleaching, if oxygen reacts with the excited fluorophore.⁶³

Overall, photoaffinity labelling (PAL) is a technique which employs a suitable linker of a fluorophore, photoreactive group and small bioactive molecule. This method has been used for identification of small molecule protein targets, using a variety of different photoactive and fluorescent groups, in order to achieve the optimum analysis environment.

An instructive example of the PAL method was described by Bringmann *et.al* (2007) who investigated the mode of action of antiplasmodial naphthylisoquinoline (NIQ) alkaloids. In this study an NIQ derivative was functionalized with benzophenone and dansyl amide moieties in order to identify the protein target for this antimalarial drug.⁶⁶ It was found that, the modified NIQ was slightly weaker than the original compound itself, however the functionalized alkaloid derivatives retained antiplasmodial activity and also microscopic studies evidenced that these molecules entered inside the cells, which is a promising model compound for applying PAL assays.

The benzophenone and dansylamide were introduced in this investigation as a photoaffinity and fluorescent moieties, respectively. In preliminary study, the dansyl functionalized derivatives with no photoaffinity functionality were also investigated showing that these molecules are good candidates for *in vitro* visualization of the alkaloids. Microscopic investigation showed that the fluorescent derivatives centred exclusively inside the infected cells (Figure 17).

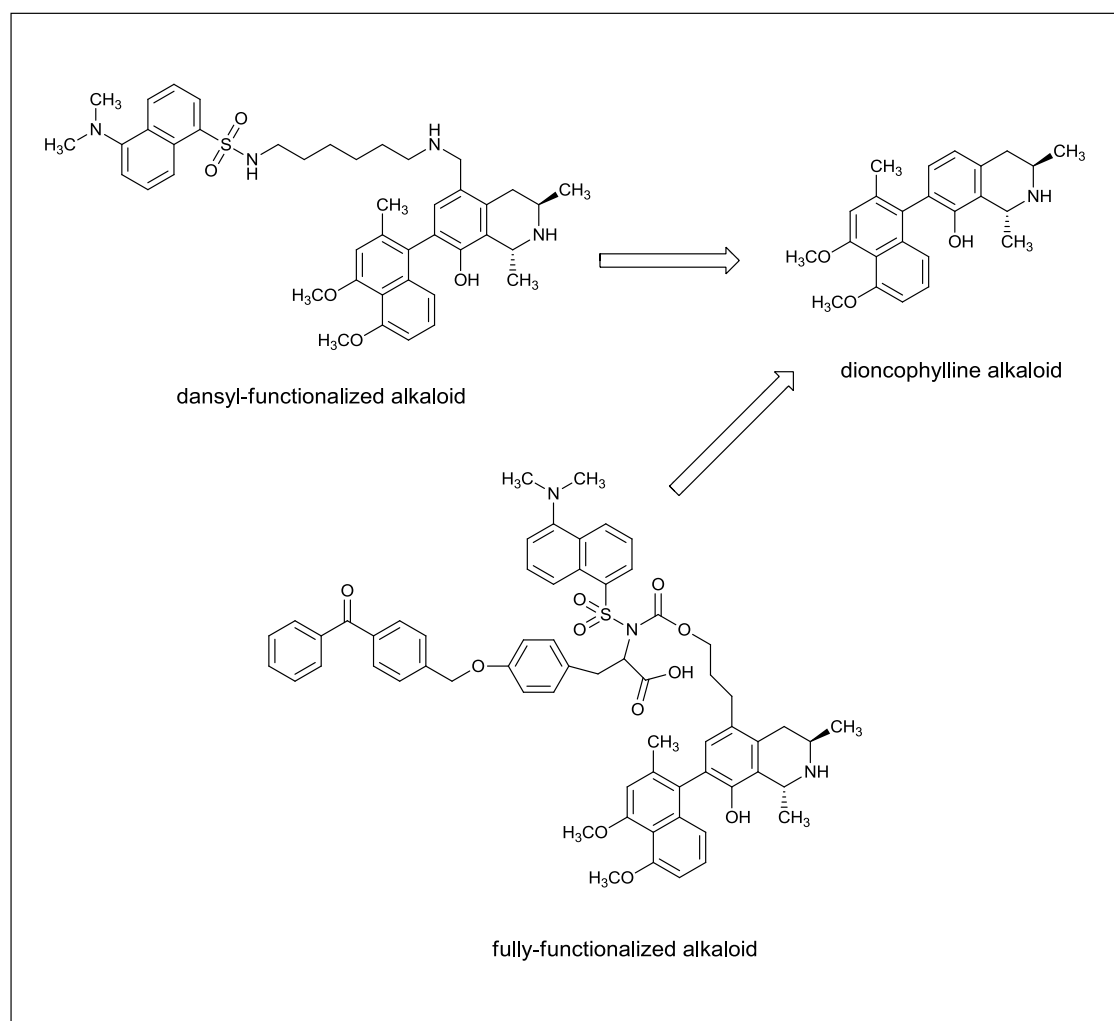


Figure 17 Dansylated and fully functionalized dioncophylline alkaloid

The general approach is illustrated by the following example. Partha *et.al* (2013) described a method of employing the tri-substituted benzenes as a tripodal template fluorescent photoaffinity probe for capturing human carbonic anhydrase.⁶⁷ In this

investigation, sulphonamide derivatives which are inhibitors for human carbonic anhydrase II (HCA II) were chosen to be a selectively function. An aryl azide was utilized as a photoaffinity molecule and a propargylated pyrene was employed as a fluorescent tag. These three molecules were joined together to build up two capture compounds. An investigation was carried out by incubation of these two molecules with a mixture of three deferent proteins, HCA II, bovine serum albumin (BSA) and lysozyme. The under UV- transillumination results showed that the only visible band corresponded to HCA II protein. A confirmation of this selectivity capture was also obtained from the MALDI mass spectrometric analysis, which provided evidence of the reliability of this method (Figure 18).

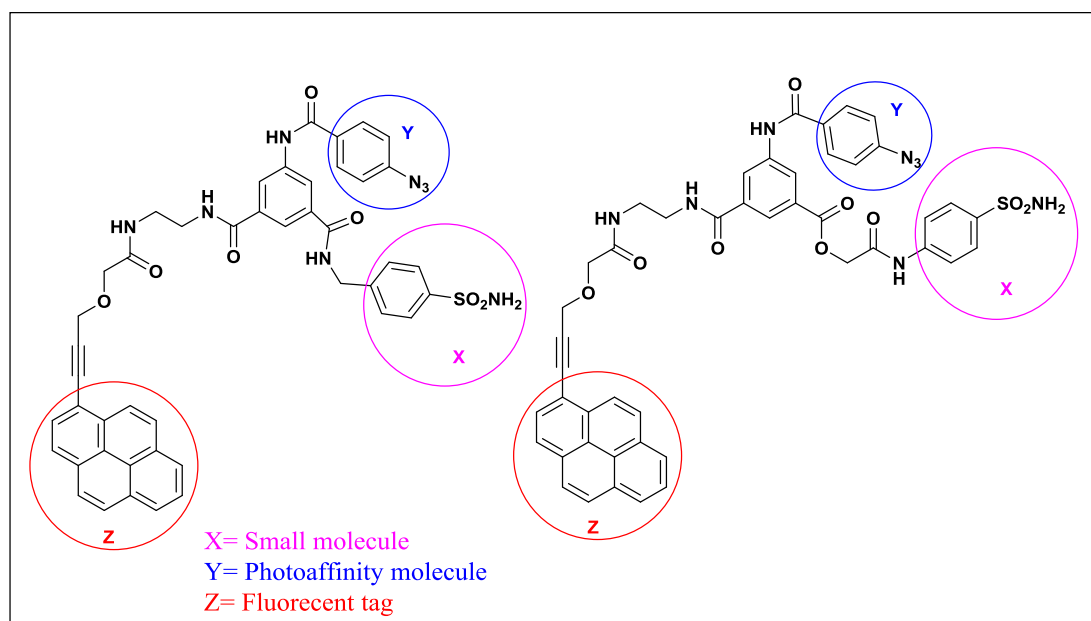


Figure 18 Photoaffinity capture compound for human carbonic anhydrase II inhibitors

1.3 The project plan

The project focused on the development of functional probes to identify protein targets of two classes of biologically active small molecules: (i) organophosphate neurotoxins and (ii) the putative targets of the cardioprotective drug diazoxide

The strategy is to design and prepare probes for the identification of biological molecules based on the non-covalent, specific binding, of the bait to a target protein. Upon exposure to light, the probes will activate and form covalent bonds and tag the target or proximal proteins. The isolation and identification of tagged proteins will be investigated by fluorescence monitoring, chromatography and mass spectrometry. However in the case of the organophosphate, the small molecule will be attached to a fluorescent tag via linker without using any photoaffinity molecules. This is because these molecules tend to bind covalently with the biomolecule targets and one of the aims is to prove the nature of binding (Figure 19).

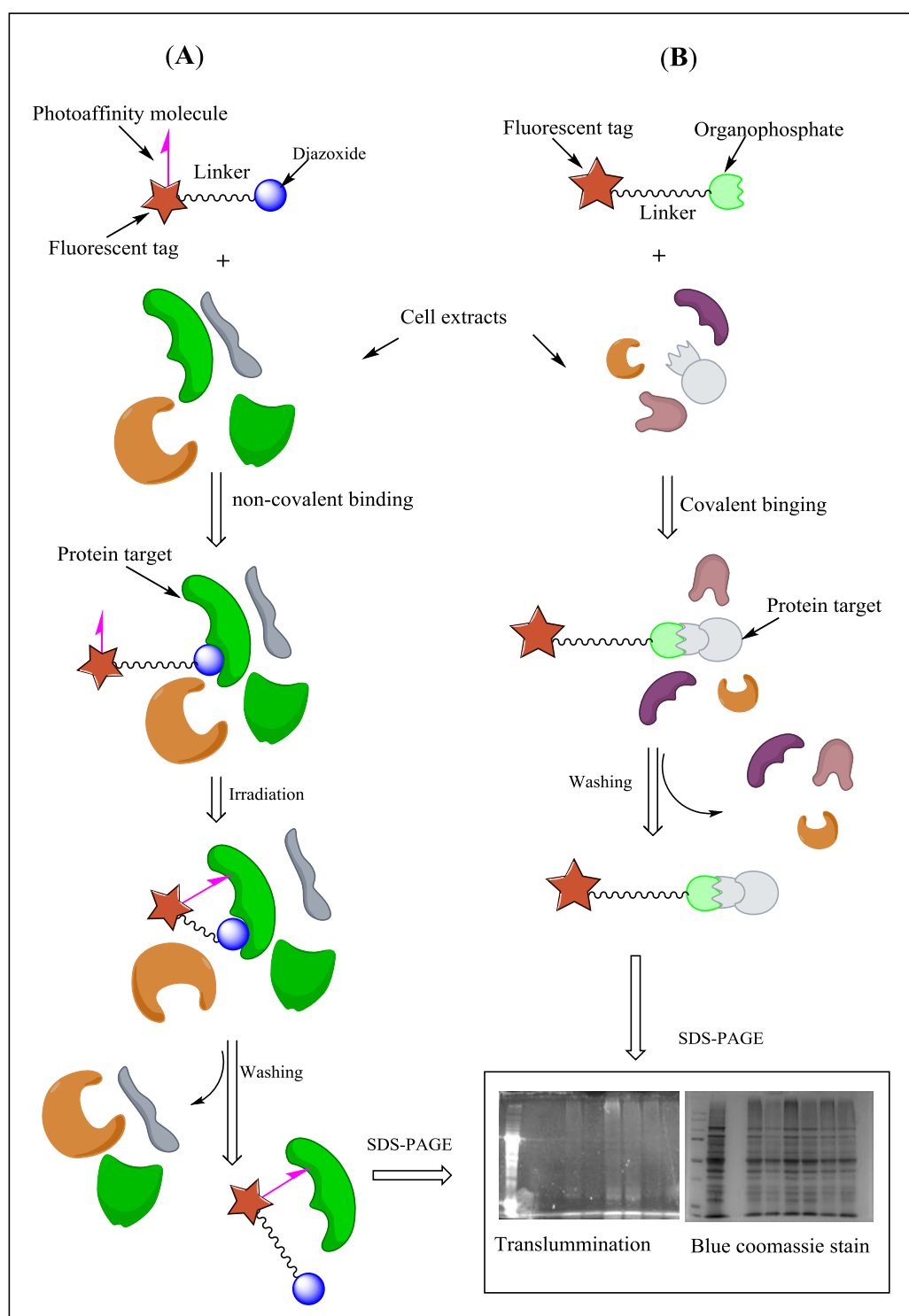


Figure 19 General strategy of the project

(A) Labelling with Photoreactive molecules; incubation followed by irradiation, washing then purification. (B) Labelling using covalent biological interactions; incubation is followed by washing then purification.

2. Chapter 2: Organophosphates

2.1 Introduction

Organophosphates are organic chemical substances that are generally produced by reacting alcohols with phosphoric acid. In the early 19th century, organophosphates were widely used as pesticides and insecticides in agriculture and as well as in wide range of chemical and industrial processes. The dangers to health posed by these species were also well known and these compounds were used as chemical weapons in World War II. The acute toxicity of these compounds is associated with the ability to inhibit the enzyme acetylcholinesterase, thereby affecting neuromuscular transmission. More recently public concern has increased regarding the frequent use of organophosphates as chemical agents, their acute toxicity and their damaging effects to the environment and human health in general.⁶⁸

Many anticholinesterase organophosphate products have been tried for therapeutic purposes. Physostigmine anticholinesterase was used to treat glaucoma in the 1870s and later after in the 1930s, synthetic cholinesterase inhibitors were being used for skeletal muscle and autonomic disorders. Some organophosphates were tried in the treatment of Parkinsonism, and they might also be useful for treating dementia

In 1986, testing began for tacrine, the first cholinesterase inhibitor to be tried for Alzheimer' disease; it was released for clinical use in 1993 and it is no longer in use. The blood-brain barrier has been the limiting factor in developing a cholinesterase inhibitor for use in dementia. Metrifonate has been used for schistosomiasis treatment and it was used for the treatment of primary degenerative dementia (Figure 20). Sung and others have reported on the ability of these substances to induce nicotinic receptor

modulation.⁶⁹ This explains the action of these drugs and may result in development of more effective agents.

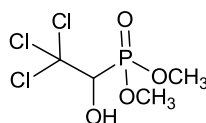


Figure 20 *Metrifonate, used for schistosomiasis treatment*

2.1.1 Acute toxicity mechanism of organophosphorus compounds

Following exposure, organophosphates are distributed widely around the body and eventually reach the nervous system. Organophosphates can be found in all parts of the nervous system, but the most serious symptoms appear due to the effect on the automatic involuntary nervous system in the parasympathetic part. The acute toxicity target of organophosphate compounds is known to be acetylcholinesterase (AChE) which normally provides the relaxation of the neurotransmitter acetylcholine (ACh).⁷⁰ Acetylcholine is one of several physiologically important neurotransmitter agents and is involved in the transmission of nerve signals. The rapid hydrolytic degradation of acetylcholine into the inactive products choline and acetic acid is performed by AChE.⁷¹ Organophosphates are non-competitive inhibitors of AChE and completely block the active site of the enzyme.⁷² These compounds are initially non-covalently and reversibly bound to the acetylcholinesterase enzyme followed by an irreversible phosphorylation of the serine oxygen atom in the active site, which causes deactivation of acetylcholinesterase enzyme in the synaptic cleft (Figure 21).⁷³ Ultimately, the increase of acetylcholine at the synapses of neuromuscular junctions can result in overstimulation of acetylcholine receptors. This causes a great influx of Na^+ into the neurons, inducing electrical signals that lead to extreme muscle contraction to the point of paralysis, secretions, and convulsions.⁷⁴

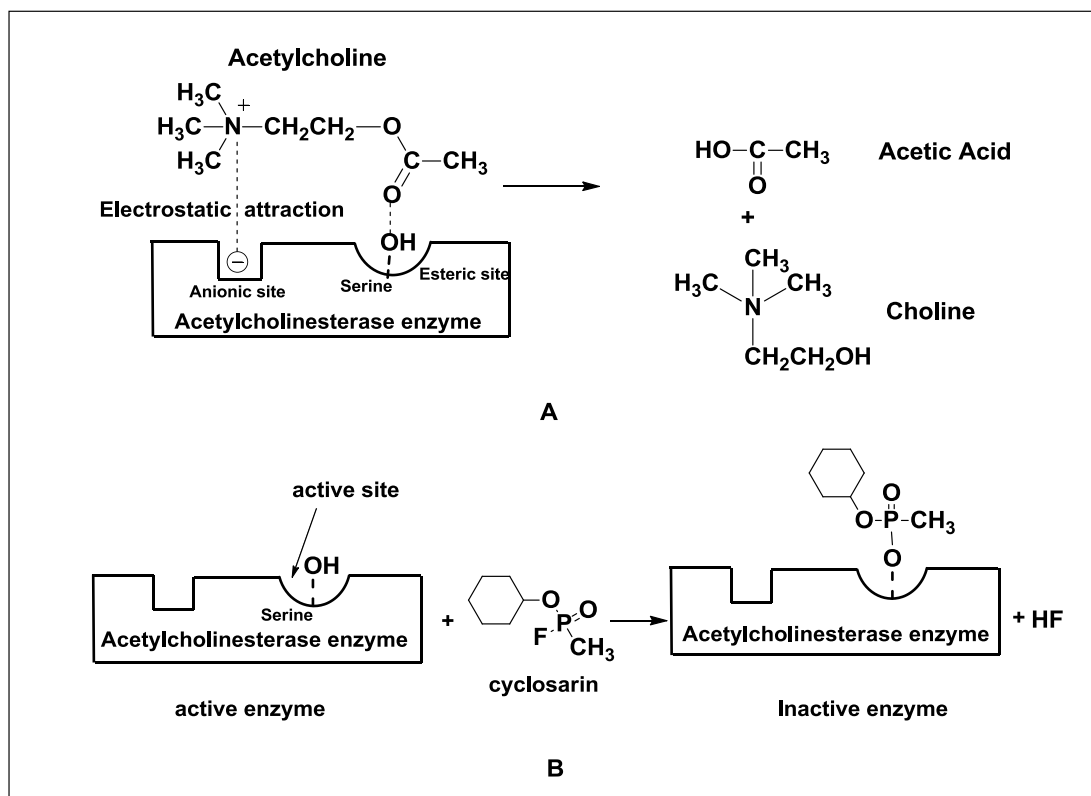


Figure 21 Inhibition of acetylcholinesterase by organophosphate; **A.** ACh hydrolysis AChE, **B.** De-activation of AChE

2.1.2 Other organophosphate targets

Many studies have demonstrated that, *in vitro*, organophosphates can interfere with many proteins, and bind to the tyrosine residues in for example transferrin, serum albumin and tubulin. Toxins which have been shown to bind to targets other than AChE are; FP-biotin, chlorpyrifos-oxon, diisopropylfluorophosphate, dichlorvos, soman, and sarin (Figure 22).^{75, 76} In addition, there is a possibility that other more reactive and low abundance proteins could react with organophosphates causing toxicity at low doses and toxic effects may also arise by mechanisms different to the inhibition of AChE.

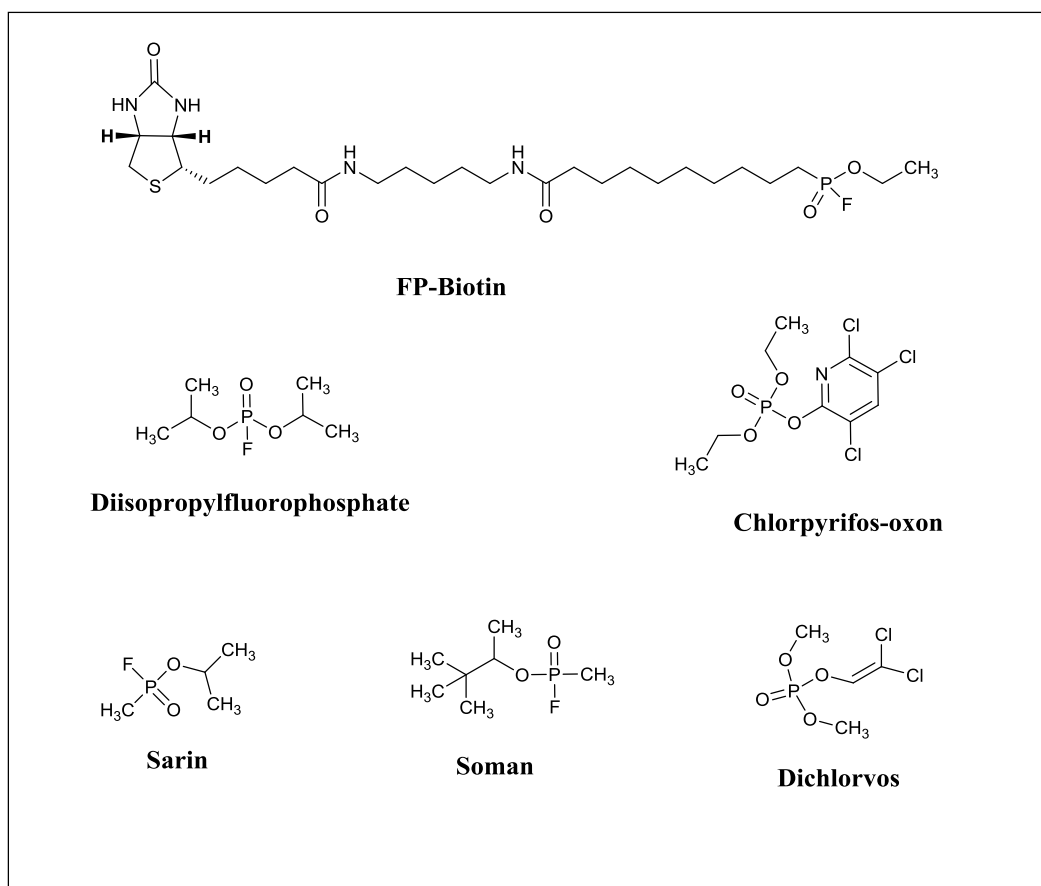


Figure 22 *Toxins bind to targets other than acetylcholinesterase*

Although exposure to low levels of organophosphates does not cause noticeable inhibition of AChE, however other neurological deficits may be caused. For example, Parkinson's disease, neurologic dysfunction and Gulf War Illness have been linked to prolonged low levels of organophosphate exposure.^{77,78}

Bronchoconstriction is a condition involving a narrowing of the airways in the lungs, which may result from low levels of exposure to organophosphorus pesticides. It is thought that some organophosphates can inhibit the function of muscarinic ACh receptors, which would facilitate transmission of an extracellular signal induced by free acetylcholine to neuronal or effector cells as opposed to inhibiting acetylcholinesterase activity.⁷⁹ These receptor proteins recognise ACh but do not belong to the serine

hydrolase family. However, the binding of a low concentration of organophosphate affects function.

More generally, signalling mechanisms in cells depend on the phosphorylation reaction of the intracellular macromolecules,⁸⁰ and it has been suggested that irreversible binding of organophosphate to a site which is normally reversibly phosphorylated can cause cellular dysfunction. The development of an understanding of the relationship between disease and low dose OP exposure will be greatly enhanced by the identification protein targets susceptible to organophosphate interference.

2.1.3 Organophosphate-induced delayed neuropathy (OPIDN)

In addition to the chronic toxic effects, acute poisoning by organophosphate compounds generally cause significant injuries to both the central and peripheral nervous systems, as well as leading to a significant effect on the spinal cord in particular. After exposure to a variety of organophosphates, an inhibition of the enzyme neuropathy target esterase (NTE) has been clearly detected in several animals. This enzyme is a phospholipase which deacylates intracellular phosphatidylcholine and hydrolyses fatty acids to generate water-soluble glycerophosphocholine.⁸¹ When this enzyme is inhibited, abnormally elevated levels of phosphatidylcholine can occur in the brain, leading to deficiency of the constitutive secretory pathway in neurons.⁸² Many studies have established that inhibition of the NTE target causes a condition called (OPIDN).⁸³ In addition, irreversible inhibition of NTE can cause a chronic cholinergic crisis associated with significant development of OPIDN after massive exposure to organophosphates.⁸⁴

While rare, OPIDN is a condition which can occur in some other mammalian species subsequent to extensive exposure to organophosphate neurotoxins. It has been stated that a number of avian and mammalian species exhibit elevated sensitivity to organophosphates.⁸⁵ Moreover, neurodegenerative forms of OPIDN has been also

observed in animals and humans, and the precise damaging impact of OPIDN in neuropathological alteration of those systems remains to be clearly diagnosed.^{86, 87}

Several organophosphates are known to cause OPIDN in sensitive mammals. These include phenyl saligenin phosphate PSP, tri-ortho-cresyl phosphate TOCP,⁸⁸ and saligenin cyclic ortho-tolylphosphate SCOTP (Figure 23).

All these compounds are pentavalent, tetra-coordinate molecules containing an oxygen atom and three substituent groups or atoms via single bonds. Each had a phenol group bonded to phosphorus by a relatively weak single P-O, which can be displaced during reaction with nucleophilic residues and allow the organophosphate to covalently attach to protein target. In the course of the phosphorylation reaction, the organophosphate compound is destroyed in a stoichiometric reaction with the enzyme. The caused inhibition is persistent, but is potentially chemically reversible. The treatment for acute organophosphate poisoning focused on the use of non-enzymatic reagents for de-phosphorylation and the consequent restoration of activity.⁸⁹

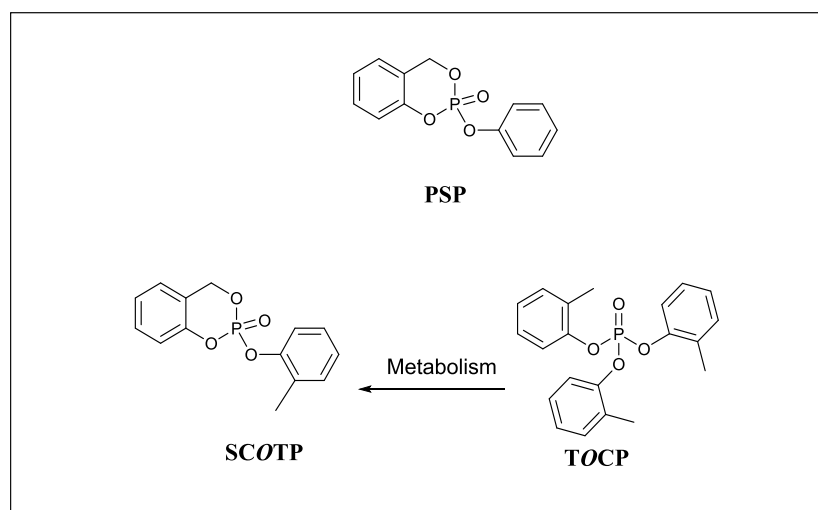


Figure 23 *Organophosphates known to induce OPIDN*

Phenyl saligenin phosphate PSP is an organophosphate neurotoxin and acetylcholinesterase was identified as a primary toxicity target. In addition, SCOTP was discovered to be a highly active metabolite of the neurotoxins, TOCP, and neurotoxin TOCP can be actively converted to SCOTP *in vivo*. Several studies have also explored the possibility that this analogue of PSP is a more potent cause of OPIDN than the parent compound itself.⁹⁰

2.1.4 The effect of phenyl saligenin phosphate (PSP) on the phosphorylation of neurofilament heavy chain (NFH) and MAP kinase activation (ERK1/2)

A number of studies have suggested that PSP is a phosphorylation promoter for many protein networks.⁹¹ For instance, a significant rise of the phosphorylation state was demonstrated for microtubule associated protein-2 (MAP-2) following exposure of the cultured neurons to PSP, whereas transient changes have been observed in the neurofilament heavy chain NFH phosphorylation after exposure of cultured neurons to this neurotoxin.^{87, 92} The NF protein subunits can be found in neurons and are considered to be essential protein classes for the regulation of axonal diameter,⁹³ while MAPs function as stabilising agents of microtubules and the interaction with different classes of protein subunits can be regulated by MAPs. The hyperphosphorylation of these proteins can eventually affect their function and lead to failure in axonal transport, which can be also clearly observed in OPIDN after extensive exposure to PSP. The obvious changes of phosphorylation in these proteins have not been well identified. However, some recent investigations have proposed that PSP might induce influx of calcium outside cells and consequent activation of the dependent enzymes which mediate the mechanism of OPIDN,⁹⁴ and phosphorylation of several proteins such as protein kinase.⁶⁸ For example, calcium calmodulin-dependent protein kinases have been implicated in (MAP-2) and NF protein phosphorylation.⁹⁵ Additionally, it was

demonstrated that calcium plays an essential role in the degeneration of axons in OPIDN after exposure to those neurotoxins.^{68, 91}

Due to its ability to phosphorylate the cytoskeletal protein networks, PSP is also an efficient neurotoxin capable of generating pharmacological and histopathological effects which are common in OPIDN.⁶⁸

2.1.5 The effect of phenyl saligenin phosphate PSP on serine/threonine phosphorylation

PSP was also demonstrated to have an effect on serine/threonine phosphorylation in experimental work using several mammalian species with high sensitivity to OPIDN such as pigs. Flaskos *et al.*, 2006 showed that PSP can induce a rise in serine phosphorylation in the presence of calcium; thus, in addition to affecting the calcium balance it may also modulate calcium dependent enzymes.⁶⁸ Most of this increased phosphorylation of serine residues occurred in tubulin with little effect on threonine phosphorylation. The increase of protein phosphorylation by PSP can be also compared with TOCP which also induced an increase in phosphorylation of α - and β -tubulin, microtubule associated protein-2 (MAP-2) and neurofilament (NF) in hen brain cytosol.⁸⁶

2.1.6 The effect of phenyl saligenin phosphate PSP on the neurite outgrowth and the activity of NTE

Hargreaves and co-workers investigated the effect of PSP on neurite outgrowth, finding it to be a selective inhibitor of the production of axon-like processes by differentiating N2a cells with no effect on outgrowth of smaller processes or cell body shape.⁸⁷ PSP is similar to the neuropathic metabolites of TOCP,⁹⁶ this was confirmed by another study that the *in vitro* inhibition of TOCP was improved by metabolic processing with

NADPH in rat liver.⁹⁷ Furthermore, it was found that the neurite outgrowth was also affected by the neuropathic influence of PSP neurotoxin and *in vitro* cellular models caused complete inhibition of neurite outgrowth.⁹⁸

NTE was the first identified target of OPIDN, and was also found to be a target of PSP, causing an inhibition upon the exposure of mouse N2a neuronal cell line.⁹⁹ It has been proposed that NTE may be able to hydrolyse lipids or perform as an ion channel,^{100, 101} and the disruption of these functions is involved in the response to organophosphates exposure.

2.1.7 The effect of phenyl saligenin phosphate on transglutaminase activity

As was previously mentioned, PSP is able to disrupt neurite outgrowth, and the inhibition of neurite outgrowth level could be the result of transglutaminase enzyme (TGase) inhibition, which is known to be important for the proper function of cytoskeletal proteins.¹⁰² These studies indicated that calcium-activated TGase enzyme is also inhibited by the effect of PSP neurotoxin. The disruption of calcium homeostasis, which was proposed to be one of the early events of OPIDN, is possibly responsible for the calcium-dependent activation of enzymes and its disruption might cause an unusual level of TGase activity.¹⁰³ TGase up-regulation could be further involved in a variety of neurodegenerative disorders including Huntington's and also Alzheimer's diseases.¹⁰⁴

TGase is implicated in the regulation of various physiological activities, which involves the cross linking of different protein subunits.¹⁰⁵ According to Harris *et al.* (2009), the protein level of TGase was reduced by sub-lethal and high doses of PSP neurotoxin as investigated *in vitro* using cell lines such as mouse N2a and human hepG2 hepatoma (HepG2) treated with different concentrations of PSP. This can be compared with low concentration of PSP that showed only little or no effect on TGase inhibition. Thus, it is

a great of interest to determine whether the disruption of neurite outgrowth by PSP is generally due to the fact that PSP has the ability to modulate TGase activity.

Taken together with the ability of organophosphates to cause transient changes in the phosphorylation of NFH in correlation with reduction of neurite outgrowth, it is likely that these agents affect not only their acute toxicity target AChE, but also other different and multiple protein targets.¹⁰⁶

2.1.8 Aim of investigation

The mode of action of organophosphate neurotoxins is more complex than originally thought, with increasing evidence for the existence of novel protein targets in addition to the acute toxicity target AChE, and the identification of proteins targeted by these toxins is central to understanding the processes involved.^{107, 108} Based on the proposed mode of toxicity, many organophosphates can react covalently with proteins and other biomolecules.¹⁰⁹ This is the reason why not to employ any affinity molecules with these molecules to build up the tool and also to investigate and prove the nature of binding, which is one of the priority goals of this study.

This work seeks to construct a probe for the fluorescent tagging of biomolecules which bind and react with the organophosphate neurotoxin PSP, by mode of covalent interaction. The design is that the organophosphate neurotoxins incorporating a linker and fluorescent tag will be prepared, and then biological activity assays of these modified toxins will be verified in in order to assess the toxicity. The active analogue will then be used for the identification of the parent toxin targets. It is envisaged that incubation of the functional probes with neuronal cell extracts followed by fluorescence directed chromatography will allow the isolation of the targeted proteins (Figure 24).

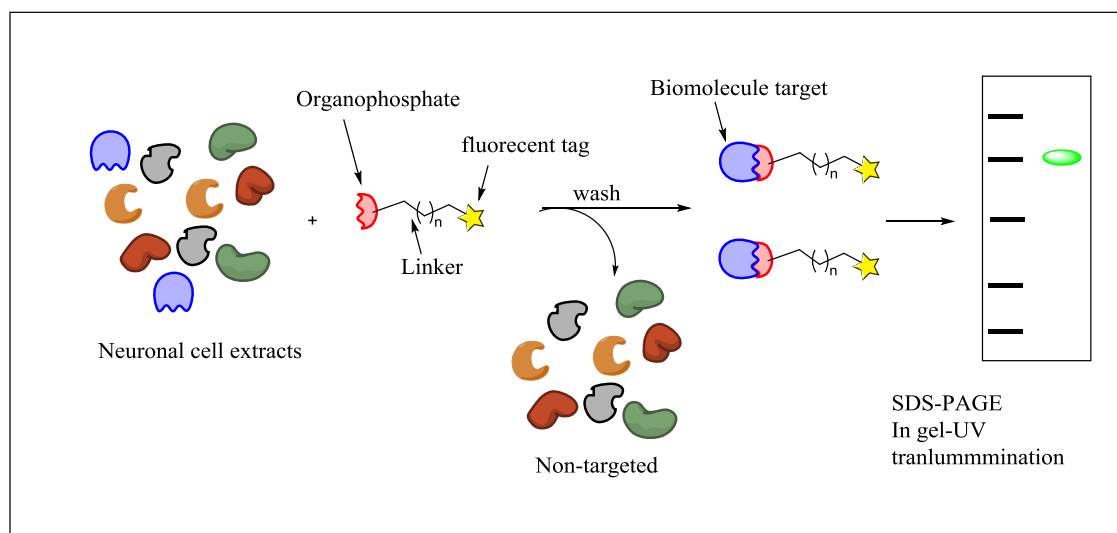


Figure 24 *Strategy of organophosphate protein targeting*

2.2 Results and Discussion

The aim of this work was to link the PSP to a fluorescent tag to explore which protein this toxin binds to. Phenyl saligenin phosphate is of interest because many studies have suggested that toxicity is caused by interaction with multiple biomolecules, as discussed above. The chemical hydrolysis of saligenin organophosphate has been studied, and the results were dependent on the nature of the attached R groups in the $\text{O}=\text{P}-(\text{OR})_3$ molecule.^{110, 111} When R is a phenyl group as in the case of PSP, there are three possible hydrolysis products, as shown in Figure 25 A. Because the phenoxy is a good leaving group, a fluorescent tag linked to the aromatic phenyl ring may be subjected to cleavage from the PSP upon the phosphorylation of the biomolecules. However, using an alkoxy linker for fluorescent tag attachment gives more stability, and the fluorescent component should not be cleaved, as described in Figure 25 B, since the alkoxy group is a much poorer leaving group than the phenoxy.

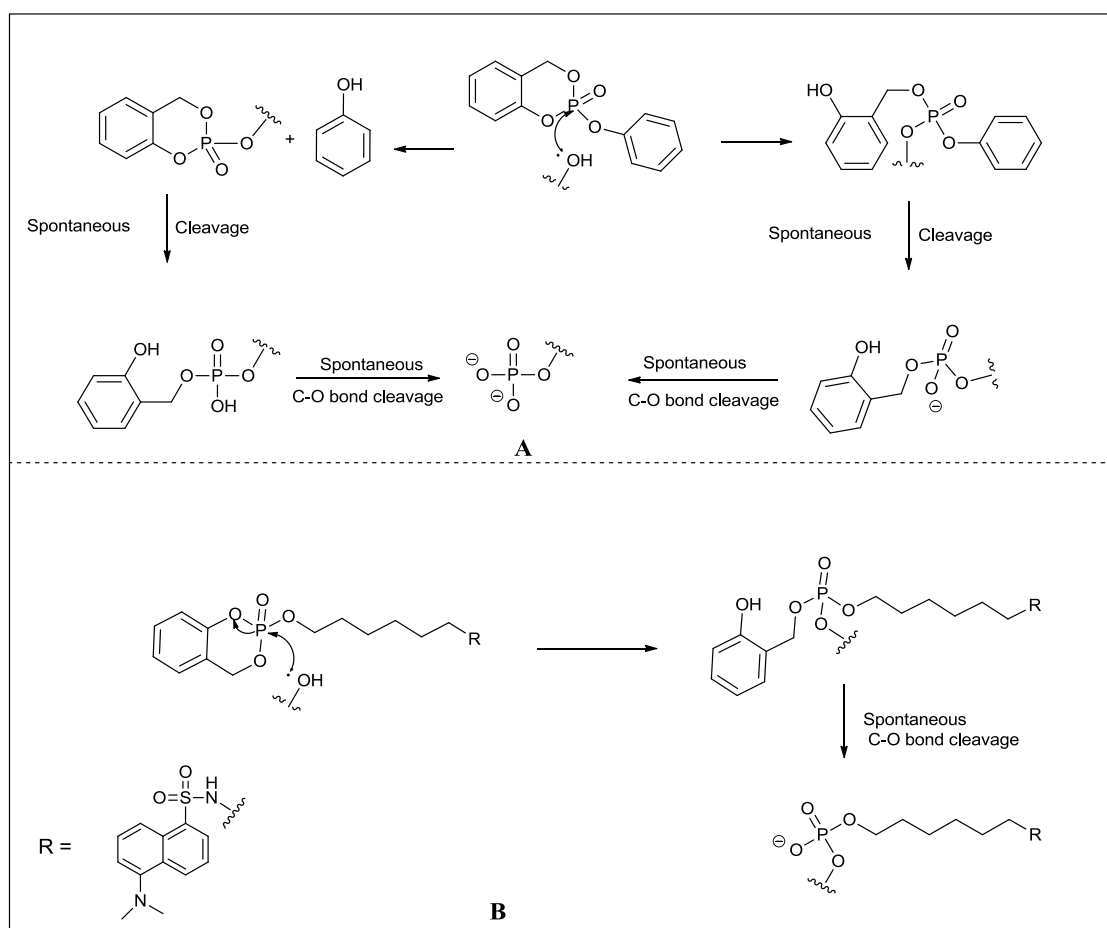


Figure 25 Possible mechanisms of the inhibition and binding of saligenin phosphate with biomolecules

Furthermore, there is evidence to suggest that the toxicity of these compounds is affected by the variation of the group attached to the phosphorus atom through the oxygen,¹¹² the toxicity of the PSP has been found to behave in a similar manner to the alkyl saligenin phosphate, which means using an alkyl linker may not affect the molecules activity significantly. For example, an investigation about the inhibition of NTE with alkyl-, alkoxy- and phenoxy- saligenin phosphate was performed by Casida, *et.al.* This study showed that the inhibition of NTE by the alkoxy-saligenin phosphate and phenoxy substituted material were relatively similar, giving IC_{50} values of 6.0 and 4.5 nM respectively (Figure 26).

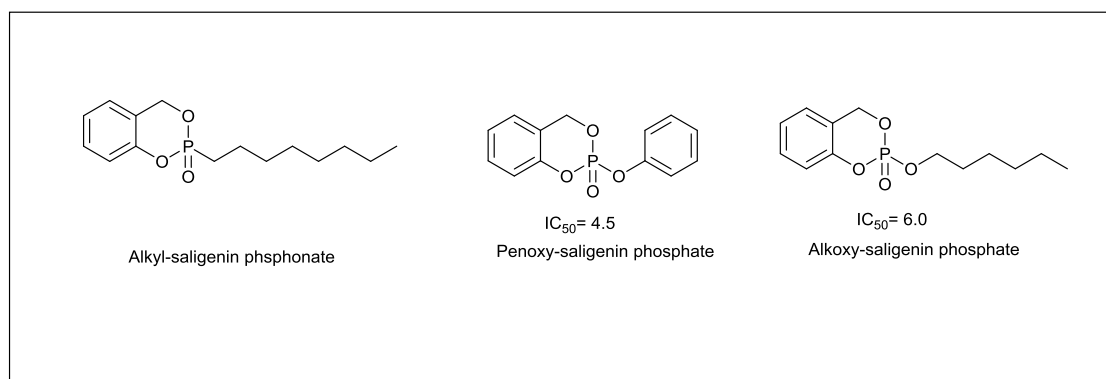


Figure 26 *Saligenin-phosphonate and phosphate analogues*

The goal of this work was to prepare organophosphate neurotoxins incorporating linkers for attachment of fluorescent tag to identify novel protein targets. The biological activity of these modified toxins was verified by esterase assays, after which they were elaborated into functional probes to identify the targets of the parent toxins (Figure 27).

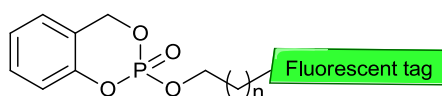
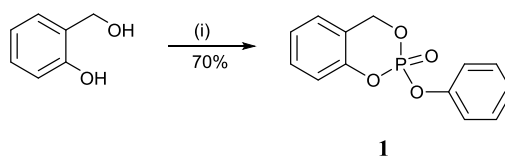


Figure 27 *Organophosphate neurotoxin linked with fluorescent tag*

2.2.1 Synthesis of phenyl saligenin phosphate

Synthesis work commenced with preparation of the parent PSP as a model reaction and for the purposes of toxicity tests. In a modification of a published procedure, commercially available 4-hydroxybenzyl alcohol (saligenin) was treated with phenyl phosphorodichloridate with triethylamine. This reaction successfully gave (PSP) phenyl saligenin phosphate **1** in a good yield (70%) after recrystallization (Scheme 2.1). Confirmation that this product was obtained was by ^1H NMR spectra, which showed that there were no peaks arising from starting materials, and a complex splitting pattern

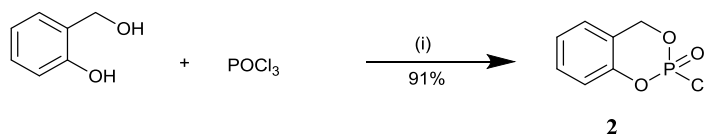
was seen and multiplet observed at 5.25-5.36 ppm for CH_2-O-P protons; in addition to a multiplet at 7.12-7.26 ppm for protons in the aromatic rings. Also, the ^{13}C NMR spectra showed a noticeable shift in the region of CH_2 carbon, from 64.6 ppm of the starting material to 69.3 ppm of the PSP product. Further the ^{31}P NMR spectra showed only one signal peak at -15.31 ppm, corresponding to an oxygenated tetrahedral phosphorus atom.



Scheme 2.1: *Reagents and conditions:* (i) Phenyl phosphodichloridate, THF, Et_3N , 0 °C- RT, 4h

2.2.2 Preparation of 2-chloro-4H-benzo[d][1, 3, 2]dioxaphosphinine 2-oxide

To finish binding the organophosphate with a linker for a further step of attachment to a fluorescent tag, compound **2** was successfully prepared by a treatment of a mixture of 4-hydroxybenzyl alcohol and triethylamine with phosphorus oxychloride ($POCl_3$) to yield the desired compound in a good yield of 91%.¹¹³ Pure product **2** was isolated after filtering the precipitate of triethylammonium chloride from dry toluene and the product used directly in the next step (Scheme 2.2). Because of the instability of this product even after being stored in the freezer, it was always necessary to use freshly prepared material.

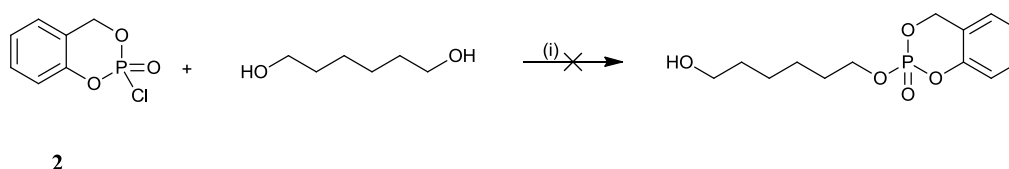


Scheme 2.2: *Reagents and conditions:* (i) DCM, Et_3N , -78 °C, 1 h, RT, 4 h

Product **2** was confirmed from the ^1H NMR spectra, which showed a complex splitting pattern and multiplet at 5.4-5.5 ppm belonging to $\text{CH}_2\text{-O-P}$, also the ^{13}C spectra showed a peak at 70.1 ppm for the $\text{CH}_2\text{-O-P}$. Further the ^{31}P NMR spectra showed one single diagnostic peak at -5.5 ppm belonging to the phosphorus atom.

2.2.3 Reaction of saligenin phosphate with 1, 6 hexane diol

The first objective after preparation of saligenin phosphate chloride **2** was to attach it to a fluorescent tag via linker. The six carbon alkyl chain was the linker of choice. Thus, 1,6 hexane diol was reacted with freshly prepared compound **2** (Scheme 2.3), but, the product was a complex mixture and the NMR spectra for the crude material did not give clear evidence for production of the desired compound. In addition, purification using a silica flash chromatography was not a suitable method for the separation, even by using very polar solvents.

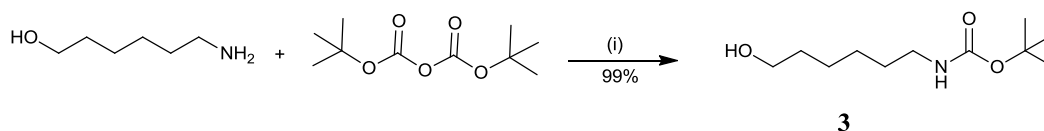


Scheme 2.3: *Reagents and conditions:* (i) THF, Et_3N , $0\text{ }^\circ\text{C}$;

2.2.4 Preparation of saligenin phosphate with a linker for attachment to a fluorescent tag

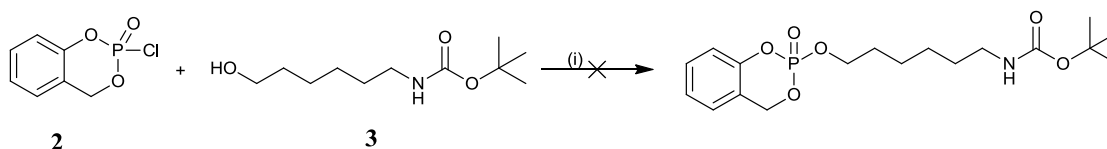
For simplicity a six carbon chain alkyl linker was chosen for the attachment with the fluorescent tag. 1, 6-Aminohexanol contains two reactive functions, a hydroxyl group that will react with the chloride attached to the phosphorus atom to create the phosphate, and the other side provides amine group to facilitate the attachment with the fluorescent

component (dansyl chloride). In order to prevent preferential amidate formation, protection of the amine group was carried out. Treatment of 1, 6-aminoheptanol with commercially available di-tert-butyl dicarbonate gave the desired compound **3** in yield of 99% (Scheme 2.4). The product was confirmed from the ^1H NMR spectra where a peak at 1.38 ppm belonging to the BOC group and a peak at 4.61 ppm for HN-CO. The ^{13}C NMR spectrum showed a diagnostic peak for the carbonyl group at 156 ppm and peak at 79 ppm belonging to the central carbon of the *t*-butyl group.



Scheme 2.4: Reagents and conditions: (i) DCM, 0 °C, RT, 2 h

The second step of the preparation, treated the freshly prepared saligenin phosphate **2** with product **3** under variety of different conditions. A number of bases (NaH, Et₃N, pyridine) were used however, no evidence of product formation was observed in ^{31}P and ^1H NMR spectra and mixtures were obtained that were highly polar and not suitable for chromatography with silica gel (Scheme 2.5).



Scheme 2.5: Reagents and conditions: (i) DCM, Et₃N, -78 °C, RT, 18 h

Examination of the ^{31}P NMR spectra indicated that a tetrahedral phosphate compound was formed, along with other phosphorus containing compounds, while the ^1H NMR spectra showed a number of compounds. Silica chromatography of the mixtures was

hampered by the high polarity of the materials and poor yields of a mixture of unidentified compounds were obtained. Investigation then turned to alternative strategies for linking the PSP moiety to the fluorescent component.

2.2.5 Preparation of BODIPY- FL fluorescent component with linker

There are many advantages of using BODIPY fluorescent derivatives, such as the high extinction coefficients, excellent photostability and high fluorescence quantum yields. A number of studies on fluorescence have suggested that BODIPY derivatives are highly recommended fluorophore for many macromolecule visualization applications including proteins.¹¹⁴ Thus, a first attempt was made to bind saligenin phosphate with BODIPY-FL via alkyl linker, starting from compound **2** to gain the desired molecule ready for biological application (Figure 28).

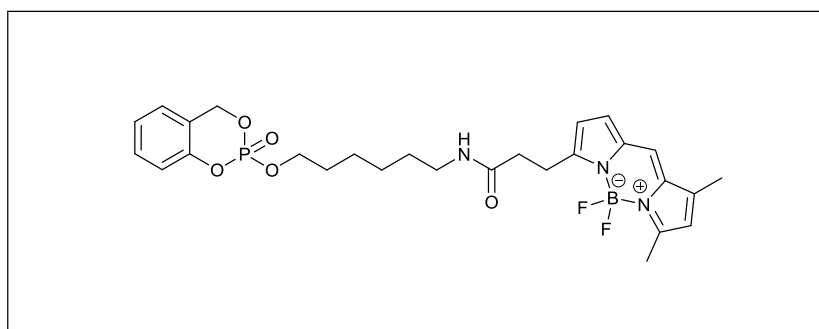
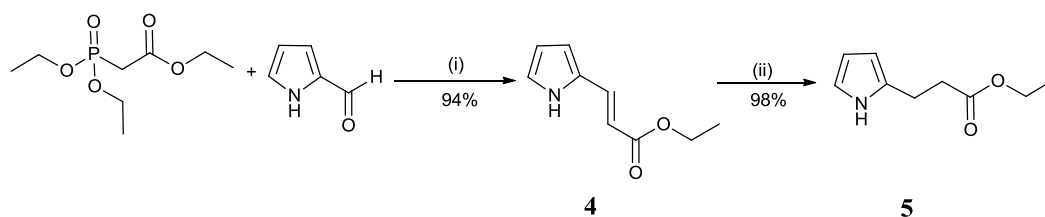


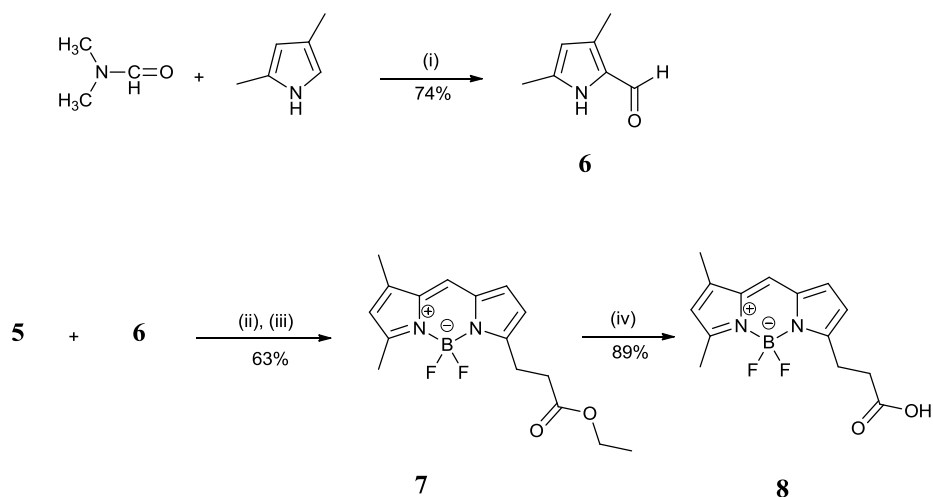
Figure 28 *Saligenin phosphate with BODIPY via alkyl linker*

BODIPY (4,4-difluoro-4-bora-3a,4a-diaza-s-indacene) has been prepared starting from commercially available 1H-pyrrole-2-carbaldehyde which was treated with ethyl 2-(diethoxymethyl)hydrophosphoryl)acetate to give the product **4**. This product was then reduced by catalytic hydrogenation,¹¹⁵ producing **5** in yield of 98% (Scheme 2.6).



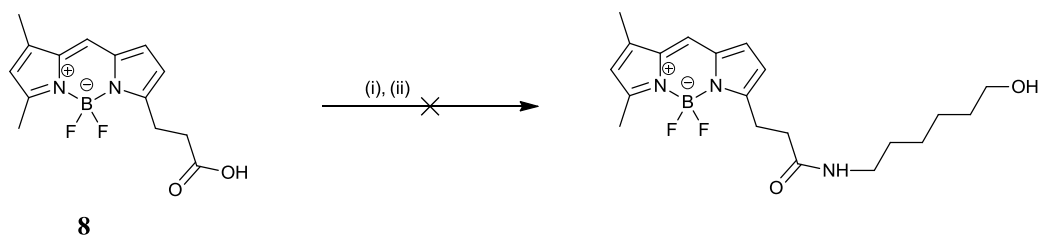
Scheme 2.6: Reagents and conditions: (i) nBuLi, THF, -78 °C to 0 °C; (ii) H₂, Pd/C, MeOH, RT

Further, the starting material 2-formyl-3,5-dimethylpyrrole **6** was prepared by reacting 2,4-dimethylpyrrole with phosphorus oxychloride and *N,N*-dimethylformamide followed by a treatment with sodium acetate, producing compound **6** in 74% yield. With compound **5** in hand, condensation reaction with 2-formyl-3,5-dimethylpyrrole **6** in presence of POCl₃ was carried out. The intermediate obtained was then reacted with BF₃.OEt₂ and DIPEA, giving the desired BODIPY- ester **7** with a yield of 63% after flash chromatography purification. The ester product **7** was then hydrolysed with 4 M HCl in dioxane yielding BODIPY acid **8** in yield of 89% after chromatography purification (Scheme 2.7). The identity of the final product was confirmed from the NMR data which were consistent with the literature.¹¹⁶



Scheme 2.7: *Reagents and conditions:* (i) a- POCl_3 , 10 °C; b- reflux 30 mins, CH_3COONa , RT;
(ii) POCl_3 , DCM, 0 °C to RT, 6 h; (iii) $\text{BF}_3 \cdot \text{OEt}_2$, DIPEA, 0 °C, RT, 12 h;
(iv) 4M HCl dioxane, RT, 2 days

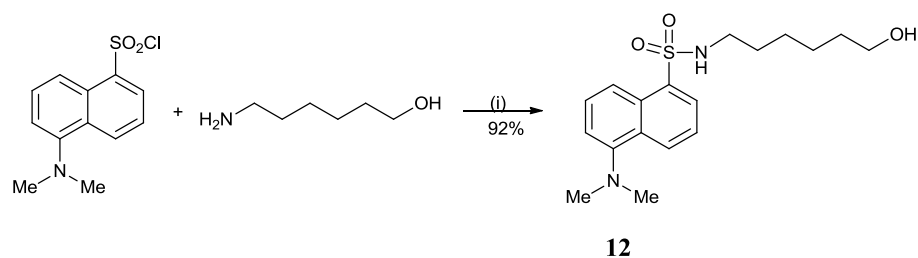
The coupling of the BODIPY **8** to alkyl linker was then briefly explored. A reaction of BODIPY **8** with commercially available 1-amino-6-hexanol was applied with employment of N-methylmorpholine and isobutylchloroformate. However, the NMR data for the crude product showed no evidence for the desired product formation (Scheme 2.8). Further work in preparing this fluorescent tag with linker was not pursued.



Scheme 2.8: *Reagents and conditions:* (i) N-methylmorpholine, isobutylchloroformate, DMF, RT, 45 min; (ii) 1-Amino-6-hexanol

2.2.6 Dansylamide with PEG linker

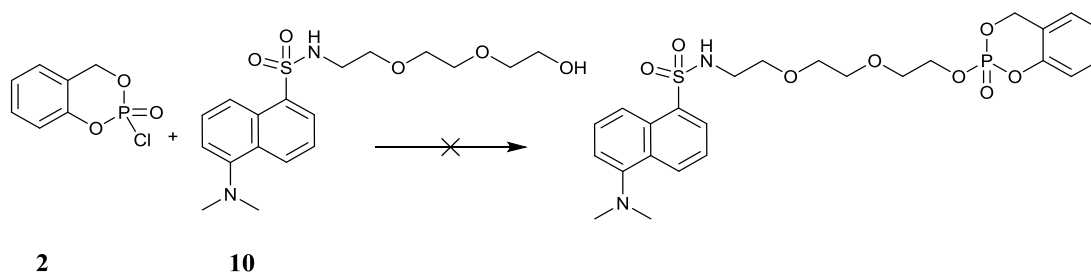
In order to investigate the impact of using a PEG spacer linker, preparation of dansylamide **10** was explored. Commercially available dansyl chloride was treated with liquid ammonia giving dansylamide **9** in yield of 87%. This product was confirmed from the NMR data which was consistent with the literature.¹¹⁷ The product **9** was then refluxed with commercially available 2-[2-(2-chloroethoxy)ethoxy]ethanol and potassium carbonate to give a 1:1 mixture of mono and di-PEG dansylamide **10** and **10a** in yield of 32% and 33%, respectively, despite the fact that the reactant materials had been used in ratio of 1:1 equivalent (Scheme 2.9). This suggests that mono substituted sulfonamide **10** might be more reactive than the sulfonamide **9**. Further evidence to support this was confirmed when the reaction was performed at room temperature and the product was more than 90% di-substituted **10a**. Therefore perhaps it might be a good suggestion if product **9** could be firstly protected via acylation reaction followed by addition of 2-[2-(2-chloroethoxy)ethoxy]ethanol, to direct the reaction undergoing a mono-substitution product. The identity of compound **10** was evidenced from the ¹H NMR spectra, showing a triplet peak at 6.08 ppm for one proton of SO₂-NH and HR-MS gave a mass consistent with the structure.



Scheme 2.10: Reagents and conditions: (i) Et_3N , DMAP, DCM, 0°C -RT, 2:30 h

2.2.8 Coupling the organophosphate compound with the florescent tag

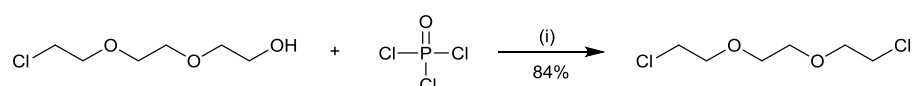
In order to couple compound **10** with saligenin phosphochloride **2**, various reaction conditions were applied, for example triethylamine at -78°C in DCM, sodium hydride at -20°C in THF, and pyridine in DCM at -78°C . However by looking to the NMR spectra for the crude product, there was no clear evidence that the desired compound was produced (Scheme 2.11).



Scheme 2.11: Reagents and condtions; (i) Et_3N , DCM, -78°C , RT, 24 h or NaH, THF, -20°C , RT, 24 h

The reaction of the dansylamide **10** with saligenin phosphochloride **2** was not successful, so an alternative plan was established to try attaching the phosphochloride group to the linker first, followed by reaction with 2-hydroxybenzyl alcohol. Phosphorus oxychloride was reacted with 2-[2-(2-chloroethoxy)ethoxy]ethanol in ratio

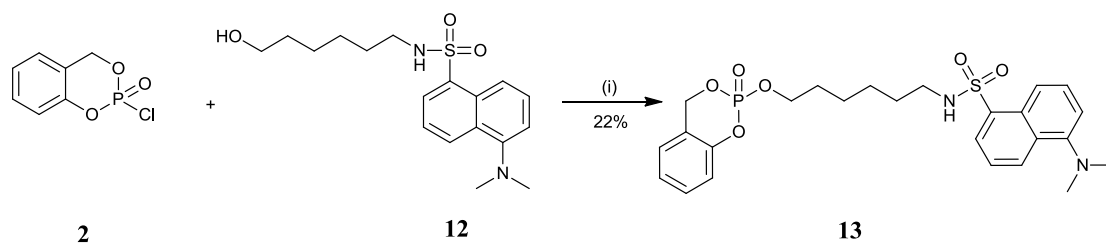
of 3: 1 equivalents, respectively, in the presence of triethylamine. The product obtained was not the desired product but unexpectedly gave 1,2-bis(2-chloroethoxy)ethane, exhibiting three peaks in the ^{13}C NMR spectrum for the symmetrical compound product (Scheme 2.12). The identity was confirmed by a comparison of spectroscopic data with the literature.¹¹⁸



Scheme 2.12: *Reagents and condtions; (i) Et₃N, Et₂O, 0 °C, RT, 3h*

2.2.9 Coupling the organophosphate compound **2** with dansyl amide **12**

Finally, after the unsuccessful coupling with dansylamide **10**, linking of the dansylamide **12** to the saligenin phosphochloridate **2** was achieved by means of a six carbon atom alkyl linker. The reaction of dansyl amide **12** with saligenin phosphochloridate **8** successfully gave dansylated saligenin phosphate **13** in yield of 22% after flash chromatography purification (Scheme 2.13). Despite the poor yield, the product was easily purified over silica gel. The ^1H NMR spectrum exhibited a difficult to recognise ABX pattern with coupling to phosphorus of three bands 14.8, 19.2 and 7.6 Hz of the CH_2 protons coupled to $\text{P}=\text{O}$ at 5.30 ppm (Figure 29). The ^{31}P NMR spectra, which showed a single peak at - 8.87 ppm for the phosphorus atom and HR-MS analysis data, are also consistent with the structure.



Scheme 13: Reagents and conditions: (i) Et₃N, DCM, -78 °C, 45 min, 20 °C, overnight

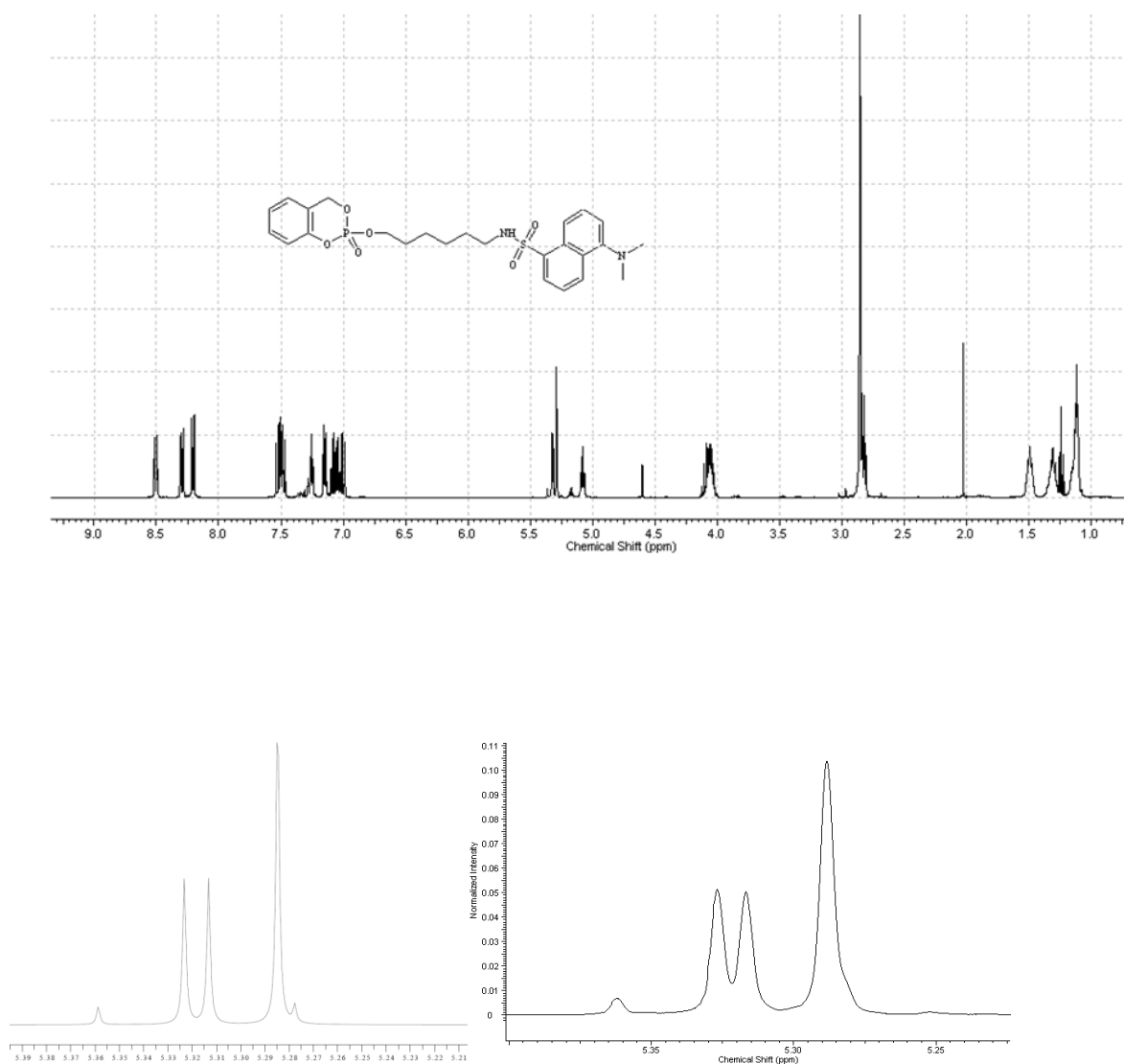


Figure 29 NMR spectra for compound **13**

2.2.10 Biological testing

In collaboration with Dr Alan Hargreaves, studies have been undertaken into the inhibition of several enzymes by phenyl saligenin phosphate. Prior to studying the biological effects of the prepared dansylated saligenin phosphate, the biochemical effects of non-dansylated PSP on serine hydrolase enzymes were studied using the known targets, trypsin and chymotrypsin, in an activity assay.

Furthermore, transglutaminase 2 is a suspected target of the PSP and the inhibition of this enzyme has also now been studied. In support of these studies, the fluorescent tagging was expected to confirm the covalent inhibition of this enzyme with PSP.

2.2.10.1 Effect of PSP on the inhibition of trypsin

Saligenin phosphate is known to inhibit the serine protease trypsin, and a colorimetric assay was used to confirm inhibition of the enzyme by PSP. Trypsin (0.025 mg/ml) was pre-incubated with PSP of various concentrations, and then the indicator substrate benzyl-L- arginine 4-nitroaniline hydrochloride, was introduced. Active trypsin cleaves the substrate producing *p*-nitroaniline which can be observed at 415 nm (Figure 30), and the concentration of the released *p*-nitroaniline indicates the enzyme activity, and the effect of the PSP on the trypsin activity.

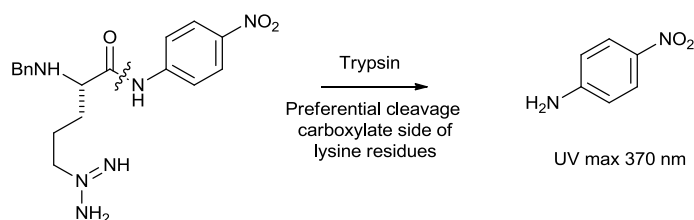


Figure 30 *Cleavage site and reaction product released by trypsin*

From the assay results obtained, it can be seen that the activity of trypsin was significantly inhibited by the increasing of the PSP concentration. The initial effect could be seen with PSP concentration of 10 μM while nearly complete inhibition was observed at 50 μM (Figure 31).

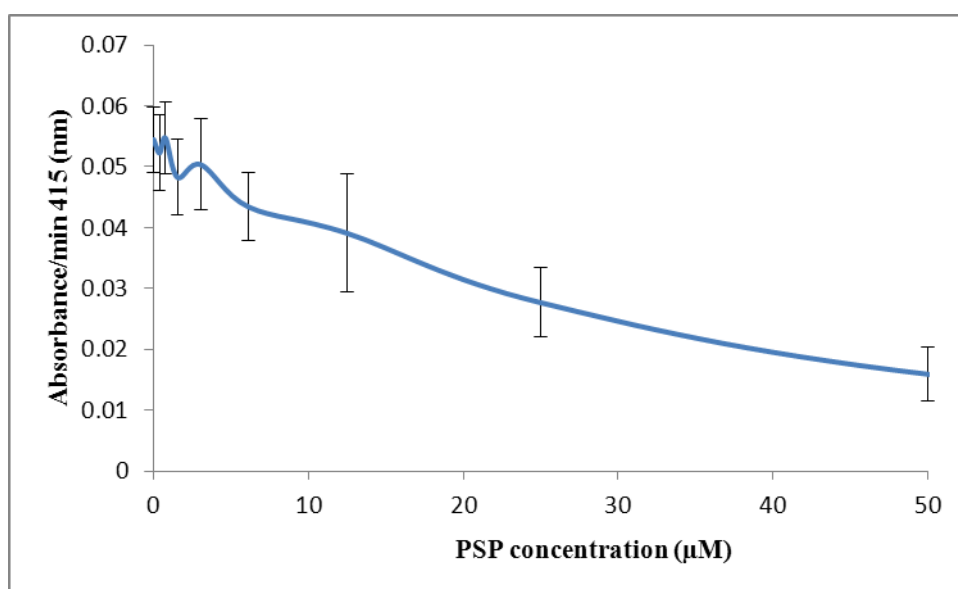


Figure 31 *Effect of PSP on trypsin activity*

2.2.10.2 Effect of PSP on the inhibition of Chymotrypsin

A similar assay to that used for trypsin was applied to chymotrypsin, in order to assess the PSP inhibition of the enzyme. Using the indicator substrate the N-Succinyl- Gly- Gly- Phe-p- nitroanilide, selective cleavage occurs on the carboxy terminal side of the phenylalanine residues releasing *p*-nitroaniline, as in the trypsin assay (Figure 32).

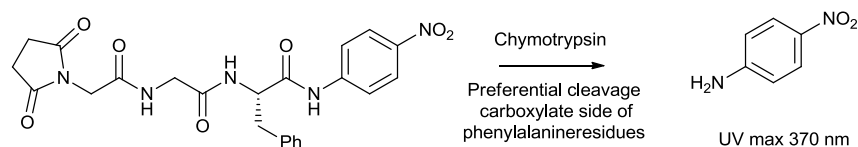


Figure 32 *Cleavage site and substrate released by chymotrypsin*

Similar incubation experiments confirmed that PSP was a potent inhibitor of chymotrypsin with significant inhibition at a PSP concentration of only 0.5 μM and the complete inhibition at 6.2 μM (Figure 33).

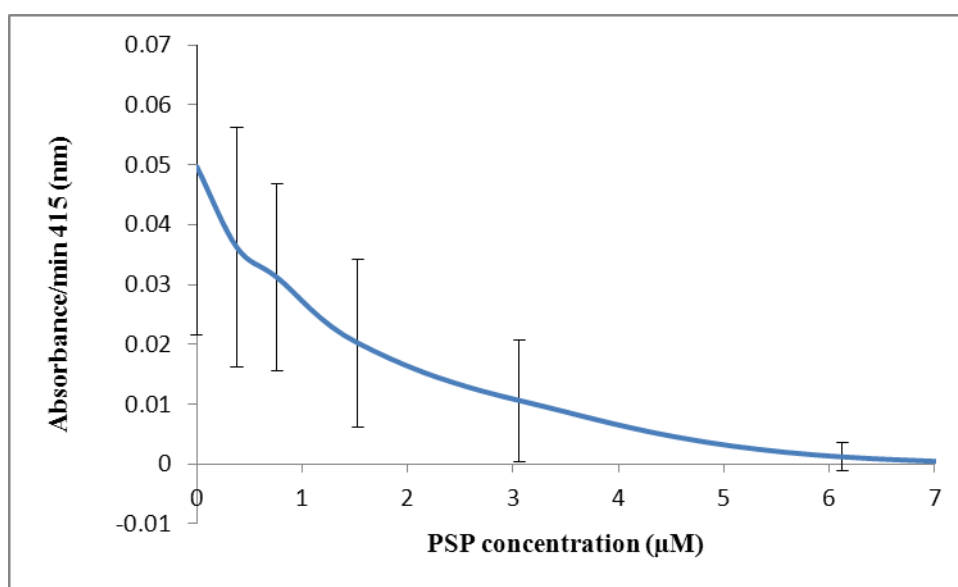


Figure 33 *Effect of PSP on chymotrypsin activity*

2.2.10.3 Effect of PSP on the inhibition of Transglutaminase 2 activity

TGase 2 catalyses the amination of protein-bound glutamine residues, an assay for TGase activity developed by Slaughter,¹¹⁹ was employed to assess inhibition of this enzyme by PSP. Purified samples of TGase 2 were pre-incubated at room temperature for 15 min with different PSP concentrations, before performing the biotin cadaverine assay to elucidate the effect of TGase 2 activity. The principle of this assay is to use N-N'-dimethyl casein as the amine acceptor substrate and biotin-cadaverine as an amine

donor. In the 1st step, TGase is primed to catalyse the covalent addition of biotinylated cadaverine to N,N'-dimethyl casein that has already been coupled to the microtitre plate. In the second step, streptavidin-coupled peroxidase is added to the wells and immobilised through the interaction with biotin. The amount of biotinylated casein is then measured by means of a coupled peroxidation reaction. The peroxidase is activated using H₂O₂ in presence of tetramethyl benzidine as electron acceptor (chromogen), and once the reaction has been stopped by the addition of sulphuric acid, the initial TGase activity is measured by the absorbance at 450 nm (Figure 34).

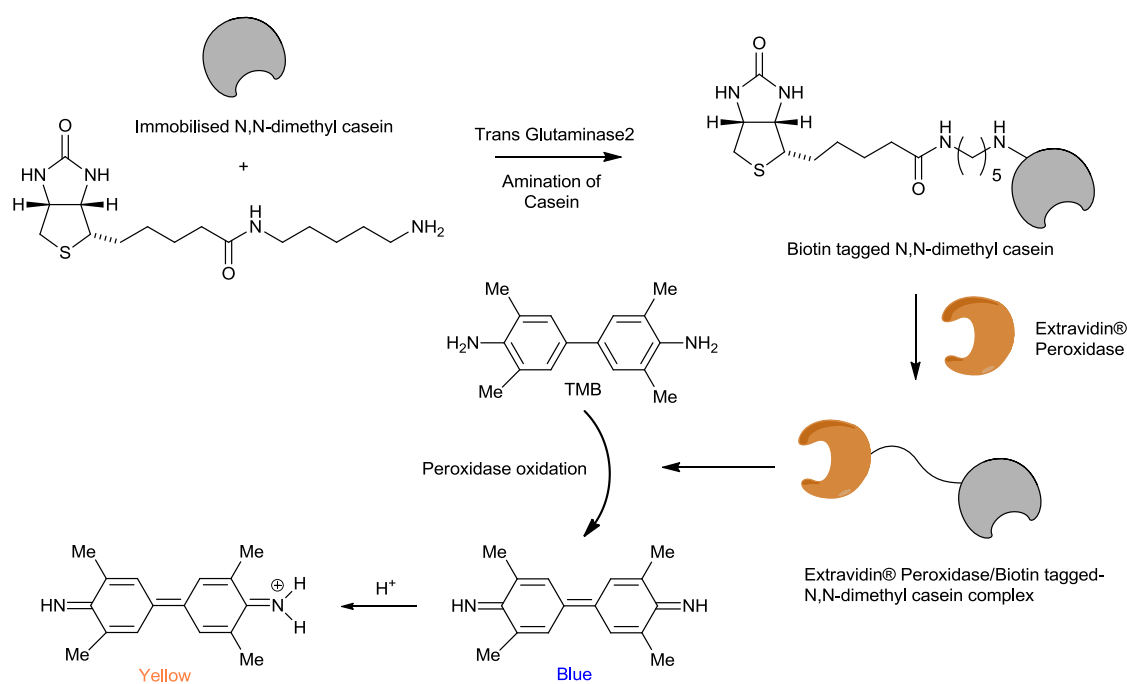


Figure 34 Biotin cadaverine assay for TGase 2 activity

In these experiments it was found that the PSP could inhibit TGase activity, and the results showed a discernible effect on the activity compared to the control at 0.09 μM to about 50% inhibition at 6.25 μM of PSP. The TGase inhibition by PSP was concentration dependent (Figure 35).

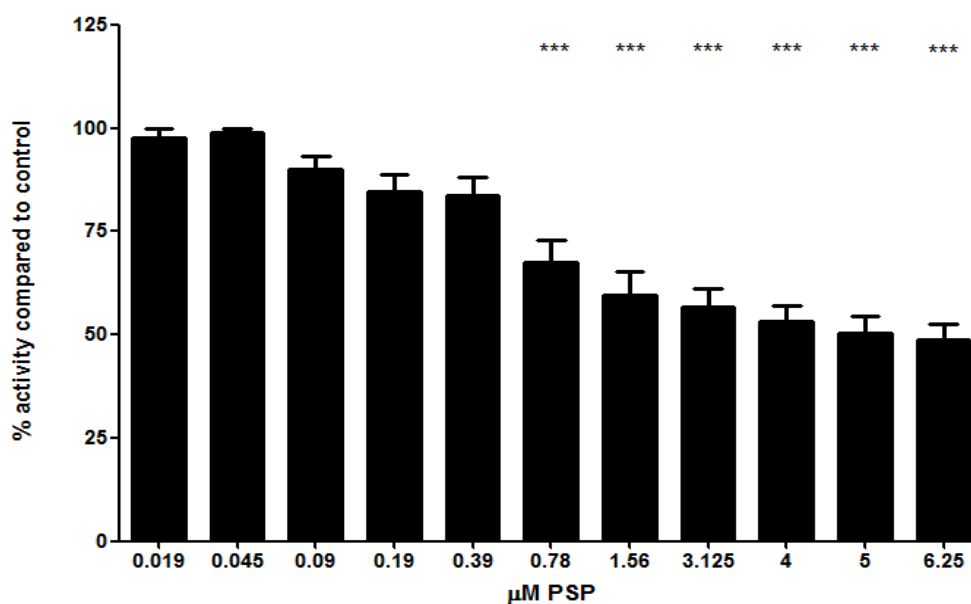


Figure 35 *In vitro* effects of different concentrations of PSP on TGase 2 activity

2.2.10.4 Gel electrophoresis and UV transillumination for dansylated PSP 13

Given the observed effect of the PSP on the activity of the three enzymes, as previously described, it was envisaged that these purified enzymes would provide an effective test for the tagging ability of the labelled saligenin phosphate. The strategy in choosing these enzymes is that the first two enzymes are established targets of PSP, while TGase 2 is thought to be a target of the same molecule.¹²⁰ Dansylated saligenin phosphate **13** was incubated with both trypsin and chymotrypsin then subjected to one dimensional gel electrophoresis. Any dansylated organophosphate **13** covalently bound to these target enzymes was then visualized using UV light. Due to the denaturing gel

electrophoresis conditions, only covalently labelled proteins should appear a fluorescent bands and unreacted neutral labelling compound will not move on the gel.

i) Trypsin and chymotrypsin gel electrophoresis

In the event, trypsin and chymotrypsin enzymes of 1mg/ml concentration were incubated with 50 μ M dansylated saligenin phosphate for 15 minutes, and then the samples were electrophoretically separated on the gel. The visualization step was carried out using a UV transilluminator, showing clear fluorescent bands for the organophosphate labelled enzyme. In quantitative terms, the labelled saligenin phosphate was covalently bonded to both enzymes; however, binding with the chymotrypsin gave much brighter bands than with trypsin. This finding is in agreement with the previous work where saligenin phosphate was a more potent inhibitor of chymotrypsin than trypsin (Figure 36).

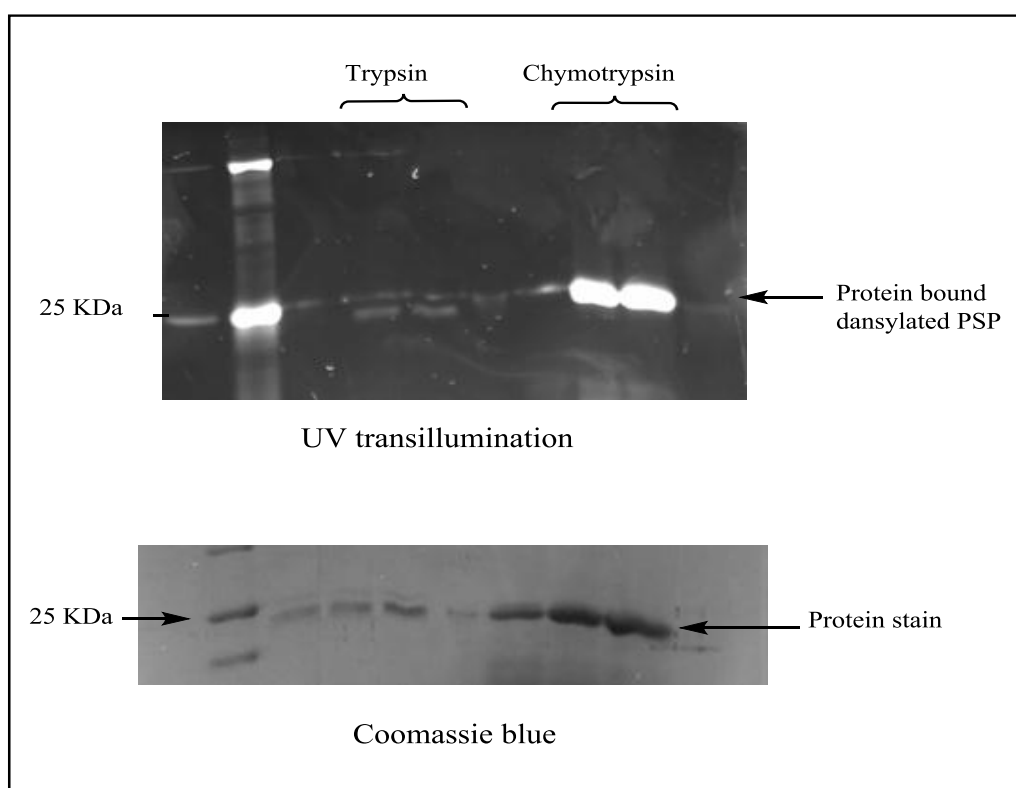


Figure 36 Incubation of dansylated saligenin phosphate with trypsin and chymotrypsin

ii) Transglutaminase 2 Gel electrophoresis

A similar experiment was then carried out using purified transglutaminase 2. The enzyme, 1mg/ml concentration, was incubated with dansylated saligenin phosphate **13**, then the samples loaded on a gel and separated by electrophoresis, and the gel was then visualized using a UV transilluminator. Examination of the gel showed a fluorescent band at a position consistent with the molecular weight of the enzyme target and confirmed that this enzyme was covalently bound to saligenin phosphate, in agreement with the inhibition studies (Figure 37).

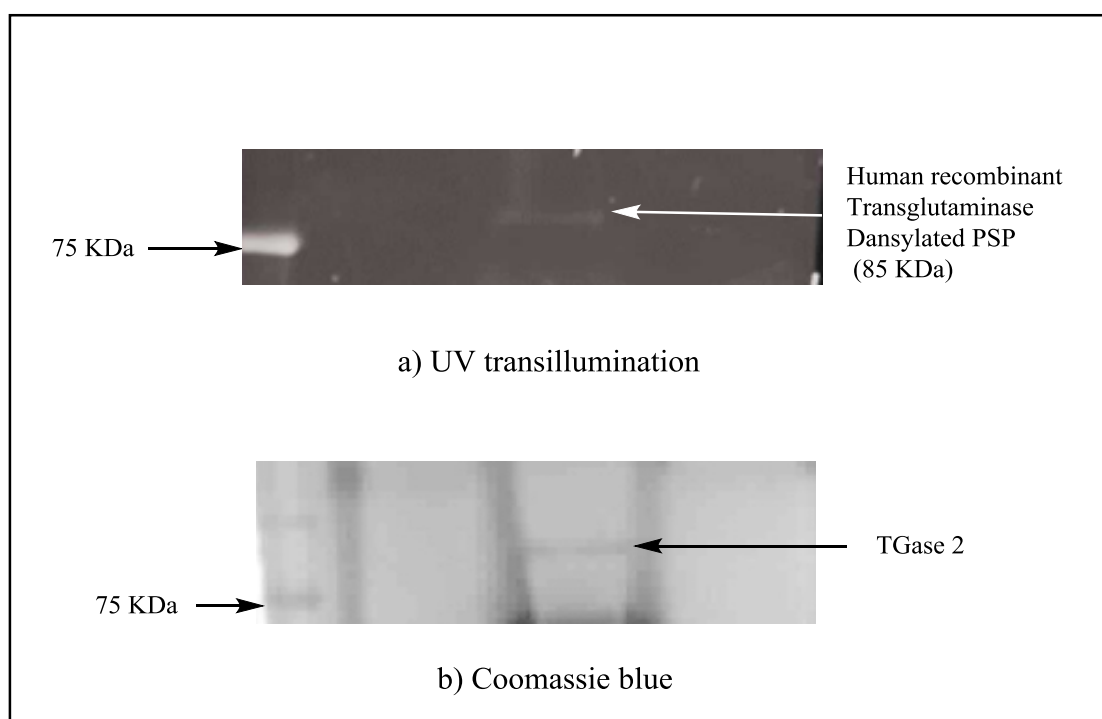


Figure 37 a) *fluorescent band of dansylated saligenin phosphate with TGase2,*
b) *TGase band with coomassie blue stain*

2.3 Conclusion

The enzyme targets of the organophosphate toxin “saligenin phosphate” have been investigated. Saligenin phosphate was coupled to a fluorescent tag via an alkyl chain linker.

In collaboration work, biological investigation on the inhibition of PSP molecule has been performed by means of established assays of saligenin phosphate **13** enzyme interactions. The inhibition of known PSP targets trypsin and chymotrypsin enzymes was established along with evidence for the inhibition of a new target, transglutaminase 2 enzyme.

Subsequent inhibition experiments using the fluorescent probe showed labelling of all three enzymes with fluorescent bands observed in all cases. This labelling was also confirmed the covalent binding of the PSP with the enzymes investigated. The experiments demonstrate the utility of using this tagging method for determination of the enzyme targets of PSP, and as a result method will find use in discovering novel targets of PSP, similar approaches may also be useful with organophosphates in general.

3. Chapter 3: The mK_{ATP} activator “diazoxide”

1. Introduction

Heart disease is one of the major causes of mortality and disability in the western world.¹²¹ The most common type of heart disease affects the arteries feeding the heart, and is termed coronary artery disease (CAD). This disease is caused by a blockage or narrowing the arteries by accumulation of lipid-containing plaques on the innermost layer of the walls of the coronary arteries. The heart muscle fed by these blocked arteries is damaged because of a lack of oxygen and blood supply.¹²² This condition affecting these arteries causes heart muscle injury called ischaemia heart syndrome, which may cause early death through heart attacks. In this event, much damage is caused not by initial loss of oxygen supply but during oxygen resupply to the heart tissue, and this is named myocardial reperfusion injury. Ischaemia injury happens when the blood supply to an area of tissue is discontinued. The time a tissue can survive a lack of oxygen differs, but eventually all ischaemic tissue becomes necrotic. Restoration of the blood supply should decrease the damage,¹²³ but studies of reperfused tissues after blockage led to the discovery that the level of injury often increased when the blood supply was restored. It has been proposed that this additional damage, reperfusion injury (IR), is due to the activity of oxygen free radicals.¹²⁴ Generally, the anti-oxidant protection systems in the aerobic myocardium can dispose of the oxygen free radicals. However, ischaemia decreases this ability, particularly in the mitochondrial compartment, causing the tissue to be highly subjected to damage.¹²⁵

The mechanism of causing such damage may be that lack of oxygen can lead to an accumulation of metabolic intermediates,¹²⁶ during the reperfusion these intermediates react causing a rapid increase in oxygen radicals (H_2O_2 , O_2^- and $\cdot\text{OH}$). This increase can

result in overcome cellular defences causing uncontrolled oxidation of cell components, leading to cell death.¹²⁷ Investigating novel ways of protecting the heart from this damage is a major research objective.

3.1.2 Introduction to cardioprotection

Cardioprotection works to find mechanisms and to preserve the heart through decreasing or even avoiding myocardial injury. The event of this protection can occur by two types of interventions. First is the endogenous activation which includes many phenomena such as classical ischaemic preconditioning, second-window or delayed ischaemic preconditioning and ischaemic postconditioning and their pharmacological recruitment. The latter involves the use of pharmacological agents to directly activate the signalling pathways involved in cardioprotection. Second is the surgical intervention.

3.1.2.1 Ischaemia preconditioning

Ischaemic preconditioning (classical preconditioning) is a powerful method of endogenous protection, and was first described by Murry and co-workers as a short-term period of intermittent ischemia and reperfusion before a prolonged ischaemic event which can give protection from cellular damage.¹²⁸ The first ischaemia event activates several signal transduction pathways, which help to keep myocytes contractility and function.¹²⁹ Current preconditioning has been achieved by applying stimuli directly to the heart muscle. It has also been discovered that ischaemia at a site distant to the heart may give the similar protection through circulating or neural mediators produced from distant tissues exposed to ischaemia.¹³⁰ It has been suggested that ischaemia preconditioning (PC) leads to cardioprotection.¹³¹

3.1.2.2 Second window of ischaemic preconditioning (SWOP)

There is another phase of preconditioning which occurs after a longer time than the first phase, which is between 24 to 72 hours after the reperfusion, and this later phase of preconditioning is called the second window of ischaemic preconditioning (SWOP). This phenomenon has been observed in many species such as dogs, rabbits and rat hearts,^{132, 133} however, it has not been found to occur in pig hearts.¹³⁴ Protection triggered by delayed preconditioning is thought to involve the prevention of the mitochondrial permeability transition pore opening by up-regulation of Bcl-2 expression.¹³⁵ Bcl-2 is member of the regulatory proteins that control apoptotic cell death,¹³⁶

3.1.2.3 Ischaemic post-conditioning

In addition to the phenomena of classical and delayed ischaemic preconditioning, a third phenomenon of ischaemic postconditioning has also been observed. Ischaemic postconditioning involves the gradual restoration of reperfusion (short periods of reperfusion) following an ischaemic insult and was first reported by Zhao *et al.* (2003).¹³⁷ It is apparent that the signalling mechanisms associated with ischaemic preconditioning and ischaemic postconditioning are very similar.¹³⁸ For example, reactive oxygen species may play a role in the protection as activators in the initial phase of postconditioning.¹³⁹ Also, postconditioning was found to be effective in reducing the generation of superoxide anion (O_2^-) in vivo in post-ischaemic myocardium.¹³⁷ Reduction of reactive oxygen species can be effected by increasing the endogenous anti-oxidant mechanisms of the myocardium.¹⁴⁰ In addition K_{ATP} channels and protein kinase C pathways are also thought to act as mediators.¹⁴¹

3.1.2.4 Role of the mitochondria in cardioprotection

Cardiac muscle cells have high numbers of mitochondria due to the dependence of heart tissue on oxidative phosphorylation.¹⁴² It is now clear that mitochondria are also central to the process causing cell death after ischaemia/reperfusion (I/R) injury.¹⁴³ Therefore, mitochondria have been identified as a key player in building a strategy of protection against I/R injury.

Activation of the mitochondrial ATP-sensitive potassium channel (mK_{ATP}) has a protective effect against many types of ischaemia.¹⁴⁴ The opening and closure of K_{ATP} channels is regulated by the ATP and ADP levels in cells, and therefore, the membrane potential is coupled to the metabolic process of the cell.¹⁴⁵ Functions of K_{ATP} channels include regulation of numerous physiological functions such as secretion, neurotransmission, contraction, and control of cell volume. In the mitochondria, mK_{ATP} is implicated in improvement of resistance for many injuries, for instance induction of apoptosis caused by a variety of stimuli.¹⁴⁶ Much interest has recently concentrated on a supposed mitochondrial K_{ATP} channel assumed to have an action in cytoprotection and myocardial preconditioning in variety of tissues; however the identity of the channel subunits remains unclear.^{147, 148}

3.1.2.5 Pharmacological preconditioning by diazoxide (PPC)

There are many studies suggesting that protection of the myocardium against ischaemia-reperfusion damage follows from activation of ATP sensitive potassium (K_{ATP}) channels.¹⁴⁹ Opening of the mK_{ATP} channels with the small molecule channel activator diazoxide can help in the early and delayed phases of preconditioning after ischaemia-reperfusion in rabbits.¹⁵⁰ This effect was also confirmed by applying the selective mK_{ATP} channel blocker sodium 5-hydroxydecanoate (5-HD), which prevented the protective effect of diazoxide. As a result, drugs with potassium channel opening

properties appear to have a broad clinical potential in pharmacological preconditioning during the ischemia/reperfusion injury. In addition, the treatment with diazoxide can also improve production of reactive oxygen species (ROS) which are thought to play an important role in cardioprotection. This effect suggests that the cardioprotective properties of diazoxide are mediated by the generation of pro-oxidants. However, the mechanism(s) of this cardioprotection are not fully understood and discovering the mechanism will enhance the potential treatment applications of this drug.

3.1.3 Potassium channel activation and diazoxide

The mK_{ATP} channel was first discovered in rat liver by Inoue *et al.*¹⁵¹ and Keith Garlid's group first isolated and characterized the mK_{ATP} channel found in the internal membrane of cow heart.¹⁵² Grover and Garlid have since demonstrated that this channel was responsible for the cardioprotection action of K_{ATP} channel openers.¹⁵³

Previous studies showed a poor correlation between sarcolemmal K^+ currents and cardioprotection for ATP-sensitive K^+ channel (K_{ATP}) openers. It has also been found that all the K_{ATP} openers can cause mitochondrial oxidation. Nevertheless, the K_{ATP} opener pinacidil for example stimulates these channels in the surface membrane, while diazoxide can particularly open the channels in mitochondria but not activate the sarcolemmal K_{ATP} . This discovery is compatible with the recognized pharmacology of several K_{ATP} channel drugs, which shows that diazoxide is the only selective drug for the $mitoK_{ATP}$ channel.¹⁵⁴ This selectivity of diazoxide can make it a powerful tool for investigating the actual mechanism of the cardioprotection and the molecular composition of these channels.¹⁵³ Moreover, it has been shown that the mK_{ATP} of cow heart varied in the sensitivity towards diazoxide, indicating heterogeneity amongst mK_{ATP} channels.¹⁵⁵ Although diazoxide is of distinctly lower potency than newer

hypotensive vasodilators like Cromakalim or Pinacidil in opening smooth muscle K^+ -channels, it is still a drug of great interest (Figure 38).¹⁵⁶

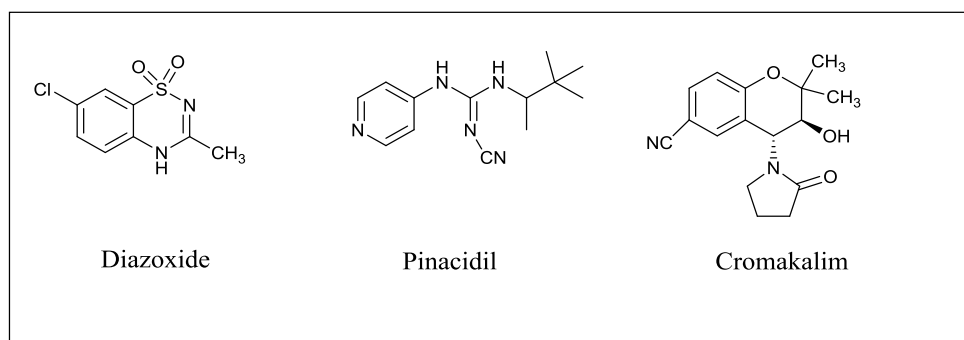


Figure 38 Hypotensive vasodilators; *Diazoxide, Cromakalim and Pinacidil*

The K_{ATP} channel opener diazoxide can provide the cardioprotection effect by opening mitochondrial K_{ATP} channels, which leads to relaxation in smooth muscles by increasing membrane permeability to potassium ions. This switches off voltage-gated calcium ion channels which inhibits the generation of an action potential. K_{ATP} channels are thought to play a key role in the cardioprotection with both K_{ATP} channel openers and ischaemic preconditioning, since in both cases, protection can be blocked by K_{ATP} channel blockers such as glibenclamide or sodium 5-hydroxydecanoate (5-HD) (Figure 39).¹⁵⁷

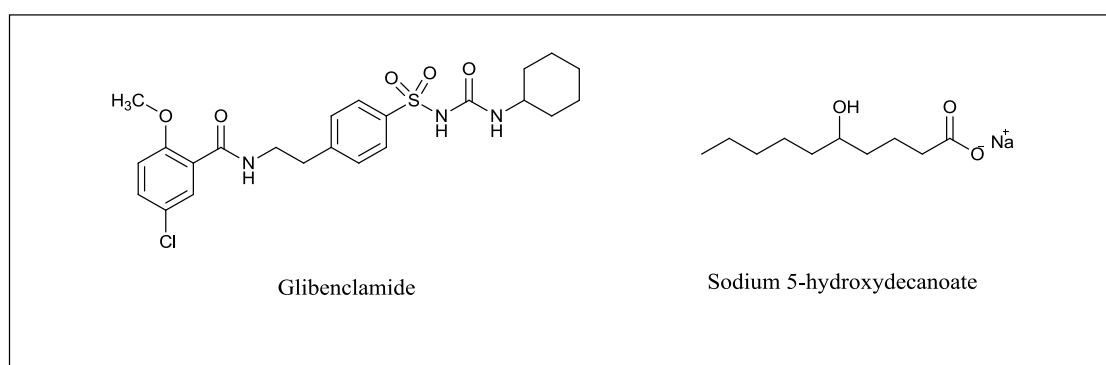


Figure 39 K_{ATP} blockers; *Glibenclamide and Sodium 5-hydroxydecanoate*

Diazoxide is also used as a vasodilator in the treatment of acute hypertension or malignant hypertension.¹⁵⁸ Diazoxide is often used in concentrations of up to several hundred μM to achieve a maximal opening of K_{ATP} channels and possible other effects are hardly ever taken into account.¹⁵⁹

3.1.4 Structure of the mK_{ATP} channel

Although the mK_{ATP} channel was first discovered in 1991, its structure and cardioprotection mechanism(s) of action are still poorly understood. Pharmacologically, mK_{ATP} can be activated and targeted by diazoxide, which can also activate the sarcolemmal K_{ATP} in the presence of ADP.¹⁶⁰ Diazoxide can also modulate the rat heart sarcolemmal K_{ATP} channel.¹⁶¹ The similar pharmacological action between these two K_{ATP} channels might suggest that the mK_{ATP} channel consists of the sulfonylurea receptors (SUR1, SUR2A, SUR2B) and the pore forming subunits (Kir6.1 and Kir6.2) as is the case with sarcolemmal K_{ATP} channels.¹⁶² However, experiments using mitochondrial-targeted SUR1 knock-out mice have revealed that diazoxide still induces protection against ischaemia-induced brain injury. These effects are also blocked by 5-HD showing that the SUR1 is not an effective component in the mK_{ATP} channel.¹⁶³ Moreover, another study using isolated rabbit myocytes has shown that transfection of a dominant negative construct of Kir6.1 did not modify the mK_{ATP} channel function, which is clear evidence that Kir6.1 is not one of the channel components.¹⁶⁴ It was also proposed that the mK_{ATP} channel contains ATP synthetase, adenine nucleotide translocator, mitochondrial ATP-binding cassette protein 1, phosphate carrier and succinate dehydrogenase (Figure 40),¹⁶⁵ if this is the case the $\text{mitoK}_{\text{ATP}}$ has completely different structure to the sarcolemmal K_{ATP} . The identification of the exact molecular structure of this channel will help in understanding the role of mK_{ATP} channels in cardioprotection and aid of development of selective drugs targeting this channel.

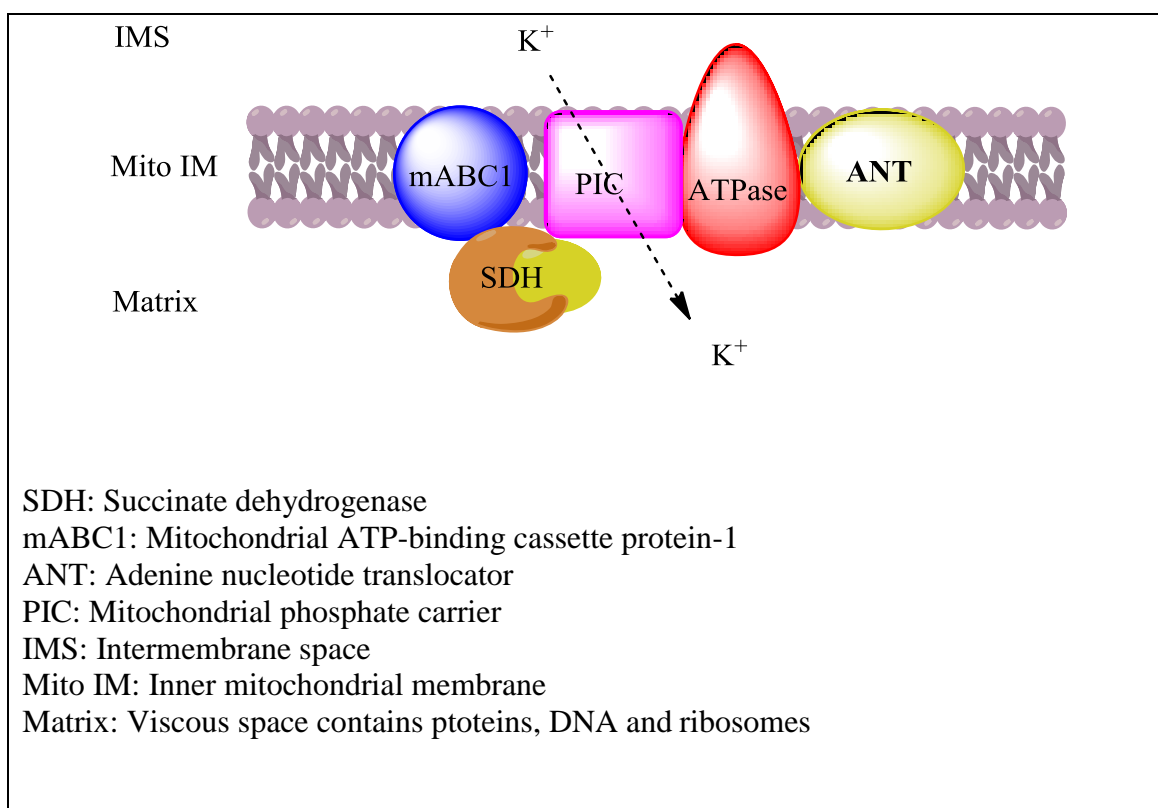


Figure 40 *Proposal Structure of the mitoK_{ATP} channel*

3.1.5 Aim of investigation

The aim of this work is to fluorescently label proteins which bind the “selective” mK_{ATP} channel opener diazoxide and potentially identify the associated proteins. This will be achieved by preparing a photochemical harpoon linked to fluorescent components and diazoxide bait, which will covalently label the targeted proteins (Figure 41).

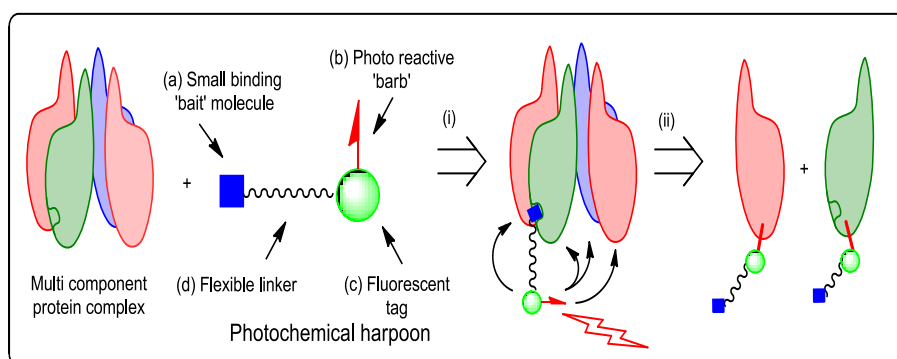
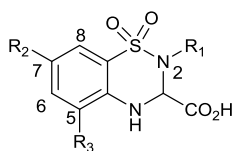


Figure 41 *Identification strategy for the protein target of drug molecule*

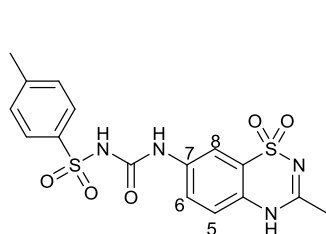
In pursuit of a chemical approach to identify the nature of the mK_{ATP} channel of the targeted by diazoxide, it was proposed to construct a chemical molecule which consists of four components: (a) a small biologically active 'bait' molecule which selectively binds to a specific protein target; (b) a photochemically activated reactive 'barb' component, which upon irradiation will covalently bond to an adjacent protein backbone (*via* a carbene or nitrene reactive intermediate); (c) a fluorescent tag attached to the photoreactive 'barb' component; and (d) a flexible linker between the bait and reactive barb/tag components.

3.2 Results and discussion

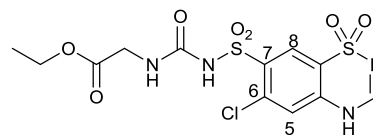
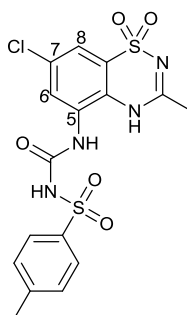
Diazoxide activates a wide number of K channels in a variety of tissue types, and structure activity relationships with different receptors and tissues have been studied. In 1994 Patrick Jimonet *et al.* synthesised and tested the activity of 2H-1,2,4-Benzothiadiazine-1,1-dioxide-3-carboxylic acid derivatives as an antagonists of the NMDA (*N*-methyl-D-aspartate) receptor-channel.¹⁶⁶ Comparing to the analogue with (R1, R2, R3= H) the affinity is greatly enhanced by appropriate introduction of chlorine atom(s) to the phenyl ring in position(s) 5 and 7 as in the followed structure.¹⁶⁷



In 2003 Smail Khelili *et al.* synthesised and evaluated diazoxide derivatives bearing NH group or sulfonylurea on positions 5 and 7.¹⁶⁸ The compounds efficiency was compared with the K_{ATP} channel openers diazoxide and Cromakalim in an assay examining the vasodilatory effects. Substitutions on these positions by means of NH group produced molecules of low efficiency, however, when sulfonylurea moiety was attached through a SO₂ group on position 7, potent vasodilators were obtained.

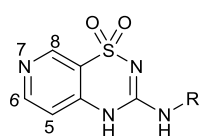


Inactive-diazoxide derivatives bearing
NH group or sulfonylurea

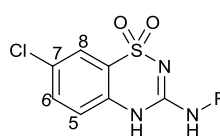


Potent-diazoxide analogue with sulfonylurea
through SO₂ group

In other study, Pascal de Tullio *et al.*¹⁶⁹ have synthesized pyridothiadiazines and benzothiadiazines bearing a variety of 3- or 4-alkyl and 3-aminoalkyl side chains. These benzothiadiazines as well as the pyridothiadiazines were tested *vs* diazoxide as inhibitors of insulin release on pancreatic B-cells and as vasorelaxants on isolated rat aorta. The pyridothiadiazines compounds were found to be powerful inhibitors of insulin release and are clearly more selective than their benzothiadiazines chlorobenzenic homolog compounds or than diazoxide.

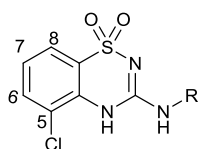


Pyridothiadiazines

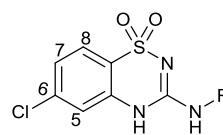


Benzothiadiazines

In 2010, Bernard Pirotte *et al.* demonstrated that the position of the chlorine atom on the benzene ring strongly affected the potency and selectivity toward pancreatic type K_{ATP} channels.¹⁷⁰ The best position for a chlorine atom on the aromatic ring of 3-alkylamino/cycloalkylamino-4H-1,2,4-benzothiadiazine 1,1-dioxides is the 6- rather than the 7-position. 6-Chloro-3-alkylamino-4H-1,2,4-benzothiadiazine 1,1-dioxide emerged as potent and highly selective pancreatic β -cell K_{ATP} channel openers, while the compounds bearing chlorine atom at the 5-position of the aromatic ring, were found to be almost inactive, at all the nature of the alkylamino side chain at the 3-positionn.



Inactive Benzothiadiazine



Active Benzothiadiazine

R= ethyl, propyl, isopropyl, cyclobutyl

The linking of the essential components of the chemical tool of investigation was the first priority. Thus, it was envisaged that the use of nitrogen atom junction would engender synthetic versatility and exceptional atom economy in connecting the three components. Because dansylamide was initially chosen as the fluorescent component, the linking of components was preformed via di alkylation of the sulfonamide group.

Overall, there is broad scope in the choice photoreactive 'barb' and fluorescent tag components for incorporation into a harpoon *via* a linker. In this work it was proposed to prepare simple fluorophore (dansyl) linked to α -trifluorodiazirene or benzophenone photoreactive component to create hybrid fluorescent tagging molecules with suitable functionality for rapid coupling and linking to the bioactive 'bait' diazoxide (Figure 42).

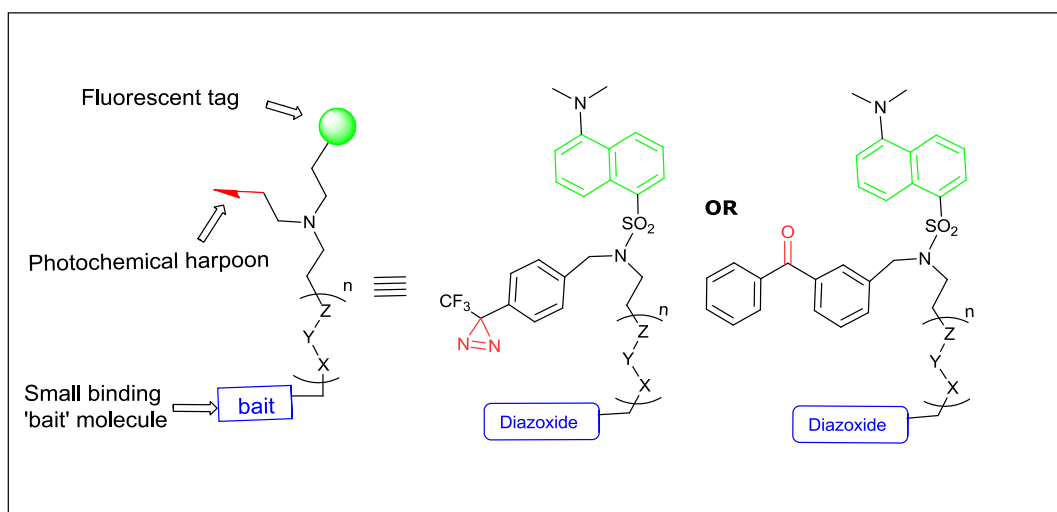


Figure 42 *Modular linked photoreactive barb and fluorescent tag with a small binding bait molecule*

3.2.1 Preparing the Photoaffinity compound (α -trifluoro diazirine)

Based on the precedent work, α -trifluoro diazirine has been chosen as a photoreactive molecule (Figure 43), because of the small molecule size and short irradiation time, which give use of this molecule more advantage.

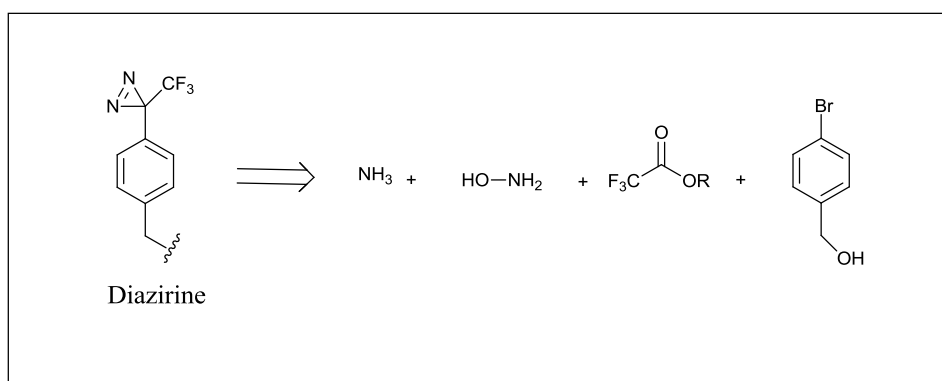
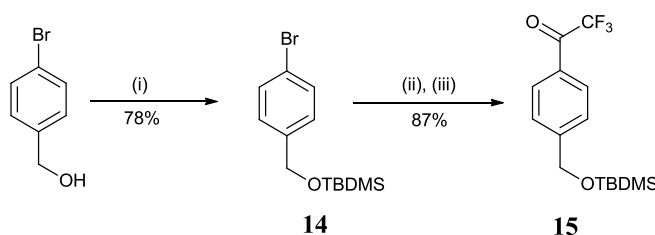


Figure 43 Retrosynthesis of diazirine

Following literature precedent, the preparation of diazirine started from commercially available 4-bromobenzyl alcohol. The synthesis commenced with protection of the hydroxyl group of the starting material by treatment with *tert*-butyldimethylsilyl chloride and imidazole to give silylether **14** in a good yield of 78%, after purification by flash chromatography.

Trifluoroacetylation was then investigated. The reported conditions¹⁷¹ of reaction with 1.1 eq *n*-BuLi with aryl bromide **14** for one hour and half and quenching with trifluoromethyl acetate gave only a low yield of ketone **15** with < 10% conversion of the starting material. Substitution of 1-trifluoroacetyl piperidine for trifluoromethyl acetate had no effect and the yield remained poor with low conversion. In order to improve the transmetalation step, the reaction time and molar equivalence of *n*-BuLi were increased to 5 eq and the reaction time increased to 4 hours. Subsequent treatment with excess of trifluoro acetate led to high conversion and good yield (87%) of ketone **15** after

chromatography. The addition of 2 and 3 equivalents of n-BuLi did not enhance the yield. The structure of product **15** was confirmed from ^1H NMR data and showed that the aromatic protons chemical shift changed from 7.16 and 7.41 ppm for **14** to 7.53 and 8.07 ppm for **15**. The presence of the CF_3 group was apparent in the ^{13}C NMR spectrum and a quartet was observed at chemical shift with $^1J = 180$ Hz belonging to CF_3 . The reaction was most easily monitored by ^{19}F NMR data which showed a single peak at δ_{F} : -71.2 ppm (Scheme 3.1).



Scheme 3.1: *Reagents and conditions:* (i) TBDMS-Cl, imidazole, DMAP, DCM, 20 h; (ii) n-BuLi, THF, -78 °C; (iii) methyl trifluoroacetate, -78 °C.

With ketone **15** in hand, elaboration to diazirine was carried out by condensation of the ketone **15** with hydroxylamine in pyridine, to give hydroxyl oxime **16** as a single diastereoisomer in a yield of 86% after chromatography. The product structure was confirmed from ^1H NMR data where it is clear that there the OH functionality gives a relatively broad peak at 8.85 to 8.96 ppm. ^{13}C NMR data showed a quartet at 119.6 ppm belonging to CF_3 , and a quartet at 146.8 ppm for the (CCF_3) . The ^{19}F NMR showed a significantly shifted signal at -66.4 ppm compared with the starting material.

Based on precedent,¹⁷² the product **16** can be exist as either the *E/Z* diastereoisomer. Comparing to the ^{13}C chemical shift of CF_3 group of oxime analogues *E* and *Z*, $\delta_{\text{C}} = 119.6$ and 124 ppm respectively,¹⁷³ suggested that the compound **16** has the *E* configuration (Figure 44).

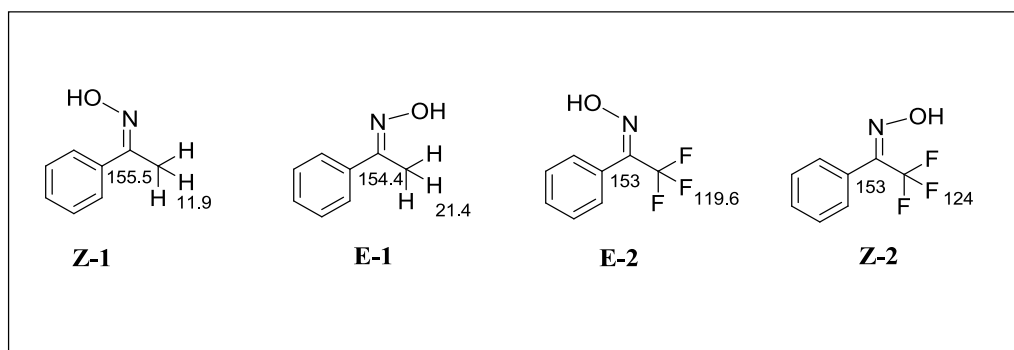
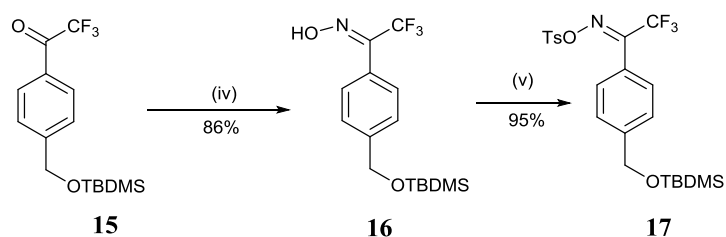


Figure 44 ^{13}C NMR for *E* and *Z* diastereoisomer

Tosylation of **16** with *p*-toluenesulfonyl chloride gave **17** in yield of 95% after purification by column chromatography, which was confirmed from ^1H NMR data that showed a single peak belonging to the tosyl methyl group at 2.35 ppm (Scheme 3.2).



Scheme 3.2: Reagents and conditions: (iv) $\text{H}_2\text{NOH} \cdot \text{HCl}$, pyridine, EtOH, 12 h; (v) TsCl, CH_2Cl_2 , Et_3N , DMAP.

Product **17** was then treated with liquid ammonia to yield diaziridine **18** in yield of 63% after chromatographic purification. The identity was confirmed from the ^1H NMR data using d -chloroform where two doublet peaks at 2.20 and 2.76 ppm belonging to HN-NH functionality can be seen. Because of these separate doublet peaks, those protons are in opposite sides on the diaziridine ring as in **S3** and **S4** and the compound exists as a pair of C_2 -symmetric conformer, shown in Figure 45, also, the ^{13}C NMR spectrum showed quartet peak at 58 ppm belonging to CF_3 and the ^{19}F NMR showed single peak at δ_{F} -75.5 ppm.

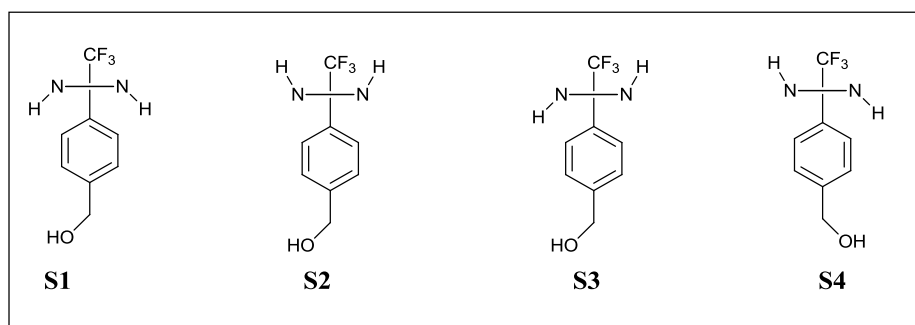
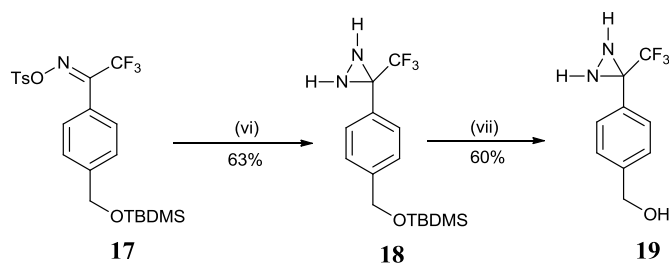


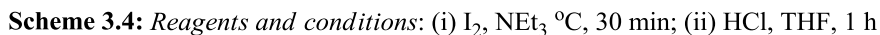
Figure 45: Symmetric possible isomers of compound **19**

A successful cleavage of the *tert*-butyldimethylsilyl protection group was obtained by treatment of diaziridine **18** with TBAF, in the presence of water to give 60% of the hydroxyl diaziridine **19** (Scheme 3.3). Structure of product **19** was evidenced from the absence of the signals in the ^1H NMR data related to the *tert*-butyldimethylsilyl protection group, while a peak at 1.82 ppm was observed belonging to the OH group using d-chloroform and a similar confirmation of HN-NH protons was obtained.

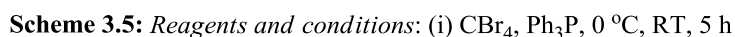


Scheme 3.3: Reagents and conditions: (vi) liquid NH_3 , THF, -78°C , 3 h; (vii) 0.1 M TBAF in THF, RT, 5 h

Finally the diazirine was prepared via a successful oxidation of diaziridine **18** with molecular iodine, and diazirine **20** was obtained in good 61% yield. Deprotection of diazirine **20** by treatment with TBAF, in the presence of water led to less than 50% conversion. A successful cleavage reaction was achieved by a treatment of 4M HCl in dioxane and yielded compound **21** as pale yellow oil in a good 81% yield (Scheme 3.4).



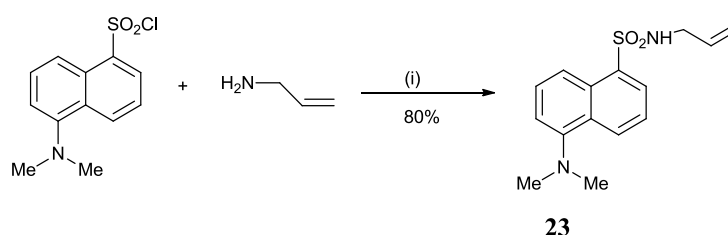
Bromo diazirine **22** was prepared by reacting hydroxyl diazirine **21** with carbon tetrabromide in presence of triphenylphosphine and gave the desired product in an excellent yield of 96% after the purification (Scheme 3.5). The ^{13}C NMR spectrum showed a diagnostic peak at 31.9 ppm for the Br-CH₂ in place of 64.4 ppm for HO-CH₂.



84

represents a compromise in fluorescent performance but provide access to the required sulfonamide functionality.

To test the feasibility of the linking strategy, allyl dansyl sulfonamide **23** was initially prepared as model compound. Commercially available dansyl chloride was reacted with allyl amine, in presence of triethylamine and DMAP, to give sulfonamide **23** in a yield of 80%. The product was easily confirmed from the ^1H NMR spectrum due to the peaks belonging to the vinyl functionality at δ_{H} : 4.86, 5.06 ppm and 5.53 ppm. The introduction of this functionality gives the opportunity to potentially apply coupling reactions on the terminal vinyl group, for example by Grubbs metathesis reactions, and provides a good handle for spectroscopic identification in the subsequent reactions (Scheme 3.6).



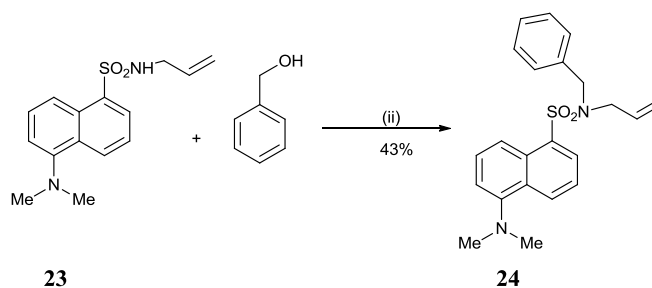
Scheme 3.6: Reagents and conditions: (i) Et_3N , DMAP, DCM, 0 °C RT, 3:30 h

3.2.3 Coupling barb with molecule of fluorescent tag and linker

3.2.3.1 Reaction with diazirine

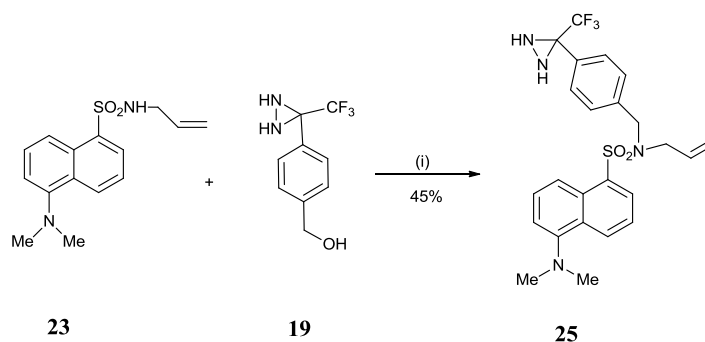
Due to the concerns about the general stability of the photoreactive diazirine ($-\text{N}=\text{N}-$) moiety, initial coupling of the dansyl sulfonamide **23** to this component focused on coupling with the precursor diaziridine ($\text{HN}-\text{NH}$) **19**. It was envisaged that the hydroxyl group of the diaziridine **19** could be activated to couple with the sulfonamide nitrogen in the presence of the two nucleophiles $\text{HN}-\text{NH}$ of diaziridine **19**, under Fukuyama/Mitsunobu conditions.¹⁷⁴ Furthermore, this coupling reaction had the

advantage of using the unoxidised diaziridine (HN-NH) compound with the benzylic OH group directly prior to conversion to the potentially unstable final diazirine product. A model Fukuyama/Mitsunobu reaction using benzyl alcohol in place of diaziridine **19** was applied to verify the reaction reliability before using the valuable prepared diaziridine **21**. Sulfonamide **23** was reacted with benzyl alcohol in the presence of DEAD and triphenylphosphine at room temperature. This protocol afforded sulfonamide **24**, in a yield of 43% after chromatographic purification. The product was confirmed from the ^1H NMR data which showed a diagnostic peak belonging to CH_2 of the benzyl group at 4.3 ppm (Scheme 3.7).



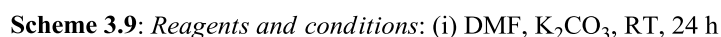
Scheme 3.7: Reagents and conditions: (ii) DEAD, Ph_3P , RT, 4 h

Based on these results, successful coupling of the diaziridine **19** was then achieved by treatment sulfonamide **23** with diaziridine **19** under the established conditions to give product **25** in yield of 45% after chromatography. The product **25** was confirmed from the ^1H NMR spectrum which shows a peak at 4.4 ppm belonging to CH_2 of the diaziridine, and the ^{19}F NMR spectrum which showed a single peak at -75.4 ppm (Scheme 3.8).



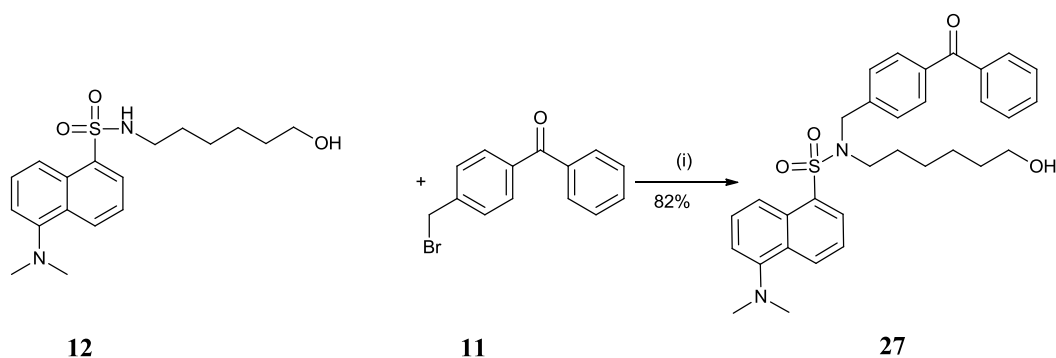
Scheme 3.8: Reagents and conditions: (i) DEAD, Ph_3P , RT, 4 h

While successful the Fukuyama/Mitsunobu conditions did not give very good conversion and yield using a reaction of diazirine **21**, alternative method was investigated by converting the hydroxyl group of diazirine **21** to a bromide, by treatment with carbon tetrabromide and triphenylphosphine, to produce 3-(α -bromo-4-tolyl)-3-(trifluoromethyl)-3H-diazirine **22** in yield of 96 % (Scheme 5). The ^{13}C NMR spectrum was diagnostic and a significant shift for the CH-OH 67.8 to 32.0 ppm for CH-Br indicated a successful conversion. The ^{19}F signal remained the same at -65 ppm indicates the presence of the diazirine group. Bromide **22** was then applied in a further coupling step with the sulphonamide **12** under mild conditions and gave product **26** in a good yield of 88%. The product structure was confirmed from the ^1H NMR spectrum with the disappearance of the signals belonging to $\text{SO}_2\text{N-H}$ proton at 5.09 ppm and the spectra were consistent with the structure of compound **26**. The ^{13}C NMR spectrum showed the $\text{CH}_2\text{-N}$ chemical shift at 51 ppm, significantly different to 36.6 ppm for the $\text{CH}_2\text{-Br}$ of the starting material. The ^{19}F NMR spectrum showed same single peak at -65.0 ppm for the diazirine **22**, confirming that the diazirine function remained intact. High resolution mass spectrum analysis has also confirmed the compound structure (Scheme 3.9).



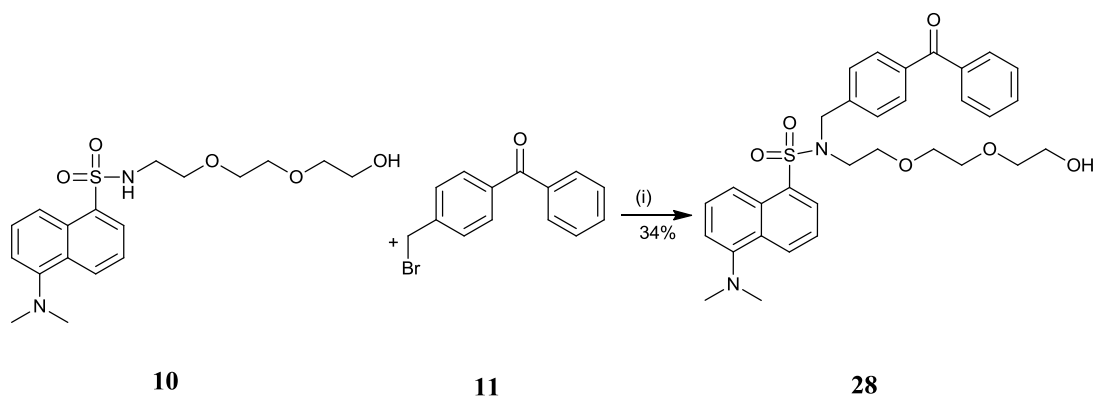
After the successful coupling of the diazirine photophore **22** with the fluorescent tag **12**, the coupling of a benzophenone photophore was investigated in order to assess the influence of the variation of the photophore nature on binding to the biomolecule targets. Moreover, two kinds of linkers (alkyl, PEG), which are already attached with the fluorescent tag, were investigated as well.

i) Initially simple alkyl chain substituted dansyl amide **12** was reacted with commercially available 4-(bromomethyl)benzophenone **11** in presence of potassium carbonate in DMF, to give molecule **27** in yield of 82 % (Scheme 3.10). Spectroscopic data was consistent with the structure shown.



Scheme 3.10: Reagents and conditions: (i) DMF, K₂CO₃, RT, 24 h

ii) Dansyl amide-PEG linker **10** was reacted with a commercially available 4-(bromomethyl)benzophenone **11** and potassium carbonate in DMF, gave molecule **28** in yield of 34 % (Scheme 3.11). The product was evidenced from the ¹H NMR spectrum which showed a significant shifting of a singlet peak from 4.51 ppm for the benzophenone CH₂-Br to 4.66 ppm for Ar-CH₂-N confirmed the alkylation reaction. Also the ¹³C NMR spectrum showed a peak for the Ar-CH₂-N at 51.7 ppm instead of 36 ppm for CH₂-Br group of the starting material and a peak for the carbonyl group at 196.2 ppm. Another confirmation was obtained from the HR-MS analysis which was consistent with the proposed structure.



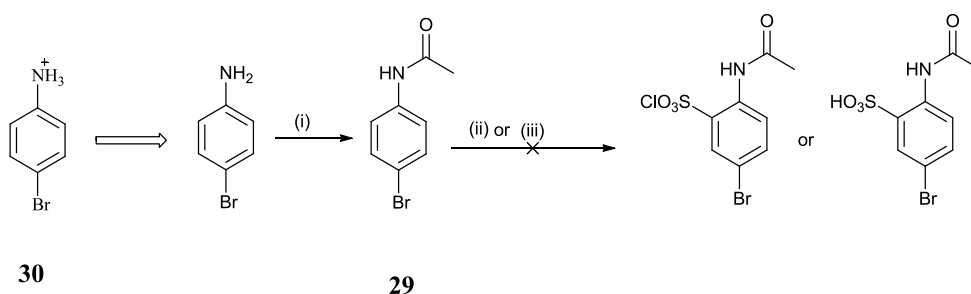
Scheme 3.11: Reagents and conditions: (i) DMF, K₂CO₃, RT, 24 h

3.2.4 Preparation of substituted diazoxides as “baits”

Having prepared a number of photoreactive fluorescent components, synthetic work then turned to the synthesis of active diazoxide analogues suitable for linking with these components.

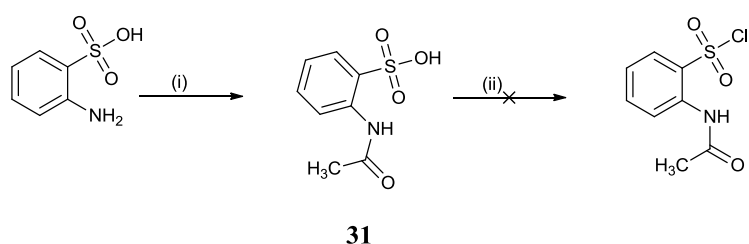
Preliminary studies focussed on the synthesis of a range of diazoxide analogues, to identify a suitable site for attachment of the fluorescent probe. A general synthesis for the preparation of diazoxide from substituted aniline was pursued. 4-Bromoaniline was chosen as a starting material and it was envisaged that a sulfonation reaction would install the sulfonyl group *ortho* to the amino group, giving the amino sulfonic acid needed to make the required diazoxide. The bromo-substituted material was also chosen because a variety of functionality can be obtained; for instance, the bromide group can be converted to a vinyl group, which after a hydroboration reaction would give the corresponding alcohol.

Commercially available 4-bromoaniline was converted to acetanilide **29** to moderate the reactivity since the protonated form **30** was more likely to be obtained from the starting material after treatment with an acid. Under a wide range of conditions the sulfonation¹⁷⁵ of the acetanilide **29** was unsuccessful and only returned starting material (Scheme 3.12).



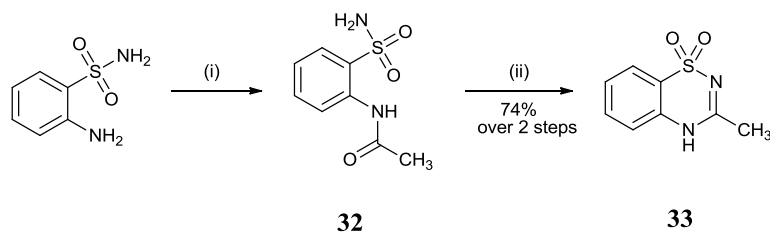
Scheme 3.12: Reagents and conditions: (i), AcOH, Ac₂O, 100 °C, 3 h; (ii) ClSO₃H, 60 °C, 2 h; (iii) H₂SO₄, 30% SO₃.

Sulfonation reaction on the bromoaniline was not a successful route. Therefore, a synthetic route starting from commercially available aniline-2-sulfonic acid was also investigated. The amine group of aniline-2-sulfonic acid was first converted to the acetamide **31** by a treatment with acetic anhydride. However, attempts to prepare the corresponding sulfonyl chloride were unsuccessful, with a variety of reagents (PCl_5 , SOCl_2 , ClSO_3H)¹⁷⁶ and wide range of temperatures and reaction times and the reactions generally returning starting materials (Scheme 3.13).



Scheme 3.13: *Reagents and Conditions:* (i) AcOH , Ac_2O , $100\text{ }^\circ\text{C}$, 3 h; (ii) PCl_5 or SOCl_2 or ClSO_3H , 50 to $70\text{ }^\circ\text{C}$, 1 h - 12 h

A successful preparation of the parent diazoxide structure was achieved starting from the more expensive but also commercially available 2-amino-benzenesulfonamide. This aniline was reacted with acetic anhydride in acetic acid at $100\text{ }^\circ\text{C}$ to give the amide **32**, which was treated with sodium hydroxide and then acidified with 2M hydrochloric acid to obtain the unsubstituted diazoxide **33** in 74% yield over two steps. The ^1H NMR data was consistent with the structure and a diagnostic resonance was observed for the NH at 12.0 ppm, while the ^{13}C NMR spectrum showed the $\text{C}=\text{N}$ resonance at 157.2 ppm (Scheme 3.14).

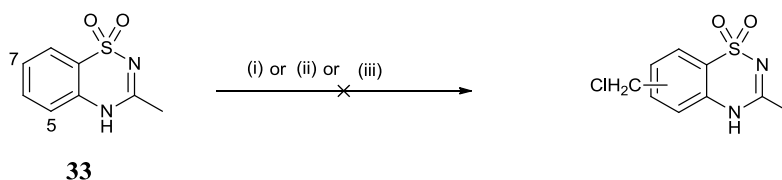


Scheme 3.14: *Reagents and conditions:* (i) AcOH, Ac₂O, 100 °C; (ii) 3% NaOH, 2N HCl

3.2.5 Substitutions on diazoxide

3.2.5.1- Halo alkylation reactions

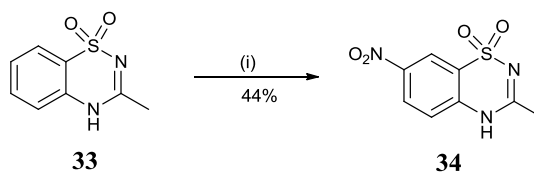
With unsubstituted diazoxide **33** in hand, elaboration to substituted diazoxides was investigated, initially via an alkylation reaction of the aromatic ring, with the substitution expected to occur to position 5 or 7 due to the amine functionality on the aromatic ring. However, all attempts at chloro-alkylation using para-formaldehyde and variety of reagents, such as zinc chloride with hydrochloric acid, zinc chloride with acetic acid and dichloromethyl methyl ether at variety different temperatures, were unsuccessful and the diazoxide **33** only returned starting material (Scheme 3.15). The low reactivity of this compound may be due to the dominant electron withdrawing effect of the SO₂ functionality; however the poor solubility of the compound may also be a contributing factor.



Scheme 3.15: *Reagents and conditions:* (i) HCHO, ZnCl₂, HCl, 60 °C, overnight; (ii) HCHO, ZnCl₂, AcOH, 60 °C, overnight; (iii) Cl₂CH-OCH₃, ZnCl₂, AcOH, 50 °C, overnight

3.2.5.2 Nitration reaction

In order to assess the reactivity of the diazoxide **33**, a nitration reaction was investigated by reacting **33** with concentrated nitric and sulfuric acid. This was successful, producing 7-nitro-diazoxide **34**, in a yield of 44%. This compound was readily identified from the ^1H NMR spectrum where three aromatic peaks can be seen with two doublets at 7.47 and 8.42 ppm and one singlet at 8.45 ppm, indicating substitution at the position 7. No product at position 5 was obtained. This nitration is useful in further elaboration but is not as good as bromination (Scheme 3.16).



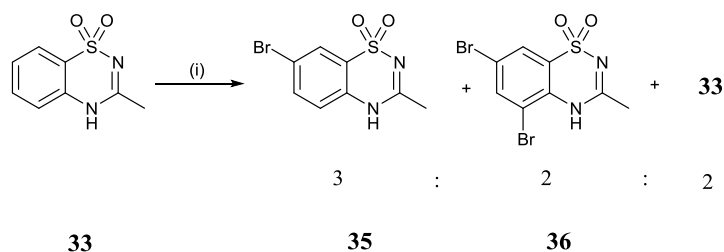
Scheme 3.16: Reagents and conditions: (i) HNO_3 , H_2SO_4 , 80 °C, 1h

3.2.5.3 Bromination reaction

While nitro-diazoxide **34** would allow access to substituted diazoxides, a more direct route is available from bromo-substituted material, which gives more opportunities for conversion to variety of different functional group. Studies focussed on finding a reliable bromination method.

Treatment of the diazoxide **33** with aqueous hydrobromic acid with H_2O_2 was not successful and the reaction returned starting materials. However, sodium bromate¹⁷⁷ proved a successful bromination reagent. Diazoxide **33** reacted with sodium bromate in sulfuric acid and sodium sulfate to give the monobromo **35** and dibromo **36**, along with unreacted starting material in ratio of 3:2:2, respectively. This result suggests that compound **35** is more reactive than **33** toward this reagent. After chromatography purification, dibrominated compound **36** was obtained in yield of 11%, characterised by ^1H NMR spectroscopy and the structure confirmed by X-ray crystallography (X-ray

data collected and solved by Prof J. D. Wallis) (Figure 46). However, diazoxide **35** could not be separated from residual starting material and this did not provide an effective route to 7-substituted diazoxides (Scheme 3.17).



Scheme 3.17: Reagents and conditions: (i) NaBrO₃, H₂SO₄, H₂O, Na₂SO₄, 50 °C, 5 h

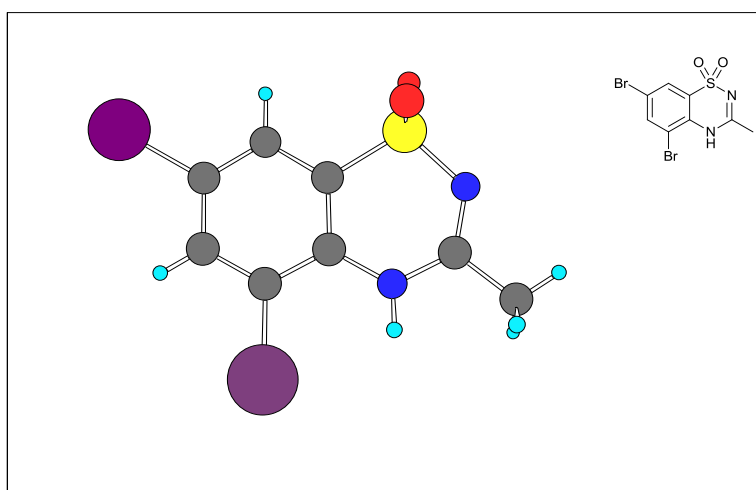
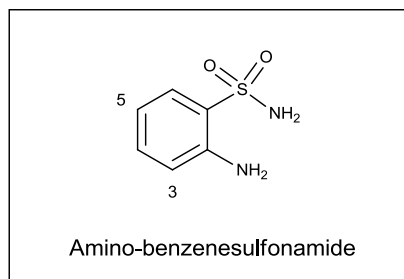


Figure 46 X-ray crystal structure of **36**

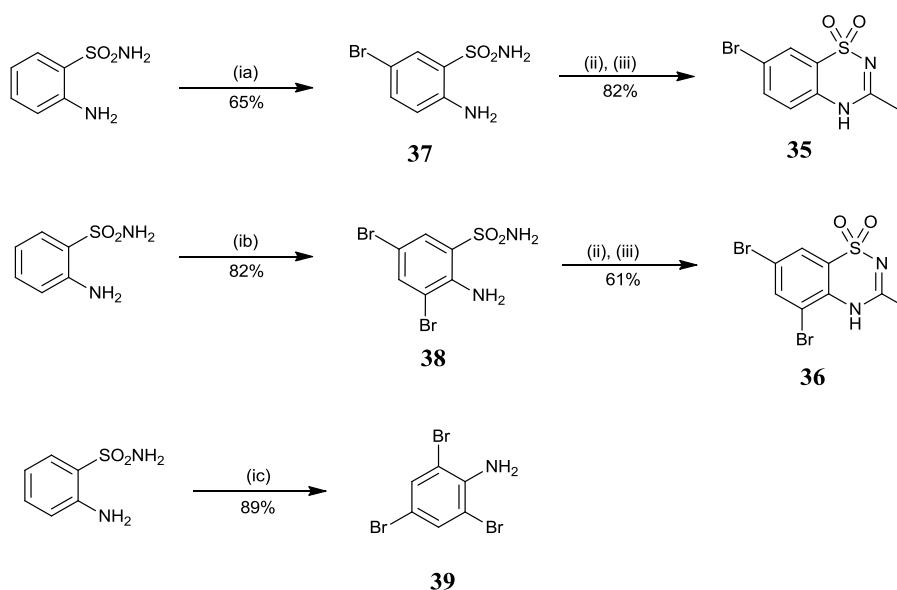
3.2.5.4 Preparation of 5'- and 7'-substituted diazoxides

Functionalization of the unsubstituted diazoxide **33** was found to be problematic due to a lack of reactivity and severely hampered by poor solubility of the diazoxides in most solvents. Therefore, it was decided to establish a general synthesis of halo-substituted diazoxide precursors for elaboration into the final product. To this end we sought to prepare chloro or bromo amino-benzenesulfonamide precursors at the 3 and 5 positions,

corresponding to the 5 and 7 positions for the final diazoxide molecule, expecting the reactivity would be directed to those positions by the effect of the amino and sulfonamide groups in the parent compound.



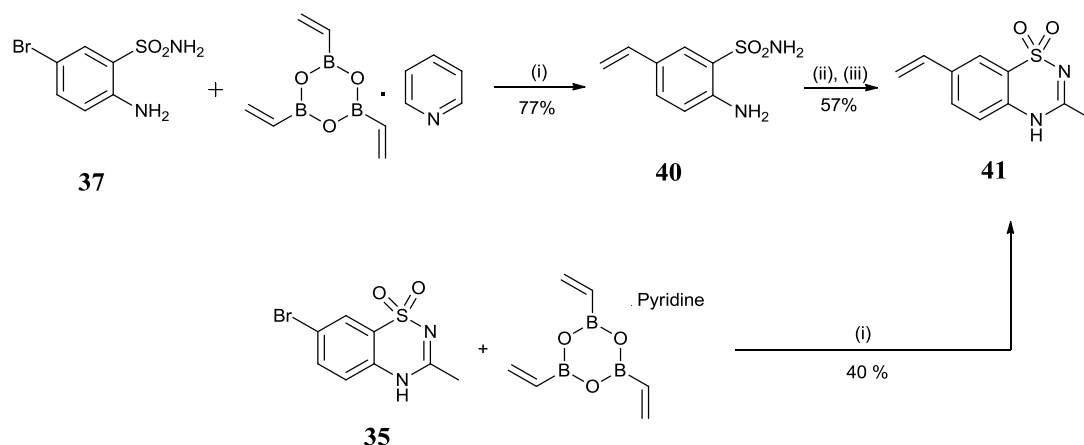
Building on this plan, 2-aminobenzenesulfonamide was used as diazoxide precursor and substitution reactions were successfully achieved. Treatment of 2-aminobenzenesulfonamide with hydrobromic acid (1eq),¹⁷⁸ in presence of hydrogen peroxide and water gave 2-amino-5-bromo-benzenesulfonamide **37** in a yield of 65% after chromatography. Furthermore, when the equivalents of hydrobromic acid were doubled, *di*-brominated **38** was formed exclusively in 82% isolated yield. When excess of the hydrobromic acid, with elevated temperatures, was applied the product was only *tri*-bromoaniline **39** in yield of 89%. Subsequently, compounds **37** and **38** were reacted with acetic anhydride, then with NaOH followed by HCl, to produce **40** and **41**, in yield of 82% and 61% respectively, the structure of which were confirmed from the ¹H NMR spectroscopy and HR-MS data (Scheme 3.18).



Scheme 3.18: Reagents and conditions: (i) HBr (aq), (a) 1eq, (b) 2eq, (c) excess, H₂O₂, H₂O, 60 °C, 15 min; (ii) Ac₂O, AcOH, 110 °C, 1h; (iii) 3% NaOH, 2M HCl, RT, (iv) HBr (aq, excess), H₂O₂, H₂O, 80 °C, 30 min

3.2.5.5 7-Vinyl-diazoxide 43

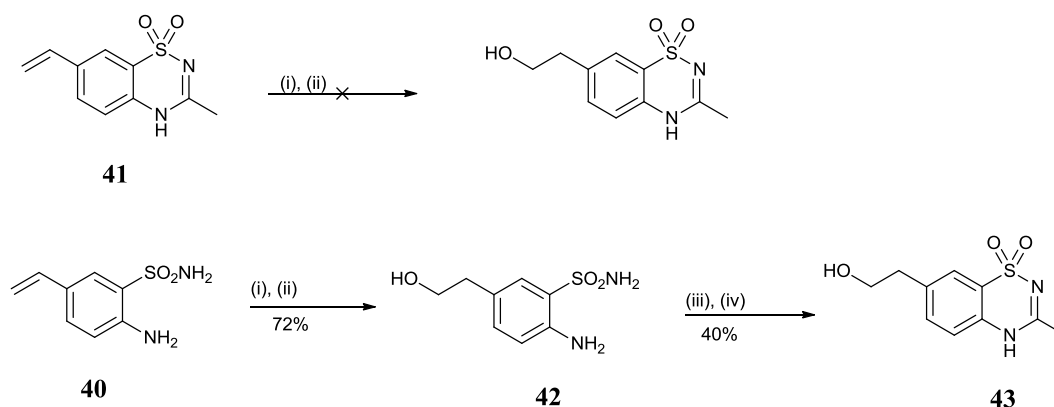
In order to prepare a variety of functionalised diazoxide analogues suitable for linking, the introduction of an appropriate group was again pursued. 2-Amino-5-bromobenzenesulfonamide **37** was reacted with 2,4,6 trivinylcyclotriboroxane-pyridine complex in presence of tetrakis(triphenylphosphine)palladium(0) and potassium carbonate,¹⁷⁹ to give the vinyl compound **40**, in a yield of 77% after purification. The product was confirmed from the ¹H NMR spectrum where the two doublets at 5.02, 5.54 ppm and one doublet-doublet (dd) at 6.57 ppm belonging to the vinyl group were apparent. The conversion of the bromide to a vinyl group offers a variety of opportunities for further functionalization. Compound **40** was then reacted with acetic anhydride and then treated with NaOH followed by HCl to give pure diazoxide **41** in yield of 57%, which was confirmed from the ¹H NMR data and HR-MS. The similar vinylation reaction of diazoxide **35** produced vinyl-diazoxide **41** in a poorer 40 % of yield (Scheme 3.19).



Scheme 3.19: Reagents and conditions: (i) $\text{Pd(PPh}_3)_4$, K_2CO_3 , DME, 80 °C, overnight; (ii) Ac_2O , AcOH, 110 °C, 1 h ; (iii) 3% NaOH, then 2M HCl, RT

3.2.5.6 Conversion of vinyl group to the corresponding alcohol-diazoxide **45**

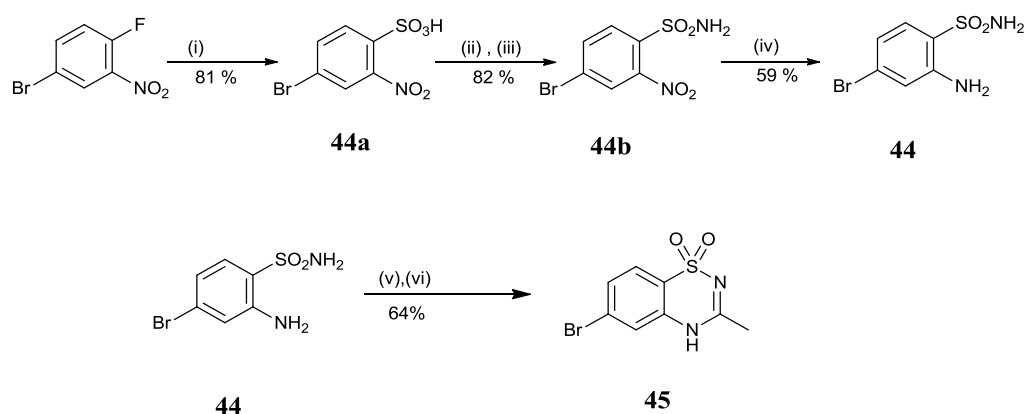
With the vinyl-products **40** and **41** in hand the hydroboration/oxidation¹⁸⁰ of these materials was explored using 9-BBN followed by oxidation with peroxide. In the event hydroboration/oxidation of diazoxide **41** returned starting material, however, treatment of the vinyl compound **40** under the same conditions gave the alcohol **42** in yield of 72%. This compound **42** was reacted with acetic anhydride and then treated with sodium hydroxide followed by hydrochloric acid and produced diazoxide **43** in an overall yield of 40% (Scheme 3.20).



Scheme 3.20: Reagents and conditions: (i) 9-BBN in THF, 25 °C, 12 h; (ii) NaOH (1M), H₂O₂ (30%); (iii) Ac_2O , AcOH, 110 °C, 1 h; (iv) 3% NaOH, then 2M HCl, RT

3.2.5.7 6-Bromo-diazoxide 45

Preparation of diazoxide functionalised at the 6 position was then performed. The 4-bromo derivative of 2-aminobenzenesulfonamide **44**, was prepared in a three step reaction,¹⁸¹ starting from commercially available 4-bromo-1-fluoro-2-nitrobenzene by reaction with aqueous sodium sulfite, followed by treatment with concentrated hydrochloric acid, to give 4-bromo-2-nitrobenzenesulfonic acid **44a**. Compound **44a** was reacted with thionyl chloride and DMF to afford intermediate, 4-bromo-2-nitrobenzenesulfonyl chloride, which was then treated with ammonia to yield 4-bromo-2-nitrobenzenesulfonamide **44b**, which was then reduced to yield the title compound **44** in 59% yield after chromatography. The obtained product was then elaborated in the usual way to produce pure diazoxide **45**, in yield of 64% (Scheme 3.21).

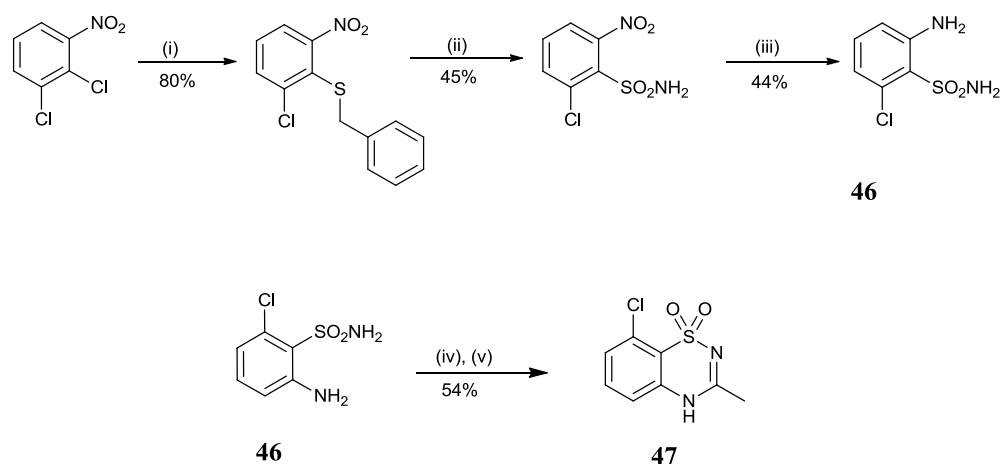


Scheme 3.21: *Reagents and conditions:* (i) Na_2SO_3 , EtOH, H_2O , 70 °C, 24h, conc HCl; (ii) SOCl_2 , DMF, 90 °C, 2h; (iii) gaseous NH_3 , CHCl_3 , -40 °C, 30 min, HCl conc.; (iv) HI, 90 °C, 24 h, $\text{Na}_2\text{S}_2\text{O}_3$, Na_2CO_3 ; (v) Ac_2O , AcOH, 110 °C, 1h ; (vi) 3% NaOH, 2M HCl, RT

3.2.5.8 8-Chloro-diazoxide 47

For the preparation of 8-chlorodiazoxide **47**, commercially available 1,2-chloro-3-nitrobenzene was reacted with benzyl mercaptan (freshly prepared) to produce 2-(benzylsulfanyl)-1-chloro-3-nitrobenzene.¹⁷⁰ Oxidation of this material with chlorine gas presumably afforded an intermediate sulfonyl chloride, which was treated directly with

aqueous ammonia to give 6-chloro-2-nitrobenzenesulfonamide. This compound was then reduced with iron powder and ammonium chloride to yield the title compound **46**, in 44% yield, which was reacted with acetic anhydride, then NaOH followed by HCl, to produce **47**, in yield of 54% (Scheme 3.22).



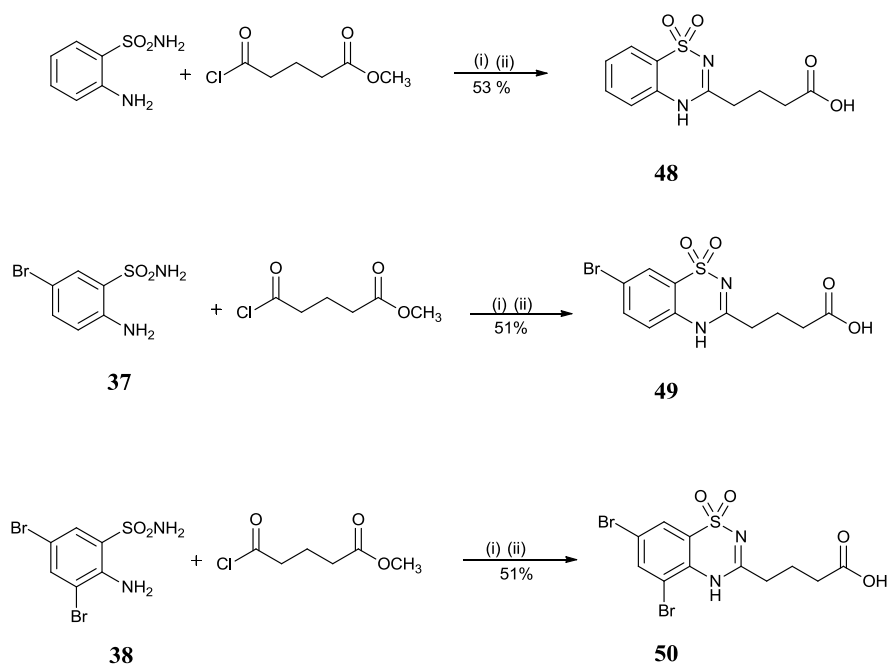
Scheme 3.22: *Reagents and conditions:* (i) $\text{C}_6\text{H}_5\text{CH}_2\text{SH}$; reflux 2 h; (ii) Cl_2 , AcOH , H_2O , 1h, NH_4OH , dioxane, 30 min; (iii) $\text{Fe}(0)$, NH_4Cl , EtOH , H_2O , reflux, 1h; (iv) Ac_2O , AcOH , 110°C , 1h ; (v) 3% NaOH , 2M HCl , RT

3.2.5.9 Preparation of C-3 side chain diazoxides

As well as preparing analogues substituted on the aromatic ring, hetero ring side chain analogues were also prepared. In order to prepare these, the unsubstituted and bromo-substituted 2-amino-benzenesulfonamides, **37** and **38** were reacted with glutaric acid monomethylester chloride.¹⁸² The amide products obtained were then treated with sodium hydroxide, followed by acidification with hydrochloric acid to give the corresponding diazoxides **48**, **49** and **50** in yield of 53%, 51% and 51% respectively. In all cases the cyclization was accompanied by ester hydrolysis, which resulted in production of the corresponding carboxylic acids (Scheme 3.23).

Pure products were obtained after washing the crude materials with ether. The structure of all three products were evident from the ^1H NMR spectra, where in the case of **48**,

resonances at 1.89, 2.32 and 2.59 ppm indicated an aliphatic chain, while those at 11.96 and 12.14 ppm indicated NH and OH groups, respectively. In addition, **49**, **50** showed signals at 1.75, 2.19 and 2.47 ppm for the aliphatic chain and 2H signal at 12.03 ppm for NH and OH functionalities. In contrast to the literature precedent, dioxane was used as a reaction solvent instead of DMF, which is hard to evaporate and remove from the final product.



Scheme 3.23: Reagents and conditions: (i) dioxane, 35 °C, 1h; (ii) 3%NaOH, 45 min, 2M HCl

3.2.6 Biologically active testing for the modified diazoxide results

Having prepared a variety of diazoxide analogues which display additional functionality in varying positions around the parent diazoxide skeleton, an assay of the biological activity of these analogues was carried out. The cardioprotection activity of the analogues were assessed by incubation with myocardial slices from the human right atrial appendage, in ischaemia/reperfusion experiments and the viability of the treated

tissue was determined as described in literatures.^{183, 184} Two biological assays were used to determine cell viability, lactic acid dehydrogenase activity (LDH) assay,¹⁸⁵ and MTT (3-[4,5-dimethylthiazol-2-yl]-2,5 diphenyl tetrazolium bromide) assay for cell viability. These assays were performed in collaboration with Dr Manuel Galiñanes, Department of Cardiac Surgery, Area University Hospital Vall d'Hebron Pg, Spain.

3.2.6.1 LDH assay

Lactate dehydrogenase (LDH) is a cellular enzyme which is released into the culture medium as a result of cell death caused by apoptosis or necrosis. LDH activity, therefore, can be used as an indicator of cell death and is used as a general means to evaluate cytotoxicity resulting from different cell treatment factors. Cayman's LDH cytotoxicity assay measures LDH activity present in the culture medium using a coupled two-step reaction. In the first step, LDH activates the reduction of NAD^+ to NADH and H^+ by oxidation of lactate to pyruvate. In the second step, a diaphorase enzyme, using NADH and H^+ , reduces the tetrazolium salt to intensively coloured formazan, then the coloured product can be measured colorimetrically with the intensity of the colour indicating how much damaged tissue or cell death is present (Figure 47). This assay is a general indicator of the presence of dangerous, acute, or chronic, tissue damage and sometimes also used to help diagnose and monitor a heart attack.

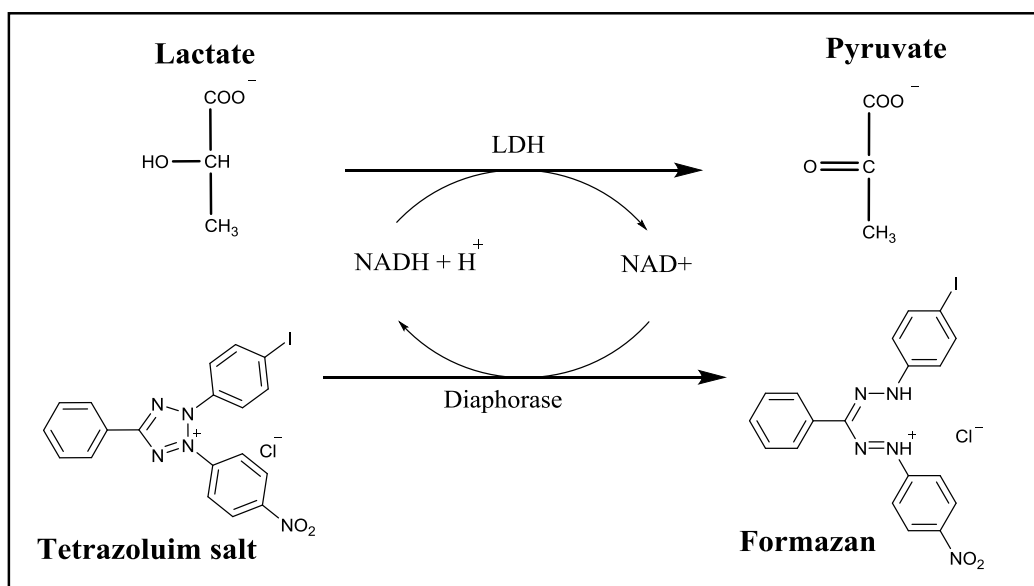


Figure 47 Mechanism of LDH assay

3.2.6.2 MTT assay

The MTT-[3-(4,5-dimethylthiazol-2-yl)-2,5-diphenyl-tetrazolium bromide] colorimetric assay has been described by Mosmann *et al.* (1983).¹⁸⁶ This assay can be used for determining the number of living cells by following the reduction the yellow tetrazolium salt to insoluble purple formazan salt by mitochondrial succinate dehydrogenase, and is a measure of residual mitochondria activity. The enzyme is produced by viable cells and the quantity of formazan produced is relative to the number of living cells present (Figure 48). Results are obtained via a simple colorimetric assay.

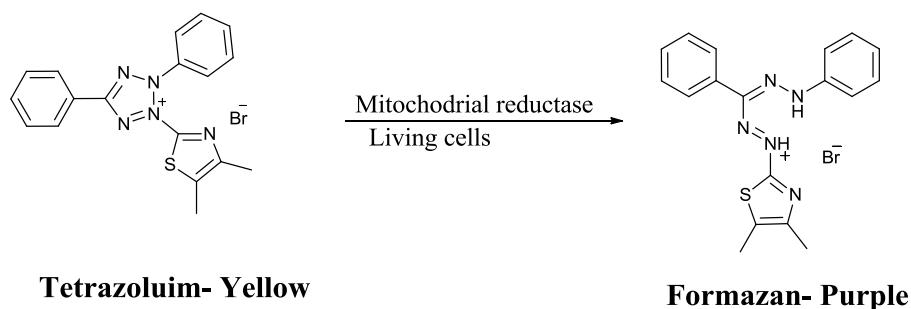


Figure 48 Reduction of MTT to Formazan

Ischaemic reperfusion experiments were performed in the presence of all the diazoxide analogues (Figure 49) six times (n=6), except for analogue **50** which was tested twice (n=2). As controls, unmodified ischaemia reperfusion (I/R) experimental were performed along with an ischaemic preconditioning experiment. The results of the LDH assays confirm that IP (preconditioning) reduces cell death and the mean values in this assay were approximately one of third of that observed in ischaemia reperfusion control (I/R). In general terms for the analogues tested, the mean LDH values vary greatly from a reduction comparable to that seen in the IP group for compounds **43** and **47**, to a negligible effect for compounds **33** and **36** (Figure 50).

The MTT assay control experiments also confirmed the protective effect of the IP protected. However, this assay suggests high levels of cell death in the ischaemia reperfusion control experiments than indicated by the LDH assay. The MTT assay results for the diazoxide analogues indicate significantly more modest protection for near all compounds when compared to I/R group. The results do not directly follow those obtained by the LDH assay. In this assay compound **35** was the only analogue showing cell viability comparable to the protective control. This compound has a very similar structure to the parent cardioprotection diazoxide, but with a direct replacement of chloride for bromide in position 7 (Figure 49).

Taking both sets of assay results into account a number of conclusions can be drawn:

- i) All the analogues provide a varying positive protective effect except for analogue **36**, which did not show a clear response assumed by both assays and has two bromo substitutions in positions 5 and 7. This negative result suggests that the protection activity may be lost when both positions 5, 7 are substituted.

- ii) The analogues **43** and **47** showed a significant reduction in the death measured by the LDH assay in contrast to a moderate cell protection as determined from the MTT assay.
- iii) A comparison between the activity of the analogues with alkyl carboxylic groups at position 3 (analogues **48** and **50**) with those with a methyl group in the same position indicate that the extended side chain is not detrimental to activity as assessed by the LDH assay. The MTT assay results are less conclusive (Figure 50).

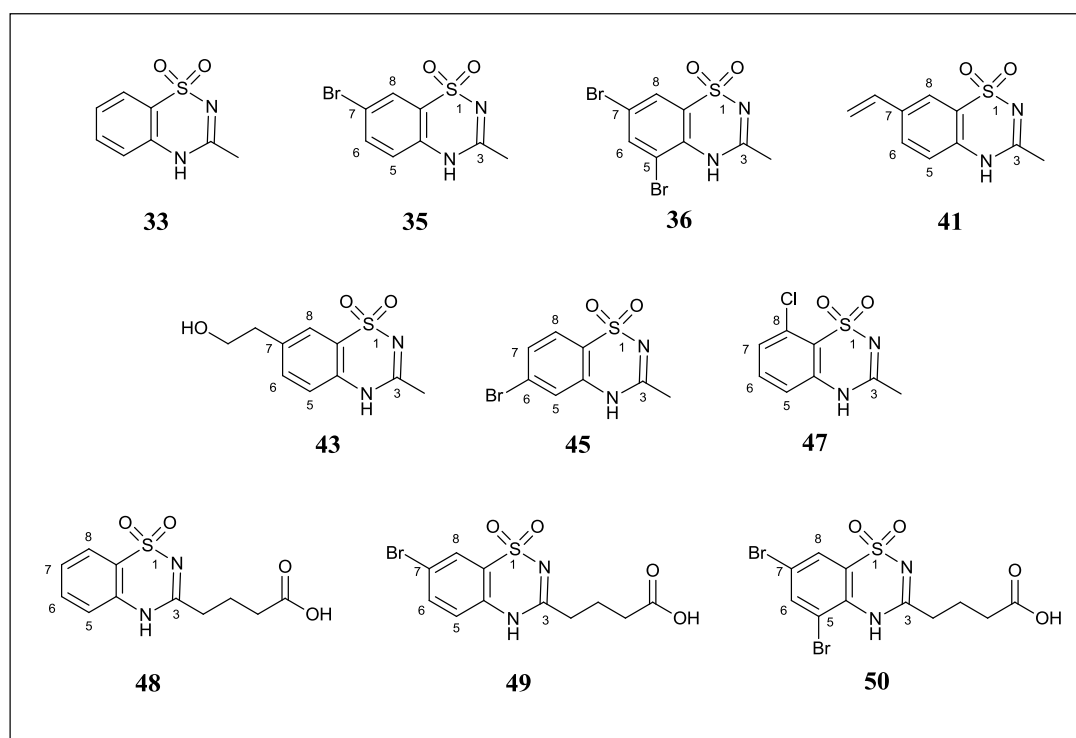


Figure 49 *Diazoxide analogues tested in cell viability assays*

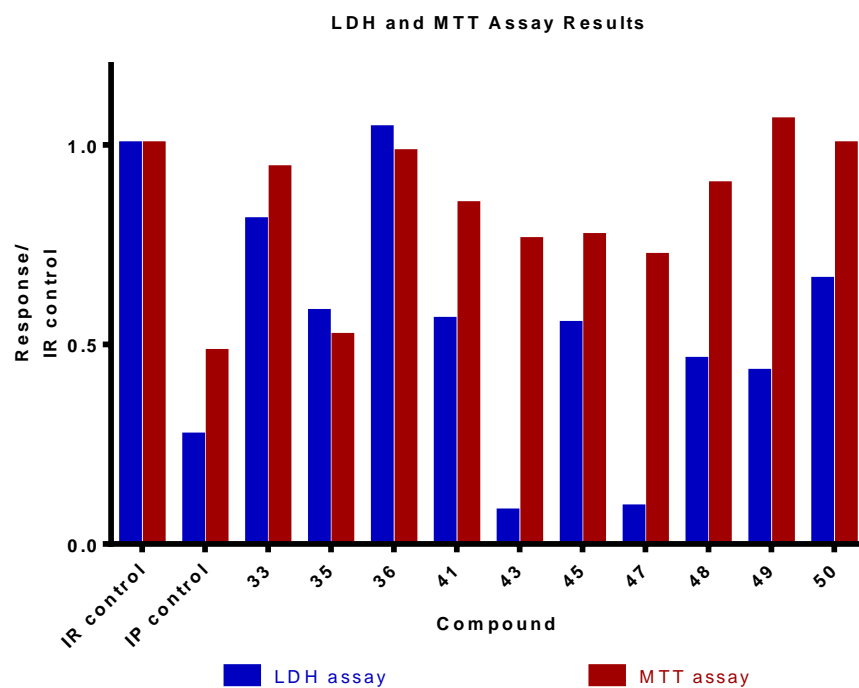


Figure 50 *LDH and MTT Assays Results; Ischaemic reperfusion experiments were performed in the presence of all the diazoxide analogues six times (n=6), except for analogue 50 which was tested twice (n=2).*

3.2.7 Fully functionalised diazoxide tagging molecules

Based on the above biological testing results, the most active analogues **43** and **47** were identified as the most promising analogues for further elaboration to the fluorescent/photoaffinity hybrid molecule. Analogue **43** has a hydroxyethyl group in position 7 which was initially installed as a handle for linking to the other components. Given that retention of activity might be expected as this group is increased in size, one proposal is to link the other components via this hydroxyl group.

For the analogue **47**, the presence of a chloro group at position 8 led to an increase in activity and elaboration of this molecule may be beneficial. However no suitable functionality for linking is present in this molecule, and given the activity of analogues **48** and **50**, it was decided to elaborate via installation of alkyl carboxylate in position 3 (Figure 51).

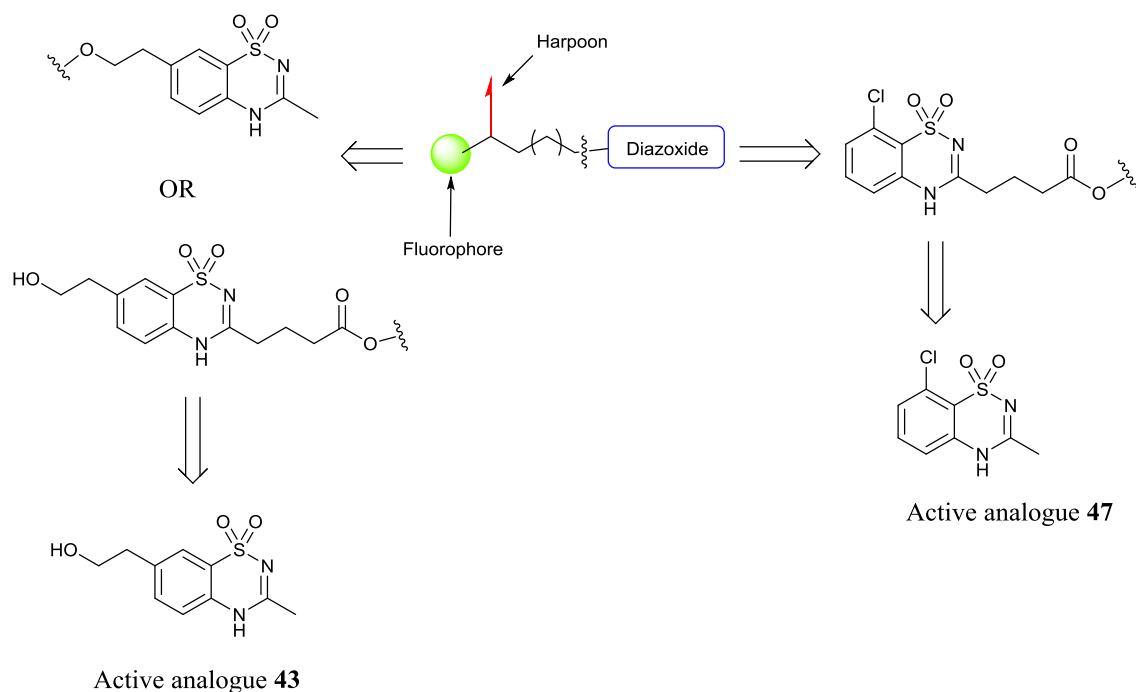
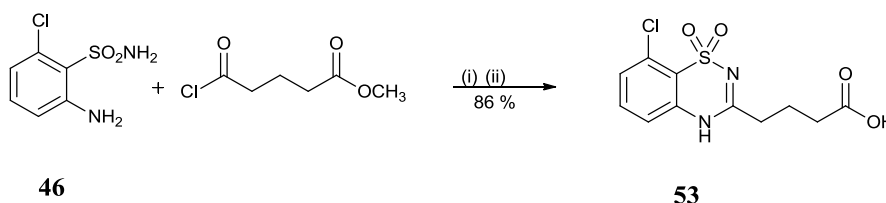


Figure 51 Elaboration plan for the analogues **43** and **47**

3.2.7.1 8-Chloro diazoxide-alkyl linker-benzophenone-dansylamide molecule

The preparation of the side chain carboxylic acid analogue of active compound **47** was then pursued. First step was to prepare the diazoxide with a side carboxylic chain by the same method as previously employed for diazoxide **48**. Thus, compound **46** was reacted with glutaric acid monomethylester chloride,¹⁸² and the intermediate amide was treated with sodium hydroxide, followed by acidification with hydrochloric acid, to give the diazoxide **53** in 86% yield (Scheme 3.24).

The identity of product **53** was easily confirmed from the ¹H NMR spectrum by the NH proton at 12.31 ppm, with no presence of the peaks belong to the NH₂ protons of the amine and sulphonamide. In addition, the ¹³C NMR spectrum showed diagnostic signals for the C=N at 117 ppm and C=O of the carboxylic acid at 173.9 ppm.



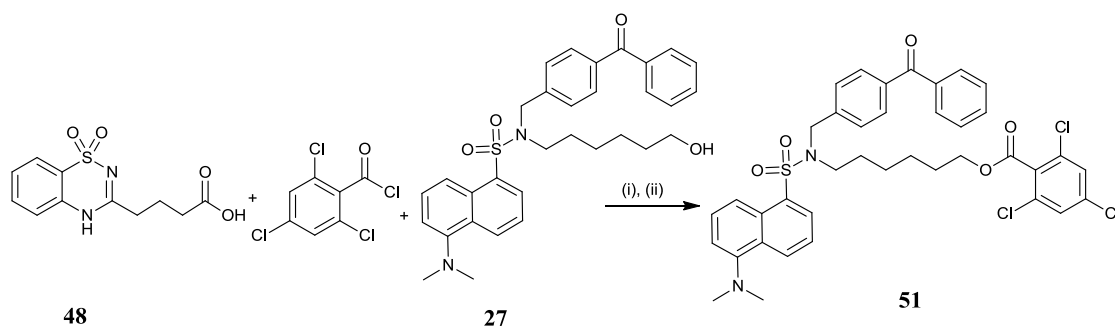
Scheme 3.24: Reagents and conditions: (i) dioxane, 35 °C, 1h; (ii) 3%NaOH, 45 min, 2M HCl

3.2.7.2 Coupling of the 8-chloro-diazoxide **48** with the hybrid molecule **27**

Having prepared compound **53**, coupling to the other components was explored. Given the long synthetic route to **43**, coupling of **47** was first explored. In a preliminary study, the more readily available diazoxide analogue **48** was used as a model compound for establishing an esterification method. A variety of different esterification conditions were tried, initially using a Brønsted acid. Treatment of diazoxide carboxylic acid **48** and hybrid molecule **27** with a catalytic amount of concentrated sulphuric acid in THF

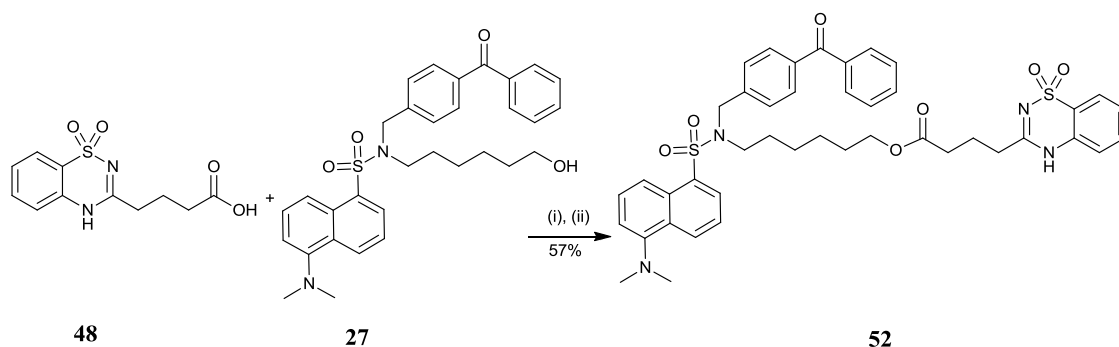
and heating at reflux for 4 hours, gave no evidence of the desired ester and returned starting materials.

Activation of the carboxylic acid was the explored using the Yamaguchi esterification method. Following the method of Dhimitruka,¹⁸⁷ diazoxide **48** was treated with 2,4,6-trichlorobenzoyl chloride, triethylamine and 4-dimethylaminopyridine for four hours, followed by alcohol **27**. However this procedure afforded only ester **51**, with no evidence of the desired coupling product. Presumably the initial formation of the intermediate anhydride was not rapid and the acid chloride preferentially reacted with alcohol **27** (Scheme 3.25).



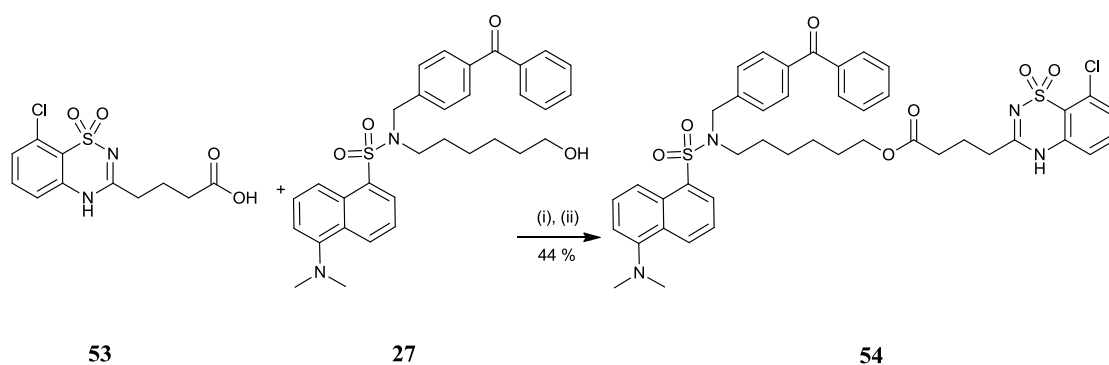
Scheme 3.25: Reagents and conditions: (i) DMF, Et₃N, DMAP, 20 °C, 4 h; (ii) DMF, DMAP 20 °C, Overnight

Pleasingly coupling was achieved by activation of the carboxylic acid using *p*-toluenesulfonyl chloride, triethylamine and 4-dimethylaminopyridine.¹⁸⁸ The reaction of *p*-toluenesulfonyl chloride with diazoxide **48** in presence of triethylamine and 4-dimethylaminopyridine for 45 minutes followed by addition of hybrid molecule **27** produced the desired ester **52** in yield of 57%. The identity of coupled product was confirmed from the ¹H NMR spectrum which showed a triplet peak at 3.81 ppm arising from the CH₂ group adjacent to the ester oxygen. The ¹³C NMR spectrum gave diagnostic peaks at 64.5 and 173.1 ppm (Scheme 3.26).



Scheme 3.26: Reagents and condtions: (i) TsCl, Et₃N, DMAP, 0 °C, 45 Min; (ii) CH₃CN, 0 °C, 25 °C, Overnight

In the event, compound **53** was reacted with *p*-toluenesulfonyl chloride in presence of triethylamine and 4-dimethylaminopyridine,¹⁸⁸ then the hybrid molecule **27** was added, to afford **54** in a purified yield of 44% (Scheme 3.27).



Scheme 3.27: Reagents and condtions: (i) TsCl, Et₃N, DMAP, 0 °C, 45 Min; (ii) CH₃CN, 0 °C, 25 °C, Overnight

The ¹H NMR spectrum was consistent with the structure with a signal at 10.26 ppm belonging to N-H and a triplet at 3.96 ppm for the two CH₂-O-C=O protons signalling the formation of ester. Moreover the ¹³C NMR spectrum showed a peak for the ester carbonyl at 173.1 ppm (Figure 52), and HR-MS analysis data also confirmed the structure of the molecule

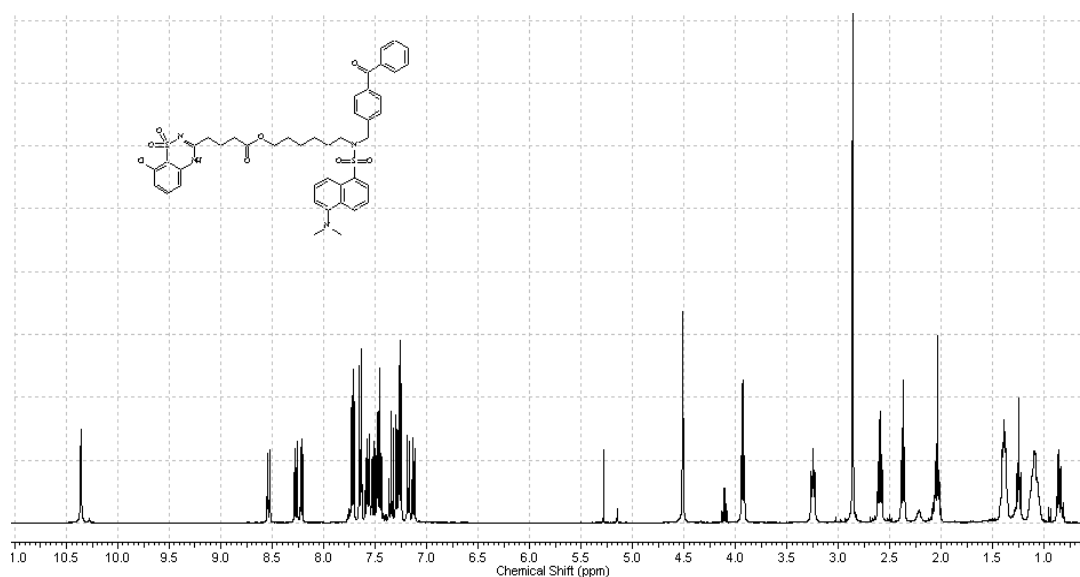
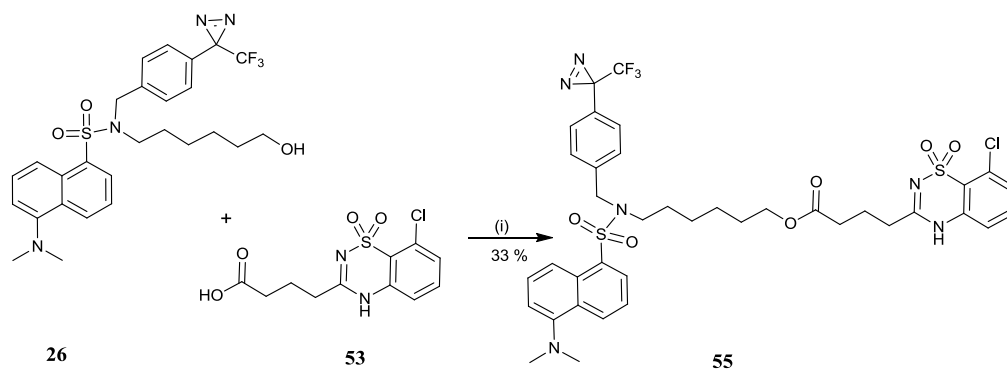


Figure 52 *NMR spectra for compound 54*

3.2.7.3 8-Chloro diazoxide-alkyl linker-diazirine-dansylamide molecule

Following the successful synthesis of benzophenone photoreactive probes, diazirine photoreactive probes were then prepared. The compound **53** was reacted with p-toluenesulfonyl chloride in presence of triethylamine and 4-dimethylaminopyridine,¹⁸⁸ then diazirine hybrid molecule **26** was introduced to give compound **55** in a yield of 33%, after column chromatography. The ¹H NMR spectrum confirmed a successful coupling with the diagnostic triplet peak at 3.92 ppm, and a singlet at 10.24 ppm belonging to the N-H of the diazoxide moiety (Figure 53). The ¹⁹F NMR spectrum once again showed a singlet peak at –65 ppm belonging to the intact diazirine functionality and HR-MS data was consistent the expected structure (Scheme 3.28).



Scheme 3.28: Reagents and conditions: (i) TsCl, Et₃N, DMAP, 0 °C, 45 Min; (ii) CH₃CN, 0 °C, 25 °C, Overnight

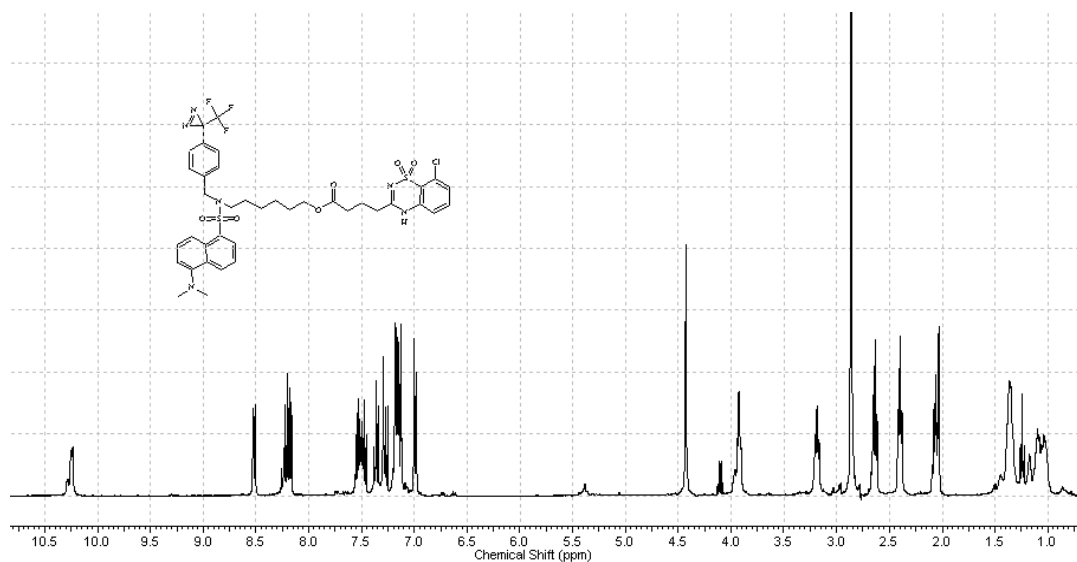
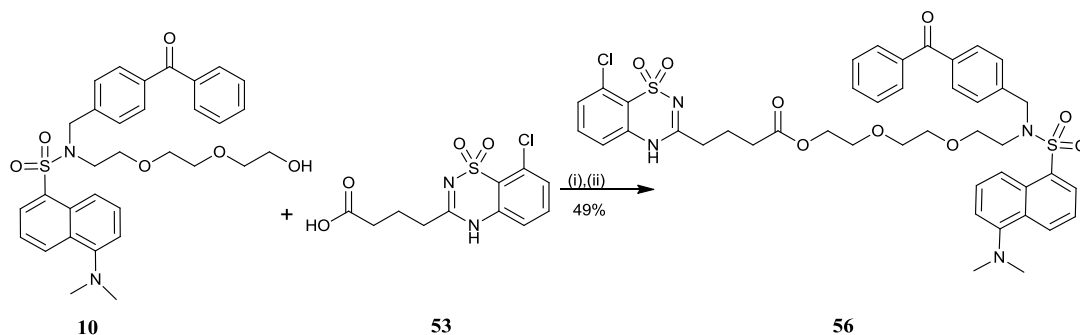


Figure 53 NMR spectra for compound **55**

3. 2.7.4 8-Chloro diazoxide-PEG linker-benzophenone-dansylamide molecule

Several further functional probes were also prepared. As stated earlier, the introduction of a polyethylene glycol (PEG) linker might confer different solubility properties on the probe and affect the binding ability of the small molecule to the biomolecule targets. Preparation of this probe was achieved by coupling of compound **53** to the hybrid molecule with PEG linker **10** using the established method, to give compound **56** in

49% yield after chromatography (Scheme 3.29). All spectroscopic data was consistent with the expected structure (Figure 54).



Scheme 3.29: Reagents and conditions: (i) TsCl, Et₃N, DMAP, 0 °C, 45 Min; (ii) CH₃CN, 0 °C, 25 °C, Overnight

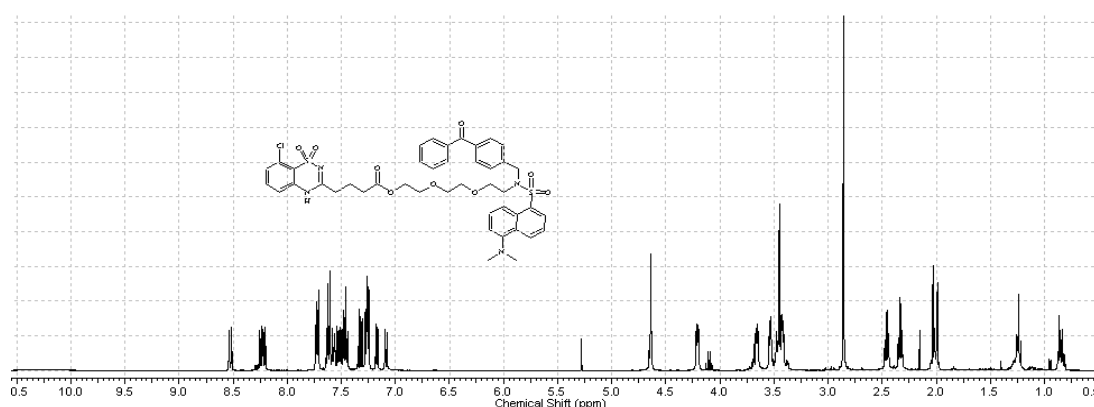
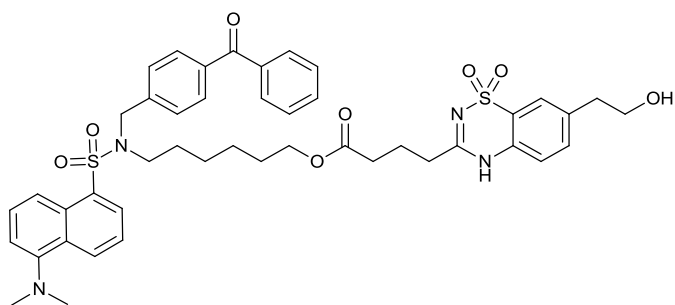


Figure 54 NMR spectra for compound **56**

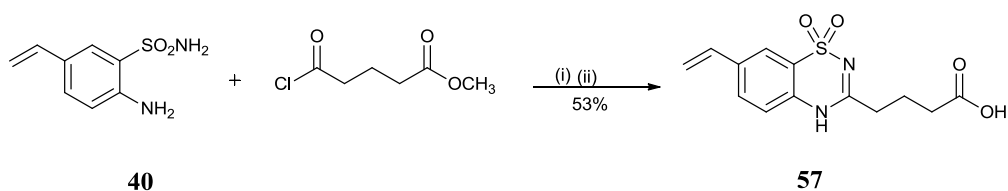
3.2.7.5 Coupling of the 7-(2-hydroxyethyl)-diazoxide with the hybrid molecule

Gives the success of the carboxy side chain installation and ester coupling protocol the preparation of compound **59** was then pursued. For this reason an alternative method was tried by preparing the fully functionalised vinyl molecule **57** then attempting conversion to the desired product **58** as follows:



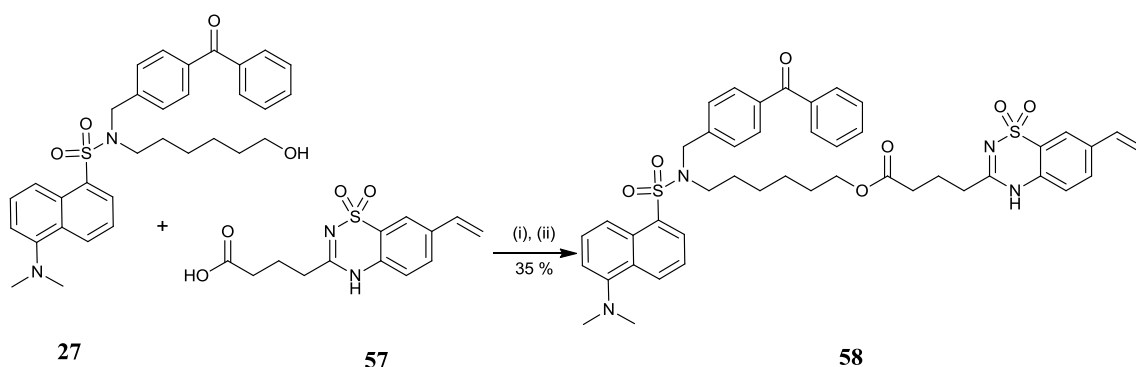
59

Due to the concerns about interference for the unprotected hydroxyl group, the strategy chosen was to elaborate vinyl sulfonamide **40**, then couple to the linker, followed by late stage oxidation to give compound **59**. Hence, 2-amino-5-vinyl-benzenesulfonamide **40** was treated with glutaric acid monomethylester chloride,¹⁸² and the amide product was then treated with sodium hydroxide, followed by acidification by hydrochloric acid to give the corresponding diazoxide **57** in purified yield of 53% (Scheme 3.30).



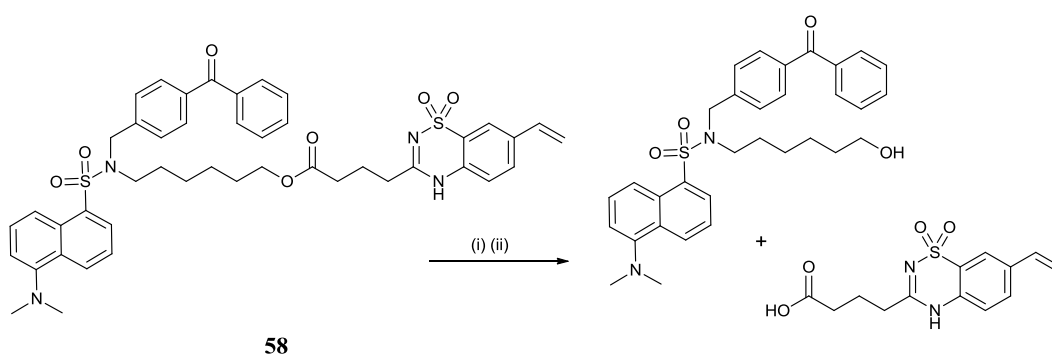
Scheme 3.30: Reagents and conditions: (i) dioxane, 35 °C, 1h; (ii) 3%NaOH, 45 min, 2M HCl

7-Vinyl-diazoxide-butric acid **57** was then coupled with photoreactive benzophenone molecule **27**, to produce the desired ester **58** in a yield of 35 % after chromatography (Scheme 3.31).



Scheme 3.31: Reagents and conditions: (i) TsCl, Et₃N, DMAP, 0 °C, 45 Min; (ii) CH₃CN, 0 °C, 25 °C, Overnight

Hydroboration-oxidation of compound **58** by reaction with 9-BBN and hydrogen peroxide was unsuccessful and the reaction returned components of starting materials the result of hydrolysis of the ester **58** (Scheme 3.32).



Scheme 3.32: Reagents and conditions: (i) 9-BBN in THF, 25 °C, 12 h; (ii) NaOH (1M), H₂O₂ (30%)

At this late stage of the project elaboration of active analogue **43**, via the hydroxyl group was abandoned and studies turned to investigation of the protein tagging probes.

3.2.8 Photolysis investigation of the fully functional molecules **54**, **55** and **56**

In order to identify the proper UV wavelength of light for the irradiation process, an investigation utilising the fully functional diazoxide **54** was established. Initially, an ethanol solution of the fully functional compound **54**, at a concentration of 10 mM was prepared. The second step was to measure the sample under a wavelength range from 250- 900 nm. UV/Vis measurements were then performed in order to assess the optimum excitation and emission wavelengths. An absorption maxima was observed at 395 nm with an emission maxima at 520 nm, both due to the dansyl amide group. The excitation maxima at 340 nm of the benzophenone moiety is presumably swamped by the strong dansyl absorption, but these promising results permitted the irradiation step to be safe for the biomolecule targets (Figure 55).

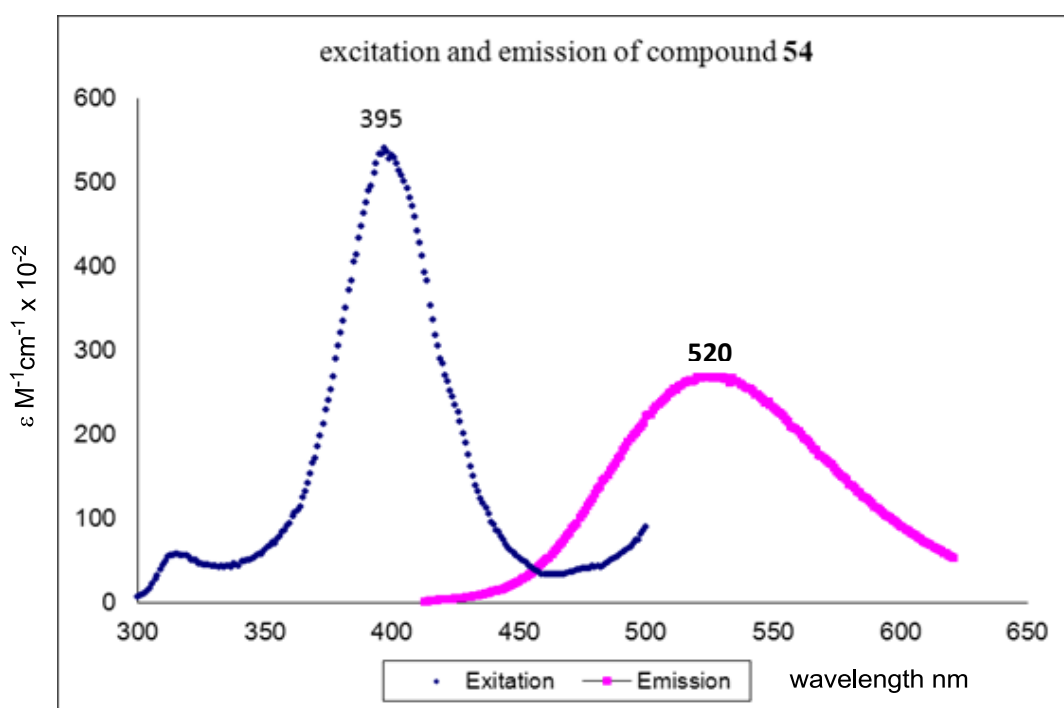


Figure 55 *Excitation and emission for **54***

In order to investigate the photo reactivity of the compounds **54**, **55** and **56** with protein molecules in general, a preliminary study was then conducted using the three analogues of the fully functional diazoxides (benzophenone probes **54** and **56**, diazirine probe molecule **55**) to assess the reactivity toward bovine serum albumin (BSA) as a representative protein target. While this protein is not expected to be a diazoxide target it is readily available and allows the photoaffinity labeling capacity and fluorescent properties of the probes to be examined. It was anticipated that the photolysis the photophore moiety would generate an active species which then covalently binds with any adjacent protein. In these preliminary experiments, 2 mM of each of the fully functional molecules **54**, **55** and **56** was incubated with the same concentration of BSA protein in ratio of 1:1. UV irradiation was then carried out under at wavelength of 360 nm, for various time periods (10, 30, 60 min). The irradiated BSA was then subjected to polyacrylamide gel electrophoresis (PAGE), with gel loading of 10 and 20 µg.

Visualization of the separated protein by UV-transillumination showed visible bands for the BSA protein bound by diazirine molecule **55** for all the applied irradiation times. However, benzophenone molecules **54** and **56**, showed no clear bands for the exposure time of 10 minutes (Figure 56), and clear bands were seen for the experiments involving at 30 and 60 minutes exposure (Figure 57). No qualitative difference in reactivity was observed between alkyl linked **54** and poly ethylene glycol (PEG) **56** in this experiment, perhaps due to the simple nature of the experiment and the high concentrations involved.

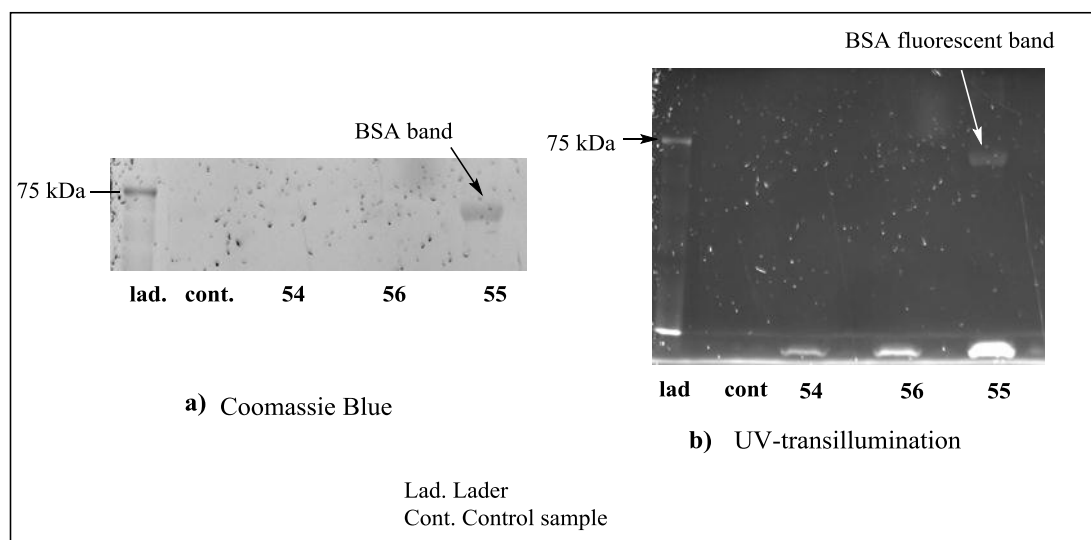


Figure 56 Exposure of BSA protein mixed with the three compounds in 10 minutes

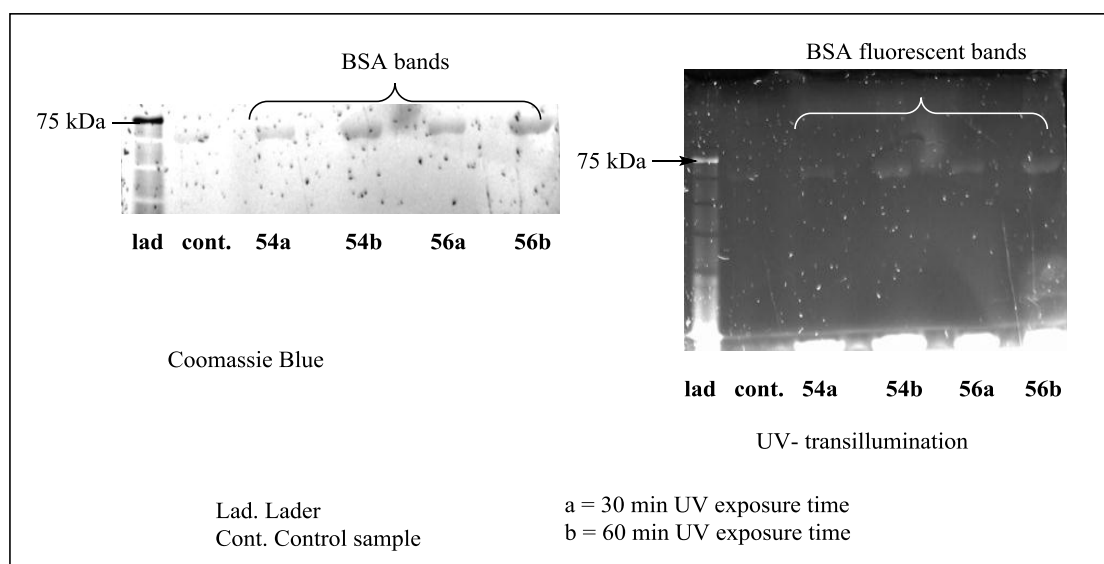


Figure 57 Exposure of BSA protein mixed with the two compounds for 30 minutes 54a, 56a and for 60 minutes 54b, 56b

Overall, the experiments for testing the validity of these molecules to bind to the adjacent proteins, and the diazirine moiety molecule has been found more efficient in short irradiation experiments, which is consistent with literature precedent.¹⁸⁹ The efficacy of the fluorescent moiety has also been established and showed discernable

bands on the gel under the UV transilluminator. Given these promising results the selective binding and tagging of mitochondrial proteins was explored.

3.2.9 Investigation of mitochondrial component targets of diazoxide analogues.

After the preliminary investigation into the binding efficiency of the functional molecules to proteins in general, the interaction with mitochondrial targets was examined. In these experiments mitochondria extracts were used instead of whole tissues or cells, in order to avoid permeability issues.

In these experiments mitochondrial extract provided by Dr Alan Hargreaves, was extracted from pig brain. Protein concentration was determined using Bio-Rad *DC* Protein assay (Bio-Rad laboratories, Hertfordshire, UK) with bovine serum albumin as the standard. Mitochondrial extract (100 µg/ml) were incubated with a 100 µM solution of the diazoxide functional molecules **54**, **55** and **56** at room temperature for 30 minutes. The samples were then divided to two parts, and one of each sample was irradiated directly under 360 nm UV light, and the other half of the samples were suspended in buffer solution and centrifuged to remove any non-binding functional molecules, then irradiated under the same UV wavelength. The irradiation period was optimised using the preliminary study results, and the diazirine analogue molecule **55** was irradiated for 10 minutes and the benzophenone **54** and **56** molecules were irradiated for 30 minutes.

Following irradiation, SDS-PAGE gel was applied to separate the biomolecule targets, and several fluorescent bands were observed on the gel under UV transillumination. Similar results were observed for all three compounds, with three major bands labelled in each experiment two at ~ 25 KDa and one at ~150 KDa. This finding indicates that

the three diazoxide molecules incubated with the mitochondria extracts specifically target only a few biomolecules found in mitochondria.

These data also showed no significant differences between the non-centrifuged and centrifuged samples, which might be related to the high specificity of these molecules. Close examination of the gels revealed that the diazirine probe gave brighter bands compared to the two benzophenone based probes. The clearer bands may be due to the greater efficiency of the diazirine functionality in photoreactive binding to the biomolecules (Figure 58).

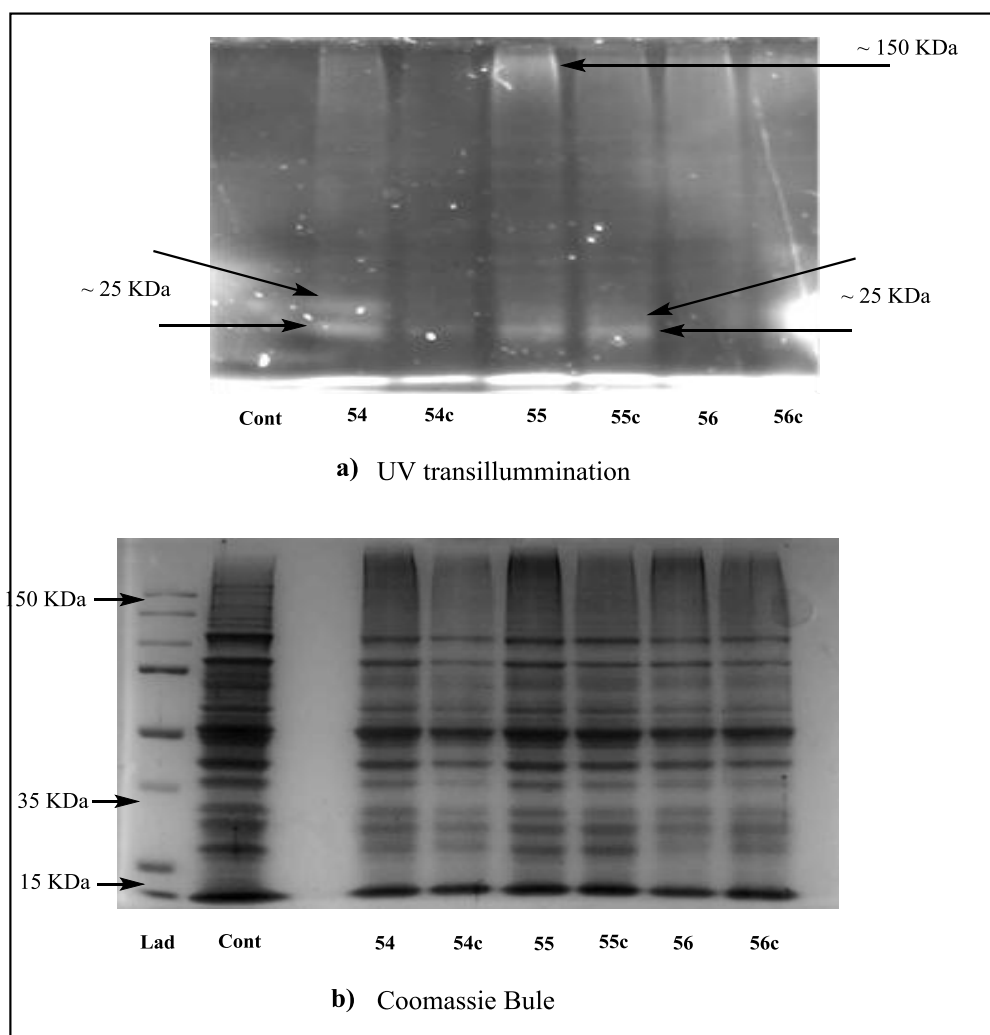


Figure 58 a) *Fluorescent bands from the incubation of molecules 54, 55 and 56 with mitochondrial extract* b) *coomassie blue pigments showing all the protein bands.*

3.2.10 Incubation of diazirine compound **55** with the mitochondrial extract

Diazirine molecule **55** demonstrated promising binding results with the mitochondrial extract in the above experiment (Figure 58). In order to further establish whether this molecule is targeting the same biomolecules as the parent diazoxide, two competition experiments were performed. In the first competition experiment molecule **55** was administered with unlabelled diazoxide, which is more likely to bind to the protein targets with high efficiency than the labelled diazoxide, displace the probe can lead to less labelling. The second strategy was to introduce a known blocker of the mK_{ATP} channel (5-HD) along with the molecule **55**. The presence of the blocker should also inhibit the binding of diazoxide probe.

In the event, mitochondrial extract was treated with the three different combinations of molecule **55** and additives. As a control mitochondrial extract with protein concentration of 100 μ M was incubated with molecule **55**, a second sample was incubated with a 1:1 mixture of molecule **55** and unlabelled diazoxide, and a third sample was incubated with a 1:1 mixture of molecule **55** and the mK_{ATP} blocker 5-HD. These samples were then irradiated by UV for 10 minutes, and an electrophoresis SDS-PAGE gel was used for separation (Figure 59).

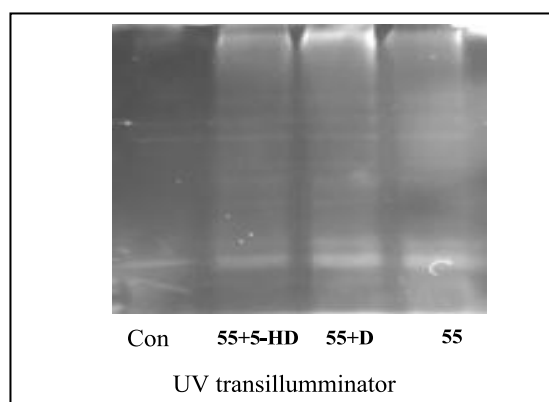


Figure 59 *Specificity targeting test; mitochondrial extract incubated with **55**+5-HD: probe with channel blocker 5-HD, **55**+ D: the probe with unlabelled diazoxide, **55**: just probe*

In these experiments, both control and competition samples exhibited similar bands to those seen in the previous results. However, slightly less bright bands were observed in the case of the mK_{ATP} blocker 5-HD competition experiment, suggesting that the probe may be labelling the mK_{ATP} channel. However, at this point in time, these experiments are inconclusive and further incubation experiments employing excess of channel blocker are required. Further work will also encompass the characterisation of the targeted biomolecules potentially using mass spectrometry of gel purified sample.

3.3 Conclusion

A number of diazoxide analogues, functionalised at different positions around the molecule, have been prepared, and biologically tested. Two analogues **43** and **47** were found to be the most active. These active analogues were then incorporated to photoreactive-fluorescent probe molecules **54**, **55** and **56**, which contain a photoaffinity component (diazirine or benzophenone), and fluorescent tag, dansylamide, attached to the diazoxide by a linker (alkyl or PEG). The probe photo reactivity was assessed by incubating these fully functional molecules with pure BSA protein, under UV light irradiation followed by gel electrophoresis. Fluorescent bands were observed consistent with the protein molecular weight, indicating covalent reaction of the probe with the BSA. Incubation and irradiation of these probes with a mitochondria extract gave three distinct fluorescent bands on the gel after electrophoresis, confirming selective binding to mitochondrial biomolecules. Finally a competitive assay was applied using diazirine molecule **55** with diazoxide and mK_{ATP} channel blocker, with the same extract to determine if the probe is labelling the targets of these small molecule. Results are inconclusive and further work is ongoing.

Future work in this project will require the application of the probes in identifying targets of diazoxide. First is to isolate and identify the biomolecules in the mitochondrial extract targeted by the diazoxide using HPLC and MS techniques. The development of second generation probes will involve the incorporation of brighter fluorescent molecules, like BODIPY, to enhance the sensitivity and allow identification of less abundant biomolecules of interest. Finally the incorporation of different length, and different polarity linkers will allow us to assess the effect of spacer variation on the affinity of the bait molecule and photoreactive binding.

4. Chapter 4: Experimental

4.1 General

For the reactions performed under anhydrous conditions, the glassware for the experiment was dried in an oven (100 °C or higher) overnight when needed and allowed to cool completely to room temperature under a flow of nitrogen before any reagents were introduced. All metal needles used were acetone washed and oven dried for at least 3 hours. Air- and moisture-sensitive liquids and solutions were transferred via syringe. Organic solutions were concentrated under reduced pressure by rotary evaporation and a vacuum pump.

4.2 Reagents and Solvents

All the reagents were analytical grade and used without further purification. The chemicals were purchased from Sigma Aldrich and Alfa Aesar and were used without further purification, unless otherwise stated. The solvents used in reactions were dried, distilled and stored under nitrogen prior to use. Ethanol was dried over Na₂SO₄. Dichloromethane was dried by distillation from CaH₂. THF was dried by distillation from sodium with benzophenone as indicator. The solvents dichloromethane, ethyl acetate, hexane, methanol and cyclohexane (Reagent grade) which were used for chromatography and some others were purchased from Fisher Scientific Ltd.

4.3 Purification Processes

Thin-layer chromatography (TLC) was carried out using silica plates, UV-active, and substances were detected in UV light with wavelength $\lambda = 254$ nm, or by dipping into iodine vapours or potassium permanganate solution. Flash column chromatography was performed using silica gel (Fluorochem, 60A, 40 ± 63 micron). The samples were either

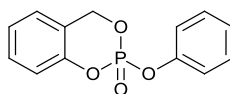
applied in solution directly to the top of the silica/solvent column or applied absorbed onto dry silica gel. Pressure was applied at the column head via hand bellows or an electric pressure pump.

4.4 Instrumentation

Proton (^1H NMR), carbon (^{13}C NMR), fluorine (^{19}F NMR) and phosphorus (^{31}P NMR) nuclear magnetic resonance spectra were measured on a Jeol ECX 400 spectrometer at 400 MHz, 100 MHz, 376 MHz and 162 MHz respectively. The chemical shifts are reported in parts per million (ppm) on the delta (δ) scale and coupling constants (J) are given in Hertz (Hz). The solvent peaks were used as reference values. For CDCl_3 ^1H NMR = 7.27 ppm, for ^{13}C NMR: CDCl_3 = 77.00 ppm; for CD_3OD , the internal reference was designated at 3.31 ppm (^1H) and 49.0 ppm (^{13}C), for $(\text{CD}_3)_2\text{SO}$ the internal reference was designated at 2.50 ppm (^1H) and 39.5 ppm (^{13}C). The abbreviations for the multiplicity for proton data were as follows: s = singlet, d = doublet, dd = doublet of doublets, dt = doublet of triplets, ddt = doublet of doublet of triplets, t = triplet, tt = triplet of triplets, q = quintet, m = multiplet, p = pentet, br = broad. Assignments were based on DEPT 135 and DEPT 90 pulse experiments and HMQC and HMBC experiments. Mass spectra were recorded under high and low resolution by the EPSRC National Mass Spectrometry Service Centre, School of Medicine, Swansea University. Melting points were determined on a Stuart melting point apparatus SMP30. The UV absorptions and emissions were measured by using a Cary Eclipse UV instrument, at a range of wavelength from 200-900 nm. Infrared (IR) absorption spectra were recorded on a Perkin Elmer Spectrum 100 FT-IR Spectrometer using an ATR attachment, and are reported in cm^{-1} .

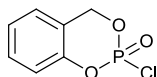
4.5 Experimental of Chapter 2

4.5.1 Synthesis of phenyl saligenin phosphate-1



Phenyl phosphorodichloridate (1.00 g, 4.73 mmol) was added to a solution of 2-hydroxy benzyl alcohol (0.50 g, 4.02 mmol) and triethylamine (5 ml, 4.37 mmol) in THF (5 ml). The mixture was stirred at 0°C for two hours, and then was refluxed for 20 hours. The product was poured into water (40 ml) and extracted with chloroform (3 × 20 ml). The combined organic layers were washed with water (3 × 15 ml) and dried (MgSO₄). The solvent was removed by rotary evaporator under low pressure to afford a crystalline compound **1** (0.70 g, 70%).¹⁹⁰ δ_H (400 MHz, CDCl₃): 5.33-5.46 (m, 2H, CH₂), 7.13-7.27 (m, 9H, Ar-H); δ_C (100 MHz, CDCl₃): 69.3 (CH₂, ²J_{PC} 6.7 Hz), 119.9 (³J_{PC} 9.5 Hz), 124.5 (²J_{PC} 4.7 Hz) 125.2, 125.5, 129.8, 129.2; δ_P (CDCl₃, 162 MHz): -15.31 ppm.

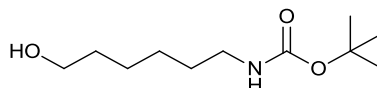
4.5.2 The preparation of 2-chloro-4H-1,3,2-benzodioxaphosphorin-2-oxide-2



To a stirred solution of saligenin (1.00 g, 8.05 mmol) and triethylamine (2.50 ml, 2.15 mmol) in dry DCM (40 ml), was added dropwise phosphorus oxychloride (0.83 ml, 8.83 mmol) in dry DCM (16 mL) at -78 °C. The mixture was stirred for 45 minutes, allowed to warm to room temperature and then was concentrated under a vacuum. Dry toluene (30 ml) was added and the mixture was allowed to stand in a fridge for one hour then filtered, the solvent was removed and the product was dried to obtain the desired compound **2** (1.50 g, 91%) in a good purity which can be used in further steps with no further purification.¹⁹¹ δ_H (400 MHz, CDCl₃): 5.40–5.50 ppm (m, 2H, CH₂), 7.03 (d, 1H, *J* 8.2 Hz), 7.11 (d, 1H, *J* 7.5 Hz), 7.19 (t, 1H, *J* 7.5 Hz), 7.32 (t, 1H, *J* 8.3 Hz); δ_C (100

MHz, CDCl₃): 70.1 (*CH*₂, *J*_{PC} 6.8 Hz), 119.0 (*J*_{PC} 9.7 Hz), 125.1, 125.5, 130.2, 148.7; δ_P (162 MHz, CDCl₃): (s, -5.35 ppm).

4.5.3 Preparation of N-Boc-6-aminohexan-1-ol-3

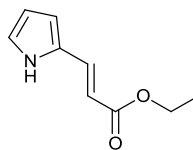


The synthesis procedure is according to Forbes *et al.*¹⁹² 6-Aminohexan-1-ol (1.00 g, 8.5 mmol) was dissolved in DCM (5 ml) and di-*tert*-butyl dicarbonate (2.05 g, 9.3 mmol) in DCM (5 ml) was added at 0 °C. The mixture was stirred at room temperature for 12 hours, then the solvent was removed under reduced pressure and the crude compound was purified using flash chromatography (silica, 1:1 ethyl acetate/cyclohexane, v/v) giving the title compound **3** (1.85 g, 99%) as a colourless oil, which crystallised to give colourless crystals after several days. δ_H (400 MHz, CDCl₃): 1.25-1.31 (m, 4H, *Hexyl*), 1.38 (s, 9H, *Boc*), 1.40-1.43 (m, 2H, *Hexyl*), 1.46-1.52 (m, 2H, *Hexyl*), 1.98 (s, 1H, *OH*), 3.0-3.7 (m, 2H, *Hexyl*), 3.48-3.6 (m, 2H, *Hexyl*), 4.61 (brs, 1H, *N-H*); δ_C (100 MHz, CDCl₃): 25.2, 26.3, 28.3, 30.0, 32.5, 40.3, 62.5, 79.0, 156.0.

4.5.4 Synthesis of a BODIPY

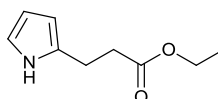
Preparation of BODIPY-FL was achieved by a five step reaction as described in a literature procedure started from commercially available 2,4-dimethylpyrrole as follows.¹¹⁶

4.5.4.1 (*E*)-Ethyl 3-(1H-pyrrol-2-yl)acrylate-4



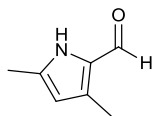
n-BuLi (2.5 M in hexanes, 5.90 ml, 14.70 mmol) was added to ethyl 2-(diethoxymethyl)hydrophosphoryl acetate (3.00 g, 13.40 mmol) in THF (30 ml, -78°C) and the mixture was stirred for 5 minutes then allowed to warm to 0 °C and kept stirring for 40 minutes. 1H-Pyrrole-2-carbaldehyde (1.27 g, 13.40 mmol) was added in a single portion, and the whole was stirred for a further 2 hours under the same conditions then warmed to room temperature and stirred overnight. The solvent was removed, the residue was portioned between water (10 ml) and ethyl acetate (15 ml) and the extracted by ethyl acetate (3 × 15 ml) and the combined organic phases were dried (MgSO₄). The solvent was removed by the rotary evaporator which afforded the desired compound **4** as yellow oil (2.21 g, 94%) which was used directly in the next step.

4.5.4.2 Ethyl 3-(1H-pyrrol-2-yl) propionate-5



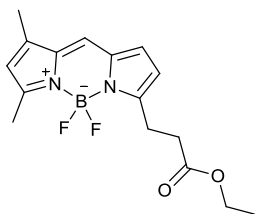
Hydrogen gas was bubbled into a solution of the product **4** (2.21 g, 13.2 mmol) and Pd/C (300 mg) in methanol (20 ml) and the mixture was placed under an atmosphere of hydrogen (balloon, ~ 1 l) and allowed to stir for 2 days at room temperature. The mixture was then filtered and the solvent was removed by rotary evaporator to afford the desired compound **5** in acceptable purity for use in the following reaction (2.23 g).¹¹⁵
 δ_H (CDCl₃, 400 MHz): 1.25 (t, 3H, *J* 7.2 Hz CH₃), 2.62 (t, 2H, *J* 6.9 Hz), 2.88 (t, 2H, *J* 6.8 Hz), 4.16 (q, 2H, *J* 6.7 Hz), 5.91 (s, 1H), 6.09 (t, 1H, *Ar-H*), 6.65 (d, 1H, *Ar-H*), 8.52 (brs, 1H, *NH*); δ_C (100 MHz, CDCl₃): 14.0, 22.4, 34.4, 60.5, 105.2, 107.8, 116.6, 130.8, 173.9.

4.5.4.3 2-Formyl-3,5-dimethylpyrrole-6



To DMF (0.90 g; 12.22 mmol) phosphorus oxychloride (1.88 g; 12.22 mmol) was added dropwise during 20 minutes under stirring at 10 °C. The mixture was stirred for 15 minutes at room temperature, then diluted with dichloromethane (5 ml) and cooled to 0 °C and a solution of 2,4-dimethylpyrrole (1.00 g, 10.51 mmol) in dichloromethane (5.00 ml) was added dropwise at 0 °C. The mixture was refluxed for 30 minutes and cooled to room temperature, and then sodium acetate (8.30 g, 61.10 mmol) in water (10 ml) was added. The mixture was refluxed for 30 minutes and cooled to room temperature and the organic layer was separated. The water layer was extracted with diethyl ether (3 × 50 ml), and the organic layers were combined, washed with a saturated aqueous solution of sodium carbonate, and dried (Na₂SO₄). The solvents were removed, and the residue was purified by column chromatography (ethyl acetate, silica) to give product **6** as a white solid (0.95 g, 74%).¹⁹³ δ_H (CDCl₃, 400 MHz): 2.21 (s, 3H, CH₃), 2.22 (s, 3H, CH₃), 5.75 (s, 1H, Ar-H), 9.35 (s, 1H, CHO), 10.74 (s, 1H, NH).

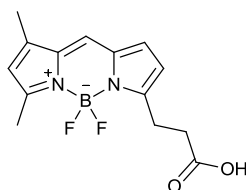
4.5.4.4 Ethyl 3-[4,4-Difluoro-5,7-dimethyl-4-bora-3a,4a-diaza-s-indacene-3-yl]propionate-7



To a stirred solution of ethyl 3-(1H-pyrrol-2-yl) propanoate **5** (1.62 g, 6.96 mmol) and 3,5-dimethyl-1H-pyrrole-2-carbaldehyde **6** (0.94 g, 7.66 mmol) in DCM (55 ml) phosphorus oxychloride (1.17 g, 7.66 mmol, 1.1eq) in DCM (4.00 ml) was added at 0 °C. The mixture stirred for 30 minutes at 0 °C then at room temperature for further 6

hours, the resulting black solution was cooled to 0 °C, and boron trifluoride etherate (3.55 ml, 28.00 mmol) and DIEA (5.10 ml, 29.25 mmol) were added. After stirring for another 12 hours at room temperature, water (100 ml) was added, and the mixture was filtered through a bed of celite. The precipitate was washed with DCM (100 ml), the aqueous layer was extracted with DCM (2 × 50 ml) and the combined organic layers have dried (Na₂SO₄) and concentrated *in vacuo*. The crude product was purified by flash chromatography (silica, dichloromethane) to give the title compound **7** as red crystals (1.41 g, 63%). δ_H (400 MHz, CDCl₃): 1.24 (t, 3H, *J* 7.2 Hz), 2.16 (s, 3H, CH₃-Ar), 2.48 (s, 3H, CH₃-Ar), 2.74 (t, 2H, *J* 7.7 Hz), 4.14 (q, 2H, *J* 6.7), 6.09 (s, 1H, Ar-H), 6.25 (d, 1H, *J* 4.0 Hz, Ar-H), 6.85 (d, 1H, *J* 3.9 Hz, Ar-H), 7.99 (s, 1H, Ar-H); δ_C (100 MHz, CDCl₃): 11.2, 14.2, 14.9, 23.9, 33.4, 60.5, 116.7, 120.3, 123.8, 128.0, 133.3, 135.1, 143.7, 157.2, 160.3, 172.5; δ_F (376 MHz, CDCl₃): -145.26 (q, *J*_{B-F} 33.2 Hz). Data were consistent with literature.¹¹⁶

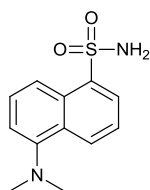
4.5.4.5 7-(2-carboxyethyl)-5,5-difluoro-1,3-dimethyl-5H-dipyrrolo[1,2-c:2',1'-f][1,3,2]diazaborinin-4-ium-5-uide -8



To a stirred solution of ethyl ester **7** (460 mg, 1.43 mmol) in THF (30 ml) was added water (24 ml) and concentrated aqueous hydrochloric acid (37%, 14.5 ml). After stirring for 48 hours at room temperature, dichloromethane (100 ml) was added, the organic phase was separated, and the aqueous layer was washed with DCM (2 × 75 ml). The combined organic layers were washed with brine (100 ml) and concentrated at the rotary evaporator under vacuum. The crude product was purified by flash chromatography (silica, dichloromethane, step gradient of 0-5% methanol) followed by

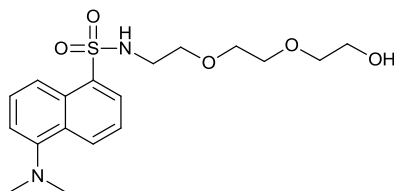
precipitation from hexane to give the title compound **8** (180 mg, 43%).¹¹⁶ δ_H (400 MHz, $CDCl_3$): 2.22 (s, 3H, CH_3 -Ar), 2.43 (s, 3H, CH_3 -Ar), 2.60 (t, 2H, J 8.0 Hz), 3.04 (t, 2H, J 7.4 Hz), 6.27 (s, 1H, Ar -H), 6.34 (d, 1H, J 4.0 Hz, Ar -H), 7.05 (d, 1H, J 4.0 Hz, Ar -H), 7.67 (s, 1H, Ar -H); 10.34 (brs, 1H, OH); δ_C (100 MHz, $CDCl_3$): 11.0, 14.5, 23.5, 32.3, 116.6, 120.4, 125.4, 128.8, 132.9, 134.5, 144.3, 156.9, 159.5, 173.4; δ_F (376 MHz, $CDCl_3$): -145.26 (q, J_{B-F} 33.23 Hz). Data consistent with literature.¹¹⁶

4.5.5 5-(Dimethyl amino)naphthalene-1-sulfonamide-9



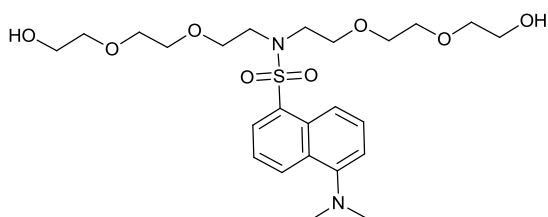
To a stirred solution of 5-(dimethylamino)naphthalene-1-sulfonyl chloride (1.1 g, 4.23 mmol) in dry THF (20 ml) at -78 °C (acetone/dry-ice) bath, ammonia gas was bubbled through the condenser until sufficient liquid ammonia had condensed (~50 ml). The reaction mixture was then stirred for a further 1 hour before being allowed to warm to room temperature overnight. After the ammonia had evaporated, the solvent was removed and the solid residue was washed with water (50 ml) then chloroform (50 ml) and filtered. The product was dried to give the title compound **9** (900 mg, 87 %) as a white solid which used in subsequent reaction with no further purification. δ_H (DMSO- d_6 , 400 MHz): 2.82 (s, 6H, $2 \times CH_3$), 7.26 (d, 1H, J 7.5 Hz), 7.51-7.58 (m, 2H), 7.59 (s, 2H, NH_2), 8.13 (d, 1H, J 8.3 Hz), 8.29 (d, 1H, J 8.6 Hz), 8.43 (d, 1H, J 8.5 Hz). Data were consistent with literature.¹¹⁷

4.5.6 5-(Dimethylamino)-N-(2-(2-(2 hydroxyethoxy)ethoxy) ethyl) naphthalene-1-sulfonamide-10



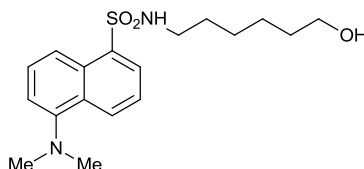
Following the precedent procedure,¹⁹⁴ in a three necked flask, dansylamide **9** (500 mg, 1.99 mmol), potassium carbonate (276 mg, 1.99 mmol), and potassium iodide (18 mg, 5% mol) were dissolved in dry DMF (95.0 ml) and the mixture was stirred at room temperature under a nitrogen atmosphere. Then 2-[2-(2-chloroethoxy)ethoxy]ethanol (335 mg, 1.99 mmol) was added to the mixture and the reaction allowed to stir at 100 °C overnight. The mixture was filtered, the filtrate collected and the solvent was evaporated. The resultant crude oil was purified by flash column chromatography (silica, ethyl acetate) to give the desired substance **10** (250 mg, 32%) as the first eluting compound. δ_H (CDCl₃, 400 MHz): 2.86 (s, 6H, 2 \times CH₃), 2.98-3.12 (m, 2H, CH₂), 3.37-3.43 (m, 4H), 3.47-3.52 (m, 2H), 3.51-3.57 (m, 2H), 3.71-3.76 (m, 2H), 6.09 (t, 1H, *J* 5.8 Hz, SO₂NH), 7.16 (d, 1H, *J* 7.5 Hz, *Ar-H*), 7.48 (t, 1H, *J* 7.8 Hz, *Ar-H*), 7.54 (t, 1H, *J* 8.0 Hz, *Ar-H*), 8.21 (d, 1H, *J* 7.3 Hz, *Ar-H*), 8.32 (d, 1H, *J* 8.6 Hz, *Ar-H*), 8.51 (d, 1H, *J* 8.5 Hz, *Ar-H*); δ_C (CDCl₃, 100 MHz): 42.9, 45.3 (2 \times CH₃-N), 61.4, 69.4, 70.1 (2C), 72.6, 115.1, 119.0, 123.1, 128.1, 129.2, 129.5, 129.7, 130.2, 135.0, 151.6. HRMS (NSI) (*m/z*), [M+H] calcd. for C₁₂H₁₄N₂O₂S 383.1635, found 383.1639.

4.5.7 5-(Dimethylamino)-N,N-bis(2-(2-(2-hydroxyethoxy)ethoxy)ethyl)naphthalene-1-sulfonamide- 10a



Further elution afforded **10a** (340 mg, 33%) as a thick red oil. δ_H (CDCl_3 , 400 MHz): 2.82 (s, 6H, $2 \times \text{CH}_3$), 3.29 (brs, 2H, $2 \times \text{OH}$), 3.47-3.66 (m, 24 H, $12 \times \text{CH}_2$), 7.13 (d, 1H, J 7.5 Hz, *Ar-H*), 7.48 (m, 2H, *Ar-H*), 8.09 (d, 1H, J 7.3 Hz, *Ar-H*), 8.23 (d, 1H, J 8.6 Hz, *Ar-H*), 8.47 (d, 1H, J 8.5 Hz, *Ar-H*); δ_C (CDCl_3 , 100 MHz): 45.3 ($2 \times \text{CH}_3\text{-N}$), 47.9 ($2 \times \text{CH}_2\text{-N-SO}_2$), 61.4 ($2 \times \text{CH}_2\text{-OH}$), 70.0 ($4 \times \text{CH}_2$), 70.1 ($2 \times \text{CH}_2$), 72.5 ($2 \times \text{CH}_2$), 115.1, 119.3, 123.0, 127.9, 128.5, 129.9, 130.1, 130.2, 135.2, 151.5; HRMS (NSI) (m/z), $[\text{M}+\text{H}]^+$ calcd, for $\text{C}_{24}\text{H}_{38}\text{N}_2\text{O}_8\text{S}$: 515.2422, found 515.2427.

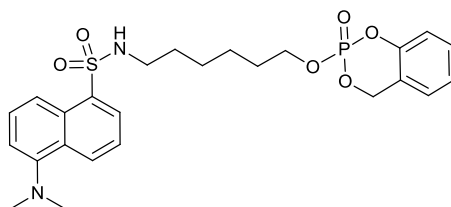
4.5.8 N-(6-hydroxy-hexyl)-5-dimethylamino-naphthalene-1-sulfonamide 12



As described in the literature procedure,¹⁹⁵ a two necked flask was charged with dansyl chloride (5.00 g, 18.53 mmol) and DMAP (250 mg, 2.04 mmol) dissolved in dry dichloromethane (80 ml); the mixture was stirred under a nitrogen atmosphere at room temperature for 20 minutes, followed by the addition of dry triethylamine (10 ml). After stirring the reaction mixture at 0 °C for 15 minutes, 6-aminohexanol (2.50 g, 21.3 mmol) was added and the whole was stirred for a further 15 minutes. The mixture was then warmed to 20 °C and stirred for 3.5 hours, diluted with DCM (50 ml) and washed with water (3×40 ml) to produce the sulphonamide **12** (6.22 g, 92%). δ_H (CDCl_3 , 400 MHz):

1.10-1.13 (m, 4H), 1.32-1.35 (m, 4H), 1.85 (brs, 1H, *OH*), 2.85 (t, 2H *J* 9.5 Hz), 2.85 (s, 6H, *N(CH₃)₂*), 3.46 (t, 2H, *J* 6.5 Hz), 5.15 (t, 1H, *J* 5.9 Hz, *SO₂NH*), 7.14 (d, 1H, *J* 7.5 Hz, *Ar-H*), 7.49-7.52 (m, 2H, *Ar-H*), 8.21 (d, 1H, *J* 8.4 Hz, *Ar-H*), 8.30 (d, 1H, *J* 8.7 Hz, *Ar-H*), 8.50 (d, 1H, *J* 8.4 Hz, *Ar-H*); δ_C (CDCl₃, 100 MHz): 24.9, 25.9, 29.3, 32.2, 42.9 (C-NH), 45.3 (2C), 62.4 (C-OH), 115.1, 118.7, 123.1, 128.2, 129.4, 129.6, 129.8, 130.2, 134.8 (C-N(CH₃)₂), 151.8 (C-SO₂N); HRMS (NSI) (*m/z*), [M+H] calcd, for C₁₉H₂₈N₂O₃S 351.1742 found 351.1737.

4.5.9 Coupling the organophosphate compound with fluorescent tag-13



To a cold (-78 °C) stirred solution of the dansylamide **12** (470 mg, 1.34 mmol) in dry dichloromethane (20 ml) and triethylamine (0.20 ml, 2.01 mmol) under nitrogen, was added dropwise the organophosphate chloride **2** (410 mg, 2.00 mmol) in dry dichloromethane (10 ml) followed by further stirring at -78 °C for 30 minutes. The reaction mixture was allowed to warm to room temperature and kept stirring for a further 24 hours. The reaction mixture was then concentrated, dry toluene (30 ml) was added, the mixture allowed to stand in a fridge for an hour then filtered and the solvent was removed from the filtrate and the residue was dried under a vacuum. Column chromatography on the resultant oil, (silica, ethyl acetate), yielded the desired compound **13** as an orange oil (150 mg, 22%). δ_H (400 MHz, CDCl₃): 1.07-1.17 (m, 2H), 1.24 (t, 2H, *J* 7.2 Hz), 1.30 (m, 2H), 1.48-1.51 (m, 2H), 2.82 (t, 2H, *J* 6.5 Hz), 2.86 (s, 6H, 2× *CH₃*), 4.02-4.10 (m, 2H), 5.08 (t, 1H, *J* 6.1 Hz, *NH*), 5.31 (d, 2H, *J* 4.0 Hz), 7.00 (d, 1H *J* 8.8 Hz), 7.02-7.10 (m, 2H), 7.15 (d, 1H, *J* 7.5 Hz), 7.26 (t, 1H, *J* 7.8 Hz), 7.47-

7.54 (m, 1H), 8.21 (d, 2H, J 8.4 Hz), 8.29 (d, 1H, J 8.6 Hz), 8.51 (d, 1H, J 8.5 Hz); δ_C (100 MHz, $CDCl_3$): 24.5, 25.5, 29.2, 29.72, 42.8, 45.3, 68.4, 115.0, 118.5, 118.5, 118.7, 123.1, 124.1, 125.2, 128.2, 129.4, 129.5, 129.6, 129.7, 130.2, 134.7, 151.8; δ_P (162 MHz, $CDCl_3$): -8.87 (q, J_{ABX} 14.8, 19.2 and 7.6 Hz); HRMS (NSI) (m/z), $[M+H]^+$ calc. 519.1713 found 519.1717.

4.6 Experimental of Chapter 3

General Procedure A

Diazoxide precursors, aminobenzenesulfonamide derivatives, were all introduced as starting materials in the following diazoxide analogue preparations; these reactions have been performed under conditions of known literature procedure.¹⁹⁶

The 2-aminobenzenesulfonamide analogue was dissolved in acetic acid, then acetic anhydride was added. The mixture was stirred at 110 °C for 1 hour. After cooling to room temperature the mixture was evaporated under reduced pressure to remove the acetic acid. The crude compound was reacted with sodium hydroxide solution (3%, 40 ml) at room temperature for 1 hour then acidified with 2 M hydrochloric acid until precipitates were formed. The solid was filtered off, washed with water then dried to give the corresponding diazoxide analogue.

General Procedure B

A two necked flask was charged with the 2-amino benzenesulfonamide analogue in dioxane. The reaction mixture was stirred under nitrogen atmosphere at 30 °C for 10 minutes then glutaric acid monomethyl ester chloride was slowly added. The reaction mixture was kept stirring for a further 1 hour, then evaporated under reduced pressure to remove the solvent. The obtained product was dissolved in 3% of sodium hydroxide

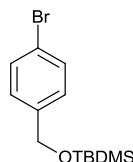
solution (10 mL) and stirred for 1 hour at room temperature, then acidified with 2 M hydrochloric acid until precipitates started forming. The mixture was allowed to stand overnight to complete the precipitation, and the product was then collected by filtration and washed with ether and dried to give the corresponding diazoxide analogue.

General Procedure C

To a stirred solution of diazoxide butyric acid analogues, triethylamine and DMAP in dry acetonitrile was added tosyl chloride in acetonitrile at 0 °C. The mixture was stirred for 30 min, then the alcohol in dry acetonitrile was added at 0 °C, and then the reaction mixture was allowed warm to 25 °C then stirred overnight.¹⁸⁸ Water was added to the mixture which was then extracted with ethyl acetate; the combined organic layers were washed with water, brine and dried (Na₂SO₄).

4.6.1 4-Bromobenzyl alcohol-O-(*tert*-butyldimethylsilyl) ether -14

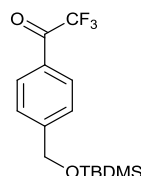
In a modified literature procedure,¹⁷¹ diazirine **22** was prepared starting from the commercially available bromobenzyl alcohol in eight reaction steps as follows.



A two necked round bottomed flask, equipped with a stirring bar, was charged with 4-bromobenzyl alcohol (25 g, 83.20 mmol) dissolved in dry DCM (125 ml) under a nitrogen atmosphere followed by addition of imidazole (21.80 g, 188 mmol) and then *tert*-butyldimethylsilyl chloride (15.00 g, 99.80 mmol) dissolved in dry DCM (25 ml) and the mixture stirred for 20 hours. The mixture was washed with water (75 ml), then the organic layer was separated, dried (MgSO₄) and the solvent was removed *in vacuo*. Column chromatography of the crude compound (silica, DCM) afforded compound **14**

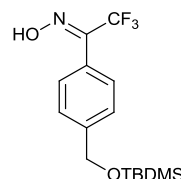
(38.00 g, 94%) as a colourless liquid. δ_H (400 MHz, $CDCl_3$): 0.07 (s, 6H, Si-(CH_3)₂), 0.91 (s, 9H, C-(CH_3)₃), 4.65 (s, 2H, CH_2), 7.16 (d, 2H, J 8.2 Hz, o -ArH), 7.41 (d, 2H, J 8.7 Hz, m -ArH). Data were consistent with literature.¹⁷¹

4.6.2 4-[(*tert*-butyldimethylsiloxy)methyl]-2,2,2-trifluoroacetophenone -15



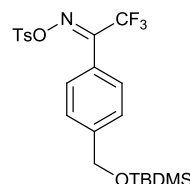
To a stirred solution of 4-bromobenzyl alcohol-O-(*tert*-butyldimethylsilyl) ether **14** (3.0 g, 9.95 mmol) in dry THF (60 ml) was added n-butyl lithium (49.70 mmol, 27 ml, 2.50 M in hexane) at -78 °C (acetone/dry ice) under a nitrogen atmosphere over a period of 10 min. The reaction mixture was stirred under these conditions for a further 1.5 hours. Methyl trifluoroacetate (5.00 ml, 49.70 mmol) was then added dropwise over 10 min and stirring continued for a further 1.5 hours. Saturated aqueous ammonium chloride (40 ml) was then added and the reaction mixture warmed to room temperature. The reaction mixture was diluted with THF (25 ml) and separated, and the organic layer washed with saturated aqueous ammonium chloride (2 × 20 ml) and then with water (2 × 20 ml). The combined aqueous layers were extracted with THF (30 ml) and then the combined organics dried over ($MgSO_4$), filtered and concentrated to give compound **15** as a colourless liquid (2.68 g, 77%). δ_H (400 MHz, $CDCl_3$) 0.15 (s, 6H, Si-(CH_3)₂) 0.98 (s, 9H, C-(CH_3)₃), 4.85 (s, 2H, CH_2), 7.53 (d, 2H, J 8.7 Hz, o -ArH), 8.07 (d, 2H, J 8.2 Hz, m -ArH); δ_F (376 MHz, $CDCl_3$): -71.27 ppm. Data were consistent with literature.¹⁷¹

4.6.3 4-[(*tert*-Butyldimethylsiloxy)methyl]-2,2,2-trifluoroacetophenone-oxime-16



To a stirred solution of 4-[(*tert*-butyldimethylsiloxy)methyl]-2,2,2-trifluoroacetophenone **15** (10.51 g, 34.60 mmol) in anhydrous pyridine (100 ml) and anhydrous ethanol (47 ml) under nitrogen, hydroxylamine hydrochloride (2.64 g, 38.00 mmol) was added and then the reaction mixture heated at 80 °C for 16 hours. The reaction mixture was then concentrated, suspended in ether (250 ml), washed with water (4 × 100 ml), dried (MgSO₄), filtered and concentrated. The resulting residue was purified by column chromatography (silica, DCM) to yield compound **16** (7.83 g, 72 %) as a colourless viscous liquid. δ_H (400 MHz, CDCl₃): 0.04 (s, 6H, Si-(CH₃)₂), 0.88 (s, 9H, C-(CH₃)₃), 4.71 (s, 2H, CH₂), 7.35 (d, 2H, *J* 8.1 Hz, *o*-ArH), 7.43 (d, 2H, *J* 7.8 Hz, *m*-ArH), 8.85 and 8.96 (brs, 1H, OH); δ_F (376 MHz, CDCl₃): -66.4 ppm. Data were consistent with literature.¹⁷¹

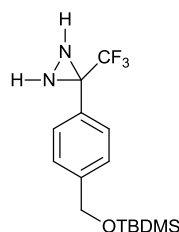
4.6.4 4-[(*tert*-Butyldimethylsiloxy)methyl]-2,2,2-trifluoroacetophenone-O-(4-toluenesulphonyl)oxime-17



A two necked round-bottomed flask equipped with a stirring bar was charged with 4-[(*tert*-butyldimethylsiloxy)methyl]-2,2,2-trifluoroacetophenone oxime **16** (230 mg, 0.71 mmol) and dry DCM (2 ml). To this stirred solution DMAP (5 mg, 0.03 mmol), *p*-toluenesulfonyl chloride (150 mg, 0.80 mmol) and triethylamine (180 mg, 0.18 mmol) were added, and the mixture was stirred under a nitrogen atmosphere at room

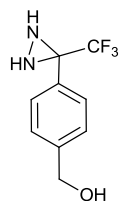
temperature for 24 hours. The reaction mixture was then partitioned between water (10 ml) and DCM (15 ml) and the organic layer washed with additional water (10 ml). Solvents were removed *in vacuo* to yield a brown oil, which was purified by column chromatography (silica, DCM/ hexane 3:4) to afford **17** as a pale green oil (290 mg, 83%). δ_H (400 MHz, $CDCl_3$): 0.00 (s, 6H, Si-(CH_3)₂), 0.83 (s, 9H, C-(CH_3)₃), 2.35 (s, 3H, $ArCH_3$), 4.66 (s, 2H, CH_2), 7.23-7.29 (m, 6H, ArH), 7.72-7.79 (m, 2H, ArH); δ_F (376 MHz, $CDCl_3$): -66.5 ppm. Data were consistent with literature.¹⁷¹

4.6.5 3-[α -(*tert*-Butyldimethylsiloxy)-4-tolyl]-3-trifluoromethyl diaziridine-**18**



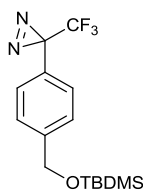
To a stirred solution of oxime **17** (330 mg, 0.67 mmol) in dry DCM (2.00 ml) at -78 °C (acetone/dry-ice bath), ammonia gas was introduced through a condenser until sufficient liquid ammonia had condensed (~15 ml). The reaction mixture was then stirred for a further 3 hours before being allowed to warm to room temperature over 2 hours. After the ammonia had evaporated, the reaction mixture was filtered and concentrated to give the title compound **18** as a white translucent paste (150 mg, 67%), which used in subsequent reactions without further purification. δ_H (400 MHz, $CDCl_3$): 0.01 (s, 6H, Si-(CH_3)₂), 0.84 (s, 9H, C-(CH_3)₃), 2.20 (d, 1H, J 8.7 Hz, NH), 2.76 (d, 1H, J 8.3 Hz, NH), 4.65 (s, 2H, CH_2), 7.27 (d, 2H, J 8.0 Hz, $o-ArH$), 7.46 (d, 2H, J 8.0 Hz, $m-ArH$); δ_F (376 MHz, $CDCl_3$): -75.5 ppm. Data were consistent with literature.¹⁷¹

4.6.6 (4-(3-(trifluoromethyl)diaziridin-3-yl)phenyl)methanol-19



In a two necked flask 3-[α -(*tert*-butyldimethylsiloxy)-4-tolyl]-3-trifluoromethyl diaziridine **18** (250 mg, 0.75 mmol) was treated with as a 1.00 M solution of tetrabutylammonium fluoride in THF (1.00 ml, 0.10 mmol) containing water (0.05 ml, 5%). The solution was stirred at room temperature for 5 hours, then diluted with ether (15 ml), washed with water (3 \times 4.00 ml), dried (Na₂SO₄), filtered and concentrated. Column chromatography of the resultant oil, (silica, DCM), yielded the title compound **19** (110 mg, 67%) as a pale yellow oil. δ_H (400 MHz, CDCl₃): 1.82 (brs, 1H, *OH*), 2.14 (d, 1H, *J* 8.4 Hz, *NH*), 2.73 (d, 1H, *J* 8.4 Hz, *NH*), 4.66 (s, 2H, *CH*₂), 7.35 (d, 2H, *J* 8.0 Hz, *o-ArH*), 7.35 (d, 2H, *J* 8.1 Hz, *m-ArH*); δ_F (376 MHz, CDCl₃): -75.4 ppm. Data were consistent with literature.¹⁷¹

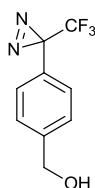
4.6.7 3-[α - (*tert*-Butyldimethylsiloxy)-4-tolyl]-3-trifluoromethyl diazirine-20



In a darkened fume hood, to a stirred solution of 3-[α -(*tert*-butyldimethylsiloxy)-4-tolyl]-3-trifluoromethyl diaziridine **18** (2.50 g, 7.53 mmol) and anhydrous triethylamine (1.75 ml, 1.27 g, 12.55 mmol) in anhydrous methanol (5 ml) was added iodine (1.60 g, 6.30 mmol) portionwise, until a red/orange colour persisted. The reaction mixture was then allowed to stir for a further 20 minutes before being neutralised with 10% aqueous citric acid solution till pH \sim 5-6 and then quenched with a few drops of 5 % aqueous

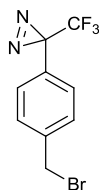
sodium meta-bisulphite solution. The reaction mixture was then poured onto ether (150 ml) dried (Na_2SO_4) filtered and concentrated. Column chromatography (silica, hexane: DCM, 2:1 (NB: column wrapped in newspaper)) afforded the title compound **20** (1.514 g, 61 %) as a light yellow oil. δ_{H} (400 MHz, CDCl_3), 0.09 (s, 6H, $2 \times \text{CH}_3$) 0.93 (s, 9H, $3 \times \text{CH}_3$), 4.74 (s, 2H, CH_2), 7.16 (d, 2H, J 7.7 Hz, ArCH), 7.35 (d, 2H, J 7.7 Hz, ArCH); δ_{F} (376 MHz, CDCl_3): -65.1 ppm. Data were consistent with literature.¹⁷¹

4.6.8 4-[3-Trifluoromethyl-3H-diazirin-3-yl] benzyl alcohol-21



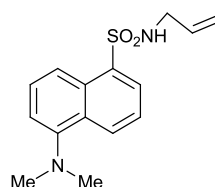
In a darkened fume hood, 3-[α -(tert-butyldimethylsiloxy)-4-tolyl]-3-trifluoromethyl diazirine **20** (1.500 g, 4.54 mmol) was treated with a solution of 4M hydrogen chloride in dioxane (5.5 ml, 5.45 mmol). The solution was allowed to stir at room temperature for 5 hours, then diluted with ether (40 ml), washed with water (3×12 ml), dried (Na_2SO_4), filtered and concentrated. Column chromatography on the resultant oil (silica, dichloromethane, (nb: column wrapped in newspaper)) yielded the title compound **21** (0.791, 81 %) as a pale yellow oil. δ_{H} (400 MHz, CDCl_3), 2.36 (brs, 1H, OH), 4.66 (s, 2H, CH_2), 7.17 (d, 2H, J 7.7 Hz, Ar-H), 7.35 (d, 2H, 8.5 J Hz, Ar-H); δ_{F} (376 MHz, CDCl_3): -65.0 ppm. Data were consistent with literature.¹⁷¹

4.6.9 3-(4-(Bromomethyl)phenyl)-3-(trifluoromethyl)-3H-diazirine-22



Diazirine **21** (1.60 g, 7.40 mmol) and carbon tetrabromide (2.70 g, 8.38 mmol) was dissolved in dry DCM (10 ml) and triphenylphosphine (2.20 g, 8.38 mmol) was slowly added to the mixture at 0 °C and the mixture was stirred at room temperature for 5 hours. Hexane (50 ml) was added to the reaction mixture and the precipitate was filtered through celite, the filtrate was evaporated *in vacuo* and the residue was purified by column chromatography (silica, hexane/ ether 1:1) to give the title compound **22** (1.99 g, 96%) as light yellow oil: δ_H (400 MHz, $CDCl_3$), 4.46 (s, 2H, CH_2), 7.17 (d, 2H, J 8.2 Hz, $ArCH$), 7.42 (d, 2H, J 8.2 Hz, $ArCH$); δ_F (376 MHz, $CDCl_3$): -65.0 ppm. Data consistent with literature.¹⁷¹

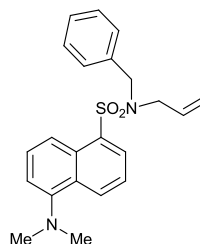
4.6.10 N-Allyl-5-(dimethylamino)naphthalene-1-sulfonamide-23



To a stirred solution of commercially available dansyl chloride (0.5 g, 1.85 mmol) in dry DCM (8.00 ml) and DMAP (220 mg, 1.8 mmol) at 0 °C, allylamine (0.15 ml, 2.03 mmol) was added, followed by triethylamine (0.50 ml, 3.58 mmol), and the mixture stirred for 20 minutes. The mixture was warmed to room temperature and stirred for 3.5 hours, then diluted with DCM (10 ml), washed with water (2 \times 10 ml), dried ($MgSO_4$) and evaporated *in vacuo*. After the addition of chloroform (10 ml), the residue re-evaporated again and dried to give **23** (0.43 g, 80%). δ_H ($CDCl_3$, 400 MHz): 2.78 (s,

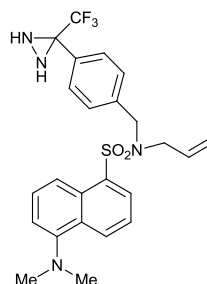
3H, CH_3), 2.88 (s, 3H, CH_3), 2.53 (d, 2H, J 5.8 Hz), 4.86 (d, 1H, J 10.1 Hz), 5.06 (d, 1H, J 17.0 Hz), 5.51-5.56 (m, 1H), 6.38 (d, 1H, J 6.5 Hz), 7.07 (d, 1H, J 7.6 Hz), 7.21 (d, 1H, J 7.3 Hz), 7.47 (t, 2H, J 7.9 Hz), 8.18 (d, 1H, J 6.5 Hz), 8.22 (d, 1H, J 8.3 Hz), 8.34 (d, 1H, J 8.5 Hz), 8.50 (d, 1H, J 8.4 Hz). δ_C ($CDCl_3$, 100 MHz): 39.0, 45.4, 45.8, 106.5, 115.1, 117.36, 117.42, 118.8, 123.1, 128.2, 128.3, 129, 129.7, 130.4, 149.6.

4.6.11 A model reaction using benzyl alcohol-24



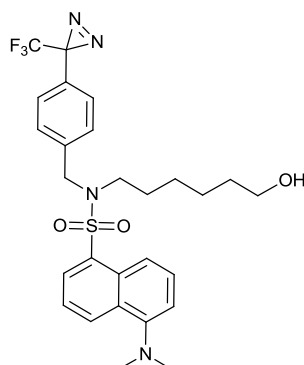
A two necked flask was charged with sulphonamide **23** (320 mg, 1.10 mmol) in dry THF (6.00 ml). The mixture was stirred under a nitrogen atmosphere followed by addition of triphenylphosphine (340 mg, 1.30 mmol) and then benzyl alcohol (0.12 ml, 1.10 mmol), and then DEAD (1.0 M in THF, 0.16 ml, 0.16 mmol) was added. The mixture was stirred at room temperature for a further 4 hours, and then concentrated *in vacuo*. The residue was purified using column chromatography (silica, ethyl acetate/hexane, 1:4), yielded the title compound **24** as a thick light brown oil (180 mg, 43%). δ_H (400 MHz, $CDCl_3$): 2.78 (s, 6H, $2 \times CH_3$), 3.72 (d, 2H, J 6.52 Hz), 4.35 (s, 2H, $Ph-CH_2$), 4.98 (dd, 2H, J 10.0, 17.0 Hz, CH_2 -vinyl), 5.42 (m, 1H, vinyl), 7.13-7.22 (m, 6H, phenyl), 7.43 (dt, 2H, J 7.4 Hz, J 7.6 Hz), 8.16 (d, 1H, J 7.3 Hz), 8.25 (d, 1H, J 8.5 Hz), 8.44 (d, 1H, J 8.4 Hz); δ_C (100 MHz, $CDCl_3$): 45.3, 48.4, 49.5 ($2 \times CH_3$), 115.1, 119.4 (2C), 123.0, 127.5, 128.0, 128.3 (3C), 128.4 (3C), 130.1, 130.4, 132.3, 135.0, 135.6, 151.7.

4.6.12 Coupling of diaziridine with fluorescent component-25



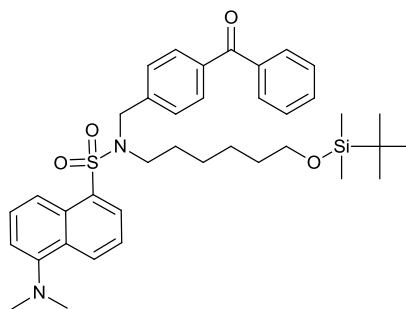
In a two necked flask, sulphonamide **23** (130 mg, 0.45 mmol) was dissolved in dry THF (5.00 mL) under a nitrogen atmosphere followed by addition of triphenylphosphine (210 mg, 0.80 mmol) diaziridine **19** (100 mg, 0.45 mmol), and finally DEAD (1.00 M in THF, 0.10 mL, 0.10 mmol). The mixture was stirred at room temperature for 4 hours then concentrated *in vacuo*. The residue was purified using column chromatography (silica, ethyl acetate/hexane, 1:4) yielded the title compound **25** as a thick brown oil (113 mg, 51%). δ_H (400 MHz, CDCl₃): 2.16 (d, 1H, *J* 8.3 Hz, *NH*), 2.75 (d, 1H, *J* 8.3 Hz, *NH*), 2.89 (s, 6H, 2 \times CH₃), 3.81 (d, *J* 6.5 Hz, 2H), 4.45 (s, 2H, CH₂), 4.96 (dd, 2H, *J* 10.0, 17.0 Hz), 5.39-5.46 (m, 1H, *vinyl*), 7.09-7.14 (m, 2H), 7.38 (d, 1H, *J* 8.13 Hz), 7.45 (dt, 2H, *J* 8.3 Hz, *J* 7.6 Hz), 8.18 (d, 1H, *J* 8.3 Hz), 8.22 (d, 1H, *J* 8.7 Hz), 8.47 (d, 1H, *J* 8.4 Hz); δ_C (100 MHz, CDCl₃): 45.5, 49, 49.3 (2 \times CH₃), 115.2, 119.3, 119.7, 123.1, 128.2 (3C), 128.8 (3C), 130, 130.4, 130.7, 131, 132.3, 134.8, 138.2, 151.8; δ_F (376 MHz, CDCl₃): -75.4; HRMS (NSI) (*m/z*), [M+H] calc. 491.1723 found 491.1714.

4.6.13 5-(Dimethylamino)-N-(6-hydroxyhexyl)-N-(4-(3-(trifluoromethyl)-3H-diazirin-3-yl)benzyl)naphthalene-1-sulfonamide-26



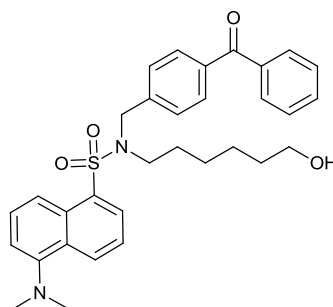
Sulfonamide compound **12** (570 mg, 1.63 mmol) was dissolved in dry DMF (15 ml), and potassium carbonate (900 mg, 0.65 mmol) was added and stirred under a nitrogen atmosphere at room temperature. To the reaction mixture, diazirine **10** (500 mg, 1.79 mmol) in DMF (15 ml) was slowly added over 10 minutes and the mixture was stirred at room temperature for a further 20 hours. The mixture was then filtered and the DMF evaporated under a vacuum, the product dissolved in DCM (40 ml) and washed with water (3 × 30 ml), saturated sodium bicarbonate solution (20 ml) and dried (MgSO₄). The product was purified by column chromatography (silica, ethyl acetate: hexane, 1:1 v/v) to produce the title compound **26** as an orange thick oil (750 mg, 84%). δ_H (400 MHz, CDCl₃): 0.96-1.02 (m, 4H), 1.18-1.23 (m, 4H), 2.07 (brs, *OH*), 2.82 (s, 6H, 2 × *CH*₃), 3.15 (t, 2H, *J* 7.4 Hz), 3.46 (t, 2H, *J* 5.5 Hz), 4.47 (s, 2H, *Ar-CH*₂), 7.04 (d, 2H, *J* 8.1 Hz), 7.17-7.22 (m, 3H), 7.49 (t, 1H, *J* 7.4 Hz), 7.55 (t, 1H, *J* 8.5 Hz), 8.21 (d, 1H, *J* 8.4 Hz), 8.26 (d, 1H, *J* 8.6 Hz), 8.52 (d, 1H, *J* 8.4 Hz); δ_C (100 MHz, CDCl₃): 24.9, 26.0, 27.1, 32.3, 45.4 (2C), 46.5, 49.8, 62.5, 115.2, 119.3, 123.1, 126.5 (2C), 128.1, 128.4, 128.6 (4C), 129.9, 130.0, 130.1, 130.5, 134.7, 138.1, 151.8; δ_F (376 MHz, CDCl₃): -65.0 ppm; HRMS (NSI) (*m/z*), [*M*+*H*] calc. 549.2142 found 549.2132.

4.6.14 Coupling the benzophenone with the dansyl amide-27a



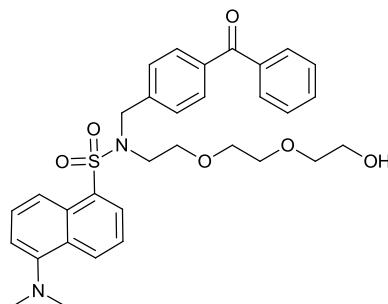
To a stirred solution of the dansyl amide **12** (470 mg, 1.01 mmol) and potassium carbonate (520 mg 3.76 mmol) in 25 mL DMF, a solution of 4-(bromomethyl)benzophenone (250 mg, 0.90 mmol) in dry DMF (5.00 ml) was added via a dropping funnel over 45 minutes. The mixture was stirred at room temperature for 24 hours, then filtered and concentrated *in vacuo*. The residue was dissolved in DCM (40 ml), the organic layer was washed with water (3 × 20 ml) then with a saturated solution of sodium bicarbonate (20 ml) and dried over anhydrous magnesium sulfate, filtered and concentrated. Column chromatography on the resultant oil (silica, ethyl acetate: cyclohexane, 1:4 v/v) yielded the title compound **27a** as a thick orange oil (492 mg, 82 %); δ_{H} (400 MHz, CDCl_3): 0.00 (s, 6H, $2 \times \text{Si-CH}_3$), 0.86 (s, 9H, $3 \times t\text{Bu-CH}_3$), 1.42 (s, 10 H), 1.09-1.15 (m, 2H), 1.22-1.28 (m, 2H), 1.39-1.45 (m, 4H), 2.05 (t, 2H, J 7.3 Hz), 2.39 (t, 2H, J 6.9 Hz), 2.59 (t, 2H, J 7.2 Hz), 2.87 (s, 6H, $2 \times \text{CH}_3$), 3.26 (t, 2H, J 7.3 Hz), 3.96 (t, 2H, J 6.5 Hz), 4.51 (s, 2H, Ar-CH_2), 7.18 (d, 1H, J 6.9 Hz), 7.29 (d, 1H, J 8.3 Hz), 7.44-7.60 (m, 6H), 7.67 (d, 2H, 8.3 J Hz), 7.75 (d, 2H, J 8.3 Hz), 8.25 (d, 1H, J 7.3 Hz), 8.32 (d, 1H, J 8.6 Hz), 8.54 (d, 1H, J 8.4 Hz); δ_{C} (100 MHz, CDCl_3): -5.2 (2C), 18.4, 25.4, 26.1 (3C), 26.5, 27.0, 27.5, 32.7, 45.5, 46.9, 50.3, 63.0, 115.3, 119.5, 123.2, 128.1(2 C), 128.2, 128.4 (3C), 130.1 (3C), 130.2, 130.4 (2C), 130.6, 132.6, 135.0, 137.0, 137.6, 141.2, 152.0, 196.3; HRMS (NSI) (m/z), $[\text{M}+\text{H}]$ calc.659.3333 found 659.3326.

4.6.15 N-(4-Benzoylbenzyl)-5-(dimethylamino)-N-(6-hydroxyhexyl)naphthalene-1-sulfonamide-27



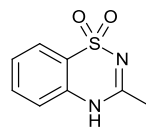
In a two necked flask (390 mg, 0.59 mmol) of the hybrid molecule **27a** was dissolved in methanol (5.00 ml), then treated with a solution of hydrochloric acid in dioxane (5 ml, 4 M). The solution was stirred at room temperature for three hours then concentrated and ethyl acetate (30 ml) was added. The organic layer was separated and washed with water (3 × 25 ml), dried (Na₂SO₄), filtered and concentrated. Column chromatography of the resultant oil, (silica, ethyl acetate: cyclohexane, 1:6), yielded the desired compound **27** as a yellow oil (230 mg, 71%). δ_H (400 MHz, CDCl₃): 0.97-1.03 (m, 4H), 1.25-1.31 (m, 4H), 1.47 (brs, OH), 2.87 (s, 6H, 2 × CH₃), 3.21 (t, 2H, *J* 7.4 Hz), 3.46 (t, 2H, *J* 5.5 Hz), 4.56 (s, 2H, *Ar-CH*₂), 7.19 (d, 1H, *J* 7.5 Hz), 7.29 (d, 2H, *J* 8.3 Hz), 7.45-7.58 (m, 5H), 7.67 (d, 2H, *J* 8.3 Hz), 7.75 (d, 2H, *J* 8.3 Hz), 8.24 (d, 1H, *J* 8.5 Hz), 8.31 (d, 1H, *J* 8.6 Hz), 8.53 (d, 1H, *J* 8.4); δ_C (100 MHz, CDCl₃): 24.9, 26.1, 27.2, 32.3, 45.4, 46.7 (2C), 50.2, 62.5, 115.2, 119.3, 123.1, 128.0 (2C), 128.1, 128.3 (3C), 129.9 (3C), 130.1, 130.2 (2C), 130.5, 132.5, 134.8, 136.9, 137.3, 141.0, 151.8, 196.3.

4.6.16 N-(4-Benzoylbenzyl)-5-(dimethylamino)-N-(2-(2-(2-hydroxyethoxy)ethoxy)ethyl)naphthalene-1-sulfonamide-28



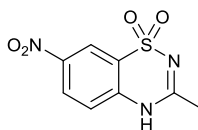
In a two necked round bottomed flask, 5-(dimethylamino)-N-(2-(2-(2-hydroxyethoxy)ethoxy)ethyl)naphthalene-1-sulfonamide **10** (180 mg, 0.47 mmol) was dissolved in dry DMF (10 ml), then potassium carbonate (260 mg, 1.88 mmol) was added to the solution under a nitrogen atmosphere. 4-Bromo-methylbenzophenone (145 mg, 0.52 mmol) in dry DMF (4.00 ml) was slowly added to the mixture and stirred for a further 24 h at room temperature. The mixture was then filtered and the DMF was removed under a vacuum, and the product dissolved in DCM (40 ml) and washed with water (3 × 30 ml), then saturated sodium bicarbonate (30 ml) and dried (MgSO₄). The product was then purified by column chromatography (silica, ethyl acetate) gave compound **28** as a yellow thick oil (92 mg, 34%). δ_H (400 MHz, CDCl₃): 2.39 (brs, 1H, OH), 2.86 (s, 6H, 2 × CH₃), 3.37 (t, 2H, *J* 4.6 Hz), 3.43-3.50 (m, 6H), 3.51 (t, 2H, *J* 4.5 Hz), 3.67 (t, 2H, *J* 4.2 Hz), 4.66 (s, 2H, *Ar-CH*₂), 7.17 (d, 1H, *J* 7.6 Hz), 7.26 (d, 2H, *J* 8.2 Hz), 7.43-7.58 (m, 6H), 7.63 (d, 2H, *J* 8.3 Hz), 7.73 (d, 2H, *J* 8.2 Hz), 8.24 (d, 1H, *J* 8.4 Hz), 8.28 (d, 1H, *J* 8.6 Hz), 8.52 (d, 1H, *J* 8.4 Hz); δ_C (100 MHz, CDCl₃): 45.3, 46.1, 51.7, 61.6, 69.6, 70.1, 72.3, 115.2, 119.3, 123.1, 128.0, 128.1, 128.2, 129.7, 129.9, 130.2, 130.5, 132.4, 134.9, 136.7, 137.3, 141.1, 151.7, 196.2.

4.6.17 3-Methyl-4H-benzo[1,2,4]thiadiazine 1,1-dioxide-33



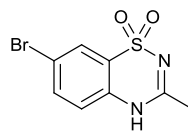
Following **General Procedure A**; 2-aminobenzenesulfonamide (3.00 g, 17.42 mmol) in acetic acid (20 ml) and acetic anhydride (2.50 ml, 26.40 mmol) gave title compound **33** (2.55 g, 74%).¹⁹⁷ δ_H (DMSO- d_6 , 400 MHz): 2.26 (s, 3H, CH_3), 7.26 (d, 1H, J 8.24 Hz, $Ar-H$), 7.39 (t, 1H, J 7.44 Hz, $Ar-H$), 7.7.64 (t, 1H, J 6.64 Hz, $Ar-H$), 7.74 (d, 1H, J 7.90 Hz, $Ar-H$) 12.00 (s, NH). δ_C (DMSO- d_6 , 100 MHz): 22.6, 117.2, 121, 123.4, 126.1, 133, 135.1, 157.2.

4.6.18 3-Methyl-7-nitro-4H-1,2,4-benzothiadiazine-1,1-dioxide-34



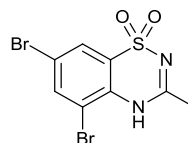
To a stirred solution of diazoxide **33** (100 mg, 0.05 mmol) in sulphuric acid (2.00 ml), concentrated nitric acid (0.15 ml) was added at) °C and the mixture was heated to 80 °C for one hour. The reaction mixture was cooled to room temperature and neutralized by solution of sodium bicarbonate and lift in the fridge overnight to complete crystalizing. Crystals were collected and dried gave the title compound **34** as a yellow solid (55 mg, 44.4%). δ_H (DMSO- d_6 , 400 MHz): 2.33 (s, 3H, CH_3), 7.47 (d, 1H, J 8.9 Hz, $Ar-H$), 8.40-8.46 (m, 2H, $Ar-H$); δ_C (DMSO- d_6 , 100 MHz): 23.3, 119.6, 120.5, 121.1, 128.4, 140.4, 144.7, 158.9. Data consistent with literature.¹⁹⁸

4.6.19 7-Bromo-3-methyl-4H-benzo[e][1,2,4]thiadiazine 1,1-dioxide-35



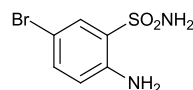
Following **General Procedure A**; 5-bromo-2-aminobenzenesulfonamide **37** (1.5 g, 5.9 mmol) in acetic acid (6.00 ml) and acid anhydride (0.7 ml, 7.4 mmol) gave title compound **35** (1.35 g, 82%).¹⁹⁹ δ_H (DMSO- d_6 , 400 MHz): 2.29 (s, 3H, CH_3), 7.27 (d, 1H, J 7.72 Hz, $Ar-H$), 7.82 (d, 1H, J 8.96 Hz, $Ar-H$), 7.91 (s, 1H, $Ar-H$), 12.24 (s, NH). δ_C (DMSO- d_6 , 100 MHz): 22.6, 117, 119.8, 122.3, 125.5, 134.4, 135.9, 157.4; ν_{max} : 3256, 3173, 3105, 1602, 1574, 1515, 1474, 1379, 1277 cm^{-1} ; HRMS (NSI) (m/z) calcd. for $C_8H_8BrN_2O_2S$ 274.9484, found 274.9490.

4.6.20 5,7-Dibromo-3-methyl-4H-benzo[e][1,2,4]thiadiazine 1,1-dioxide-36



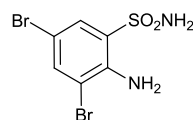
Following **General Procedure A**; 3,5-dibromo-2-aminobenzenesulfonamide **38** (200 mg, 0.56 mmol) in acetic acid (3.00 ml) and acetic anhydride (0.15 ml, 158 mmol) to give compound **36** as a pale yellow solid (120 mg, 61%). δ_H (DMSO- d_6 , 400 MHz): 2.31 (s, 3H, CH_3), 7.87 (s, 1H, $Ar-H$), 8.16 (s, 1H, $Ar-H$), 10.83 (s, 1H, NH); δ_C (DMSO- d_6 , 100 MHz): 23.32, 111.46, 117.55, 123.54, 125.39, 132.80, 138.81, 159.3; ν_{max} : 3295, 3074, 1613, 1569, 1496, 1443, 1372, 1293 cm^{-1} ; x-ray crystal data for **36**: $C_8H_6Br_2N_2O_2S$, M_r = 354.03, monoclinic, a = 18.7013(9), b = 5.3063(2), c = 10.5662(5) Å, β = 97.264(4), V = 1040.12(8) Å³, Z = 4, $P2_1/c$, D_c = 2.26 g/cm³, μ = 7.973 mm⁻¹, T = 120(2) K, 2417 unique reflections (R_{int} =0.0243), 1915 with $F^2 > 2\sigma$, $R(F, F^2 > 2\sigma)$ = 0.027, $R_w(F^2, \text{all data})$ = 0.064. Crystals grown from 10% MeOH in DCM.

4.6.21 5-Bromo-2-amino-benzenesulfonamide-37



A two necked round-bottomed flask equipped with a stirring bar was charged with 2-aminobenzenesulfonamide (4.00 g, 23 mmol), and water (20 ml) was added. Concentrated hydrobromic acid (4.20 ml, 23.30 mmol, 45% w/v in acetic acid) was added, the mixture was stirred until it became clear, and then the stirred solution warmed gently to 45°C. Hydrogen peroxide 30% in water, (5.00 ml, 0.58 mmol) was added and rapid stirring initiated. The mixture was then stirred for 15 minutes at 60°C, and then the reaction flask cooled in an ice bath. When the temperature had fallen to about 25°C, the mixture was filtered at once and the product was washed with water and dried to afford **37**. (3.80 g, 65%). δ_H (DMSO- d_6 , 400 MHz): 5.99 (s, 2H, *Ar-NH₂*), 6.76 (d, 1H, *J* 8.8 Hz, *Ar-H*), 7.34 (d, 1H, *J* 2.4 Hz, *Ar-H*), 7.36 (s, 2H, *SO₂NH₂*), 7.61 (s, 1H, *Ar-H*). δ_C (DMSO- d_6 , 100 MHz): 104.9, 119.0, 125.6, 129.7, 135.3, 144.8. Data consistent with literature.²⁰⁰

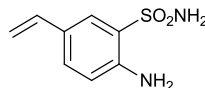
4.6.22 3,5-Dibromo-2-aminobenzenesulfonamide-38



A two necked round-bottomed flask equipped with a stirring bar was charged with 2-aminobenzenesulfonamide (2.00 g, 11.50 mmol) and then water (10 ml) was added. Concentrated hydrobromic acid (4.20 ml, 23.30 mmol, 45% w/v in acetic acid) was added, and the mixture was stirred until a clear solution was obtained. The stirred solution was warmed gently to 45°C. Hydrogen peroxide (30% in water, 5.00 ml, 0.58 mmol) was added and rapid stirring initiated. The mixture was stirred at 60°C for 30 minutes and then an ice bath was raised about the flask. When the temperature had

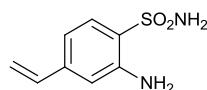
fallen to about 25°C, the mixture was filtered, and the product was washed with water and dried to give **38** (3.30 g, 82%). δ_H (DMSO- d_6 400 MHz): 6.01 (s, 2H, $ArNH_2$), 7.65 (s, 2H, SO_2NH_2), 7.70 (s, 1H, $Ar-H$), 7.84 (s, 1H, $Ar-H$); δ_C (DMSO- d_6 , 100 MHz): 105.1, 110.6, 127.0, 129.7, 137.6, 141.5. Data consistent with literature.²⁰¹

4.6.23 2-Amino-5-vinyl-benzenesulfonamide-40



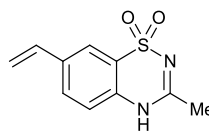
A two-necked round-bottomed flask was equipped with a magnetic stirring bar, and a reflux condenser fitted with a nitrogen inlet. The flask was charged with 5-bromo-2-aminobenzenesulfonamide **37** (1.50 g, 5.97 mmol), 1,2-dimethoxyethane (20 ml) and tetrakis (triphenylphosphine) palladium (0) (0.25 g, 0.21 mmol). Under an atmosphere of nitrogen the reaction mixture was stirred at room temperature for 15 minutes then a solution of potassium carbonate (1.60 g, 11.30 mmol) in water (6.00 ml) was added, followed by 2,4,6- trivinylcyclotriboroxane-pyridine complex (2.00 g, 8.31 mmol).¹⁷⁹ The reaction mixture was stirred under reflux for 20 hours and then cooled to ambient temperature. Distilled water (20 ml) was added, and the resulting mixture was filtered, the filtrate extracted with diethyl ether (3 × 20 ml), the combined organic layers were dried over (MgSO₄), filtered and concentrated by rotary evaporation. The crude product was purified by flash chromatography (silica, ethyl acetate/cyclohexane 4:3 parts per volume) to give the title compound **40** as a white solid (0.92 g, 77%). δ_H (CD₃OD, 400 MHz): 4.82 (s, 4H, 2 × NH_2), 5.03 (d, 1H, J 11.7 Hz, *vinyl*), 5.55 (d, 1H, J 17.5 Hz, *vinyl*), 6.57 (dd, 1H, J 10.5, 10.9 Hz, *vinyl*), 6.78 (d, 1H, J 8.5 Hz, $Ar-H$), 7.37 (d, 1H, J 8.4 Hz, $Ar-H$), 7.68 (s, 1H, $Ar-H$); δ_C (CD₃OD, 100 MHz): 109.7, 117.2, 124.1, 126.0, 126.5, 130.5, 135.5, 145.2; HRMS (NSI) (m/z), [M+H] calc.199.0538 found 199.0536.

4.6.24 2-Amino-4-vinylbenzenesulfonamide **40a**



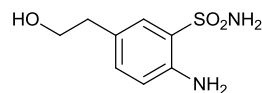
A two-necked round-bottomed flask was equipped with a magnetic stirring bar, and a reflux condenser fitted with a nitrogen inlet. The flask was charged with 4-bromo-2-aminobenzenesulfonamide **44** (400 mg, 1.59 mmol), 1,2-dimethoxyethane (10 ml) and tetrakis (triphenylphosphine)palladium(0) (60 mg, 0.05 mmol). Under an atmosphere of nitrogen, the reaction mixture was stirred at room temperature for 20 min then potassium carbonate (350 mg, 2.50 mmol) dissolved in distilled water (3.00 ml), was added, followed by 2,4,6- trivinylcyclotriboroxane-pyridine complex (310 mg, 1.29 mmol).¹⁷⁹ The reaction mixture was stirred at 82 °C for 20 hours and then cooled to ambient temperature, distilled water (10 ml) was added and the resulting mixture was filtered. The filtrate was extracted with diethyl ether (3 × 20 ml), and the combined organic phases were dried (MgSO₄), filtered and concentrated *in vacuo*. The product was then purified by flash chromatography (silica, ethyl acetate/cyclohexane 4:3 v/v) to give the title compound **40a** (190 mg, 60%). δ_H (DMSO-d₆, 400 MHz): 5.31 (d, 1H, *J* 10.7 Hz, *vinyl*), 5.76 (d, 1H, *J* 17.6 Hz, *vinyl*), 5.80 (s, 2H, *Ar-NH*₂), 6.61 (dd, 1H, *J* 17.6, 11 Hz, *vinyl*), 6.74 (d, 1H, *J* 8.2 Hz, *Ar-H*), 6.81 (s, 1H, *Ar-H*), 7.08 (s, 2H, *SO*₂*NH*₂), 7.49 (d, 1H, *J* 8.2 Hz, *Ar-H*); δ_C (DMSO-d₆, 100 MHz): 112.6, 114.4, 116.1, 123.5, 128.3, 136.1, 141.2, 145.7; HRMS (NSI) (*m/z*), [*M*+*H*] calc.199.0539 found 199.0537

4.6.25 3-Methyl-7-vinyl-4H-benzo[e][1,2,4]thiadiazine 1,1-dioxide-41



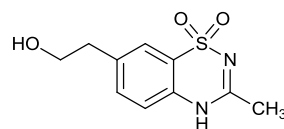
A two-necked round-bottomed flask was equipped with a magnetic stirring bar and a reflux condenser fitted with a nitrogen inlet. The flask was charged with 7-bromo-3-methyl-4H-benzo[e][1,2,4]thiadiazine-1,1-dioxide **35** (450 mg, 1.63 mmol), a (2:1) mixture of 1,2-dimethoxyethane and acetonitrile (15 ml) and tetrakis(triphenylphosphine)palladium(0) (370 mg, 0.30 mmol). The mixture was stirred at room temperature for 20 minutes then a solution of potassium carbonate (250 mg, 1.80 mmol) in water (2.00 ml) was added, followed by 2,4,6-trivinylcyclotriboroxane-pyridine complex (220 mg, 0.91 mmol). The reaction mixture was stirred at 82 °C for 20 hours and then cooled to ambient temperature, distilled water (15 ml) was added and the resulting mixture was filtered through celite. The filtrate was extracted with DCM/acetonitrile, 4:1 (3 × 2 ml), the combined organic phases dried (MgSO₄), then filtered and the filtrate was concentrated under rotary evaporation. The white solid was washed with DCM then dried gave the title compound **41** (160 mg, 44%). δ_H (DMSO-d₆, 400 MHz): 2.28 (s, 3H, CH₃), 5.32 (d, 1H, *J* 10.8 Hz, *vinyl*), 5.89 (d, 1H, *J* 17.6 Hz, *vinyl*), 6.81 (dd, 1H, *J* 17.6, 11.0 Hz, *vinyl*), 7.25 (d, 1H, *J* 8.44 Hz, *Ar-H*), 7.80 (d, 1H, *J* 8.7 Hz, *Ar-H*), 7.82 (s, 1H, *Ar-H*), 12.0 (brs, 1H, *NH*); δ_C (DMSO-d₆, 100 MHz): 22.5, 115.4, 117.6, 121.1, 121.2, 123.0, 134.5, 134.7, 135.2, 157.0; HRMS (NSI) (*m/z*), [M+H] calc. 223.0536 found 223.0538.

4.6.26 2-Amino-5-(2-hydroxy-ethyl)-benzenesulfonamide-42



In a two necked flask, 2-amino-5-vinyl-benzenesulfonamide **40** (510 mg, 2.57 mmol) was dissolved in 9-BBN solution (0.5 M in THF, 17.00 mL, 8.80 mmol) and stirred at 25 °C for 12 h. At 0 °C, hydrogen peroxide (30% in H₂O, 0.20 mL, 13.00 mmol) and 1M sodium hydroxide solution (13.50 mL, 13.50 mmol) were carefully added.¹⁸⁰ The mixture was stirred at 25 °C for 2 hours, diluted with saturated aqueous ammonium chloride (100 mL) and extracted with ethyl acetate (3 × 50 mL). The combined organic phases were dried (Na₂SO₄), filtered, and evaporated. The product was purified by flash chromatography (silica, ethyl acetate) to produce **42** as a white solid (350 mg, 63 %). δ_H (CD₃OD, 400 MHz): 2.70 (t, 2H, *J* 6.9 Hz, *ethyl*), 3.68 (t, 2H, *J* 7.0 Hz, *ethyl*), 4.85 (s, 4H, 2 × *NH*₂), 6.79 (d, 1H, *J* 8.3 Hz, *Ar-H*), 7.16 (d, 1H, *J* 8.2 Hz, *Ar-H*), 7.54 (s, 1H, *Ar-H*); δ_C (CD₃OD, 100 MHz): 38.9, 64.0, 118.9, 125.9, 128.8, 129.1, 135.3, 144.6.

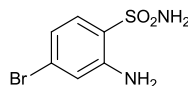
4.6.27 7-(2-Hydroxyethyl)-3-methyl-4H-benzo[e][1,2,4]thiadiazine 1,1-dioxide-43



Following **General Procedure A**; 2-amino-5-(2-hydroxy ethyl) benzenesulfonamide **42** (350 mg, 1.62 mmol), in acetic acid (6.00 ml) and acetic anhydride (0.17 ml, 1.78 mmol) gave the title compound **43** (170 mg, 40%). δ_H (DMSO-*d*₆, 400 MHz): 1.67 (brs, 1H, *OH*), 2.24 (s, 3H, *CH*₃), 2.27 (t, 2H, *J* 6.5 Hz, *CH*₂), 3.57 (t, 2H, *J* 6.5 Hz, *CH*₂), 7.17 (d, 1H, *J* 8.3 Hz, *Ar-H*), 7.47 (d, 1H, *J* 8.4 Hz, *Ar-H*), 7.58 (s, 1H, *Ar-H*), 11.92 (s, *NH*); δ_C (DMSO-*d*₆, 100 MHz): 22.4, 38.0, 61.5, 116.9, 120.8, 122.9, 133.1, 133.3,

133.8, 138.3, 156.8; ν_{max} : 3412, 2933, 2880, 2533, 2312, 1614, 1527, 1583, 1272 cm^{-1} ;
HRMS (NSI) (m/z), calcd. 241.0641, found 241.0645.

4.6.28 2-Amino-4-bromobenzenesulfonamide-44



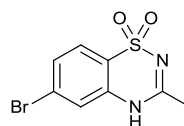
In a two necked flask, 4-bromo-1-fluoro-2-nitrobenzene (2.40 g, 10.90 mmol) was dissolved in ethanol (30 ml). Subsequently, a suspension of sodium sulphate (3.00 g) in a mixture of ethanol (50 ml) and water (62 ml) was added and then the whole was stirred at 70°C for 24 hours. Thereafter, at room temperature the reaction mixture was adjusted to PH 2 with concentrated HCl. The mixture was filtered and the filtrate was concentrated *in vacuo*. The remaining residue was dissolved under reflux in brine (saturated aqueous sodium chloride solution) (50 ml). Subsequently, water (5.00 ml) was added and the solution was then cooled in an ice bath. The precipitate was collected by filtration and dried to yield 4-bromo-2-nitrobenzenesulfonic acid **44a** (2.50 g, 81%) as a light yellow crystalline solid, which was used directly in the next step without purification.

4-Bromo-2-nitrobenzenesulfonic **44a** (2.50 g, 8.86 mmol) was dissolved in thionyl chloride (3.00 ml) and DMF (0.50 ml) and stirred at 90 °C for 2 hours. Subsequently, excess thionyl chloride was distilled off under reduced pressure. The residue was co-evaporated with chloroform (2 × 10 ml). Thereafter, the 4-bromo-2-nitrobenzenesulfonyl chloride intermediate was dissolved in chloroform (50 ml), then the solution was cooled to -40°C and ammonia gas was passed through the reaction mixture for 30 minutes. The mixture was stirred at room temperature to allow the ammonia to evaporate, and the solution was acidified with concentrated HCl to adjust to

pH 2. Subsequently, the mixture was concentrated *in vacuo* to yield 4-bromo-2-nitrobenzenesulfonamide **44b** (2.00 g, 80%).

The compound **44b** (2.00 g, 7.11 mmol) was dissolved in hydriodic acid (57 vol%, 18.50 ml). The solution was heated at 90°C for 24 hours. After cooling to room temperature, ethyl acetate (30 ml) was added. Thereafter, the solution was cooled in an ice bath and solid of (Na₂S₂O₃) was added under stirring until decolourization of the solution occurred, and then Na₂CO₃ was added as a solid for neutralization of the mixture. The layers were separated and the aqueous layer was extracted with ethyl acetate (10 ml), and the combined organic layers were dried over Na₂SO₄. After filtration and concentration *in vacuo* the crude product was purified by flash chromatography (silica, dichloromethane/ethanol, 10:1 parts per volume) to yield the title compound **44** (1.1 g, 61%). δ_H (CD₃OD, 400 MHz): 4.77 (s, 4H, 2 x NH₂), 6.71 (d, 1H, *J* 8.8 Hz, *Ar-H*), 6.94 (s, 1H, *Ar-H*), 7.45 (1H, d, *J* 8.4 Hz, *Ar-H*); δ_C (CD₃OD, 100 MHz): 119.9, 120.3, 124.7 (*C-Br*), 128.5 (*C-SO₂*), 130.9, 148.3 (*C-NH₂*).

4.6.29 6-Bromo-3-methyl-4H-benzo[e][1,2,4]thiadiazine 1,1-dioxide-45

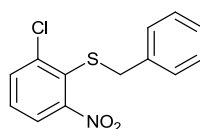


Following **General Procedure A**; 2-amino-4-bromobenzenesulfonamide **44** (200 mg, 0.72 mmol) in acetic acid (3.00 ml) and acetic anhydride (0.09 ml, 0.80 mmol) gave compound **45** (140 mg, 64%).¹⁹⁹ δ_H (DMSO-d₆, 400 MHz): 2.22 (s, 3H, CH₃), 7.37 (s, 1H, *Ar-H*), 7.51 (d, 1H, *J* 8.0 Hz, *Ar-H*), 7.65 (d, 1H, *J* 8.16 Hz, *Ar-H*), 11.96 (s, 1H, NH); δ_C (DMSO-d₆, 100 MHz): 23.2, 120.1, 120.5, 126.25, 126.31, 129.6, 137, 158.1; ν_{max} : 3285, 3189, 3125, 1607, 1574, 1530, 1464, 1383, 1277 cm⁻¹; HRMS (NSI) (*m/z*), calcd. for C₈H₈BrN₂O₂S 274.9484, found 274.9491.

4.6.30 2-Amino-6-chlorobenzenesulfonamide-46

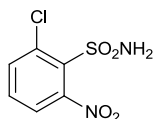
Preparation of this compound was achieved by applying a known procedure starting from 1,2-chloro-3-nitrobenzene,¹⁷⁰ using a three step reaction as described below:

i) 2-(Benzylsulfanyl)-1-chloro-3-nitrobenzene **46a**



A solution of benzyl chloride (5.70 ml, 49.80 mmol) and thiourea (3.80 g, 49.90 mmol) in a (1:1) mixture of ethanol and water (20 ml) supplemented with a few drops of ammonia solution was heated at reflux for 3 hours. 1,2-Chloro-3-nitrobenzene (9.60 g, 50 mmol) in ethanol (20 ml) was added under stirring to this solution and then an aqueous solution potassium hydroxide (7.00 g/ 50 ml) was added dropwise and the mixture was then heated at reflux for 2 hours. After cooling in an ice bath, the resulting precipitate was collected by filtration, washed with water (50 ml), and dried to give 2-(benzylsulfanyl)-1-chloro-3-nitrobenzene **46a** as a yellow crystalline solid (11.20 g, 80%). The crude compound was used in the next step without further purification.

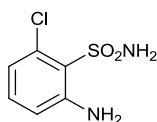
ii) 6-Chloro-2-nitrobenzenesulfonamide **46b**



Gaseous chlorine, obtained from the reaction of concentrated hydrochloric acid (8.08 g, 0.08 mmol) on potassium permanganate (1.60 g, 0.01 mmol), was introduced under stirring into a solution of 2-(benzylsulfanyl)-1-chloro-3-nitrobenzene **46a** (0.50 g, 1.78 mmol) in acetic acid (12.50 ml) and water (0.25 ml) at room temperature during 30 minutes. The mixture was poured onto ice (~ 50 g) and extracted twice with diethyl ether (25 ml). The organic layer was washed with water (15 ml), dried (MgSO₄),

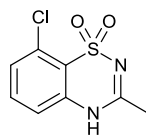
filtered, and concentrated under reduced pressure. The resulting oily residue was dissolved in dioxane (5.00 ml) and a 30% aqueous solution of ammonia (10 ml) was added dropwise. After 30 minutes of stirring, the mixture was concentrated under reduced pressure to a volume of 7.00 ml, giving rise to the formation of a precipitate. The aqueous suspension was made alkaline with sodium hydroxide (10% m/v aqueous solution) until completed dissolution of the insoluble material. The alkaline solution was treated with charcoal, filtered, and adjusted to pH 3 with 6 M hydrochloric acid. The resulting precipitate was collected by filtration, washed with water, and dried to give 6-chloro-2-nitrobenzenesulfonamide **46b** (130 mg, 40 %); mp 129-131, lit. mp 128-132 °C.¹⁷⁰

iii) **2-Amino-6-chlorobenzenesulfonamide-46**



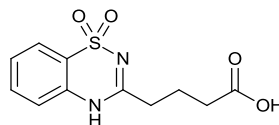
Product **46b** was dissolved in a hot (1:1) mixture of ethanol and water (3.00 ml) and then treated with ammonium chloride (80 mg, 1.50 mmol) and iron powder (0.16 g, 2.87 mmol), and the suspension heated at reflux for 45 minutes. The reaction mixture was filtered, and the filtrate was concentrated under reduced pressure to half of the volume and then extracted with dichloromethane (3 × 10 ml). The combined organic layers were dried (MgSO₄), filtered and the filtrate was concentrated under reduced pressure. After addition of hexane (2.00 ml), the resulting precipitate was collected by filtration, washed with hexane (20 ml), and dried to give the title compound **46** as a light brown solid (55 mg, 48%). δ_H (CD₃OD, 400 MHz): 4.86 (s, 4H, 2 × NH₂), 6.66-6.72 (m, 2H, Ar-H), 7.03-7.10 (m, 1H, Ar-H); δ_C (CD₃OD, 100 MHz): 118.1, 119.6, 129.5, 131.9, 133.4, 134.1. Data was consistent with the literature.¹⁷⁰

4.6.31 8-Chloro-3-methyl-4H-benzo[e][1,2,4]thiadiazine 1,1-dioxide-47



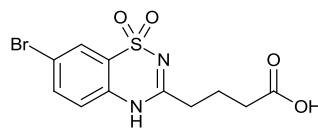
Following **General Procedure A**; 2-Amino-6-chlorobenzenesulfonamide **46** (200 mg, 0.96 mmol) in acetic acid (2.00 mL) and acetic anhydride (0.10 mL, 1.01 mmol) gave the title compound **47** as a white solid (120 mg, 54%). δ_H (DMSO- d_6 , 400 MHz): 2.28 (s, 3H, CH_3), 7.29 (d, 1H, J 8.2 Hz, $Ar-H$), 7.45 (d, 1H, J 8.0 Hz, $Ar-H$), 7.62 (t, 1H, J 8.1 Hz, $Ar-H$), 12.22 (s, 1H, NH); δ_C (DMSO- d_6 , 100 MHz): 22.3, 116.6, 127.5, 129.4, 133.3, 137.1, 139.6, 155.6; ν_{max} : 3254, 3174, 3100, 1602, 1580, 1522, 1460, 1417 cm^{-1} ; HRMS (NSI) (m/z), calc. 230.9990, found 230.9993.

4.6.32 4-(1,1-Dioxido-4H-benzo[e][1,2,4]thiadiazin-3-yl)butanoic acid-48



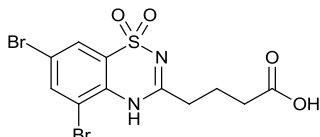
Following **General Procedure B**; 2-Aminobenzenesulfonamide (1.00 g 5.80 mmol) in dioxane (10 mL) and glutaric acid monomethyl ester chloride (1.00 mL, 7.20 mmol) gave the title compound **48** as a white solid (820 mg, 53%).¹⁸² M.p. 183-185 °C; δ_H (DMSO- d_6 , 400 MHz): 1.86-1.92 (m, 2H, CH_2) 2.32 (t, 2H, J 7.1 Hz, CH_2), 2.59 (t, 2H, J 7.3 Hz, CH_2), 7.30 (d, 1H, J 8.3 Hz, $Ar-H$), 7.41 (t, 1H, J 7.6 Hz, $Ar-H$), 7.64 (t, 1H, J 7.5 Hz $Ar-H$), 7.77 (d, 1H, J 7.9 Hz, $Ar-H$), 11.96 (s, 1H, NH), 12.14 (s, 1H, OH); δ_C (DMSO- d_6 , 100 MHz): 21.2, 32.4, 34.2, 117.3, 121.2, 123.4, 126.2, 133.0, 135.1, 159.7, 173.9; ν_{max} : 3252, 3204, 3168, 3120, 1735, 1609, 1529, 1478, 1279 cm^{-1}

4.6.33 4-(7-Bromo-1,1-dioxido-4H-benzo[e][1,2,4]thiadiazin-3-yl)butanoic acid-49



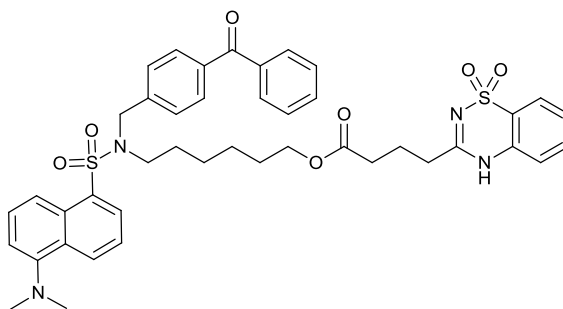
Following **General Procedure B**; 2-Amino-5-bromo benzenesulfonamide **37** (200 mg 0.79 mmol) in dioxane (10 ml) and glutaric acid monomethylester chloride (1.00 ml, 7.20 mmol) gave the title compound **49** as a white solid (25 mg, 33%).¹⁸² M.p. 246-249 °C; δ_H (DMSO- d_6 , 400 MHz): 1.72-1.78 (m, 2H, CH_2) 2.19 (t, 2H, J 7.1 Hz, CH_2), 2.47 (t, 2H, J 7.4 Hz, CH_2), 7.15 (d, 1H, J 8.6 Hz, $Ar-H$), 7.70 (d, 1H, J 8.7 Hz, $Ar-H$), 7.80 (s, 1H, $Ar-H$), 12.03 (s, 2H, NH , OH); δ_C (DMSO- d_6 , 100 MHz): 21.0, 32.4, 34.2, 117.1, 119.9, 122.5, 125.5, 134.4, 135.9, 159.9, 173.9; ν_{max} : 3274, 3184, 3113, 1692, 1605, 1574, 1526 cm^{-1}

4.6.34 4-(5,7-Dibromo-1,1-dioxido-4H-benzo[e][1,2,4]thiadiazin-3-yl)butanoic acid-50



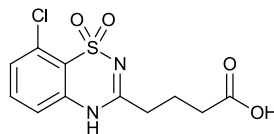
Following **General Procedure B**; 2-Amino-3,4-dibromobenzenesulfonamide **38** (200 mg 0.60 mmol) in dioxane (10 ml) and glutaric acid monomethyl ester chloride (0.10 mL, 0.75 mmol) gave the title compound **50** as a white solid (170 mg, 66%).¹⁸² M.p. 236-239 °C; δ_H (DMSO- d_6 , 400 MHz): 1.70 (m, 2H, CH_2) 2.14 (t, 2H, J 7.18 Hz, CH_2), 2.42 (t, 2H, J 7.40 Hz, CH_2), 7.81 (d, 1H, J 8.68 Hz, $Ar-H$), 8.3 (s, 1H, $Ar-H$), 10.83 (s, 1H, NH), 12.38 (s, 1H, OH); δ_C (DMSO- d_6 , 100 MHz): 21.1, 32.4, 34.2, 111.5, 117.5, 123.5, 125.4, 132.8, 138.8, 159.3, 173.7.

4.6.35 Hybrid with the non-substituted diazoxide-52



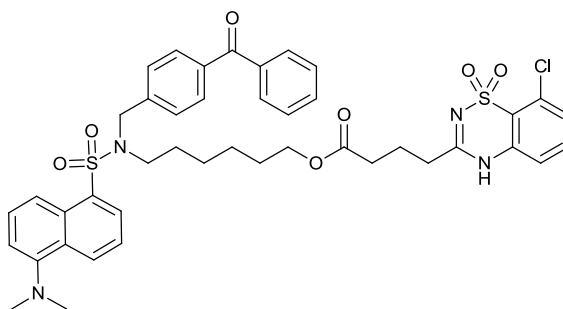
Following **General Procedure C** using diazoxide butyric acid **48** (100 mg, 0.37 mmol), triethylamine (0.15 ml, 0.44 mmol) and DMAP (4.5 mg, 10% mol) in dry acetonitrile (2 ml), tosyl chloride (85 mg, 0.44 mmol) in acetonitrile (1.50 ml), and alcohol **27** (210 mg, 0.38 mmol) in acetonitrile (3.00 ml). The product was purified using column chromatography (silica, ethyl acetate/cyclohexane, 1:1 v/v) yielded the desired compound **52** as an orange thick oil (170 mg, 57 %). δ_H (400 MHz, $CDCl_3$): 0.93-0.99 (m, 2H), 1.12-1.19 (m, 2H), 1.23-1.30 (m, 4H), 1.94 (t, 2H, J 8.0 Hz), 2.27 (t, 2H, J 7.2 Hz), 2.51 (t, 2H, J 7.5 Hz), 2.76 (s, 6H, $2 \times CH_3$), 3.15 (t, 2H, J 7.5 Hz), 3.81 (t, 2H, J 6.5 Hz), 4.45 (s, 2H, $Ar-CH_2$), 7.09 (d, 1H, J 7.0 Hz), 7.11 (d, 1H, J 7.7 Hz), 7.19 (d, 2H, J 8.2 Hz), 7.23 (t, 1H, J 7.0 Hz), 7.34-7.50 (m, 7H), 7.56 (d, 2H, J 8.2 Hz), 7.63 (d, 2H, J 8.5 Hz), 7.76 (d, 1H, J 8.0 Hz), 8.13 (d, 1H, J 8.5 Hz), 8.20 (d, 1H, J 8.7 Hz), 8.44 (d, 1H, J 8.2 Hz), 10.37 (s, 1H, NH); δ_C (100 MHz, $CDCl_3$): 21.4, 25.3, 26.0, 27.4, 28.2, 32.9, 35.1, 45.4 (2C), 47.1, 50.5, 64.5, 115.4, 117.3, 119.2, 121.2, 123.2, 124.0, 126.6, 128.1 (2C), 128.4 (3C), 130.0 (3C), 130.4 (2C), 130.8, 132.7, 133.1, 134.6, 135.1, 136.8, 137.3, 141.3, 152.0, 159.8, 173.1, 196.6; ν_{max} : 3267, 2937, 2861, 1727, 1654, 1608, 1577, 1478 cm^{-1} ; HRMS (NSI) (m/z), $[M+H]^+$ calc. 795.2881 found 795.2882.

4.6.36 4-(8-Chloro-1,1-dioxido-4H-benzo[e][1,2,4]thiadiazin-3-yl)butanoic acid-53



Following **General Procedure B**; 2-Amino-6-chlorobenzenesulfonamide **46** (260 mg, 1.26 mmol) in dioxane (15 ml) and glutaric acid monomethylester chloride (0.20 ml, 1.50 mmol) gave the title compound **53** (330 mg, 86%). M.p. 208-210 °C; δ_H (DMSO- d_6 , 400 MHz): 1.80-1.88 (m, 2H, CH_2), 2.30 (t, 2H, J 7.3 Hz, CH_2), 2.58 (t, 2H, J 7.4 Hz, CH_2), 7.33 (d, 1H, J 8.3 Hz, $Ar-H$), 7.44 (d, 1H, J 7.8 Hz, $Ar-H$), 7.60 (t, 1H, J 8.1 Hz, $Ar-H$), 12.16 (s, 1H, OH), 12.31 (s, 1H, NH); δ_C (DMSO- d_6 , 100 MHz): 21.0, 32.4, 33.8, 116.82, 119.4, 127.6, 129.4, 133.4, 137.0, 158.1, 173.9; ν_{max} : 3293, 3193, 3117, 1696, 1603, 1580, 1524, 1416, 1287 cm^{-1} ; HRMS (NSI) (m/z), calc. for $C_{11}H_{11}ClN_2O_4S$ 301.0047, found 301.0055.

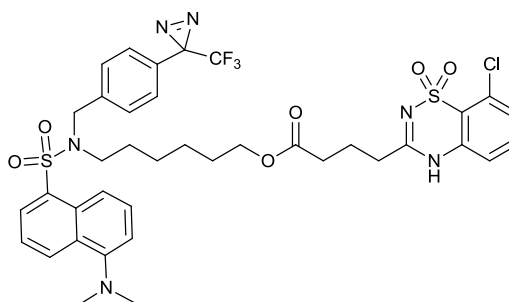
4.6.37 Benzophenone-hybrid with 8-chloro- diazoxide-54



Following **General Procedure C** using 8-chlorodiazoxide butyric acid **53** (58 mg, 0.19 mmol), triethylamine (0.08 ml, 0.57 mmol), DMAP (2.30 mg, 10% mol) in acetonitrile (2.00 ml), tosyl chloride (44 mg) in acetonitrile (1.50 ml) and alcohol **27** (105 mg, 0.19 mmol) in acetonitrile (1.50 ml). The product was purified using column chromatography (silica, ethyl acetate/cyclohexane, 1:1 v/v) to yield the title compound **54** as a yellow oil (70 mg, 44%). δ_H (400 MHz, $CDCl_3$): 1.09-1.15 (m, 2H), 1.22-1.27

(m, 2H), 1.38-1.43 (m, 4H), 2.05 (t, 2H, J 7.3 Hz), 2.39 (t, 2H, J 6.9 Hz), 2.59 (t, 2H, J 7.2 Hz), 2.87 (s, 6H, $2 \times CH_3$), 3.26 (t, 2H, J 7.3 Hz), 3.96 (t, 2H, J 6.5 Hz), 4.51 (s, 2H, $Ar-CH_2$), 7.08 (d, 1H, J 7.8 Hz), 7.19 (d, 1H, J 7.2 Hz), 7.26 (d, 2H, J 7.2 Hz), 7.28-7.36 (m, 2H), 7.45-7.59 (m, 6H), 7.65 (d, 2H, J 8.3 Hz), 7.72 (d, 2H, J 8.4 Hz), 8.22 (d, 1H, J 8.4 Hz), 8.28 (d, 1H, J 8.6 Hz), 8.54 (d, 1H, J 8.4 Hz), 10.26 (s, 1H, NH); δ_C (100 MHz, $CDCl_3$): 21.1, 25.1, 25.8, 27.3, 28.1, 32.8, 34.8, 45.4 (2C), 47.1, 50.5, 64.4, 115.3, 116.1, 119.0, 119.8, 123.1, 128.0 (2C), 128.2, 128.3 (3C), 129.9 (3C), 130.0, 130.3 (2C), 130.7, 131.3, 132.7, 132.8, 134.4, 136.6, 136.7, 137.2, 141.2, 151.9, 157.8, 173.1, 196.7; ν_{max} : 3265, 3182, 2936, 1727, 1655, 1602, 1580, 1524, 1461, 1309, 1156 cm^{-1} ; HRMS (NSI) (m/z), $[M+H]^+$ calc. 829.2491 found 829.2494.

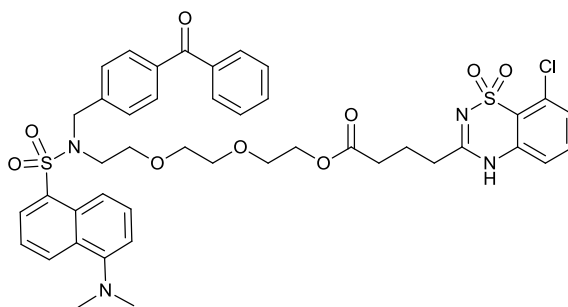
4.6.38 Diazirine alkyl linker hybrid with 8-chloro diazoxide-55



Following **General Procedure C** using 8-chlorodiazoxide butyric acid **53** (265 mg, 0.87 mmol), triethylamine (4.00 ml, 3.50 mmol), DMAP (10 mg, 10% mol) in acetonitrile (5.00 ml), tosyl chloride (106 mg, 1.05 mmol) in acetonitrile (5.00 ml) and alcohol **26** (480 mg, 0.87 mmol) in acetonitrile (3.00 ml). The product was purified using column chromatography (silica, ethyl acetate/cyclohexane, 1:1 v/v) gave the title compound **55** as an orange thick oil (240 mg, 33 %). δ_H (400 MHz, $CDCl_3$): 1.02-1.11 (m, 2H), 1.20-1.28 (m, 2H), 1.31-1.39 (m, 4H), 2.06, (d, 2H, J 7.3 Hz), 2.40 (t, 2H, J 7.3 Hz), 2.64 (t, 2H, J 7.3 Hz), 2.86 (s, 6H, $2 \times CH_3$), 3.19 (t, 2H, J 7.0 Hz), 3.92 (t, 2H, J 6.5 Hz), 4.43

(s, 2H, *Ar-CH*₂), 6.99 (d, 2H, *J* 8.1 Hz), 7.14 (d, 2H, *J* 8.2 Hz), 7.17 (d, 2H, *J* 7.6 Hz), 7.28 (d, 1H, *J* 7.8 Hz), 7.36 (t, 1H, *J* 8.0 Hz), 7.48 (t, 1H, *J* 7.6 Hz), 7.54 (t, 1H, *J* 7.7 Hz), 8.18 (d, 1H, *J* 7.3 Hz), 8.21 (d, 1H, *J* 8.5 Hz), 8.52 (d, 1H, *J* 8.2 Hz), 10.24 (s, 1H, *NH*); δ_C (100 MHz, CDCl₃): 21.3, 25.3, 26.0, 27.4, 28.3, 33.0, 34.9, 45.5 (2C), 46.9, 50.2, 64.6, 115.4, 116.5, 119.1, 119.8, 123.3, 126.6 (2C), 128.4 (2C), 128.6, 128.7 (4C), 130.0, 130.2, 130.9, 131.3, 133.0, 134.6, 136.8, 138.0, 152.0, 158.2, 173.3; δ_F (376 MHz, CDCl₃): -65.0; ν_{max} : 3263, 3182, 2936, 1727, 1602, 1580, 1524, 1461, 1307, 155 cm⁻¹; HRMS (NSI) (*m/z*), [M+H] calc. 833.2164 found 833.2164.

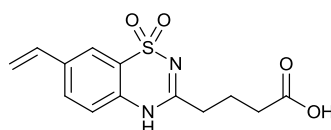
4.6.39 Benzophenone and PEG linker hybrid with 8-chlorodiazoxide-56



Following **General Procedure C** using 8-chlorodiazoxide butyric acid **53** (78 mg, 0.26 mmol), triethylamine (0.10 ml, 0.78 mmol), DMAP (3.00 mg, 10% mol) in acetonitrile (3.00 ml), tosyl chloride (60 mg) in acetonitrile (2.00 ml) and alcohol **28** (150 mg, 0.26 mmol) in acetonitrile (2.00 ml). The product was purified using column chromatography (silica, ethyl acetate) gave the title compound **56** as a red thick oil (120 mg, 53 %). δ_H (400 MHz, CDCl₃): 0.81-0.87 (m, 2H), 1.24 (t, 2H, *J* 7.2 Hz), 1.98-2.05 (m, 2H), 2.33 (t, 2H, *J* 7.0 Hz), 2.46 (t, 2H, *J* 7.2 Hz), 2.86 (s, 6H, 2 × *CH*₃), 3.41-3.48 (m, 2H), 3.54 (t, 2H, *J* 4.3 Hz), 3.66 (t, 2H, *J* 3.2 Hz), 4.21 (t, 2H, *J* 4.4 Hz), 4.64 (s, 2H, *Ar-CH*₂), 7.08 (d, 1H, *J* 8.1 Hz), 7.17 (d, 1H, *J* 7.5 Hz), 7.21-7.29 (m, 4H), 7.32 (d, 2H, *J* 8.1 Hz), 7.44-7.54 (m, 2H), 7.62 (d, 3H, *J* 8.3 Hz), 7.72 (d, 2H, *J* 6.9 Hz), 8.21 (d, 1H, *J* 8.4 Hz), 8.24 (d, 1H, *J* 8.5 Hz), 8.43 (d, 1H, *J* 8.5 Hz), 10.26 (brs, 1H, *NH*); δ_C (100

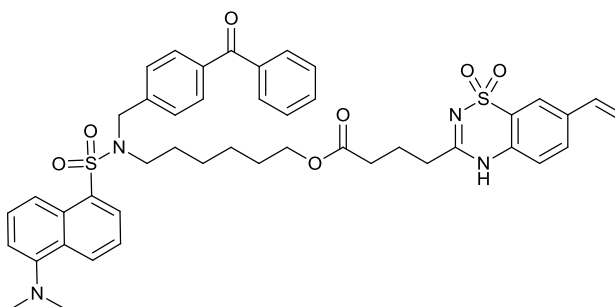
MHz, CDCl₃): 21.4, 32.8, 34.7, 45.5 (2C), 46.4, 51.9, 63.4, 69.1, 69.6, 70.2, 70.4, 115.5, 116.1, 119.2, 120.1, 123.3, 128.3 (3C), 128.5 (3C), 129.7, 130.0, 130.1 (3C), 130.4 (2C), 130.9, 131.6, 132.9 (2C), 134.9, 136.7, 136.9, 137.3, 141.4, 152.0, 157.7, 172.9, 196.8; ν_{max} : 3266, 3182, 2867, 1731, 1654, 1604, 1580, 1525, 1461, 1310, 1157 cm⁻¹; HRMS (NSI) (m/z), [M+H] calc. 861.2389 found 861.2384.

4.6.40 4-(1,1-Dioxido-7-vinyl-4H-benzo[e][1,2,4]thiadiazin-3-yl)butanoic acid-57



Following **General Procedure B**; 2-Amino-5-vinylbenzenesulfonamide **40** (250 mg 1.26 mmol) in dioxane (10 ml) and glutaric acid monomethylester chloride (0.20 ml, 1.50 mmol) gave the title compound **57** (260 mg, 70%). M.p. 207-209 °C; δ_H (DMSO-d₆, 400 MHz): 1.75-1.86 (m, 2H, CH₂) 2.25 (t, 2H, J 7.3 Hz, CH₂), 2.53 (t, 2H, J 7.4 Hz, CH₂), 5.29 (d, 1H, J 10.9 Hz), 5.88 (d, 1H, J 17.5 Hz), 6.78 (dd, 1H, J 11.1, 10.9 Hz), 7.27, (d, 1H, J 8.3 Hz), 7.78 (d, 1H, J 10.9 Hz), 7.80 (s, 1H), 12.10 (s, 2H, NH, OH); δ_C (DMSO-d₆, 100 MHz): 21.2, 32.4, 34.2, 115.5, 117.8, 121.1, 121.4, 130.1, 134.5, 134.8, 135.3, 159.6, 174.0.

4.6.41 Benzophenone-hybrid with 7-vinyl diazoxide-58



Following **General Procedure C** using 7-vinyldiazoxide butyric acid **57** (290 mg, 0.98 mmol), triethylamine (0.42 ml, 2.95 mmol), DMAP (12 mg, 10% mol) in acetonitrile

(5.00 ml), tosyl chloride (230 mg, 1.18 mmol) in acetonitrile (3.00 ml) and alcohol **27** (530 mg, 0.98 mmol) in acetonitrile (5.00 ml). The product was purified using column chromatography (silica, ethyl acetate/cyclohexane, 1:1 v/v) yielded the title compound **58** as a yellow oil (160 mg, 20 %). δ_H (400 MHz, $CDCl_3$): 1.07-1.18 (m, 2H), 1.10-1.29 (m, 2H), 1.36-1.47 (m, 4H), 2.05 (t, 2H, J 7.3 Hz), 2.38 (t, 2H, J 6.8 Hz), 2.57 (t, 2H, J 7.2 Hz), 2.87 (s, 6H, $2 \times CH_3$), 3.26 (t, 2H, J 7.3 Hz), 3.96 (t, 2H, J 6.5 Hz), 4.51 (s, 2H, $Ar-CH_2$), 5.30 (d, 1H, J 10.9 Hz), 5.73 (d, 1H, J 17.5 Hz), 6.64 (dd, 1H, J 10.6, 10.9 Hz), 7.06 (d, 1H, J 8.5 Hz), 7.18 (d, 1H, J 7.4 Hz), 7.26 (d, 2H, J 8.2 Hz), 7.45-7.59 (m, 6H), 7.65 (d, 2H, J 8.2 Hz), 7.72 (d, 2H, J 8.4 Hz), 7.87 (s, 1H), 8.22 (d, 1H, J 7.3 Hz), 8.28 (d, 1H, J 8.5 Hz), 8.54 (d, 1H, J 8.3 Hz), 10.21 (s, 1H, NH); δ_C (100 MHz, $CDCl_3$): 21.4, 25.3, 25.9, 27.0, 27.5, 28.2, 33.0, 35.2, 45.5 (2C), 47.3, 50.8, 64.6, 115.5, 115.8, 117.3, 119.2, 121.7, 123.3, 128.2 (2C), 128.5 (3C), 130.1 (3C), 130.5 (2C), 130.9, 132.9, 134.1, 134.6, 1236.5, 136.9, 137.4, 141.3, 152.1, 159.2, 173.5, 196.

4.7 Biological experimental

4.7.1 UV irradiation test

A solution of bovine serum albumin protein (BSA) 2.00 mM was prepared by dissolving BSA solid (660 mg) in phosphate buffer saline (PBS) solution (5.00 mL), then solutions of the fully functional diazoxides were prepared at a final concentration of 40 mM in DMSO as shown in Table 2. The diazoxide solutions (25 μ L) were added to 500 μ L of the protein solution and the mixture sample were shaken for 15 min at room temperature. ~100 μ L of each sample was loaded in a 384 well plate, and then exposed to light of 360 nm wave length for variable times of 10, 30 and 60 min.

Compound No	Molecular Wight	Mass in 250 μ ml DMSO	Final concentration
54	829.42	8.29 mg	40 mM
55	833.34	8.33 mg	40 mM
56	861.42	8.61 mg	40 mM

Table 2 *Preparation of solutions of functional molecules for VU irradiation*

4.7.2 SDS Polyacrylamide Gel Electrophoresis

i) Preparation of samples

The irradiated samples were very concentrated therefore, a dilution was carried out to prepare samples can be directly loaded to the gel. The overall concentration of the sample was (127 μ g/ 1 μ L), so dilution of 100 times by using the same buffer solution PBS was done and a concentration of (1.27 μ g/ 1 μ L) was obtained.

ii) Preparation of polyacrylamide gels

SDS-PAGE was carried out by the method described by Laemmli (1970) with some modifications,²⁰² using the Bio-Rad Mini-PROTEAN III electrophoresis cell, which was assembled according to the manufacturer's instructions. Two glass plates (one with 1.5 mm spacers) were thoroughly cleaned with 70% (v/v) ethanol and dried before use. The plates were then clamped into position in the gel casting stand. Ten ml of resolving gel mix were prepared as shown in Table 2.4. TEMED was used as a polymerisation inducing agent and was added to the solution immediately before the gel was poured. Sufficient space was left above the resolving gel mixture to allow for a stacking gel. Distilled water was carefully added by a 1ml pipette above the resolving gel to create a smooth overlay. The gel mix was allowed to polymerise at room temperature for 40 min. After polymerisation of the resolving gel, the distilled water overlay was removed. Then TEMED was added to the 4 % (w/v) acrylamide stacking gel mix immediately prior to pouring the gel mix on top of the resolving gel to the top of the glass plates. A 10 tooth comb was placed within the gel to make 10 individual wells. The gel was then allowed to polymerise for 20 min at room temperature before the comb was carefully removed. The gel assembly was then transferred to an electrophoresis running chamber containing SDS-PAGE running buffer as in Table 3.

Resolving gels	
Reagent	10 % gel
Resolving Buffer (1.5M Tris–HCl , 0.4 % (w/v) SDS , pH 8.8)	2.5 ml
40% (w/v) 29:1 Acrylamide Bis Acrylamide solution	2.5 ml
Distilled water	4.88 ml
10 % (w/v) ammonium persulphate (APS)	100 µl
TEMED	20 µl
Total volume	10 ml
Stacking gels	
Reagent	volume
4% Stacking Buffer (0.5 M Tris–HCl , 0.4 % SDS , pH 6.8)	2.5 ml
40% (w/v) 29:1 Acrylamide Bis Acrylamide solution	1 ml
Distilled water	6.4 ml
10 % (w/v) ammonium persulphate	100 ml
TEMED	20 µl
Total volume	10 ml
Electrophoresis running buffer	
25 mM Tris, 192 mM glycine, 0.1% (w/v) SDS, pH 8.3	

Table 3 *Preparation and reagents for SDS-PAGE*

iii) One dimensional gel electrophoresis of samples

Samples were mixed with Laemmli x4 buffer (

Table 4) in a 1:3 ratio and boiled for 5 min. Samples were allowed to cool down to room temperature prior to loading into the gel. 10 and 20 µg of protein was loaded into

each well, to obtain even loading across the gel. After the gel was made up according to section above, 2 µl of Blueye prestained protein ladder, (molecular weight range 11-245 kDa) was added to the well. Gels were then placed vertically in a Mini-PROTEAN III™ electrophoresis chamber from Bio-Rad and run in electrode running buffer at 50 volts for 10 min using Bio-Radpower pac 300. This initial voltage allows the samples to enter the stacking gel. After that, the voltage was increased to 150 volts and run for around 1 h. As the dye front approached the base of the gel plates, the voltage was switched off. Gels were carefully removed and placed in 10% methanol in water solution to stop protein moving. Gels were then visualised under UV transillumination imaging system.

Reagent	Volume (ml)
Distilled water	0.8
1 M Tris HCl pH 6.8	2.4
Glycerol	4.0
10 % (w/v) SDS	1.6
β-mercaptoethanol	1.0
Bromophenol blue 0.05% (w/v)	0.2
Total volume	10.0

Table 4 *Laemmli x4 SDS – PAGE sample buffer*

4.7.3 Incubation of the mitochondrial extract proteins with the diazoxide molecules.

Mitochondrial extract provided by Dr Alan Hargreaves, which was extracted from pig brain. The protein concentration was determined using, Bio-Rad *DC* Protein assay (Bio-

Rad laboratories, Hertfordshire, UK) with bovine serum albumin as the standard.

Protein concentration was 6.5 µg/µl; the samples were prepared as follow:

Mitochondrial extract 50 µl was diluted with TBS buffer solution 64 µl, then diazoxides molecule (100 µM, 3 µl) were added and incubated at room temperature for 30 minutes.

Sample were then divided to two parts 60 µl each, one part was suspended in TBS buffer solution and centrifuged at 1000 r/m for 5 minutes, the pellets were separated and collected. All the samples were loaded in a 384 well plate, and irradiated under 360 nm UV light for 10 and 30 minutes for the diazirine and benzophenone respectively. Then 40 µg of each sample was loaded in a polyacrylamide gel for electrophoresis separation, as described above.

References

1. M. A. Lampson and T. M. Kapoor, in *Chemical Biology*, ed. anonymous Wiley-VCH Verlag GmbH, 2007, pp.71-94.
2. D. B. Martin, L. S. Stuart, *Angew Chem Int Ed Engl.*, 2004, **43**, 46-58.
3. K. R. Yamamoto, *Annu. Rev. Genet.*, 1985, **19**, 209-252.
4. D. T. Hung, T. F. Jamison and S. L. Schreiber, *Chem. Biol.*, 1996, **3**, 623-639.
5. P. J. Belshaw, J. G. Schoepfer, K. Liu, K. L. Morrison and S. L. Schreiber, *Angew. Chem., Int. Ed.*, 1995, **34**, 2129-2132.
6. J. Westbrook, Z. Feng, L. Chen, H. Yang and H. M. Berman, *Nucleic Acids Research*, 2003, **31**, 489-491.
7. C. M. Crews and U. Splittgerber, *Trends Biochem. Sci.*, 1999, **24**, 317-320.
8. S. J. Haggarty, T. U. Mayer, D. T. Miyamoto, R. Fathi, R. W. King, T. J. Mitchison and S. L. Schreiber, *Chem. Biol.*, 2000, **7**, 275-286.
9. J. Inglese, R. L. Johnson, A. Simeonov, M. Xia, W. Zheng, C. P. Austin and D. S. Auld, *Nat Chem Biol*, 2007, **3**, 466-479.
10. S. Ong, M. Schenone, A. A. Margolin, X. Li, K. Do, M. K. Doud, D. R. Mani, L. Kuai, X. Wang, J. L. Wood, N. J. Tolliday, A. N. Koehler, L. A. Marcaurelle, T. R. Golub, R. J. Gould, S. L. Schreiber and S. A. Carr, *Proc. Natl. Acad. Sci. U. S. A.*, 2009, **106**, 4617-4622.
11. M. Rogawski, *Amino Acids*, 2000, **19**, 133-149.
12. D. C. Swinney and J. Anthony, *Nature*, 2011, **10**, 507-519.
13. J. L. DV. Titov, *Bioorg Med Chem.*, 2012, **20**, 1902-1909.
14. T. U. Mayer and T. M. Kapoor, *Science*, 1999, **286**, 971.
15. T. M. Kapoor, T. U. Mayer, M. L. Coughlin and T. J. Mitchison, *J. Cell Biol.*, 2000, **150**, 975-988.
16. T. N. Glasnov, H. Tye and C. O. Kappe, *Tetrahedron*, 2008, **64**, 2035-2041.

17. J. Bajorath, *Nat Rev Drug Discov*, 2002, **1**, 882-894.
18. H. Gohlke and G. Klebe, *Angew. Chem. , Int. Ed.*, 2002, **41**, 2644-2676.
19. T. J. Mitchison, *Chem Biol*, 194, **1**, 3-6.
20. J. Heitman, N. R. Movva and M. N. Hall, *Science*, 1991, **253**, 905-909.
21. J. P. Yan, ME. Colon, L. A. Beebe and P. Melancon, *J Cell Biol.*, 1994, **126**, 65-75.
22. G. Rigaut, A. Shevchenko, B. Rutz, M. Wilm, M. Mann and B. Seraphin, *Nat Biotech*, 1999, **17**, 1030-1032.
23. P. A. Wallrabe H, *Curr. Opin. Biotechnol.*, 2005, **16**, 19-27.
24. T. Fukui, *J. Biochem. (Tokyo, Jpn.)*, 1995, **117**, 1139-1144.
25. B. F. Cravatt and E. J. Sorensen, *Curr. Opin. Chem. Biol.*, 2000, **4**, 663-668.
26. R. Garcia-Serna and J. Mestres, *Drug Discov. Today*, 2011, **16**, 99-106.
27. M. B. Goshe and R. D. Smith, *Curr. Opin. Biotechnol.*, 2003, **14**, 101-109.
28. I. H. Takahiro Hayashi, *Acc. Chem. Res.*, 2012, **45**, 1460.
29. D. A. Jeffery and M. Bogyo, *Curr. Opin. Biotechnol.*, 2003, **14**, 87-95.
30. D. Greenbaum, A. Baruch, L. Hayrapetian, Z. Darula, A. Burlingame, K. F. Medzihradszky and M. Bogyo, *Mol. Cell. Proteomics*, 2002, **1**, 60-68.
31. M. Patricelli, D. Giang, L. Stamp and J. Burbaum, *Proteomics*, 2001, **1**, 1067.
32. A. Borodovsky, B. M. Kessler, R. Casagrande, H. S. Overkleeft, K. D. Wilkinson and H. L. Ploegh, *EMBO J.*, 2001, **20**, 5187-5196.
33. A. Singh, E. R. Thornton and F. H. Westheimer, *J. Biol. Chem.*, 1962, **237**, PC3006-PC3008.
34. D. Robinette, N. Neamati, K. B. Tomer and C. H. Borchers, *Expert Rev Proteomics*, 2006, **3**, 399-408 (DOI:10.1586/14789450.3.4.399).
35. A. E. Ruoho, H. Kiefer, P. E. Roeder and S. J. Singer, *Proc. Natl. Acad. Sci. U. S. A.*, 1973, **70**, 2567-2571.

36. E. W. Chan, S. Chattopadhyaya, R. C. Panicker, X. Huang, S. Q. Yao, *J. Am. Chem. Soc.*, 2004, **126**, 14435-14446.
37. T. Kan, Y. Kita, Y. Morohashi, Y. Tominari, S. Hosoda, T. Tomita, H. Natsugari, T. Iwatsubo and T. Fukuyama, *Org. Lett.*, 2007, **11**, 2055-2058.
38. J. Bunner, S. Serin, F. Richards, *J Biol Chem.*, 1980, **255**, 3313-3318.
39. Y. Sadakane and Y. Hatanaka, *Anal. Sci.*, 2006, **22**, 209-218.
40. A. L. MacKinnon, J. L. Garrison, R. S. Hegde and J. Taunton, *J. Am. Chem. Soc.*, 2007, **129**, 14560-14561.
41. K. L. Buchmueller, B. T. Hill, M. S. Platz and K. M. Weeks, *J. Am. Chem. Soc.*, 2003, **125**, 10850-10861.
42. Y. Z. Li, J. P. Kirby, M. W. George, M. Poliakoff and G. B. Schuster, *J. Am. Chem. Soc.*, 1988, **110**, 8092-8098.
43. R. J. Bergeron, J. B. Dionis and M. J. Ingeno, *J. Org. Chem.*, 1987, **52**, 144-149.
44. W. L. Karney and W. T. Borden, *J. Am. Chem. Soc.*, 1997, **119**, 3347-3350.
45. C. J. Shields, D. E. Falvey, G. B. Schuster, O. Buchardt and P. E. Nielsen, *J. Org. Chem.*, 1988, **53**, 3501-3507.
46. Q. Liu and Y. Tor, *Org. Lett.*, 2003, **5**, 2571-2572.
47. E. Goddard-Borger and R. V. Stick, *Org. Lett.*, 2007, **9**, 3797-3800.
48. A. Sinz, *ChemMedChem*, 2007, **2**, 425-431.
49. J. Brunner, H. Senn and F. M. Richards, *J. Biol. Chem.*, 1980, **255**, 3313-3318.
50. M. Platz, A. S. Admasu, S. Kwiatkowski, P. J. Crocker, N. Imai and D. S. Watt, *Bioconjugate Chem.*, 1991, **2**, 337-341.
51. S. A. Fleming, *TETRAHEDRON*, 1995, **51**, 12479-12520.
52. G. Dorman and G. D. Prestwich, *Biochemistry (N. Y.)*, 1994, **33**, 5661-5673.
53. A. M. Sadaghiani, S. H. Verhelst, M. Bogoy, *Curr Opin Chem Biol.*, 2007, **11**, 20-28.

54. M. D. Savage, *Avidin-biotin chemistry: a handbook*, Pierce Chemical Company, 1992.
55. X. Tong and L. Smith, *Anal. Chem.*, 1992, **64**, 2672-2677.
56. N. M. Green, *Methods Enzymol*, 1990, **84**, 51-67.
57. M. Wilchek and E. A. Bayer, *Meth. Enzymol.*, 1990, **184**, 5-13.
58. H. Zhou, J. A. Ranish, J. D. Watts and R. Aebersold, *Nat. Biotechnol.*, 2002, **20**, 512.
59. M. Grabolle, M. Spieles, V. Lesnyak, N. Gaponik, A. Eychmuller and U. Resch-Genger, *Anal. Chem.*, 2009, **81**, 6285-6294.
60. A. Bilenca, J. Cao, M. Colice, A. Ozcan, B. Bouma, L. Raftery and G. Tearney, *Ann. N. Y. Acad. Sci.*, 2008, **1130**, 68-77.
61. M. Chalfie, Y. Tu, G. Euskirchen, W.W. Ward and D. C. Prasher, *Science*, 1994, **263**, 802-805.
62. R. Hovius, B. H. Meyer, E. G. Guignet and H. Vogel, in *Struct.Genomics Membr.Proteins*, ed. anonymous CRC Press LLC, 2006, pp.199-210.
63. K. Truong and M. Ikura, *Curr. Opin. Struct. Biol.*, 2001, **11**, 537-538.
64. M. W. MS. Dillingham, *Org Biomol Chem.*, 2008, **6**, 3031-3037.
65. F. Koehn, J. Hofkens, R. Gronheid, d. A. Van and F. C. De Schryver, *J Phys Chem A*, 2002, **106**, 4808-4814.
66. B. Gerhard, M. Christian Gampe, R. Yanina, B. Torsten, H. Johan Faber, M. Martin, R. Matthias, L. Matthias, B. Reto and G. and Christoph, *J. Med. Chem.*, 2007, **50**, 6104-6112.
67. P. Sarathi Addy, B. Saha, N. D. Pradeep Singh, A. K. Das, J. T. - Bush, C. Lejeune, C. J. Schofield and A. Basak, *Chem. Commun.*, 2013, **49**, 1930-1932.
68. J. Flaskos, M. Sachana, M. Pen, W.Harris, A.J. Hargreaves, *Environ. Toxicol. Pharmacol.*, 2006, **22**, 70-74.

69. J. J. Sung, S. J. Kim, H. B. Lee, J. M. Chung, M.Y. Choi, C. L. Cha, Y. H. Chun, K.W. Lee, *Muscle Nerve*, 1998, **21**, 1135-1144.
70. D. J. Read, L. Langford, H. R. Barbour, P. J. Forshaw and P. Glynn, *Toxicol. Appl. Pharmacol.*, 2007, **219**, 190-195.
71. A. G. Karczmar, E. Usdin and J. H. Wills , *Anticholinesterase agents.*, Pergamon Press, Oxford; New York, 1970.
72. T. Eleršek and M. Filipič, *InTech*, Available from: <http://www.intechopen.com/book>, 2011.
73. K. Zilles, CM. Becker, A. Schleicher, *Bibl Anat.*, 1982, **23**, 40-55.
74. T. C. Tsao, Y. C. Juang, R. S. Lan, W. B. Shieh and C. H. Lee, *CHEST*, 1990, **98**, 631-636.
75. B. Li, L. M. Schopfer, H. Grigoryan, C. M. Thompson, S. H. Hinrichs, P. Masson and O. Lockridge, *Toxicol. Sci*, 2009, **107**, 144-155.
76. Li B Schopfer, M.Lawrence, LM. Schopfer, SH.Hinrichs, P.Masson and O. Lockridge, *Anal Biochem.*, 2007, **361**, 263-272.
77. R. Toomey, R. Alpern, J. J. Vasterling, D. G. Baker, D. J. Reda, M. J. Lyons, W. G. Henderson, H. K. Kang, S. A. Eisen and F. M. Murphy, *J Int Neuropsychol Soc.*, 2009, **15**, 717-729.
78. D. B. Hancock, E. R. Martin, G. M. Mayhew, J. M. Stajich, J. Rita, M. A. Stacy, B. L. Scott, J. M. Vance and W. K. Scott, *BMC Neurol.*, 2008, **8**, 6.
79. P. J. Lein and A. D. Fryer, *Toxicol. Sci.*, 2005, **83**, 166-176.
80. S. Roy, B. Zhang, V. -. Lee and J. Trojanowski, *Acta Neuropathol.*, 2005, **109**, 5-13.
81. P. Glynn, *Biochim Biophys Acta.*, 2005, **1736**, 87-93.
82. M. Mühlig-Versen, A. B. da Cruz, J. Tschäpe, M. Moser, R. Büttner, K. Athenstaedt, P. Glynn and D. Kretschmar, *J. Neurosci. Res.*, 2005, **25**, 2865-2873.
83. G. Schmuck and H. J. Ahr, *Toxicol In Vitro*, 1997, **3**, 263-270.

84. P. Glynn, *Prog Neurobiol*, 2002, **1**, 61-74.
85. J. A. Johnson and K. B. Wallace, *Toxicol. Appl. Pharmacol.*, 1987, **88**, 234-241.
86. M. B. Abou-Donia, *Chem. Biol. Interact.*, 1993, **87**, 383-393.
87. A. J. Hargreaves, M. J. Fowler, M. Sachana, J. Flaskos, M. Bountouri, I. C. Coutts, P. Glynn, W. Harris, M. W. Graham, *Biochem. Pharmacol.*, 2006, **71**, 1240-1247.
88. K. Solbu, S. Thorud, M. Hersson, S. Øvrebø, D. G. Ellingsen, E. Lundanes and P. Molander, *J. Chromatogr. , A*, 2007, **1161**, 275-283.
89. J. E. Chambers and S. F. Oppenheimer, *Toxicological Sciences*, 2004, **77**, 185-187.
90. M. Eto, H. Ohkawa, K. Kobayashi and T. Hosoi, *Agric. Biol. Chem.*, 1968, **32**, 1056-1058.
91. H. A. N. El-Fawal and W. C. McCain, *Neurotoxicol. Teratol.*, 2008, **30**, 161-166.
92. S. Elizabeth, L. Daniel M. and A. Mohamed B., *Proc Natl Acad Sci U S A.*, 1986, **83**, 6174-6178.
93. R. Lalonde and C. Strazielle, *Rev Neurosci.*, 2003, **14**, 369-385.
94. H. A. N. El-Fawal, B. S. Jortner and M. Ehrich, *Toxicol. Appl. Pharmacol.*, 1989, **97**, 500-511.
95. R. K. Sihag, A. Y. Jeng and R. A. Nixon, *FEBS Lett.*, 1988, **233**, 181-185.
96. B. Jortner and M. Ehrich, *Neurotoxicology*, 1987, **8**, 303-314.
97. M. J. Fowler, J. Flaskos, W. G. McLean and A. J. Hargreaves, *J. Neurochem.*, 2001, **76**, 671-678.
98. D. Henschler, G. Schmuck, M. van Aerssen and D. Schiffmann, *Toxicol. in Vitro*, 1992, **6**, 327-335.
99. M. Ehrich, L. Correll and B. Veronesi, *Neurotoxicology*, 1994, **15**, 309-313.
100. M. van Tienhoven, J. Atkins, Y. Li and P. Glynn, *J. Biol. Chem.*, 2002, **277**, 20942-20948.

101. P. J. Forshaw, J. Atkins, D. E. Ray and P. Glynn, *J. Neurochem.*, 2001, **79**, 400-406.
102. W. Harris, D. Muñoz, P. L. R. Bonner and A. J. Hargreaves, *Toxicol. in Vitro*, 2009, **23**, 1559-1563.
103. D. Muñoz, P. L. R. Bonner and A. J. Hargreaves, *Toxicol. in Vitro*, 2010, **24**, 2104-2107.
104. A. J. L. Cooper, T. M. Jeitner and J. P. Blass, *Neurochem. Int.*, 2002, **40**, 1-5.
105. M. Griffin, R. Casadio, C.M. Bergamini, *Biochem. J.*, 2002, **368**, 377-396.
106. C. N. Pope, *J. Toxicol. Environ. Health, Pt. B*, 1999, **2**, 161-181.
107. A. Hargreaves and J. Avila, *J. Neurochem.*, 1985, **45**, 490-496.
108. A. J. Hargreaves and W. G. McLean, *Neurosci. Lett.*, 1993, **163**, 201-204.
109. M. S. Liyasova, L. M. Schopfer and O. Lockridge, *Chem. Res. Toxicol.*, 2012, **25**, 1752-1761.
110. U. Muus, C. Kranz, T. Marquardt and C. Meier, *Eur. J. Org. Chem.*, 2004, **2004**, 1228-1235.
111. C. Meier, U. Muus, J. Renze, L. Naesens, E. De Clercq and J. Balzarini, *Antivir Chem Chemother.*, 2002, **2**, 101-114.
112. S. Y. Wu and J. E. Casida, *Chem. Res. Toxicol.*, 1992, **5**, 680-684.
113. E. H. Rios Morales, J. Balzarini and C. Meier, *Chem. Eur. J.*, 2011, **17**, 1649-1659.
114. J. Karolin, L. B. -. Johansson, L. Strandberg and T. Ny, *J. Am. Chem. Soc.*, 1994, **116**, 7801-7806.
115. E. Cuevas-Yañez, J. M. Muchowski and R. Cruz-Almanza, *Tetrahedron*, 2004, **60**, 1505-1511.
116. K. Gießler, H. Griesser, D. Göhringer, T. Sabirov and C. Richert, *Eur. J. Org. Chem*, 2010, **2010**, 3611-3620.

117. H. Zhang, P. Wang, Y. Yang and H. Sun, *Chem. Commun.*, 2012, **48**, 10672-10674.
118. Y. Gao, P. Ma, Y. Chen, Y. Zhang, Y. Bian, X. Li, J. Jiang and C. Ma, *Inorg. Chem.*, 2009, **48**, 45-54.
119. T. F. Slaughter, K. E. Achyuthan, T. Lai and C. S. Greenberg, *Anal. Biochem.*, 1992, **205**, 166-171.
120. W. Harris, D. Munoz, P. Bonner and A. J. Hargreaves, *Toxicol In Vitro.*, 2009, **23**, 1559-1563.
121. D. A. Cecilie, J.V. Lars, N. Tom Ivar, M. Kristian and W. Rune, *BMJ*, 2008, **337**.
122. J. Bogaert, S. Dymarkowski and A. Taylor M., in *in Clinical Cardiac MRI*, ed. ed. J. Bogaert, S. Dymarkowski and A. Taylor M., Springer Berlin Heidelberg, 2005, pp.381-437.
123. D. M. Yellon and D. J. Hausenloy, *N. Engl. J. Med.*, 2007, **357**, 1121-1135.
124. V. Braunersreuther and V. Jaquet, *Curr Pharm Biotechnol*, 2012, **1**, 97-114.
125. R. Ferrari, L. Agnoletti, L. Comini, G. Gaia, T. Bachetti, A. Cargnoni, C. Ceconi, S. Curello and O. Visioli, *Eur. Heart J.*, 1998, **19 Suppl B**, B2-11.
126. N. J. Davies, R. Schulz, P. M. Olley, K. D. Strynadka, D. L. Panas and G. D. Lopaschuk, *Circulation Research*, 1992, **70**, 1161-1168.
127. K. Ogasawara, T. Inoue, M. Kobayashi, H. Endo, T. Fukuda and A. Ogawa, *Neurosurgery*, 2004, **55**, 1060-1067.
128. C. E. Murry, R. B. Jennings and K. A. Reimer, *Circulation*, 1986, **74**, 1124-1136.
129. R. Schulz, M. V. Cohen, M. Behrends, J. M. Downey and G. Heusch, *Cardiovasc. Res.*, 2001, **52**, 181-198.
130. B. C. G. Gho, R. G. Schoemaker, M. A. van den Doel, D. J. Duncker and P. D. Verdouw, *Circulation*, 1996, **94**, 2193-2200.
131. R. Wong, Aponte, AM. Aponte, C. Steenbergen, E. Murphy, *AJP-Heart Circ Physiol*, 2010, **298**, 75-91.

132. T. Kuzuya, S. Hoshida, N. Yamashita, H. Fuji, H. Oe, M. Hori, T. Kamada and M. Tada, *Circ. Res.*, 1993, **72**, 1293-1299.
133. M. S. Marber, D. S. Latchman, J. M. Walker and D. M. Yellon, *Circulation*, 1993, **88**, 1264-1272.
134. J. Z. Sun, X. L. Tang, S. W. Park, Y. Qiu, J. F. Turrens and R. Bolli, *J. Clin. Invest.*, 1996, **97**, 562-576.
135. S. Javadov, M. Karmazyn and N. Escobales, *J. Pharmacol. Exp. Ther.*, 2009, **330**, 670-678.
136. Y. Tsujimoto, L. Finger, J. Yunis, P. Nowell and C. Croce, *Science*, 1984, **226**, 1097-1099.
137. Z. Zhao, J. S. Corvera, M. E. Halkos, F. Kerendi, N. Wang, R. A. Guyton and J. Vinten-Johansen, *Am J Physiol Heart Circ Physiol*, 2003, **285**, H579-H588.
138. J. Vinten-Johansen, Z. Zhao, R. Jiang, A. J. Zatta and G. P. Dobson, *J. Appl. Physiol.*, 2007, **103**, 1441-1448.
139. C. Penna, R. Rastaldo, D. Mancardi, S. Raimondo, S. Cappello, D. Gattullo, G. Losano and P. Pagliaro, *Basic Res. Cardiol.*, 2006, **101**, 180-189.
140. G. Serviddio, N. Di Venosa, A. Federici, D. D'Agostino, T. Rollo, F. Prigigallo, E. Altomare, T. Fiore and G. Vendemiale, *FASEB J.*, 2005, **19**, 354-361.
141. Z. Zhao and J. Vinten-Johansen, *Cardiovasc. Res.*, 2006, **70**, 200-211.
142. M. Hüttemann, I. Lee, L. Samavati, H. Yu and J. W. Doan, *Biochim. Biophys. Acta*, 2007, **1773**, 1701-1720.
143. P. Bernardi, L. Scorrano, R. Colonna, V. Petronilli and F. Di Lisa, *Eur. J. Biochem.*, 1999, **264**, 687-701.
144. S. Roth, J. Dreixle, A. Shaikh, K. Lee and V. Bindokas, *Invest Ophthalmol Vis Sci.*, 2006, **47**, 2114-2124.
145. M. A. Burke, R. K. Mutharasan and H. Ardehali, *Circ. Res.*, 2008, **102**, 164-176.
146. M. Murata, M. Akao, B. O'Rourke and E. Marbán, *Circ. Res.*, 2001, **89**, 891-898.

147. H. Ardehali and B. O'Rourke, *J. Mol. Cell. Cardiol.*, 2005, **39**, 7-16.
148. S. Sandler, A. K. Andersson, J. Larsson, N. Makeeva, T. Olsen, P. O. G. Arkhammar, J. B. Hansen, F. A. Karlsson and N. Welsh, *Biochem. Pharmacol.*, 2008, **76**, 1748-1756.
149. N. B. Standen, *J. Physiol. (Lond.)*, 2002, **542**, 666-666.
150. R. Ockaili, V. R. Emani, S. Okubo, M. Brown, K. Krottapalli and R. C. Kukreja, *Am J Physiol-Heart C.*, 1999, **277**, H2425-H2434.
151. I. Inoue, H. Nagase, K. Kishi and T. Higuti, *Nature*, 1991, **352**, 244-247.
152. P. Paucek, G. Mironova, F. Mahdi, A. D. Beavis, G. Woldegiorgis and K. D. Garlid, *J. Biol. Chem.*, 1992, **267**, 26062-26069.
153. K. D. Garlid, P. Paucek, V. Yarov-Yarovoy, H. N. Murray, R. B. Darbenzio, A. J. D'Alonzo, N. J. Lodge, M. A. Smith and G. J. Grover, *Circ. Res.*, 1997, **81**, 1072-1082.
154. Y. Liu, T. Sato, B. O'Rourke and E. Marban, *Circulation*, 1998, **97**, 2463-2469.
155. K. D. Garlid, P. Paucek, V. Yarov-Yarovoy, X. Sun and P. A. Schindler, *J. Biol. Chem.*, 1996, **271**, 8796-8799.
156. G. Edwards and A. H. Weston, *Annu. Rev. Pharmacol. Toxicol.*, 1993, **33**, 597-637.
157. G. J. Gross and R. M. Fryer, *Circulation Research*, 1999, **84**, 973-979.
158. H. W. van Hamersvelt, H. J. Kloke, H. J. Kloke, D. J. de Jong, R. A. Koene, R. A. Koene, F.T. Huysmans, *J Hypertens.*, 1996, **14**, 1041-1045.
159. A. Björklund and V. Grill, *Endocrinology*, 1993, **132**, 1319-1328.
160. N. D'hahan, C. Moreau, A. Prost, H. Jacquet, A. E. Alekseev, A. Terzic and M. Vivaudou, *Proc. Natl. Acad. Sci. U. S. A.*, 1999, **96**, 12162-12167.
161. H. Zhang, T. P. Flagg and C. G. Nichols, *J. Mol. Cell. Cardiol.*, 2010, **48**, 71-75.
162. S. Seino, *Annu. Rev. Physiol.*, 1999, **61**, 337-362.

163. A. Muñoz, M. Nakazaki, J. C. Goodman, R. Barrios, C. G. Onetti, J. Bryan and L. Aguilar-Bryan, *Stroke*, 2003, **34**, 164-170.
164. J. Seharaseyon, A. Ohler, N. Sasaki, H. Fraser, T. Sato, D. C. Johns, B. O»Rourke and E. Marbán, *J. Mol. Cell. Cardiol.*, 2000, **32**, 1923-1930.
165. H. Ardehali, Z. Chen, Y. Ko, R. Mejía-Alvarez and E. Marbán, *Proc. Natl. Acad. Sci. U. S. A.*, 2004, **101**, 11880-11885.
166. W. Danysz and C. G. Parsons, *Pharmacological Reviews*, 1998, **50**, 597-664.
167. P. Jimonet, F. Audiau, J. Aloup, M. Barreau, J. Blanchard, A. Bohme, A. Boireau, M. Chevé, D. Damour, A. Doble, J. Lavayre, G. Dutruc-Rosset, J. C. R. Randle, J. Rataud, J. Stutzmann and S. Mignani, *Bioorg. Med. Chem. Lett.*, 1994, **4**, 2735-2740.
168. S. Khelili, *Med Chem Res*, 2003, **12**, 457-470.
169. P. deTullio, B. Pirotte, P. Lebrun, J. Fontaine, L. Dupont, M. Antoine, R. Ouedraogo, S. Khelili, C. Maggetto, B. Masereel, O. Diouf, T. Podona and J. and Delarge, *J. Med. Chem.*, 1996, **39**, 937-948.
170. B. Pirotte, P. de Tullio, Q. Nguyen, F. Somers, P. Fraikin, X. Florence, P. Wahl, J. B. Hansen and P. Lebrun, *J. Med. Chem.*, 2010, **53**, 147-154.
171. D. P. Smith, J. Anderson, J. Plante, A. E. Ashcroft, S. E. Radford, A. J. Wilson and M. J. Parker, *Chem. Commun.*, 2008, **0**, 5728-5730.
172. A. V. Afonin, I. A. Ushakov, O. A. Tarasova, E. Y. Shmidt, A. I. Mikhaleva and V. K. Voronov, *Russ. J. Org. Chem.*, 2000, **36**, 1777-1783.
173. A. C. Garner and J. Furniss, *Unpublished data*, Nottingham Trent University.
174. T. Fukuyama, M. Cheung, C. Jow, Y. Hidai and T. Kan, *Tetrahedron Lett.*, 1997, **38**, 5831-5834.
175. A. K. Imtiyaz and Y. S. Jung, *lett. Org. Chem.*, 2007, **4**, 423-428.
176. A. Gopalsamy, R. Chopra, K. Lim, G. Ciszewski, M. Shi, K. J. Curran, S. F. Sukits, K. Svenson, J. Bard, J. W. Ellingboe, A. Agarwal, G. Krishnamurthy, A.

- Y. Howe, M. Orlowski, B. Feld, J. O'Connell and T. S. Mansour, *J. Med. Chem.*, 2006, **49**, 3052-3055.
177. A. Groweiss, *Org. Process Res. Dev.*, 2000, **4**, 30-33.
178. D. Phillips, J. Sonnenberg, A. C. Arai, R. Vaswani, P. O. Krutzik, T. Kleisli, M. Kessler, R. Granger, G. Lynch and A. Richard Chamberlin, *Bioorg. Med. Chem.*, 2002, **10**, 1229-1248.
179. F. Kerins and D. O'Shea, *J. Org. Chem.*, 2002, **67**, 4968-4971.
180. Y. Takashima, Y. Kaneko and Y. Kobayashi, *Tetrahedron*, 2010, **66**, 197-207.
181. T. Fuchss, A. Strub, C. Hesslinger, W. Ulrich and R. Boer, 2007, , 51pp.
182. C. Parenti, L. Costantino, M. D. Bella, L. Raffa, G. G. Baggio and P. Zanolli, *Arch. Pharm. (Weinheim)*, 1985, **318**, 903-911.
183. J. Linares-Palomino, M. A. Husainy, V. K. Lai, J. M. Dickenson and M. Galiñanes, *J. Physiol. (Lond.)*, 2010, **588**, 2173-2191.
184. M. A. Husainy, J. M. Dickenson and M. Galiñanes, *J. Surg. Res.*, 2012, **174**, 62-72.
185. T. Decker and M. Lohmann-Matthes, *J. Immunol. Methods*, 1988, **115**, 61-69.
186. T. Mosmann, *J. Immunol. Methods*, 1983, **65**, 55-63.
187. I. Dhimitruka and J. SantaLucia, *Org. Lett.*, 2006, **8**, 47-50.
188. K. Wakasugi, A. Iida, T. Misaki, Y. Nishii and Y. Tanabe, *Adv. Synth. Catal.*, 2003, **345**, 1209-1214.
189. M. Hashimoto and Y. Hatanaka, *Eur. J. Org. Chem*, 2008, **2008**, 2513-2523.
190. M. Kainosho and A. Nakamura, *Tetrahedron*, 1969, **25**, 4071-4081.
191. E. F. Rios Morales, J. F. Balzarini and C. Meier, *J Med Chem.*, 2012, **55**, 7245-7252.
192. C. C. Forbes, K. M. DiVittorio and B. D. Smith, *J. Am. Chem. Soc.*, 2006, **128**, 9211-9218.

193. E. V. Antina, G. B. Guseva, A. E. Loginova, A. S. Semeikin and A. I. V'yugin, *Russian Journal of General Chemistry*, 2010, **80**, 2374-2381.
194. H. Liu, Z. Gao, Z. Yao, S. Zheng, Y. Li, W. Zhu, X. Tan, X. Luo, J. Shen, K. Chen, G. Hu and H. Jiang, *J. Med. Chem.*, 2007, **50**, 83-93.
195. R. F. G. Fröhlich, R. H. Furneaux, D. J. Mahuran, B. A. Rigat, A. E. Stütz, M. B. Tropak, J. Wicki, S. G. Withers and T. M. Wrodnigg, *Carbohydr. Res.*, 2010, **345**, 1371-1376.
196. *Beijing Nhwa Medicine Research Institute, Peop. Rep. China. Pat.*, CN101092405A, 12/26.
197. D. Yang, H. Fu, L. Hu, Y. Jiang and Y. Zhao, *J. Comb. Chem.*, 2009, **11**, 653-657.
198. A. Cherepakha, V. O. Kovtunenکو, A. Tolmachev and O. Lukin, *Tetrahedron*, 2011, **67**, 6233-6239.
199. A. Cherepakha, V. O. Kovtunenکو, A. Tolmachev, O. Lukin and K. G. Nazarenko, *Synthetic Communications*, 2011, **41**, 1977-1989.
200. M. A. H. Ismail, D. A. Abou El Ella, K. A. M. Abouzid and A. H. Mahmoud, *Bioorg. Med. Chem.*, 2012, **20**, 2455-2478.
201. L. Raffa, A. Monzani and A. Albasini, *Farmaco, Ed. Sci.*, 1964, **19**, 35-46.
202. U. K. Laemmli, *Nature*, 1970, **227**, 680-685.